

ENANTIOSELECTIVE SULFA-MICHAEL ADDITION TO *TRANS*-
CHALCONE DERIVATIVES WITH QUININE DERIVED BIFUNCTIONAL
ORGANOCATALYSTS

A THESIS SUBMITTED TO
THE GRADUATE SCHOOL OF NATURAL AND APPLIED SCIENCES
OF
MIDDLE EAST TECHNICAL UNIVERSITY

BY

DENİZ TÖZENDEMİR

IN PARTIAL FULFILLMENT OF THE REQUIREMENTS
FOR
THE DEGREE OF DOCTOR OF PHILOSOPHY
IN
CHEMISTRY

DECEMBER 2020

Approval of the thesis:

**ENANTIOSELECTIVE SULFA-MICHAEL ADDITION TO TRANS-
CHALCONE DERIVATIVES WITH QUININE DERIVED
BIFUNCTIONAL ORGANOCATALYSTS**

submitted by **DENİZ TÖZENDEMİR** in partial fulfillment of the requirements for the degree of **Doctor of Philosophy in Chemistry, Middle East Technical University** by,

Prof. Dr. Halil Kalıpçılar
Dean, Graduate School of **Natural and Applied Sciences**

Prof. Dr. Cihangir Tanyeli
Head of the Department, **Chemistry**

Prof. Dr. Cihangir Tanyeli
Supervisor, **Chemistry, METU**

Examining Committee Members:

Prof. Dr. Metin Zora
Chemistry, METU

Prof. Dr. Cihangir Tanyeli
Chemistry, METU

Prof. Dr. Özdemir Doğan
Chemistry, METU

Prof. Dr. Aliye Alaylı Altundaş
Chemistry, Gazi University

Assist. Prof. Dr. Yunus Emre Türkmen
Chemistry, Bilkent University

Date: 28.12.2020

I hereby declare that all information in this document has been obtained and presented in accordance with academic rules and ethical conduct. I also declare that, as required by these rules and conduct, I have fully cited and referenced all material and results that are not original to this work.

Name, Last name : Deniz Tözendemir

Signature :

ABSTRACT

ENANTIOSELECTIVE SULFA-MICHAEL ADDITION TO *TRANS*- CHALCONE DERIVATIVES WITH QUININE DERIVED BIFUNCTIONAL ORGANOCATALYSTS

Tözendemir, Deniz
Doctor of Philosophy, Chemistry
Supervisor: Prof. Dr. Cihangir Tanyeli

December 2020, 181 pages

The use of organocatalysts has brought profound advantages in the context of asymmetric synthesis, in terms of ease of use and better compatibility with the environment. More than 20 organocatalysts of four different classes (squaramide, urea, thiourea, and sulfonamide) have been developed and used to catalyze various asymmetric reactions in our research group. In this thesis, asymmetric sulfa-Michael type additions were carried out in the presence of cinchona alkaloid derived squaramide and sulfonamide-type organocatalysts of our design. The first part of the thesis focuses on sulfa-Michael addition of methyl thioglycolate to *trans*-chalcones. 23 enantiomerically enriched chalcone derivatives (>99% yield, 68-99% ee) and 4 enantiomerically enriched aryl butenone derivatives (31-71% yield, 61-77% ee) were synthesized in the presence of a squaramide/quinine type organocatalyst. A nitro-substituted sulfa-Michael adduct was selected for further reactions which yielded optically and biologically active 1,4-benzothiazepin-2-one derivative. In the second part of the study, 1-naphthalenethiol was added to *trans*-chalcones in the similar fashion, in the presence of a sulfonamide/quinine type bifunctional organocatalyst. A total of 15 enantiomerically enriched sulfa-Michael adducts (β -

aryl- β -sulfanyl ketones) containing thionaphthol moiety were synthesized with moderate to excellent enantioselectivities (51-96% ee). Selected β -aryl- β -sulfanyl ketones were oxidized to obtain corresponding optically active sulfones.

Keywords: Asymmetric Synthesis, Asymmetric Catalysis, Organocatalysis, Sulfa-Michael Reaction, Conjugate Addition

ÖZ

KİNİN TÜREVİ BİFONKSİYONEL ORGANOKATALİZÖRLER İLE TRANS-ÇALKON TÜREVLERİNE ENANTİYOSEÇİCİ SÜLFA-MICHAEL KATILMALARI

Tözendemir, Deniz
Doktora, Kimya
Tez Yöneticisi: Prof. Dr. Cihangir Tanyeli

Aralık 2020, 181 pages

Asimetrik sentez bağlamında organokatalizörlerin kullanımı, kullanım kolaylığı ve çevreyle uyum bakımından önemli avantajlar getirmiştir. Araştırma grubumuzda dört ayrı sınıftan (skuaramit, üre, tiyoüre ve sülfonamit) 20'den fazla organokatalizör sentezlenmiş ve bu katalizörler çok çeşitli asimetrik tepkimeyi katalizlemede kullanılmaktadır. Bu tez çalışmasında, kendi tasarımı olan kinkona alkaloid türevi skuaramit ve sülfonamit tipi organokatalizörler varlığında asimetrik sülfamichael tepkimeleri gerçekleştirilmiştir. Tezin ilk kısmı, metal tiyoglikolatın *trans*-çalkonlara sülfamichael katılmaları üzerinde yoğunlaşmaktadır. Sentezlenen skuaramit/kinin tipi organokatalizör kullanılarak 23 adet enantiyomerce zengin çalkon türevi (>99% verim, 68-99% ee) ve 4 adet enantiyomerce zengin aril bütenon türevi (31-71% yield, 61-77% ee) elde edilmiştir. Oluşturulan nitro-sübsitüentli bir sülfamichael katılma ürünün seçilerek ilave tepkimelere tabi tutulması ile optikçe ve biyolojik olarak aktif 1,4-benzotiyazepin-2-on türevi elde edilmiştir. Çalışmanın ikinci kısmında, 1-tiyonaftolün sülfonamit/kinin tipi organokatalizör varlığında *trans*-çalkonlara katılması incelenmiştir. Toplam 15 adet enantiyomerce zengin sülfamichael katılma ürünü (β -aril- β -sülfanil ketonlar) ortalamadan çok yüksek

değerlere varan enantioseçiciliklerle (%51-96 ee) elde edilmiştir. Seçilen β -aril- β -sülfanil ketonların yükseltgenmesiyle optikçe aktif sülfonlar elde edilmiştir.

Anahtar Kelimeler: Asimetrik Sentez, Asimetrik Kataliz, Organokataliz, Sülfamichael Tepkimesi, Konjuge Katılma

“Choose love, and don’t ever let fear turn you against your playful heart”

-Jim Carrey

ACKNOWLEDGMENTS

This thesis is the product of a long and tiresome journey. Before finally bringing it to a close, I want to pay my respects to some wonderful people.

Before anyone else, I would like to express my deepest gratitude to my doctor father Prof. Dr. Cihangir Tanyeli. I went through dark times, and he was there for me with his endless patience. I am sincerely grateful, not only for his academic guidance and wisdom, but also the moral support.

Throughout my graduate studies, I got to share the laboratory with many people and all of them somehow contributed to this work. For that, I am thankful to all Tanyeli Research Group members, old and new. A special thanks with sprinkles on top goes to Zeynep Dilşad Susam. I do not regret the days and nights we spent together in the laboratory in vain, even one bit. Thanks for everything you have done for and with me.

None of these would have been possible without the financial support of TÜBİTAK (113Z156 and 217Z035). I also would like to thank Zeynep Erdoğan (UNAM) for HRMS experiments, Ömür Çelikbıçak and Melis Şardan Ekiz (HÜNİTEK) for MALDI-MS experiments and all the NMR operators of METU Chemistry Department for their contributions.

A synthetic organic chemist is in constant need of all sorts of glassware and chemicals. Thankfully, I was always covered by Halil Memiş, Hamit Çağlar and Nizamettin Kavut. They were truly the pillars of the department during my labwork.

It was never all work and no play. All my breaks in the department were accompanied by 3 wonderful people: Eda Karadeniz, Seda Karahan and Halil İpek. I enjoyed and miss every sip of stale tea and dull Social Building food with them. Another person I was blessed to have in my life during my PhD was Zeki Seskir. Although we seldom had enough time to spend together, it was always invigorating

to converse with him. Of course, another special thanks goes to Burcu Tekin for managing to strip me off of my academic anxiety with a hearty laugh, juicy conversations and quality food.

What kind of an acknowledgement would this be if I did not thank my parents, right? I was not the easiest young adult to deal with, and I surely took them to hell and back since I started grad school. There isn't a simple phrase I can use to express my gratitude to them. I am lucky to have them as my mother and father.

I saved the best person on earth for the last. The biggest, fattest, and fanciest of thanks goes to my partner in life, to Gökhan Demirkıran. Countless times I felt broken down and lost faith in myself. But each time, he believed in me more strongly than I could ever do. On top of that, he made me believe in and be proud my own work, which was the main catalyst for me to finish up what I started. I am eternally grateful for his presence.

Last but not least, thank you, dear reader for your precious time.

TABLE OF CONTENTS

ABSTRACT	v
ÖZ.....	vii
ACKNOWLEDGMENTS	x
TABLE OF CONTENTS	xii
LIST OF TABLES	xvii
LIST OF FIGURES	xviii
LIST OF ABBREVIATIONS	xxvii
CHAPTERS	
1 INTRODUCTION	1
1.1 Sulfur Containing Drugs.....	1
1.2 The Importance of Asymmetric Synthesis	2
1.3 Asymmetric Organocatalysis.....	4
1.3.1 Cinchona Alkaloids as a Motif in Bifunctional Organocatalysis	6
1.4 Sulfa-Michael Addition Reactions	9
1.4.1 Asymmetric Sulfa-Michael Addition Reactions.....	10
1.5 1,4-Benzothiazepin-2-ones	14
1.6 β -Aryl- β -Sulfanyl Ketones	15
1.7 Chiral Sulfones	15
1.8 Aim of the Study	16
2 RESULTS AND DISCUSSION.....	19
2.1 Synthesis of Bifunctional Organocatalysts.....	19
2.2 Synthesis of the <i>trans</i> -Chalcone Derivatives	21

2.3	Asymmetric Sulfa-Michael Addition of Methyl Thioglycolate to <i>trans</i> -Chalcones	22
2.3.1	Optimization Studies	22
2.3.2	Substrate Scope	26
2.3.3	Synthesis of 1,4-Benzothiazepin-2-one Derivative.....	32
2.4	Asymmetric Sulfa-Michael Addition of 1-Thionaphthol to <i>trans</i> -Chalcones	34
2.4.1	Optimization Studies	34
2.4.2	Substrate Scope	39
2.4.3	Synthesis of Sulfones	44
3	EXPERIMENTAL.....	47
3.1	Materials and Methods.....	47
3.2	Synthesis of Bifunctional Quinine-type Organocatalysts	48
3.2.1	Synthesis of Quinine Amine 77	48
	Synthesis of 2-Adamantyl Monosquaramide 76b	49
3.2.2	Synthesis of Bifunctional Organocatalyst 58b	49
3.2.3	Synthesis of 2,4,6-Trimethyl-3-nitrobenzene-1-sulfonyl chloride (79)	50
3.2.4	Synthesis of Bifunctional Catalyst 59	50
3.3	General Procedure for the Synthesis of Products 61a-v	51
3.3.1	Methyl 2-((3-oxo-1,3-diphenylpropyl)thio)acetate (61a)	52
3.3.2	Methyl 2-((3-oxo-3-phenyl-1-(<i>m</i> -tolyl)propyl)thio)acetate (61b)	52
3.3.3	Methyl 2-((3-oxo-3-phenyl-1-(<i>p</i> -tolyl)propyl)thio)acetate (61c).....	52
3.3.4	Methyl 2-((3-oxo-1-phenyl-3-(<i>p</i> -tolyl)propyl)thio)acetate (61d)	53
3.3.5	Methyl 2-((1-(2-methoxyphenyl)-3-oxo-3-phenylpropyl)thio)acetate (61e)	53

3.3.6	Methyl 2-((1-(3-methoxyphenyl)-3-oxo-3-phenylpropyl)thio)acetate (61f)	53
3.3.7	Methyl 2-((1-(4-methoxyphenyl)-3-oxo-3-phenylpropyl)thio)acetate (61g)	54
3.3.8	Methyl 2-((1-(furan-2-yl)-3-oxo-3-phenylpropyl)thio)acetate (61h)	54
3.3.9	Methyl 2-((3-oxo-3-phenyl-1-(thiophen-2-yl)propyl)thio)acetate (61i)	54
3.3.10	Methyl 2-((1-(2-bromophenyl)-3-oxo-3-phenylpropyl)thio)acetate (61j)	55
3.3.11	Methyl 2-((1-(3-bromophenyl)-3-oxo-3-phenylpropyl)thio)acetate (61k)	55
3.3.12	Methyl 2-((3-(4-bromophenyl)-3-oxo-1-phenylpropyl)thio)acetate (61l)	56
3.3.13	Methyl 2-((1-(2-chlorophenyl)-3-oxo-3-phenylpropyl)thio)acetate (61m)	56
3.3.14	Methyl 2-((1-(3-chlorophenyl)-3-oxo-3-phenylpropyl)thio)acetate (61n)	56
3.3.15	Methyl 2-((1-(4-chlorophenyl)-3-oxo-3-phenylpropyl)thio)acetate (61o)	57
3.3.16	Methyl 2-((1-(3-fluorophenyl)-3-oxo-3-phenylpropyl)thio)acetate (61p)	57
3.3.17	Methyl 2-((3-oxo-3-phenyl-1-(2-(trifluoromethyl)phenyl)propyl)thio)acetate (61q)	58
3.3.18	Methyl 2-((3-oxo-3-phenyl-1-(4-(trifluoromethyl)phenyl)propyl)thio)acetate (61r)	58
3.3.19	Methyl 2-((1-(2-nitrophenyl)-3-oxo-3-phenylpropyl)thio)acetate (61s)	59
3.3.20	Methyl 2-((1-(3-nitrophenyl)-3-oxo-3-phenylpropyl)thio)acetate (61t)	59
3.3.21	Methyl 2-((1-(4-nitrophenyl)-3-oxo-3-phenylpropyl)thio)acetate (61u)	60
3.3.22	Methyl 2-((3-(4-nitrophenyl)-3-oxo-1-phenylpropyl)thio)acetate (61v)	60

3.4	General Procedure for the Synthesis of Products 63a-d	60
3.4.1	Methyl 2-((3-oxo-1-phenylbutyl)thio)acetate (63a).....	61
3.4.2	Methyl 2-((1-(4-methoxyphenyl)-3-oxobutyl)thio)acetate (63b)	61
3.4.3	Methyl 2-((3-oxo-1-(4-(trifluoromethyl)phenyl)butyl)thio)acetate (63c).....	61
3.4.4	Methyl 2-((1-(4-nitrophenyl)-3-oxobutyl)thio)acetate (63d).....	62
3.5	Procedure for the Synthesis of Product 84	62
3.6	Procedure for the Dithiolane Protection of Sulfa-Michael Adduct 88	63
3.7	Procedure for Synthesis of Benzothiazepinone Derivative 81	64
3.8	General Procedure for the Synthesis of Products 66a-x	65
3.8.1	3-(Naphthalen-1-ylthio)-1,3-diphenylpropan-1-one (66a).....	65
3.8.2	3-(Naphthalen-1-ylthio)-1-phenyl-3-(m-tolyl)propan-1-one (66b)	66
3.8.3	3-(Naphthalen-1-ylthio)-1-phenyl-3-(p-tolyl)propan-1-one (66c)	66
3.8.4	3-(Naphthalen-1-ylthio)-3-phenyl-1-(p-tolyl)propan-1-one (66d)	67
3.8.5	3-(3-Methoxyphenyl)-3-(naphthalen-1-ylthio)-1-phenylpropan-1-one (66f)	68
3.8.6	3-(4-Methoxyphenyl)-3-(naphthalen-1-ylthio)-1-phenylpropan-1-one (66g)	68
3.8.7	3-(3-Bromophenyl)-3-(naphthalen-1-ylthio)-1-phenylpropan-1-one (66k)	69
3.8.8	1-(4-Bromophenyl)-3-(naphthalen-1-ylthio)-3-phenylpropan-1-one (66l)	70
3.8.9	3-(2-Chlorophenyl)-3-(naphthalen-1-ylthio)-1-phenylpropan-1-one (66m)	70
3.8.10	3-(3-Chlorophenyl)-3-(naphthalen-1-ylthio)-1-phenylpropan-1-one (66n)	71

3.8.11	3-(4-Chlorophenyl)-3-(naphthalen-1-ylthio)-1-phenylpropan-1-one (66o)	71
3.8.12	3-(Naphthalen-1-ylthio)-1-phenyl-3-(4-(trifluoromethyl)phenyl) propan-1-one (66r)	72
3.8.13	3-(Naphthalen-1-ylthio)-3-(4-nitrophenyl)-1-phenylpropan-1-one (66u)	73
3.8.14	3-(Naphthalen-1-ylthio)-1-phenyl-3-(3,4,5-trimethoxyphenyl) propan-1-one (66w)	73
3.8.15	3-(Naphthalen-1-ylthio)-1-(2-nitrophenyl)-3-phenylpropan-1-one (66x)	74
3.9	General Procedure for the Synthesis of Sulfones	74
3.9.1	3-(Naphthalen-1-ylsulfonyl)-1,3-diphenylpropan-1-one (67a)	75
3.9.2	3-(3-Methoxyphenyl)-3-(naphthalen-1-ylsulfonyl)-1-phenylpropan-1-one (67f)	75
3.9.3	3-(3-Methoxyphenyl)-3-(naphthalen-1-ylsulfonyl)-1-phenylpropan-1-one (67g)	76
3.9.4	3-(4-Chlorophenyl)-3-(naphthalen-1-ylsulfonyl)-1-phenylpropan-1-one (67o)	77
4	CONCLUSION	79
	REFERENCES	81
A.	NMR SPECTRA	85
B.	HPLC CHROMATOGRAMS	134
	CURRICULUM VITAE	181

LIST OF TABLES

TABLES

Table 2.1. Catalyst and solvent screening ^a	23
Table 2.2. Further screening for SMA of methyl thioglycolate to <i>trans</i> -chalcone ^a	24
Table 2.3. Substrate scope of SMA of methyl thioglycolate to <i>trans</i> -chalcones ^a ...	27
Table 2.4. SMA of methyl thioglycolate with aryl butenones under optimized conditions ^a	29
Table 2.5. SMA of methyl thioglycolate with aryl butenones under mild conditions ^a	30
Table 2.6. Catalyst and solvent screening ^a	35
Table 2.7. Further screening for SMA of 1-thionaphthol to <i>trans</i> -chalcone ^a	37
Table 2.8. SMA of 1-thionaphthol to substituted <i>trans</i> -chalcones in THF.....	39
Table 2.9. Further solvent screening results for the selected derivative 66c ^a	41
Table 2.10. SMA of 1-thionaphthol to substituted <i>trans</i> -chalcones in DCM.....	42
Table 2.11. Synthesis of enantioenriched sulfones from β -aryl- β -sulfanyl ketones	45

LIST OF FIGURES

FIGURES

Figure 1.1. Structures of selected sulfur containing drug molecules	1
Figure 1.2. Structures and odors of linalool enantiomers.....	2
Figure 1.3. Structures of ibuprofen and penicillamine enantiomers	3
Figure 1.4. Classes and modes of activation of asymmetric organocatalysts	5
Figure 1.5. Comparison of resonance structures and distances between the hydrogens of thiourea and squaramide moieties	8
Figure 1.6. Structure of CGP-37151 and its benzothiazepine core	14
Figure 1.7. Structures of raloxifene and <i>seco</i> -raloxifene	15
Figure 1.8. The leprosy drug dapsone	16
Figure 1.9. Structures of organocatalysts	17
Figure 2.1. Structures of surveyed organocatalysts	22
Figure 2.2. Structures of surveyed organocatalysts	35
Figure 2.3. Comparison of the ee's of SMA in the presence of THF and DCM as solvent.....	44
Figure 2.4. Comparison of FTIR spectra of 66a (red, top) and 67a (blue, bottom)	45
Figure A. 1 ¹ H NMR spectrum of 59	85
Figure A. 2 ¹³ C NMR spectrum of 59	85
Figure A. 3 ¹ H NMR spectrum of 61a	86
Figure A. 4 ¹³ C NMR spectrum of 61a	86
Figure A. 5 ¹ H NMR spectrum of 61b	87
Figure A. 6 ¹³ C NMR spectrum of 61b	87
Figure A. 7 ¹ H NMR spectrum of 61c	88
Figure A. 8 ¹³ C NMR spectrum of 61c	88
Figure A. 9 ¹ H NMR spectrum of 61d	89
Figure A. 10 ¹³ C NMR spectrum of 61d	89
Figure A. 11 ¹ H NMR spectrum of 61e	90
Figure A. 12 ¹³ C NMR spectrum of 61e	90

Figure A. 13 ^1H NMR spectrum of 61f	91
Figure A. 14 ^{13}C NMR spectrum of 61f	91
Figure A. 15 ^1H NMR spectrum of 61g	92
Figure A. 16 ^{13}C NMR spectrum of 61g	92
Figure A. 17 ^1H NMR spectrum of 61h	93
Figure A. 18 ^{13}C NMR spectrum of 61h	93
Figure A. 19 ^1H NMR spectrum of 61i	94
Figure A. 20 ^{13}C NMR spectrum of 61i	94
Figure A. 21 ^1H NMR spectrum of 61j	95
Figure A. 22 ^{13}C NMR spectrum of 61j	95
Figure A. 23 ^1H NMR spectrum of 61k	96
Figure A. 24 ^{13}C NMR spectrum of 61k	96
Figure A. 25 ^1H NMR spectrum of 61l	97
Figure A. 26 ^{13}C NMR spectrum of 61l	97
Figure A. 27 ^1H NMR spectrum of 61m	98
Figure A. 28 ^{13}C NMR spectrum of 61m	98
Figure A. 29 ^1H NMR spectrum of 61n	99
Figure A. 30 ^{13}C NMR spectrum of 61n	99
Figure A. 31 ^1H NMR spectrum of 61o	100
Figure A. 32 ^{13}C NMR spectrum of 61o	100
Figure A. 33 ^1H NMR spectrum of 61p	101
Figure A. 34 ^{13}C NMR spectrum of 61p	101
Figure A. 35 ^1H NMR spectrum of 61q	102
Figure A. 36 ^{13}C NMR spectrum of 61q	102
Figure A. 37 ^1H NMR spectrum of 61r	103
Figure A. 38 ^{13}C NMR spectrum of 61r	103
Figure A. 39 ^1H NMR spectrum of 61s	104
Figure A. 40 ^{13}C NMR spectrum of 61s	104
Figure A. 41 ^1H NMR spectrum of 61t	105
Figure A. 42 ^{13}C NMR spectrum of 61t	105

Figure A. 43 ^1H NMR spectrum of 61u	106
Figure A. 44 ^{13}C NMR spectrum of 61u	106
Figure A. 45 ^1H NMR spectrum of 61v	107
Figure A. 46 ^{13}C NMR spectrum of 61v	107
Figure A. 47 ^1H NMR spectrum of 63a	108
Figure A. 48 ^{13}C NMR spectrum of 63a	108
Figure A. 49 ^1H NMR spectrum of 63b	109
Figure A. 50 ^{13}C NMR spectrum of 63b	109
Figure A. 51 ^1H NMR spectrum of 63c	110
Figure A. 52 ^{13}C NMR spectrum of 63c	110
Figure A. 53 ^1H NMR spectrum of 63d	111
Figure A. 54 ^{13}C NMR spectrum of 63d	111
Figure A. 55 ^1H NMR spectrum of 84	112
Figure A. 56 ^{13}C NMR spectrum of 84	112
Figure A. 57 ^1H NMR spectrum of 88	113
Figure A. 58 ^{13}C NMR spectrum of 88	113
Figure A. 59 ^1H NMR spectrum of 81	114
Figure A. 60 ^{13}C NMR spectrum of 81	114
Figure A. 61 ^1H NMR spectrum of 66a	115
Figure A. 62 ^{13}C NMR spectrum of 66a	115
Figure A. 63 ^1H NMR spectrum of 66b	116
Figure A. 64 ^{13}C NMR spectrum of 66b	116
Figure A. 65 ^1H NMR spectrum of 66c	117
Figure A. 66 ^{13}C NMR spectrum of 66c	117
Figure A. 67 ^1H NMR spectrum of 66d	118
Figure A. 68 ^{13}C NMR spectrum of 66d	118
Figure A. 69 ^1H NMR spectrum of 66f	119
Figure A. 70 ^{13}C NMR spectrum of 66f	119
Figure A. 71 ^1H NMR spectrum of 66g	120
Figure A. 72 ^{13}C NMR spectrum of 66g	120

Figure A. 73 ^1H NMR spectrum of 66k	121
Figure A. 74 ^{13}C NMR spectrum of 66k	121
Figure A. 75 ^1H NMR spectrum of 66l	122
Figure A. 76 ^{13}C NMR spectrum of 66l	122
Figure A. 77 ^1H NMR spectrum of 66m	123
Figure A. 78 ^{13}C NMR spectrum of 66m	123
Figure A. 79 ^1H NMR spectrum of 66n	124
Figure A. 80 ^{13}C NMR spectrum of 66n	124
Figure A. 81 ^1H NMR spectrum of 66o	125
Figure A. 82 ^{13}C NMR spectrum of 66o	125
Figure A. 83 ^1H NMR spectrum of 66r	126
Figure A. 84 ^{13}C NMR spectrum of 66r	126
Figure A. 85 ^1H NMR spectrum of 66u	127
Figure A. 86 ^{13}C NMR spectrum of 66u	127
Figure A. 87 ^1H NMR spectrum of 66w	128
Figure A. 88 ^{13}C NMR spectrum of 66w	128
Figure A. 89 ^1H NMR spectrum of 66x	129
Figure A. 90 ^{13}C NMR spectrum of 66x	129
Figure A. 91 ^1H NMR spectrum of 67a	130
Figure A. 92 ^{13}C NMR spectrum of 67a	130
Figure A. 93 ^1H NMR spectrum of 67f	131
Figure A. 94 ^{13}C NMR spectrum of 67f	131
Figure A. 95 ^1H NMR spectrum of 67g	132
Figure A. 96 ^{13}C NMR spectrum of 67g	132
Figure A. 97 ^1H NMR spectrum of 67o	133
Figure A. 98 ^{13}C NMR spectrum of 67o	133
Figure B. 1 HPLC chromatogram of <i>rac</i> - 61a	134
Figure B. 2 HPLC chromatogram of enantiomerically enriched 61a	134
Figure B. 3 HPLC chromatogram of <i>rac</i> - 61b	135
Figure B. 4 HPLC chromatogram of enantiomerically enriched 61b	135

Figure B. 5 HPLC chromatogram of <i>rac</i> - 61c	136
Figure B. 6 HPLC chromatogram of enantiomerically enriched 61c	136
Figure B. 7 HPLC chromatogram of <i>rac</i> - 61d	137
Figure B. 8 HPLC chromatogram of enantiomerically enriched 61d	137
Figure B. 9 HPLC chromatogram of <i>rac</i> - 61e	138
Figure B. 10 HPLC chromatogram of enantiomerically enriched 61e	138
Figure B. 11 HPLC chromatogram of <i>rac</i> - 61f	139
Figure B. 12 HPLC chromatogram of enantiomerically enriched 61f	139
Figure B. 13 HPLC chromatogram of <i>rac</i> - 61g	140
Figure B. 14 HPLC chromatogram of enantiomerically enriched 61g	140
Figure B. 15 HPLC chromatogram of <i>rac</i> - 61h	141
Figure B. 16 HPLC chromatogram of enantiomerically enriched 61h	141
Figure B. 17 HPLC chromatogram of <i>rac</i> - 61i	142
Figure B. 18 HPLC chromatogram of enantiomerically enriched 61i	142
Figure B. 19 HPLC chromatogram of <i>rac</i> - 61j	143
Figure B. 20 HPLC chromatogram of enantiomerically enriched 61j	143
Figure B. 21 HPLC chromatogram of <i>rac</i> - 61k	144
Figure B. 22 HPLC chromatogram of enantiomerically enriched 61k	144
Figure B. 23 HPLC chromatogram of <i>rac</i> - 61l	145
Figure B. 24 HPLC chromatogram of enantiomerically enriched 61l	145
Figure B. 25 HPLC chromatogram of <i>rac</i> - 61m	146
Figure B. 26 HPLC chromatogram of enantiomerically enriched 61m	146
Figure B. 27 HPLC chromatogram of <i>rac</i> - 61n	147
Figure B. 28 HPLC chromatogram of enantiomerically enriched 61n	147
Figure B. 29 HPLC chromatogram of <i>rac</i> - 61o	148
Figure B. 30 HPLC chromatogram of enantiomerically enriched 61o	148
Figure B. 31 HPLC chromatogram of <i>rac</i> - 61p	149
Figure B. 32 HPLC chromatogram of enantiomerically enriched 61p	149
Figure B. 33 HPLC chromatogram of <i>rac</i> - 61q	150
Figure B. 34 HPLC chromatogram of enantiomerically enriched 61q	150

Figure B. 35 HPLC chromatogram of <i>rac-61r</i>	151
Figure B. 36 HPLC chromatogram of enantiomerically enriched 61r	151
Figure B. 37 HPLC chromatogram of <i>rac-61s</i>	152
Figure B. 38 HPLC chromatogram of enantiomerically enriched 61s	152
Figure B. 39 HPLC chromatogram of <i>rac-61t</i>	153
Figure B. 40 HPLC chromatogram of enantiomerically enriched 61t	153
Figure B. 41 HPLC chromatogram of <i>rac-61u</i>	154
Figure B. 42 HPLC chromatogram of enantiomerically enriched 61u	154
Figure B. 43 HPLC chromatogram of <i>rac-61v</i>	155
Figure B. 44 HPLC chromatogram of enantiomerically enriched 61v	155
Figure B. 45 HPLC chromatogram of <i>rac-63a</i>	156
Figure B. 46 HPLC chromatogram of enantiomerically enriched 63a	156
Figure B. 47 HPLC chromatogram of <i>rac-63b</i>	157
Figure B. 48 HPLC chromatogram of enantiomerically enriched 63b	157
Figure B. 49 HPLC chromatogram of <i>rac-63c</i>	158
Figure B. 50 HPLC chromatogram of enantiomerically enriched 63c	158
Figure B. 51 HPLC chromatogram of <i>rac-63d</i>	159
Figure B. 52 HPLC chromatogram of enantiomerically enriched 63d	159
Figure B. 53 HPLC chromatogram of <i>rac-84</i>	160
Figure B. 54 HPLC chromatogram of enantiomerically enriched 84	160
Figure B. 55 HPLC chromatogram of <i>rac-81</i>	161
Figure B. 56 HPLC chromatogram of enantiomerically enriched 81	161
Figure B. 57 HPLC chromatogram of <i>rac-66a</i>	162
Figure B. 58 HPLC chromatogram of enantiomerically enriched 66a	162
Figure B. 59 HPLC chromatogram of <i>rac-66b</i>	163
Figure B. 60 HPLC chromatogram of enantiomerically enriched 66b	163
Figure B. 61 HPLC chromatogram of <i>rac-66c</i>	164
Figure B. 62 HPLC chromatogram of enantiomerically enriched 66c	164
Figure B. 63 HPLC chromatogram of <i>rac-66d</i>	165
Figure B. 64 HPLC chromatogram of enantiomerically enriched 66d	165

Figure B. 65 HPLC chromatogram of <i>rac</i> - 66f	166
Figure B. 66 HPLC chromatogram of enantiomerically enriched 66f	166
Figure B. 67 HPLC chromatogram of <i>rac</i> - 66g	167
Figure B. 68 HPLC chromatogram of enantiomerically enriched 66g	167
Figure B. 69 HPLC chromatogram of <i>rac</i> - 66k	168
Figure B. 70 HPLC chromatogram of enantiomerically enriched 66k	168
Figure B. 71 HPLC chromatogram of <i>rac</i> - 66l	169
Figure B. 72 HPLC chromatogram of enantiomerically enriched 66l	169
Figure B. 73 HPLC chromatogram of <i>rac</i> - 66m	170
Figure B. 74 HPLC chromatogram of enantiomerically enriched 66m	170
Figure B. 75 HPLC chromatogram of <i>rac</i> - 66n	171
Figure B. 76 HPLC chromatogram of enantiomerically enriched 66n	171
Figure B. 77 HPLC chromatogram of <i>rac</i> - 66o	172
Figure B. 78 HPLC chromatogram of enantiomerically enriched 66o	172
Figure B. 79 HPLC chromatogram of <i>rac</i> - 66r	173
Figure B. 80 HPLC chromatogram of enantiomerically enriched 66r	173
Figure B. 81 HPLC chromatogram of <i>rac</i> - 66u	174
Figure B. 82 HPLC chromatogram of enantiomerically enriched 66u	174
Figure B. 83 HPLC chromatogram of <i>rac</i> - 66w	175
Figure B. 84 HPLC chromatogram of enantiomerically enriched 66w	175
Figure B. 85 HPLC chromatogram of <i>rac</i> - 66x	176
Figure B. 86 HPLC chromatogram of enantiomerically enriched 66x	176
Figure B. 87 HPLC chromatogram of <i>rac</i> - 67a	177
Figure B. 88 HPLC chromatogram of enantiomerically enriched 67a	177
Figure B. 89 HPLC chromatogram of <i>rac</i> - 67f	178
Figure B. 90 HPLC chromatogram of enantiomerically enriched 67f	178
Figure B. 91 HPLC chromatogram of <i>rac</i> - 67g	179
Figure B. 92 HPLC chromatogram of enantiomerically enriched 67g	179
Figure B. 93 HPLC chromatogram of <i>rac</i> - 67o	180
Figure B. 94 HPLC chromatogram of enantiomerically enriched 67o	180

LIST OF SCHEMES

SCHEMES

Scheme 1.1. The work of Bredig & Fiske: The first example of asymmetric organocatalysis.....	5
Scheme 1.2. Pioneering work of Hiemstra and Wynberg.....	7
Scheme 1.3. Rawal's pioneering work on asymmetric conjugate addition with chiral squaramide catalyst.....	7
Scheme 1.4. The sulfonamide/quinine catalytic system of Song and co-workers....	9
Scheme 1.5. The first attempt for asymmetric sulfa-Michael addition.....	10
Scheme 1.6. Asymmetric SMA of benzylthiol with cinchona alkaloids as organocatalysts.....	11
Scheme 1.7. Asymmetric SMA of thiols to 2-cyclohexene-1-one	12
Scheme 1.8. Selected works on asymmetric organocatalytic sulfa-Michael addition	13
Scheme 1.9. General synthesis methods for 1,4-benzothiazepin-2-ones.....	14
Scheme 1.10. The general synthetic route for sulfones	16
Scheme 1.11. Synthetic pathway for the SMA of methyl thioglycolate to chalcones and generation of 1,4-benzothiazepin-2-one.....	18
Scheme 1.12. Synthetic pathway for the SMA of 1-thionaphthol to chalcones and subsequent oxidation.....	18
Scheme 2.1. Synthesis of aminoDMAP derived bifunctional organocatalysts	19
Scheme 2.2. Synthesis of quinine derived bifunctional organocatalysts	21
Scheme 2.3. Synthetic route for <i>trans</i> -chalcone derivatives.....	22
Scheme 2.4. The proposed transition state model for SMA of methyl thioglycolate to <i>trans</i> -chalcone derivatives	26
Scheme 2.5. SMA of cinnamoyl benzotriazole with methyl thioglycolate under optimized conditions	32
Scheme 2.6. Updated pathway to obtain 84	32

Scheme 2.7. Reduction of amino chalcone and transformation to 2-phenylquinoline	33
Scheme 2.8. Dithiolane protection of the 2-nitro substituted sulfa-Michael adduct 61s	34
Scheme 2.9. Synthesis of chiral 1,4-benzothiazepin-2-one.....	34
Scheme 2.10. Proposed transition state for the SMA of 1-thionaphthol to <i>trans</i> -chalcones	39

LIST OF ABBREVIATIONS

ABBREVIATIONS

ATR	attenuated total reflectance
DIAD	diisopropyl azodicarboxylate
DPPA	diphenylphosphoryl azide
MALDI	matrix-assisted laser desorption/ionization
SMA	sulfa-Michael addition
SOMO	singly occupied molecular orbital
TOF	time-of-flight

CHAPTER 1

INTRODUCTION

1.1 Sulfur Containing Drugs

Sulfur is an important element in biological systems. Because of the ability of sulfur containing compounds to exhibit a large variety of biological activities, they have long been used in pharmaceutical industry. By 2016, the most abundant heteroatom (excluding nitrogen and oxygen) in the drug market was sulfur, with 362 FDA approved sulfur derived drugs.¹

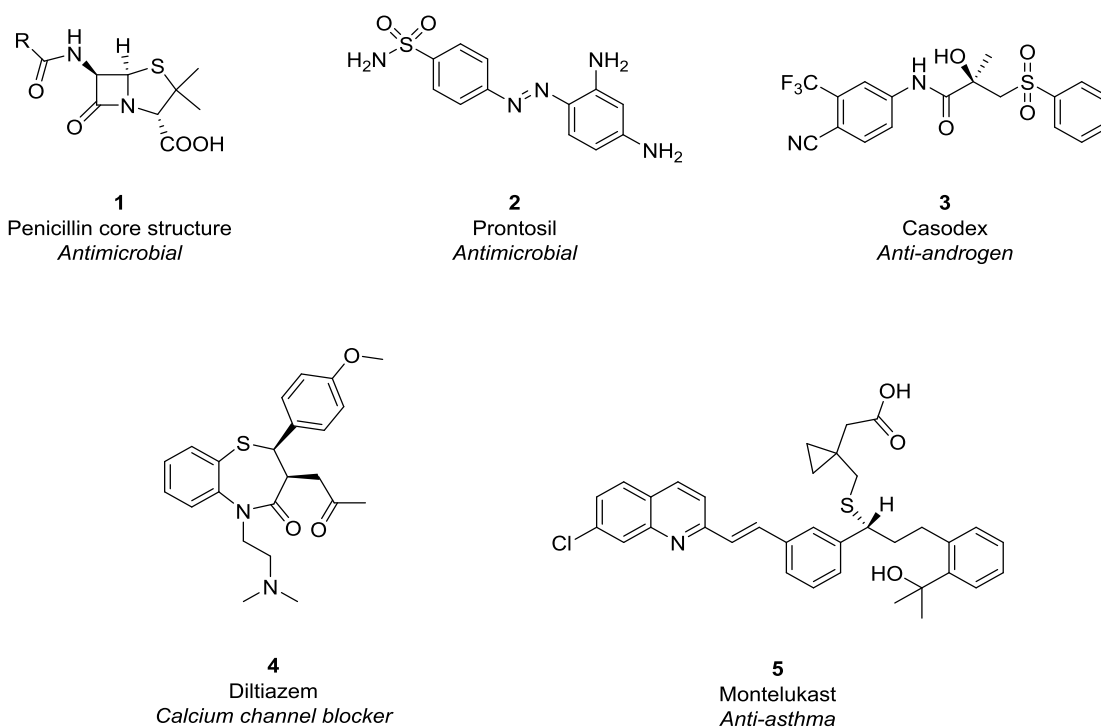


Figure 1.1. Structures of selected sulfur containing drug molecules

Penicillin (1),² the pioneering antibiotic for the treatment of bacterial infections has a thiazolidine ring in its core structure. After the impact of penicillin, sulfonamides

emerged as the first systematically administered antibiotics with Prontosil (**2**) being the first of the class.³ Casodex (**3**), a sulfone derived drug, is an anti-androgen which is used in the treatment of prostate cancer.⁴ Thioethers are another class of drugs with a wide range of biological activities; Diltiazem (**4**)⁵ is known for its use as a calcium channel blocker to treat cardiovascular diseases and Montelukast (**5**)⁶ is a successful drug for the treatment of seasonal allergies and asthma. (Figure 1.1).

1.2 The Importance of Asymmetric Synthesis

Life is chiral; 19 of the amino acids that make up our bodies and govern the processes ongoing in our bodies are chiral. Therefore, our physiological response to individual stereoisomers of optically active compounds are different. For instance, (*R*)-(-)-linalool (**6**) is the compound that gives lavender its characteristic woody-floral aroma that we all know. On the other hand, (*S*)-(+)-linalool (**7**) odor is perceived as bitter or sour orange (Figure 1.2).⁷

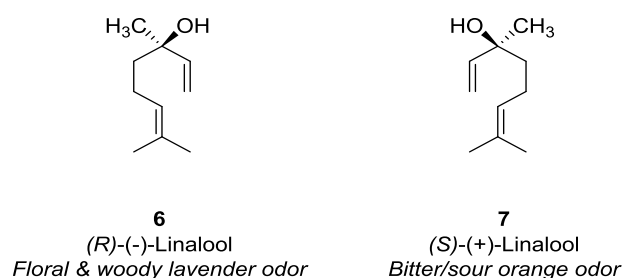


Figure 1.2. Structures and odors of linalool enantiomers

In a similar manner, despite their physical and chemical properties being the same in achiral media, a patient's physiology can react differently to the two enantiomers of a chiral drug. The (*S*)-isomer of the well-known anti-inflammatory drug ibuprofen (Figure 1.3) is over 100 times more potent than the (*R*)-isomer.⁸ In some cases, one enantiomer of the drug molecule can even be toxic, while the other has the desired therapeutic effect. D-Penicillamine is used in the treatment of Wilson's disease by working as a chelating agent. L-Penicillamine, on the other hand, can lead to

blindness by causing the inflammation of the optic nerve (Figure 1.3).⁹ By 2006, chiral drugs were composing more than half of the commercial drugs,¹⁰ and some of the chiral drugs that had been previously marketed as racemates have been switched with their single enantiomers in the last decades.¹¹ Due to the possible biological activity differences between the enantiomers of the drug molecule, the enantiopurity of those single-enantiomer drugs should be strictly controlled.

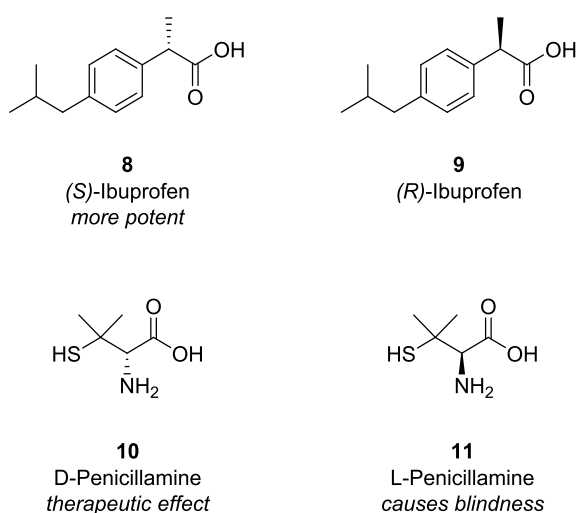


Figure 1.3. Structures of ibuprofen and penicillamine enantiomers

A group of Japanese scientists worked on the statistics of chiral drug market and drug development in Japan. According to their paper published in 2008,¹² 76 new drugs were approved between January 2001 and July 2003. 61% of those drugs were chiral and only a 13% portion was marketed as a racemic mixture. Their study also showed that, only 8% of the single-enantiomer drugs were developed through asymmetric synthesis; a technique which involves the synthetic pathways that favors the formation of one stereoisomer over the other. Other means of obtaining those molecules include starting from the single enantiomer of a chiral starting material (78%), and resolution of the racemic reaction mixture of a non-stereoselective pathway (18%). Undoubtedly, asymmetric synthesis did come far in the past 16 years and currently it is the most powerful tool for obtaining enantiopure or

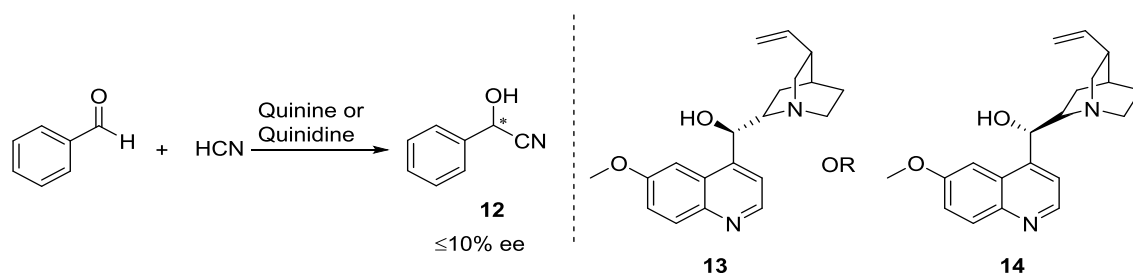
enantioenriched compounds.¹³ However, there is still a demand for the development of new and more efficient asymmetric synthesis methods, and the subject remains as a hot topic in organic synthesis.

1.3 Asymmetric Organocatalysis

Among the techniques to obtain enantioenriched organic molecules, catalytic asymmetric synthesis methods are superior over other means of asymmetric synthesis. Due to the use of a substoichiometric amount of a chiral catalyst to bring about the desired enantioselective transformation, it is an atom economic method compared to the methods that use chiral auxiliaries or stoichiometric amount of catalysts.¹⁴ The catalyst chosen for asymmetric catalysis can be either an enzyme or a biocatalyst, a transition metal complex with chiral ligands or an organocatalyst. Biocatalytic methods present with limitations due to the single-handedness of nature. Transition metal catalysis comes with the issue of metal toxicity, which may require special disposal methods due to environmental concerns, or it may pose a serious health concern especially in the synthesis of drug molecules if traces of the catalyst remain. Moreover, transition metal complexes can be susceptible to moisture and air. Compared with the two aforementioned methods, organocatalysts are relatively inexpensive, non-toxic, more resistant to air and moisture; so that they do not require inert atmosphere, easily obtained and designed without resorting to complicated synthetic procedures.¹⁵

Although it is widely accepted that MacMillan¹⁶ invented the term “Organocatalysis”, the concept was first introduced as “Organic Catalysis” in 1935 by Wolfgang Langenbeck.¹⁷ However, the earliest example of asymmetric organocatalysis goes back to 1912; to the work of Bredig and Fiske (Scheme 1.1).¹⁸ In the work, the chiral cyanohydrin **12** was synthesized with up to of 10% ee by the reaction of benzaldehyde with hydrogen cyanide in the presence of cinchona alkaloids quinine (**13**) or quinidine (**14**). Despite this unsatisfactory result, the work served as the basis of asymmetric organocatalysis. The real interest in the field began to increase exponentially after the publication of two pioneering works by List,

Lerner and Barbas¹⁹ (on proline catalyzed asymmetric aldol reactions); and MacMillan¹⁶ (iminium catalyzed asymmetric Diels-Alder reaction).



Scheme 1.1. The work of Bredig & Fiske: The first example of asymmetric organocatalysis

Organocatalysts for asymmetric transformations can be classified into two broad categories based on the interactions they undergo with the substrates: Covalent and non-covalent catalysis (Figure 1.4).²⁰

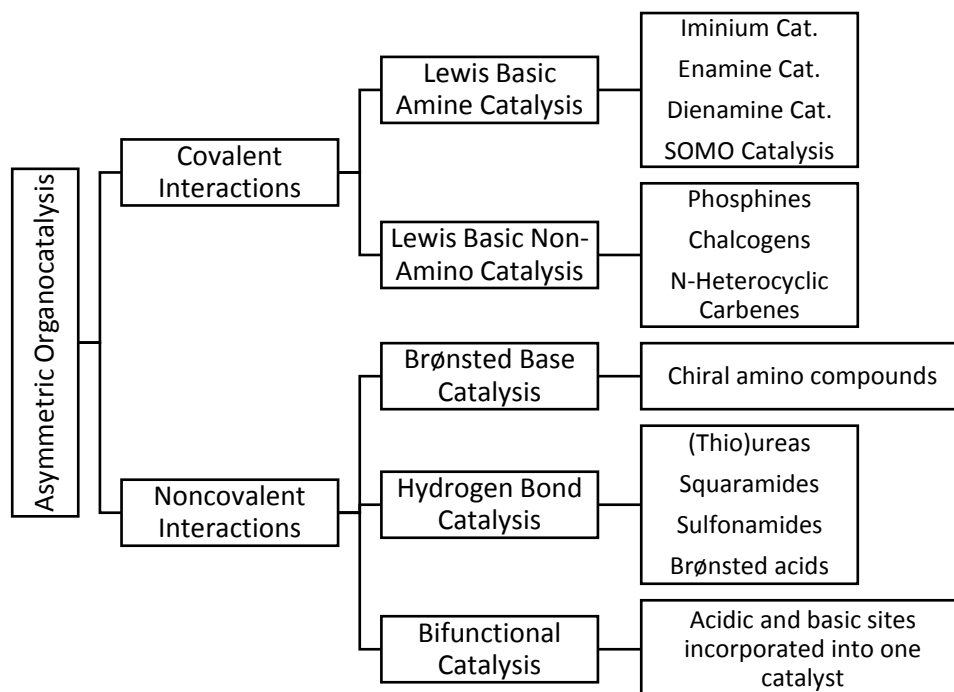


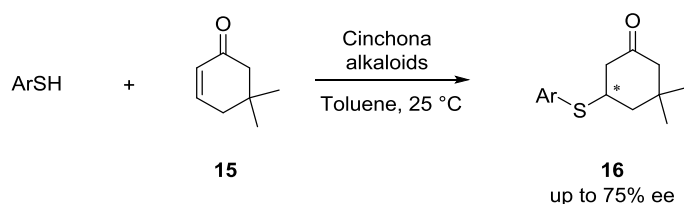
Figure 1.4. Classes and modes of activation of asymmetric organocatalysts

A special class of organocatalysts with a noncovalent activation mode deserves recognition; “bifunctional catalysts” possess both acidic and basic units.²¹ Urea,²² thiourea,²³ guanidine,²⁴ sulfonamide²⁵ and squaramide²⁶ moieties are some of the powerful acidic parts credited in the literature. Those acidic units can act as H-bond donors, which in turn, activate the electrophile. The nucleophile is activated via complete or partial deprotonation by the Lewis/Brønsted basic units. Remarkable results were obtained in the literature with DMAP,²⁷ cyclohexyldiamine²⁸ and cinchona alkaloid derived²⁹ catalysts. The acidic and basic units are linked together with chiral spacer to induce enantioselectivity.

1.3.1 Cinchona Alkaloids as a Motif in Bifunctional Organocatalysis

Cinchona alkaloids are a family of naturally occurring compounds isolated from the bark of *cinchona officinalis* plants.³⁰ The members of this family are considered as one of the most attractive organocatalysts due to their low cost, availability and the ease of modification by incorporating acidic units to obtain structures that allow bifunctional mode of activation.

Although cinchona alkaloids were known to catalyze asymmetric transformations via the activation of the nucleophile by its quinuclidine moiety,¹⁸ the most influential paper on the family was Hiemstra and Wynberg’s work published in 1981.³¹ The work consists of the addition of aromatic thiols to cyclic enones in the presence of cinchona alkaloids as organocatalysts with enantioselectivities up to 75% ee. Although their ee’s were moderate at best, this work is regarded as a pioneer in asymmetric organocatalysis due to the elaborate investigation of thermodynamic parameters and thorough screening studies (Scheme 1.2).

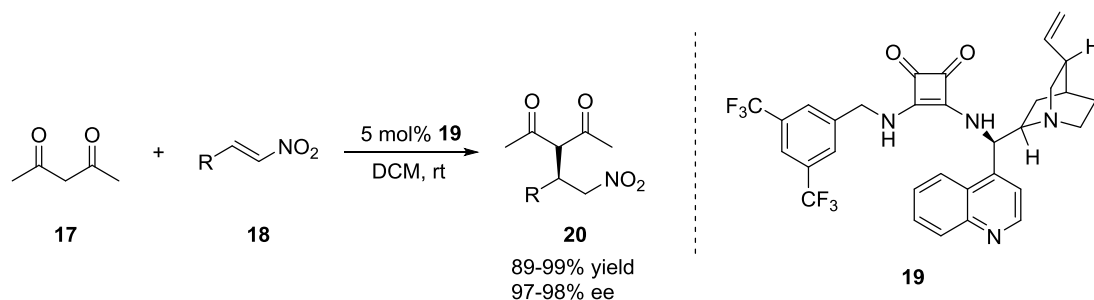


Scheme 1.2. Pioneering work of Hiemstra and Wynberg

Quinine is a member of the cinchona alkaloid family and has outstanding applications as an important moiety in organocatalysts. After quinine was adapted to the dual activation mode of bifunctional organocatalysts by the incorporation of acidic units, the reaction and substrate scope of quinine derived organocatalysts increased exponentially. In this work, the best catalysts for systems under investigation are quinine derived sulfonamide and squaramide. Thus, the next part of the literature will focus on sulfonamide and squaramide functionalized cinchona alkaloid-derived organocatalysts.

1.3.1.1 Squaramides

Squaramides were first introduced as organocatalysts by Rawal and co-workers in 2008.³² Their sulfonamide/cinchonine catalyst **19** gave excellent results in the asymmetric conjugate addition of β -dicarbonyl compounds to nitrostyrene derivatives (Scheme 1.3).



Scheme 1.3. Rawal's pioneering work on asymmetric conjugate addition with chiral squaramide catalyst

Squaramide derivatives are claimed to be superior organocatalysts for asymmetric reactions than corresponding ureas and thioureas in terms of rigidity and H-bond dynamics; compared to (thio)ureas, squaramides have an extended conjugation throughout the dione moiety (Figure 1.5), resulting in a more rigid structure and therefore limited degree of conformational changes. In addition, the acidity of the NH hydrogens is greater in squaramides, leading to stronger H-bonds.³³ When Rawal's group compared the distance between the two NH hydrogens of thiourea and squaramide by using the crystallographic data and computational methods, they found that the spacing for squaramide is 2.72 Å, which was 0.6 Å greater than of thiourea. They interpret this finding as an evidence for better H-bonding in the case of squaramides.

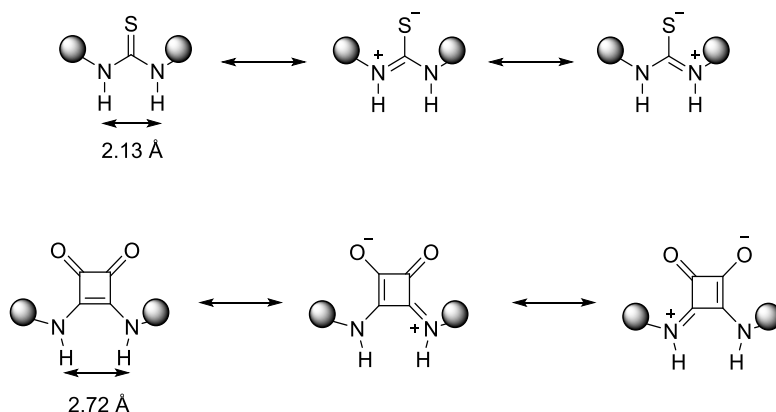


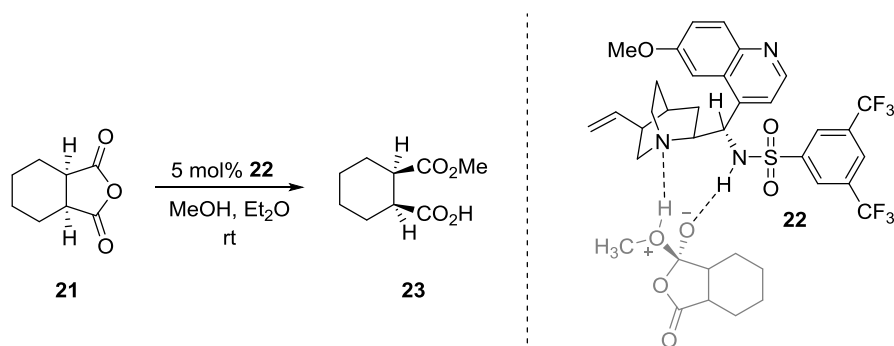
Figure 1.5. Comparison of resonance structures and distances between the hydrogens of thiourea and squaramide moieties

Since this successful entry of squaramides in the realm of organocatalysis, it attracted tremendous interest and have been employed in a large variety of asymmetric transformations.³⁴

1.3.1.2 Sulfonamides

The first quinine derived sulfonamide organocatalyst was developed by Song and co-workers in 2008,³⁵ as an alternative catalytic system to (thio)ureas for the

methanolytic desymmetrization of cyclic anhydrides. The latter system was found to be vulnerable, since intermolecular H-bonding between the NH groups and sulfur/oxygen atom of (thio)ureas could lead to aggregation or dimerization of the catalyst, hindering its activity. Their newly designed catalyst was not only more thermally stable than (thio)ureas, but also allowed the group to attain 95% ee for the desired product (Scheme 1.4). According to the transition state model they suggested by computational approach, the quinuclidine moiety activates methanol by acting as a general base, while the sulfonamide part stabilizes the newly forming oxyanion by H-bonding.



Scheme 1.4. The sulfonamide/quinine catalytic system of Song and co-workers

Not long after Song's group published this new type of organocatalyst, many successful examples employing sulfonamides were added to the literature³⁶ and sulfonamides continue to be a desired scaffold for asymmetric bifunctional organocatalysis.

1.4 Sulfa-Michael Addition Reactions

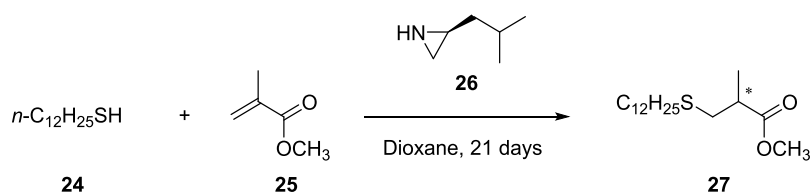
The ultimate goal in synthetic organic chemistry is to form more complex structures from small building blocks via formation of new carbon-carbon bonds. To achieve this, one of the most indispensable tools is Michael reaction, in which a carbanion is added to an α,β -unsaturated carbonyl compound in a conjugate manner. Variants of Michael addition were developed over the years to extend the reaction scope in order

to form new carbon-heteroatom bonds by the use of heteroatom-centered nucleophiles.³⁷ Sulfa-Michael (also mentioned as thia-Michael or thio-Michael in the literature) addition reaction is a variant of Michael reaction, in which a sulfur-centered nucleophile is employed as the donor, rather than a carbanion.³⁸ It is a frequently sought method for the incorporation of carbon-sulfur bonds to the substrates, thanks to the large variety of possible donor and acceptor systems available.

1.4.1 Asymmetric Sulfa-Michael Addition Reactions

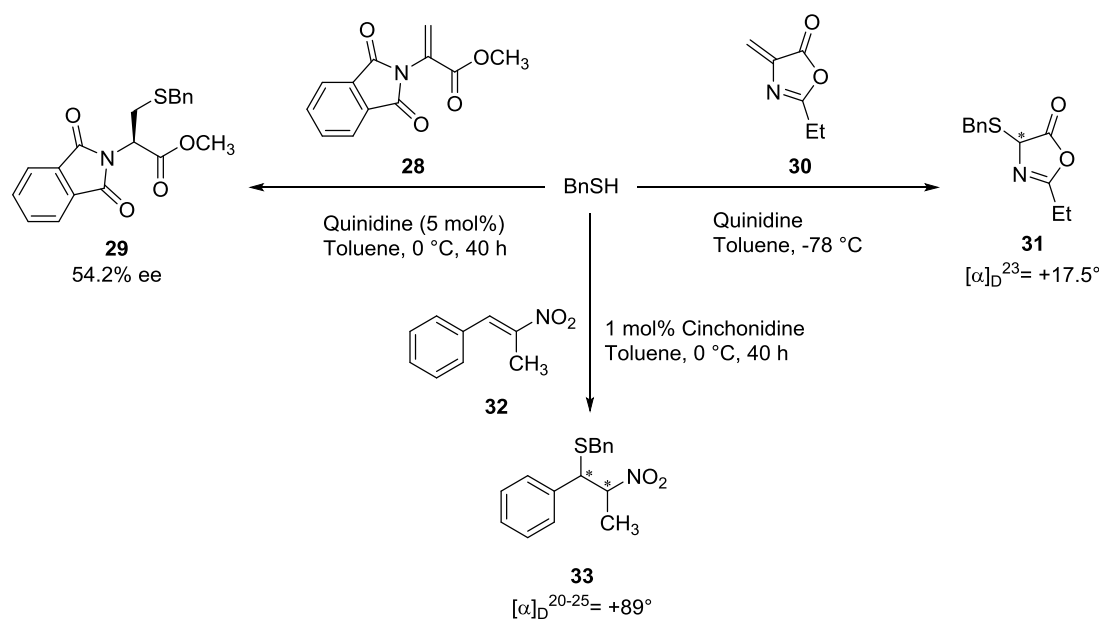
Due to the nature of α,β -unsaturated carbonyl compounds, sulfa-Michael addition (SMA) allows the formation of new stereocenters, which makes SMA a reaction of interest for asymmetric catalysis.³⁹

The first attempt for asymmetric SMA in the literature was the preliminary study of the development of polymeric catalyst systems for the polyaddition of dithiols to bis(enones).⁴⁰ To evaluate the reactivity of their substrates, Inoue and co-workers first carried out a model reaction with lauryl mercaptan (**24**) and methyl methacrylate (**25**), in the presence of poly *S*-isobutylethyleneimine monomer (**26**) as the catalyst to induce stereoselectivity (Scheme 1.5). After observing a nonzero specific rotation for the product solution as the proof of asymmetry, they proceeded to the polyaddition with poly *S*-isobutylethyleneimine as the catalyst. Then the group turned their interest completely toward polyadditions and adding thiols to unsaturated polymers in the following decade.



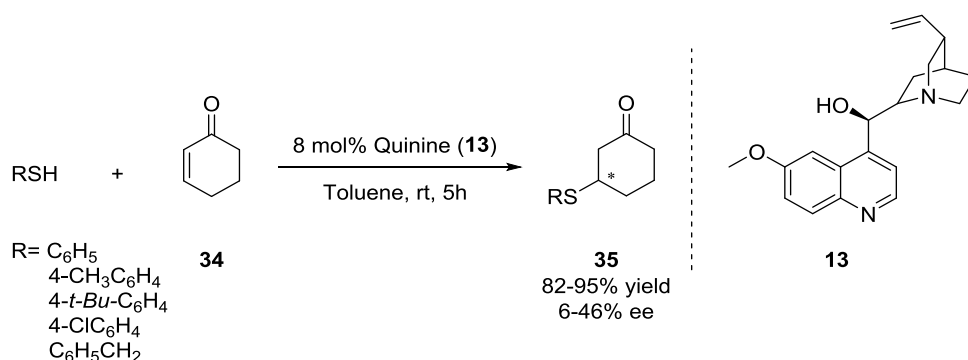
Scheme 1.5. The first attempt for asymmetric sulfa-Michael addition

Asymmetric organocatalytic SMA in a more conventional sense was published by Pracejus⁴¹ and Helder⁴² concurrently in 1977. Inspired by the works of Inoue, Pracejus and co-workers focused on the addition of thiols to methyl α -phthalimidoacrylate (**28**), 2-ethyl-4-methylene-1,3-oxazolin-5-one (**30**) and nitrostyrene derivatives (**32**) by using a number of cinchona alkaloids as organocatalysts (Scheme 1.6). The target enantioenriched products were obtained with low to moderate selectivities.



Scheme 1.6. Asymmetric SMA of benzylthiol with cinchona alkaloids as organocatalysts

Helder's asymmetric SMA study consists of the reaction of thiols with 2-cyclohexene-1-one (**34**), in the presence of quinine (**13**) (Scheme 1.7). Although neither study shows a striking stereinduction with the selected systems, they were the pioneers of a field which would attract the interest of synthetic chemists for decades to come.



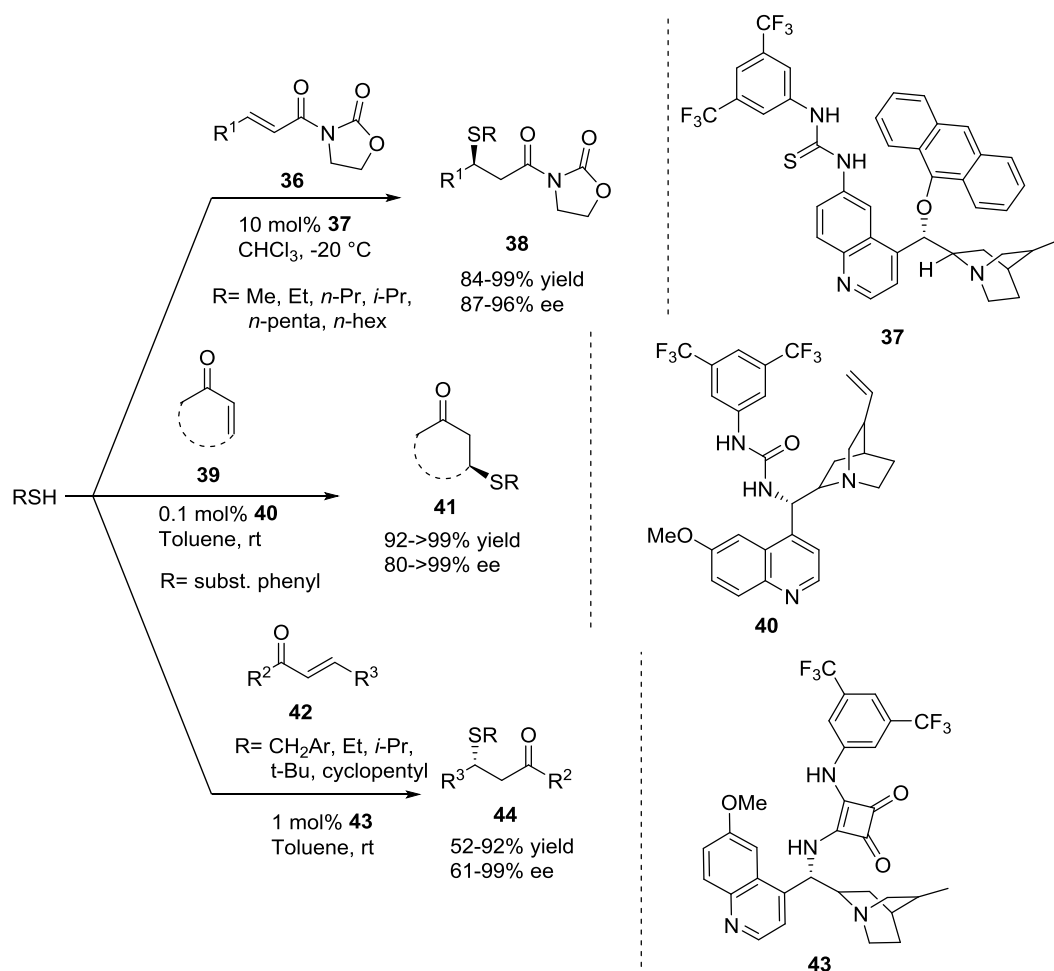
Scheme 1.7. Asymmetric SMA of thiols to 2-cyclohexene-1-one

Since then, many examples of asymmetric SMA reactions were added to the literature that employs different thiols to react with a large variety of enones.

Despite the interest, asymmetric SMA reactions still remain relatively less explored, compared to other asymmetric transformations. The main challenge of SMA is the high nucleophilic power of sulfur, compared to carbon and other commonly studied heteroatoms, causing a high rate of background reaction. In other words, due to the high nucleophilicity of the donor, the reaction can occur even without the presence of a chiral catalyst, which will result in no stereoselectivity. To suppress this undesired background reaction, low temperatures and/or high catalyst loadings are generally employed.⁴³ Liu et al.^{43b} demonstrated the addition of thiols to α,β -unsaturated *N*-acylated oxazolidine-2-ones **36** with a cinchona alkaloid derived thiourea catalyst **37** with 87-96% ee. But this high result demanded a relatively high (10 mol%) catalyst loading and low temperatures (-20 °C) (Scheme 1.8). The studies which employ mild conditions and low catalyst loading use thiophenol derivatives or simple alkyl thiols as nucleophiles.⁴⁴ Rana and co-workers attained excellent ee's with a very low quinine derived urea catalyst **40** for the SMA of simple substituted thiophenols and cyclic enones (Scheme 1.8).^{44b}

Being a versatile pharmacophore itself, *trans*-chalcone is an important core for the synthesis of biologically active compounds.⁴⁵ Despite being an α,β -unsaturated compound, it is not a very good Michael acceptor, relatively.⁴⁶ Consequently, sulfa-

Michael additions to chalcones are less studied than other electrophiles. In 2010, Dai et al.^{44c} investigated the SMA of simple alkyl thiols to *trans*-chalcone derivatives. With a low (1 mol%) loading of quinine/squaramide catalyst **43**, they obtained the target thioethers **44** with moderate to excellent (61-99%) ee's (Scheme 1.8).



Scheme 1.8. Selected works on asymmetric organocatalytic sulfa-Michael addition

As nucleophiles, thionaphthols and thioglycolic esters, however, are overlooked in sulfa-Michael addition reactions. To our best knowledge, no study is present concerning the organocatalytic asymmetric SMA of 1-thionaphthol to chalcones. Thus, they are chosen to be investigated within this thesis. The enantioselective reaction of methyl thioglycolate with *trans*-chalcones were explored only with

catalytic methods that employ $\text{La}(\text{OTf})_3$.⁴⁷ Considering the striking advantages organocatalysis offer in asymmetric reactions over organometallic catalysts, the aforementioned system has been studied as another part of this thesis.

1.5 1,4-Benzothiazepin-2-ones

Benzothiazepines are a class of organic heterocyclic compounds that contain nitrogen and sulfur in their 7-membered rings. 1,4-Benzothiazepin-2-one, a member of the aforementioned class, has a proven inhibitory effect against mitochondrial Na^+ - Ca^{2+} exchanger (mNCE),⁴⁸ which is crucial in cell metabolism. Regulation of the Na^+ - Ca^{2+} in the cell also allows the neuroprotection of the cell, which was tested with the benzothiazepine derivative CGP-37151 (**45**) (Figure 1.6) on *C. elegans* worms. The study showed that CGP-37151 is effective for lengthening the lifespan of the worms.⁴⁹ Inhibition of mNCE also affects the insulin secretion mechanism. Pei et al. demonstrated that the 1,4-benzothiazepin-2-one core could be utilized in the treatment of type II diabetes.⁵⁰

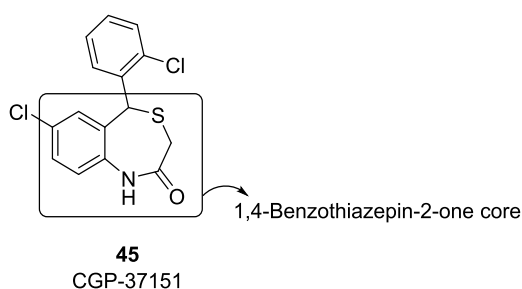
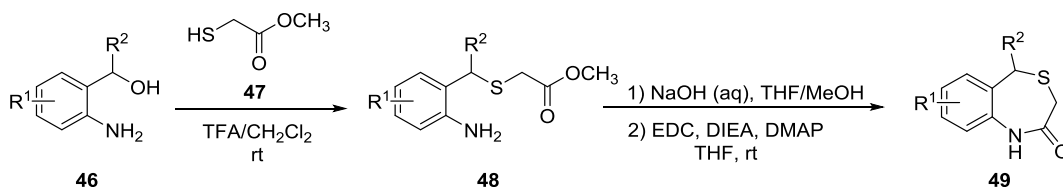


Figure 1.6. Structure of CGP-37151 and its benzothiazepine core

The general strategy for the synthesis of 1,4-benzothiazepin-2-ones **49** are outlined below in Scheme 1.9.⁵⁰



Scheme 1.9. General synthesis methods for 1,4-benzothiazepin-2-ones

1.6 β -Aryl- β -Sulfanyl Ketones

The general name of the sulfa-Michael addition products of aromatic thiols and chalcones are called “ β -aryl- β -sulfanyl ketones” (also 1,3-biarylsulfanyl compounds). These core motifs are regarded as estrone analogues⁵¹ and found in the structure of *seco*-raloxifene **51**. *seco*-Raloxifene is the non-cyclic bioisostere of raloxifene (**50**), which is a selective estrogen receptor modulator, employed in the treatment of osteoporosis and also has anti-proliferative activity against breast cancer cells (Figure 1.6).⁵² Study of Kumar and co-workers showed that β -aryl- β -sulfanyl ketones have potent anti-breast cancer activity, which is comparative to tamoxifen; the well-known breast cancer drug.⁵³ In addition to the aforementioned biological activities, a group of Iranian scientists showed that these motifs are also potent urease inhibitors.⁵⁴

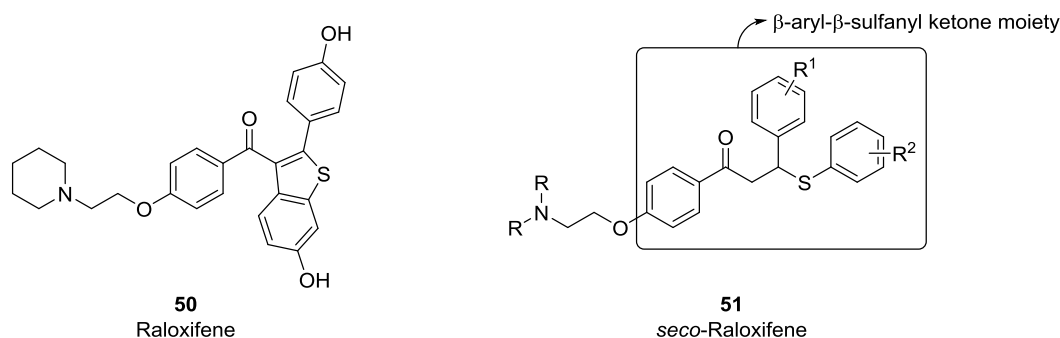


Figure 1.7. Structures of raloxifene and *seco*-raloxifene

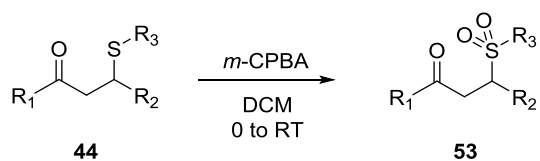
1.7 Chiral Sulfones

The most well-known sulfone drug is dapsons (**52**), which is used for the treatment of leprosy as an antibacterial (Figure 18.8).⁵⁵ Despite sulfones have been overshadowed in pharmacology by sulfonamides, they have a large array of biologic activities which may pave their way for their use as anti-HIV-1⁵⁶, anti-hepatitis C⁵⁷, antifungal,⁵⁸ acaricidal/insecticidal⁵⁹ and antimalarial agents.



Figure 1.8. The leprosy drug dapsone

Although there are several possible methods of synthesis for obtaining sulfones, the most convenient pathway is the oxidation of corresponding sulfides. As oxidants, generally peroxides, peracids or permanganates are employed (Scheme 1.10).⁶⁰ Konduru et al. studied the oxidation of racemic chalcone-based sulfides to corresponding sulfones, which also showed promising antibacterial and antifungal activity.⁶¹



Scheme 1.10. The general synthetic route for sulfones

1.8 Aim of the Study

Sulfa-Michael addition reaction is a versatile tool for the construction of new C-S bonds. The organosulfur compounds obtained via this route can serve as building blocks for sulfur-containing drug molecules. Considering more than half of the drugs on the market are chiral, synthesizing these building blocks in an asymmetric manner is essential. In this context, this thesis focuses on the enantioselective organocatalytic sulfa-Michael addition of selected thiol compounds to *trans*-chalcones. The chiral bifunctional organocatalysts designed for this purpose (Figure 1.9) were synthesized in the first part of this work.

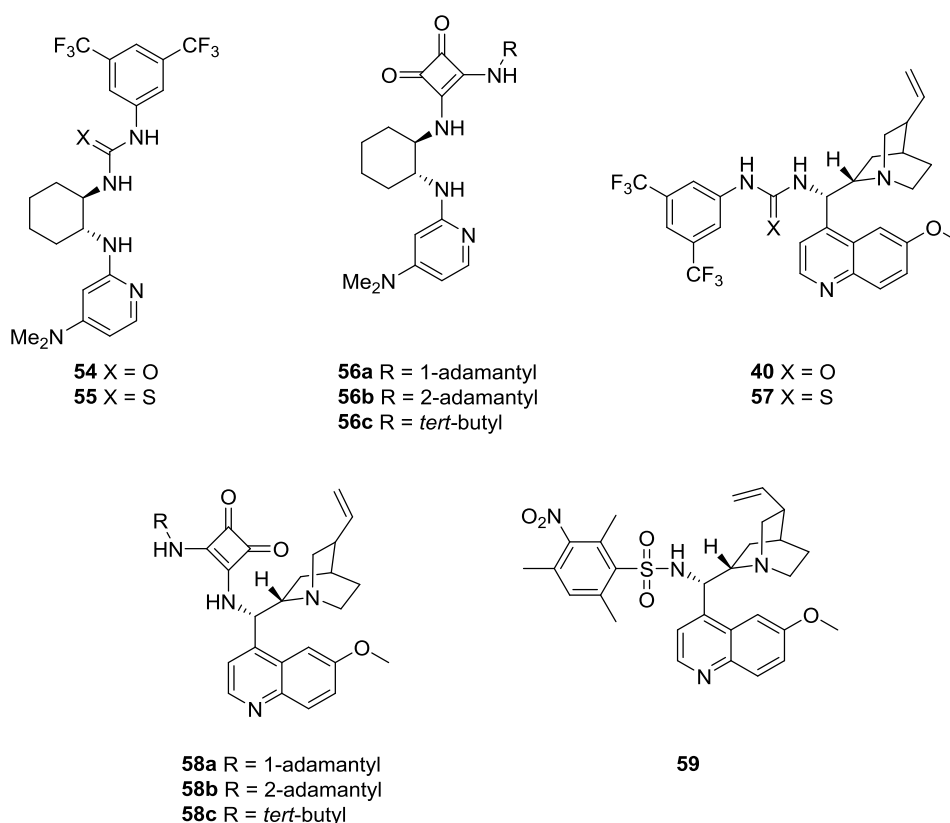
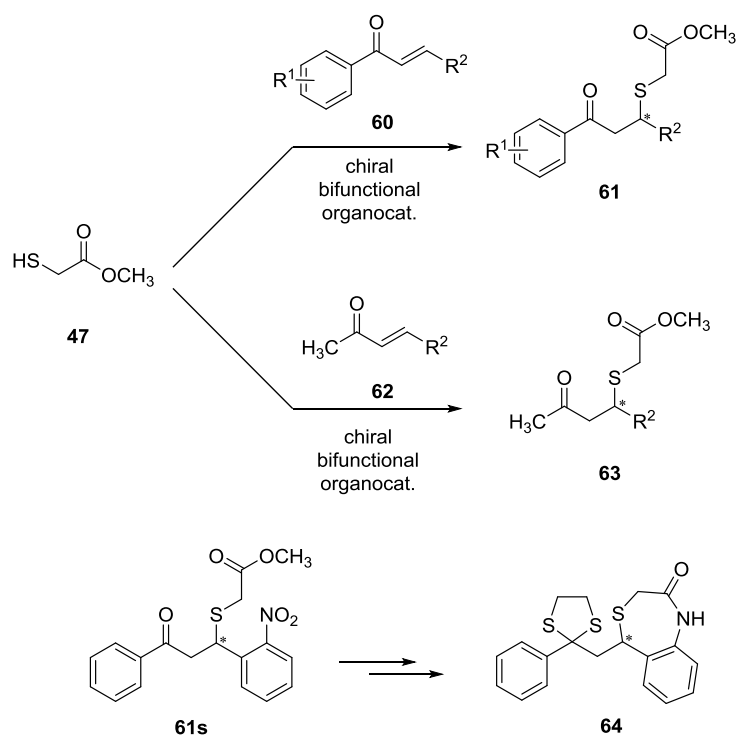


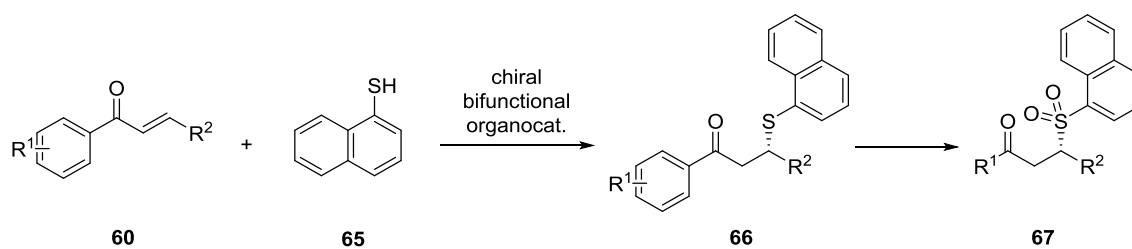
Figure 1.9. Structures of organocatalysts

In the second part of the thesis, these catalysts were surveyed in the enantioselective SMA of methyl thioglycolate (**47**) to *trans*-chalcones **60**. Among the chalcone derivatives chosen for this transformation, 2-amino substituted derivative **61s** was selected to carry out a model reaction towards the synthesis of chiral and enantiomerically rich 1,4-benzothiazepin-2-one motif **64**. Despite the significant biological activity of this motif, synthesis of their chiral counterparts had not been previously explored (Scheme 1.11).



Scheme 1.11. Synthetic pathway for the SMA of methyl thioglycolate to chalcones and generation of 1,4-benzothiazepin-2-one

In the last part of the work, our attention was directed to the SMA of 1-thionaphthol (**65**) to *trans*-chalcone derivatives **60** to obtain biologically active β -aryl- β -sulfanyl ketones (**66**). Then we targeted the transformation of the enantiomerically rich sulfa-Michael products to the corresponding sulfones (**67**) via oxidation (Scheme 1.12).



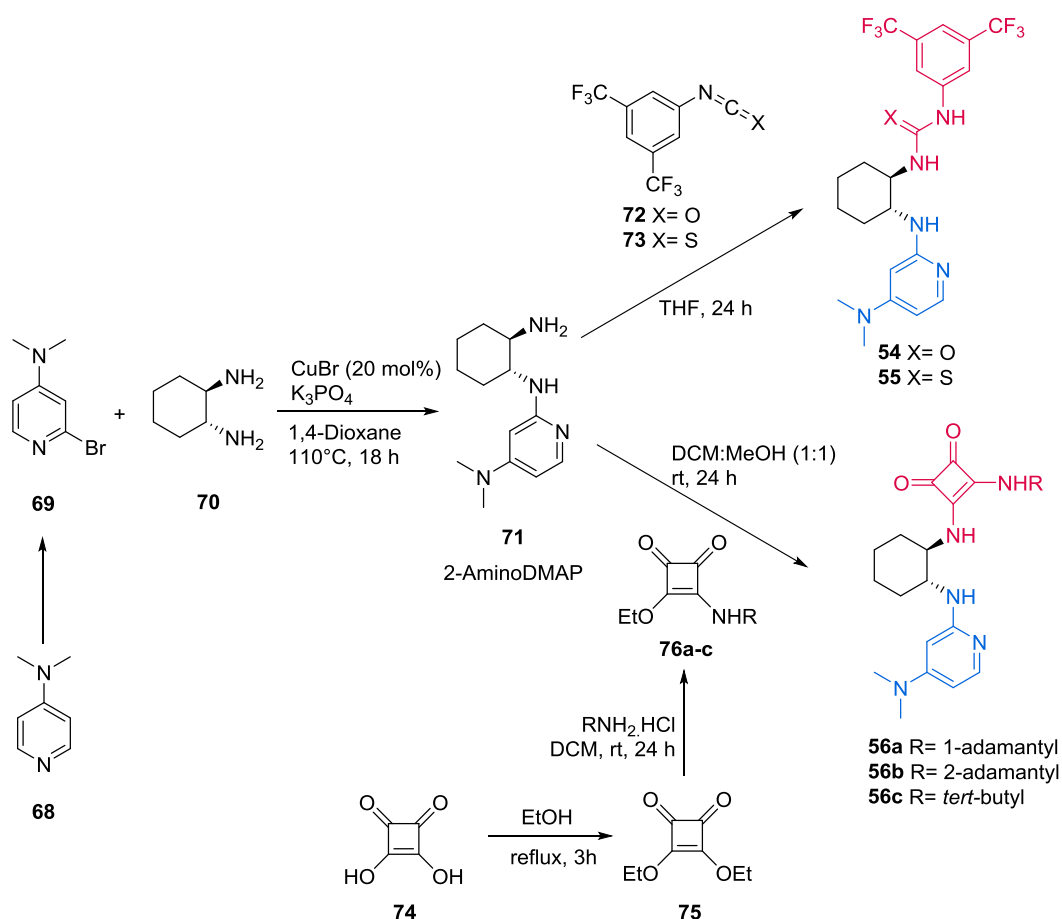
Scheme 1.12. Synthetic pathway for the SMA of 1-thionaphthol to chalcones and subsequent oxidation

CHAPTER 2

RESULTS AND DISCUSSION

2.1 Synthesis of Bifunctional Organocatalysts

The organocatalysts employed in this work can be divided into two classes as 2-aminoDMAP and quinine derived. The design and successful applications of organocatalysts having the 2-amino DMAP basic core was previously reported by our research group in the addition of 1,3-dicarbonyls to nitrostyrene derivatives.⁶²



Scheme 2.1. Synthesis of aminoDMAP derived bifunctional organocatalysts

Synthesis of 2-aminoDMAP catalysts starts from 4-dimethylaminopyridine (**68**), which is converted to the “2-bromoDMAP” unit **69**. Then this unit is tethered to the chiral spacer (*1R,2R*)-(-)-1,2-diaminocyclohexane (**70**) by the modified Ullmann coupling reaction (Scheme 2.1). The resulting “2-aminoDMAP” moiety serves as the basic unit of the catalyst. Then the acidic part is introduced to achieve the bifunctionality; to obtain urea (**54**) and thiourea type (**55**) organocatalysts, **70** is reacted with 3,5-bis(trifluoromethyl)phenyl isocyanate (**72**) or bis(trifluoromethyl)phenyl isothiocyanate (**73**), respectively.

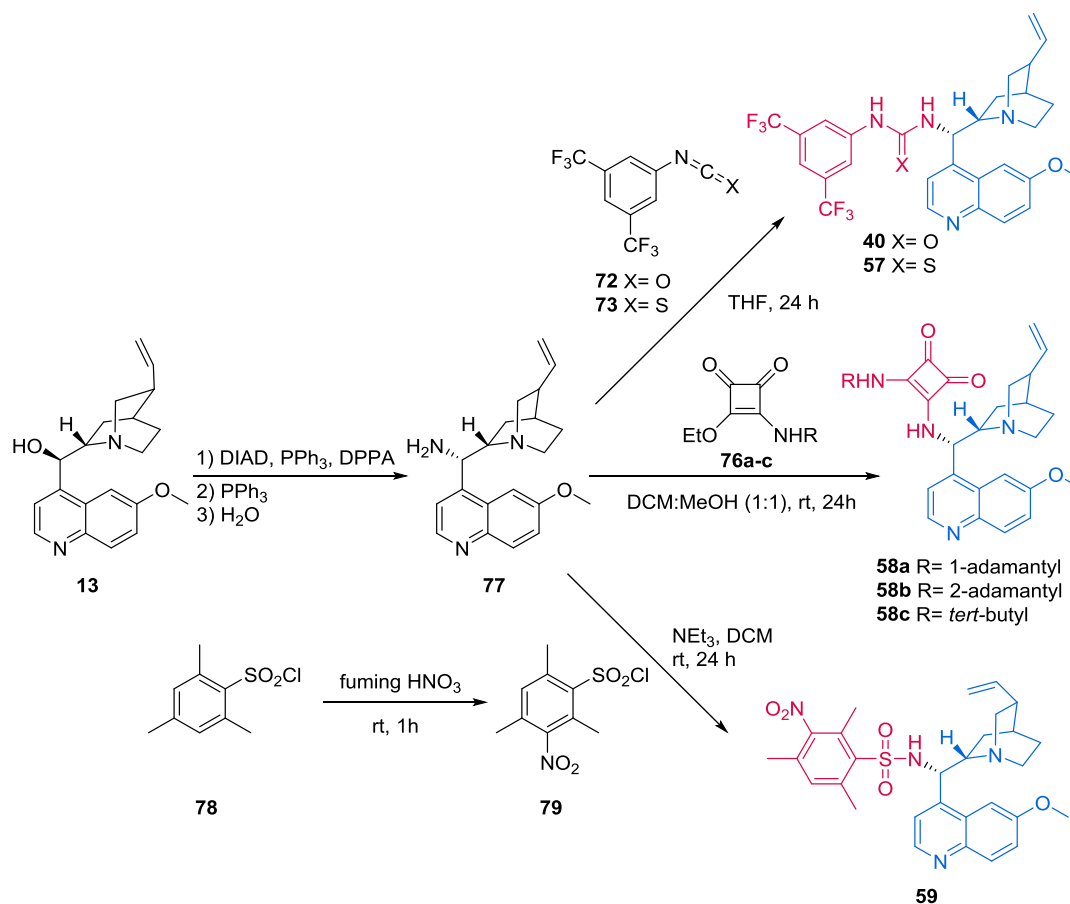
For the synthesis of squaramide-type catalysts, initially the monosquaramide motif **76** was constructed. The protocol starts with the conversion of squaric acid (**74**) to diethyl squarate (**75**). Then the selected bulky amine was allowed to react with freshly synthesized diethyl squarate to yield the corresponding monosquaramide **76**. This monosquaramide was then coupled with the basic part to obtain the bifunctional squaramide/DMAP organocatalysts (**56a-c**).

The quinine-derived organocatalysts of our design were also previously reported with their outstanding demonstrations on Michael,⁶³ aza-Henry⁶⁴ and aza-Friedel-Crafts⁶⁵ reactions. The basic “quinine amine” unit **77** is obtained via the Mitsunobu reaction of quinine (**13**), followed by Staudinger reduction of the in situ-formed azide.⁶⁶ Then this unit is coupled by the acidic unit of choice to complete the bifunctional organocatalyst skeleton. Analogous to 2-aminoDMAP type catalysts, introduction of 3,5-bis(trifluoromethyl)phenyl isocyanate (**72**) or bis(trifluoromethyl)phenyl isothiocyanate (**73**) according to Soós’ procedure yields the corresponding urea **40** or thiourea **57**, respectively.

The squaramide/quinine organocatalysts **58a-c** were synthesized by reacting the basic quinine amine moiety **77** with the selected monosquaramide, similar to the pathway for squaramide/DMAP catalysts.

The acidic sulfonyl chloride unit **79** of the sulfonamide catalyst was obtained via the nitration of 2,4,6-trimethylbenzenesulfonyl chloride (**78**).⁶⁷ It was then tethered to

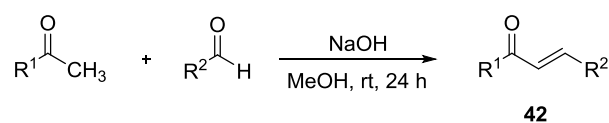
the quinine amine (**77**) to obtain the bifunctional sulfonamide/quinine organocatalyst **59** (Scheme 2.2).



Scheme 2.2. Synthesis of quinine derived bifunctional organocatalysts

2.2 Synthesis of the *trans*-Chalcone Derivatives

The chalcone derivatives used in this work were obtained by Claisen-Schmidt condensation, using Murphy's protocol (Scheme 2.3).⁶⁸



Scheme 2.3. Synthetic route for *trans*-chalcone derivatives

2.3 Asymmetric Sulfa-Michael Addition of Methyl Thioglycolate to *trans*-Chalcones

2.3.1 Optimization Studies

The studies were started with the screening of the synthesized quinine or 2-aminoDMAP derived chiral bifunctional catalysts (Figure 1.18). Among the eleven catalysts surveyed (Figure 2.1), sterically bulky organocatalysts with adamantyl moieties at their acidic part showed relatively better selectivities with the best one being the quinine-derived catalyst **58b** which gave the desired product with almost stoichiometric yield and 83% ee (Table 2.1, entry 9).

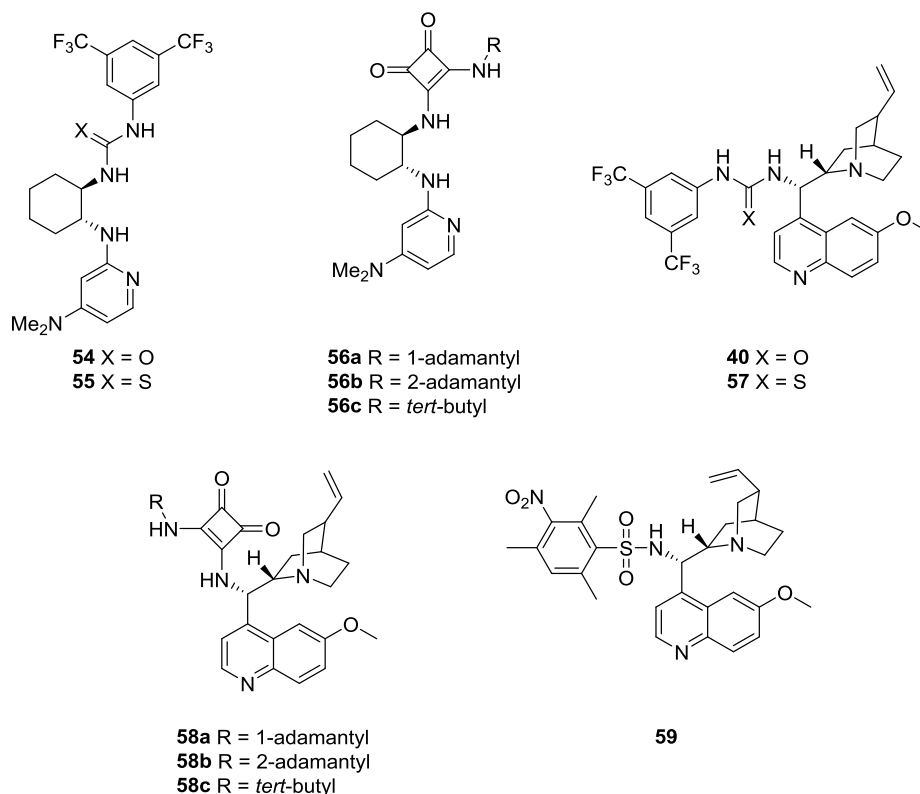
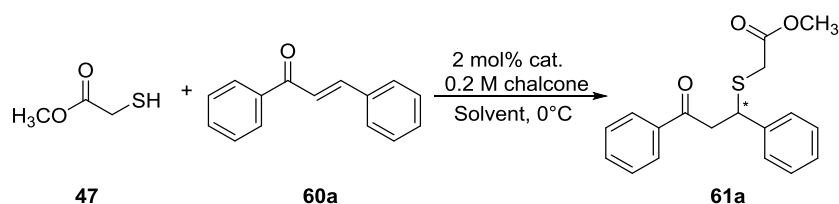


Figure 2.1. Structures of surveyed organocatalysts

Table 2.1. Catalyst and solvent screening^a



Entry	Cat	Solvent	Time (h)	Yield ^b (%)	ee ^c (%)
1	54	DCM	1	>99	23
2	55	DCM	6	15	8
3	56a	DCM	2	81	40
4	56b	DCM	1	>99	68
5	56c	DCM	6	83	5
6	40	DCM	6	86	9
7	57	DCM	6	70	15
8	58a	DCM	5	80	50
9	58b	DCM	1	>99	83
10	58c	DCM	6	32	14
11	59	DCM	6	80	47
12	58b	Hexane	6	54	86
13	58b	Toluene	1	>99	87
14	58b	THF	1	>99	22
15	58b	Chloroform	6	99	84
16	58b	Dioxane	1	>99	45
17	58b	MTBE	2	89	84
18	58b	EtOAc	5	96	26
19	58b	MeCN	2	92	15
20	58b	Et ₂ O	5	92	84

^a Unless stated otherwise, all reactions were performed with 0.10 mmol *trans*-chalcone and 0.20 mmol methyl thioglycolate in 0.5 mL of solvent, in the presence of 2 mol% organocatalyst at 0°C. ^b Isolated yields. ^c Determined by chiral HPLC analysis, AD-H column, 80:20 Hexane/isopropanol, 1.0 mL/min, 254 nm.

After selecting the best working catalyst, we tested several solvents for the reaction of interest to improve the stereoselectivity. Nonpolar solvents were found to work better than polar solvents and solvents that have hydrogen bond acceptor character gave lower ee's due to their possible interference with the H-bond dynamics of the

catalyst and electrophile. The best results were obtained with hexane, toluene, chloroform, methyl *tert*-butyl ether and diethyl ether with small differences in ee's (Table 2.1, entries 12, 13, 15, 17 and 20). However, the reaction was sluggish in hexane, diethyl ether and chloroform compared to toluene and methyl *tert*-butyl ether. And among the last two, toluene gave the desired product with both higher yield and ee (>99% yield and 87% ee versus 89% yield and 84% ee, respectively). Hence, toluene was selected as the best working solvent, and was used in further optimizations.

Next, we investigated the effect of catalyst loading on enantioselectivity (Table 2.2, entries 1-4). The previous screenings were done with 2 mol% catalyst loading, and the reaction was carried out again with the catalyst loading varied between 1 and 10 mol%. The selectivity was found to be increasing with increased catalyst loading and the reaction durations required for full conversion became shorter. The best selectivity (91% ee) was obtained in the presence of 10 mol% catalyst (Table 2.2, entry 4).

Then, the effect of dilution was observed by changing the chalcone concentration from 0.2 M to 0.05, 0.1 and 0.4 M (Table 2.2, entries 4-7). 92% of enantiomeric excess was attained when we decreased the concentration to 0.1 M (Table 2, entry 6). It seems dilution has a positive effect on selectivity, presumably because of the reduced possibility of the self-aggregation of the catalyst via hydrogen bonding. However, further dilution had a detrimental effect on ee (Table 2.2, entry 5).

Table 2.2. Further screening for SMA of methyl thioglycolate to *trans*-chalcone^a

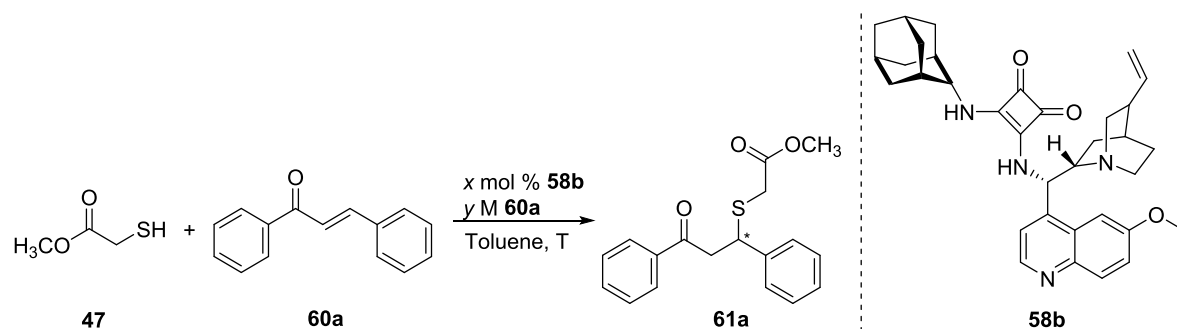


Table 2.2. Continued.^a

Entry	Cat. Loading	T (°C)	Conc. (M)	Time (h)	Yield ^b (%)	ee ^c (%)
1	1%	0	0.2	23	76	48
2	2%	0	0.2	1	>99	87
3	5%	0	0.2	1	>99	89
4	10%	0	0.2	0.5	>99	91
5	10%	0	0.05	0.5	>99	88
6	10%	0	0.1	0.5	>99	92
7	10%	0	0.4	0.5	>99	91
8 ^d	10%	0	0.1	0.5	86	91
9 ^e	10%	0	0.1	0.5	>99	79
10	10%	RT	0.1	0.5	>99	93
11	10%	-20	0.1	3	>99	94
12	10%	-40	0.1	25	>99	97
13	1%	RT	0.1	1	>99	90

^a Unless stated otherwise, all reactions were performed with 1:2 ratio of *trans*-chalcone to methyl thioglycolate in toluene, in the presence of organocatalyst **58b** at the indicated temperature.

^b Isolated yields. ^c Determined by chiral HPLC analysis, AD-H column, 80:20 *n*-hexane / isopropanol, 1.0 mL/min, 254 nm. ^d The reaction was carried out using 1:1 ratio of *trans*-chalcone to methyl thioglycolate. ^e The reaction was carried out using 1:3 ratio of *trans*-chalcone to methyl thioglycolate.

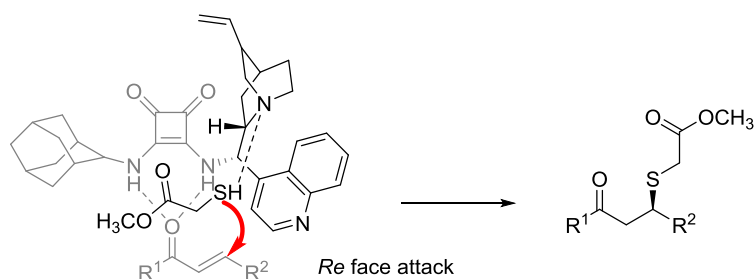
Next, the effect of the ratio of reactants on selectivity was brought under investigation. Using an equimolar mixture of *trans*-chalcone and methyl thioglycolate resulted in a slight decrease in ee and a rather larger decrease in yield (Table 2.2, entry 8). Further increasing methyl thioglycolate amount to 3 molar equivalents showed a sudden drop in selectivity (entry 9). Thus, we moved on with a 1:2 ratio of reactants as before.

Since sulfur nucleophiles are rather good nucleophiles, the background reaction which yields a racemic mixture of the product was of concern; when the reactants were allowed to react without the presence of any catalyst, formation of some sulfa-Michael addition product **61a** was observed. To minimize the rate of background reaction, we investigated the effect of temperature as the final parameter. Carrying out the reaction at room temperature resulted in a slight increase in ee to 93% (Table 2.2, entry 10). However, there was an even better improvement on selectivity when

the reaction medium was cooled. By running the reaction at $-40\text{ }^{\circ}\text{C}$, almost full conversion and an excellent ee of 97% was achieved (entry 12), and the homogeneity of the reaction medium was retained despite this low temperature.

To test the applicability of a milder reaction condition, we carried out the model reaction at room temperature with 1 mol% organocatalyst **58b**. The desired product (**61a**) was obtained with almost quantitative yield and 90% ee. Unfortunately, this excellent enantioselectivity wasn't maintained for substituted sulfa-Michael adducts under this condition. Thus, the optimal catalyst loading and reaction temperature were selected as 10 mol % and -40°C , respectively.

The absolute configuration of chiral adducts were assigned as *R* by comparing the obtained data with the literature.^{47a} The rest were tentatively assigned by analogy. A transition state model was proposed to elucidate the source of enantioselectivity (Scheme 2.4), in which the nucleophile is activated by the quinuclidine nitrogen, whereas the acidic squaramide hydrogens activate chalcone by H-bonding. The nucleophilic attack occurs on the *Re* face of chalcones, affording the *R* enantiomer.

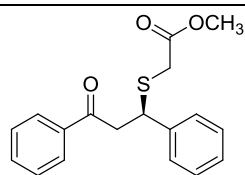
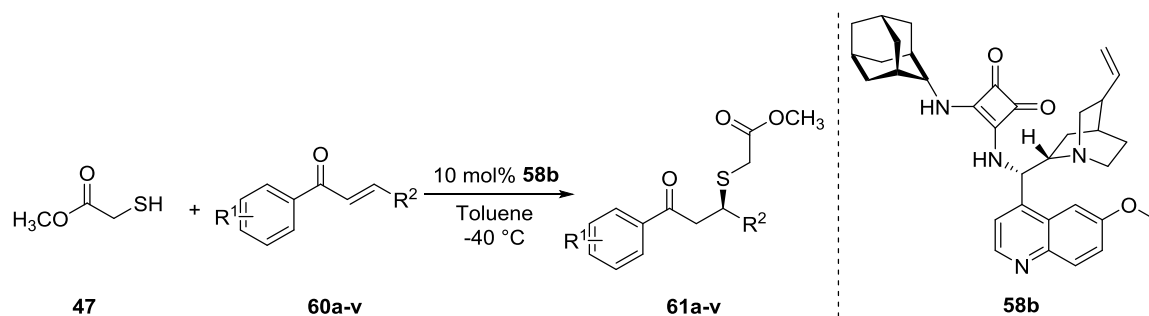


Scheme 2.4. The proposed transition state model for SMA of methyl thioglycolate to *trans*-chalcone derivatives

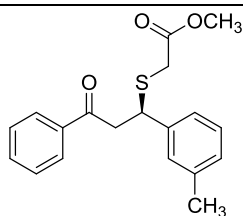
2.3.2 Substrate Scope

With the optimized conditions in hand, we synthesized a series of sulfa-Michael adducts by using various substituted chalcones and enones (Table 2.3).

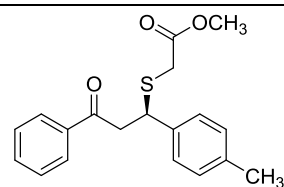
Table 2.3. Substrate scope of SMA of methyl thioglycolate to *trans*-chalcones^a



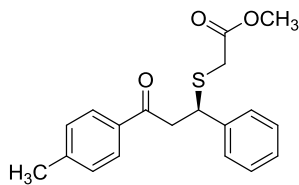
61a
>99% yield, 97% ee
25 h,
>99% yield, 93% ee^b
24 h



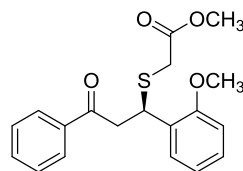
61b
>99% yield, 95% ee
22 h



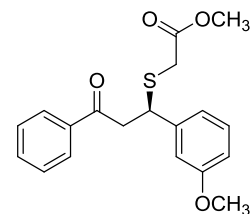
61c
>99% yield, 96% ee
23 h



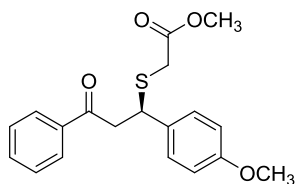
61d
>99% yield, 97% ee
22 h



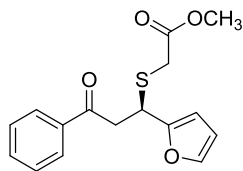
61e
>99% yield, 82% ee
21 h



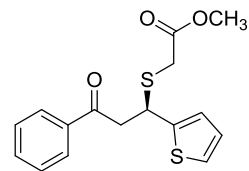
61f
>99% yield, 96% ee
25 h



61g
>99% yield, 99% ee
42 h

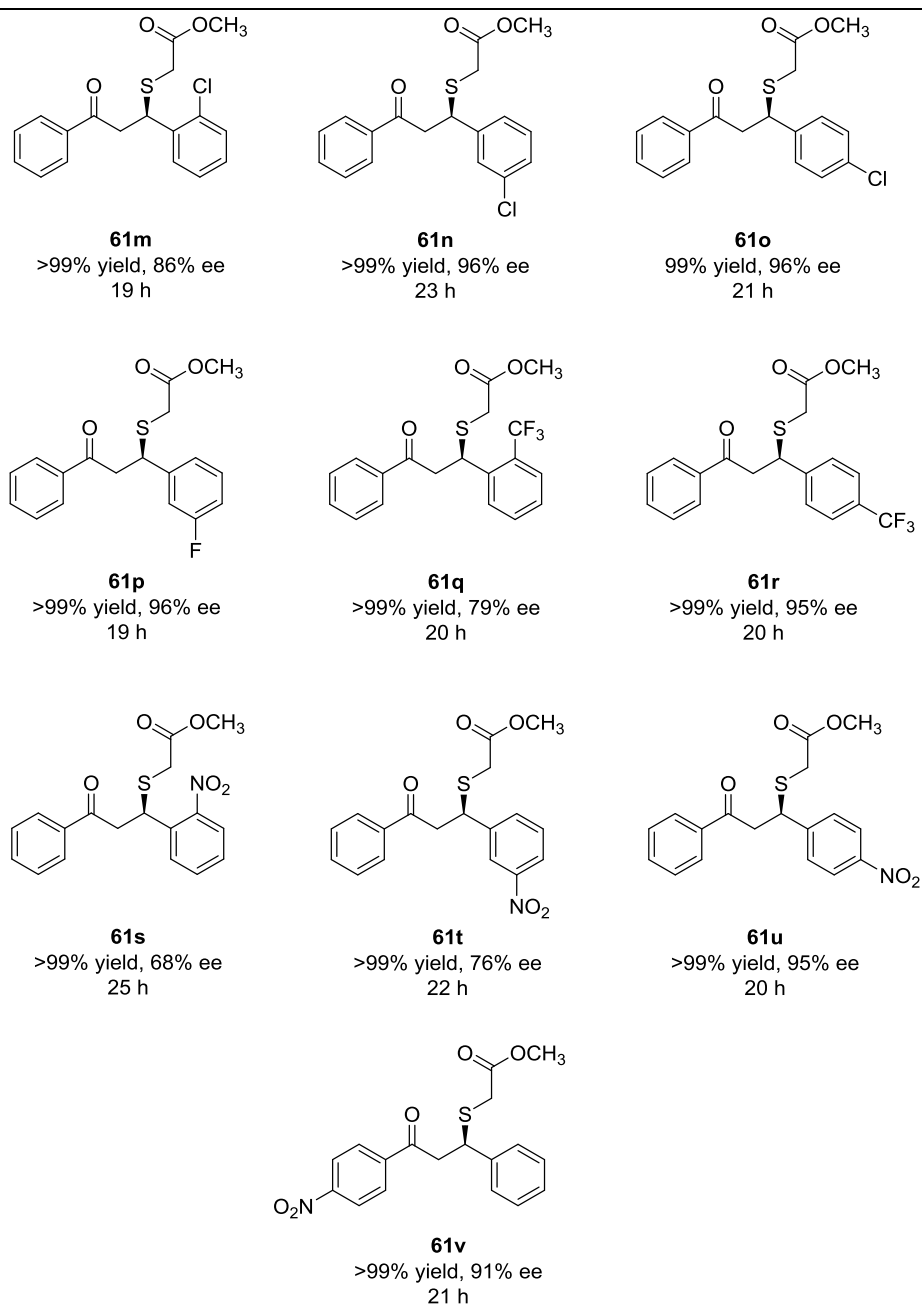


61h
>99% yield, 91% ee
41 h



61i
>99% yield, 95% ee
41 h

Table 2.3. Continued.^a



^a Unless stated otherwise, all reactions were performed with 0.10 mmol *trans*-chalcone and 0.20 mmol methyl thioglycolate in 1.0 mL of solvent, in the presence of 10 mol % **58b** at -40°C. ^b Performed with 4.9 mmol (1.02 g) of **60a**, at gram-scale.

Among the employed chalcone derivatives, the best ee's were obtained with the ones having substituents at *para*- or *meta*- positions, giving rise to excellent selectivities ranging between 95-99% (Table 2.3) regardless of the electronic character of the substituents. One exception was the 3-nitro substituted chalcone (76% ee). 2-Furyl and 2-thienyl moieties were also well tolerated (91 and 96% ee, respectively). Substituents on *ortho*-positions, however, gave rise to rather lower ee's ranging between 68-86%. The lowest ee was obtained with the 2-nitro substituent (68% ee). When the electron donating and withdrawing nature of the substituents and the stereochemical outcomes of their reactions are evaluated, it can be deduced that the decrease in the selectivity for *ortho*-substituted derivatives is related to the steric effect. To demonstrate the efficiency of the catalyst system, a scale-up reaction was performed by using 4.9 mmol of **60a**. The gram-scale synthesis yielded **61a** with >99% yield and 93% ee.

Next, the substituent scope was widened to aryl butenones **62a-d**. When the reactions were carried out under the same optimized conditions as for chalcone derivatives, the reactions were sluggish and the products **63a-d** were obtained with poor yields (Table 2.4).

Table 2.4. SMA of methyl thioglycolate with aryl butenones under optimized conditions^a

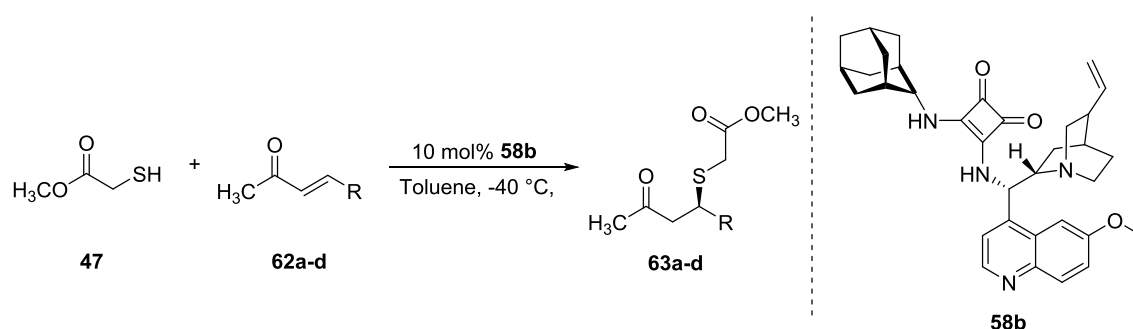
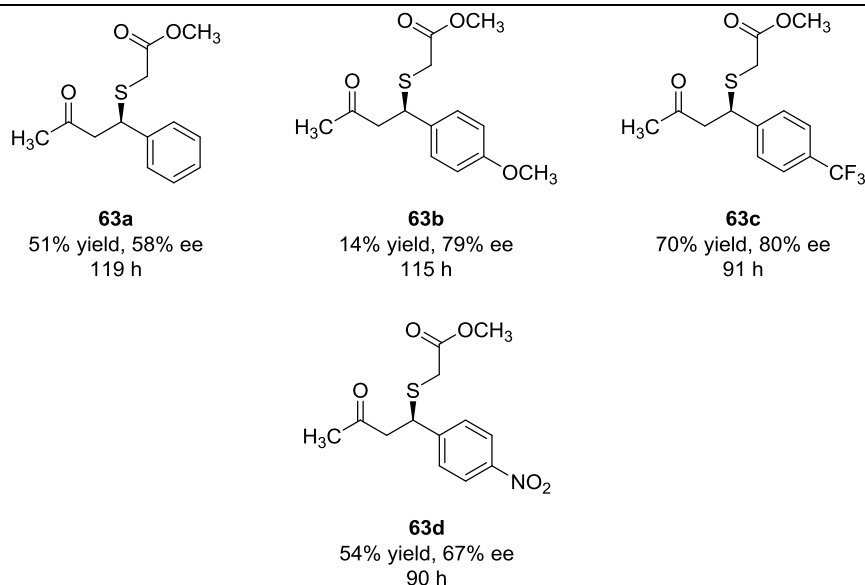


Table 2.4. Continued.^a



^a Unless stated otherwise, all reactions were performed with 0.10 mmol aryl butenone derivative and 0.20 mmol methyl thioglycolate in 1.0 mL of solvent, in the presence of 10 mol% **58b** at -40 °C.

Seeing those results, the reactions of aryl butenones were performed at room temperature for improved rate of conversion and yield and the target adducts were obtained with shorter reaction times and higher yields (Table 2.5). For **63b** and **63c**, the selectivities were a little lower than the previous condition, but there was a small increase for the other entries.

Table 2.5. SMA of methyl thioglycolate with aryl butenones under mild conditions^a

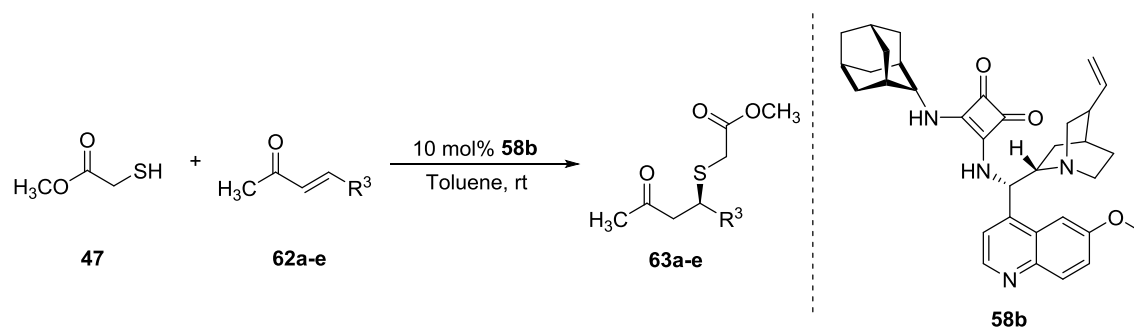
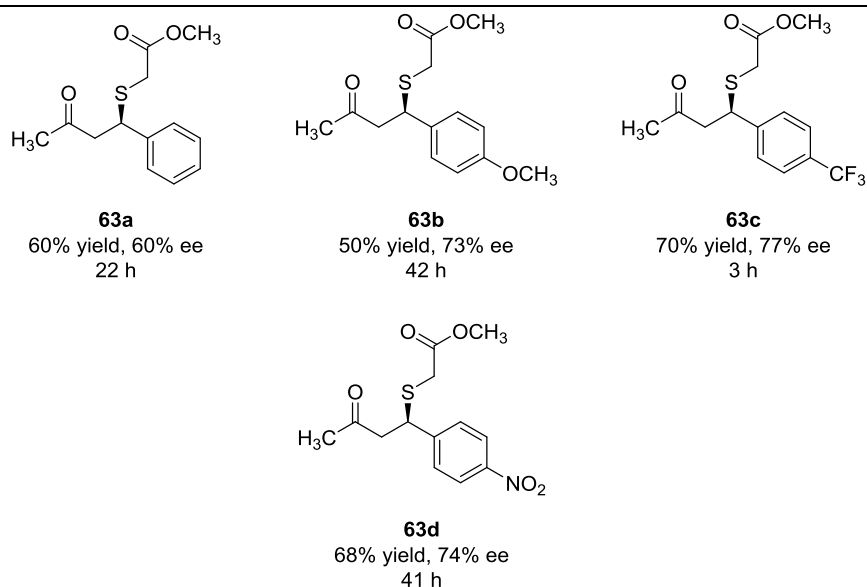
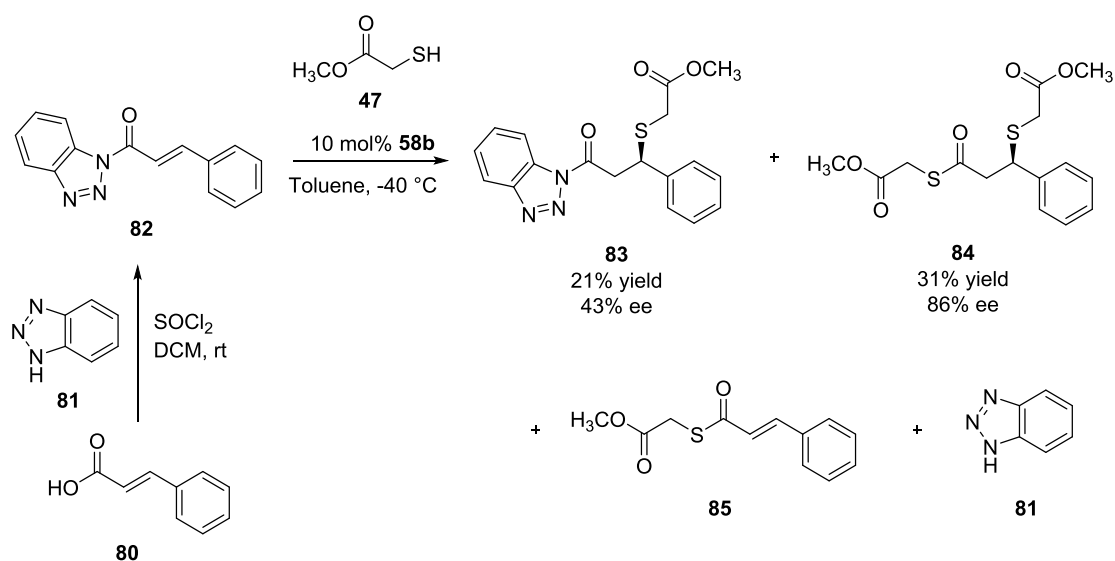


Table 2.5. Continued.^a



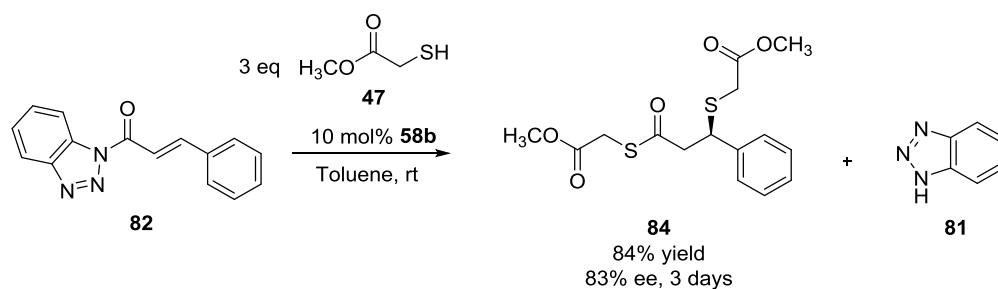
^a Unless stated otherwise, all reactions were performed with 0.10 mmol aryl butenone derivative and 0.20 mmol methyl thioglycolate in 1.0 mL of solvent, in the presence of 10 mol% **58b** at room temperature.

Another enone chosen for this part of the work was cinnamoyl benzotriazole **82**. The starting material was synthesized by the reaction of cinnamic acid and benzotriazole in the presence of SOCl_2 .⁶⁹ After obtaining the enone, we proceeded with the addition of methyl thioglycolate under optimized conditions. Against our initial goal, the reaction gave the thiol substituted thioester **84** as the major product (31% yield, 86% ee) instead of the 1,4-adduct (Scheme 2.5).



Scheme 2.5. SMA of cinnamoyl benzotriazole with methyl thioglycolate under optimized conditions

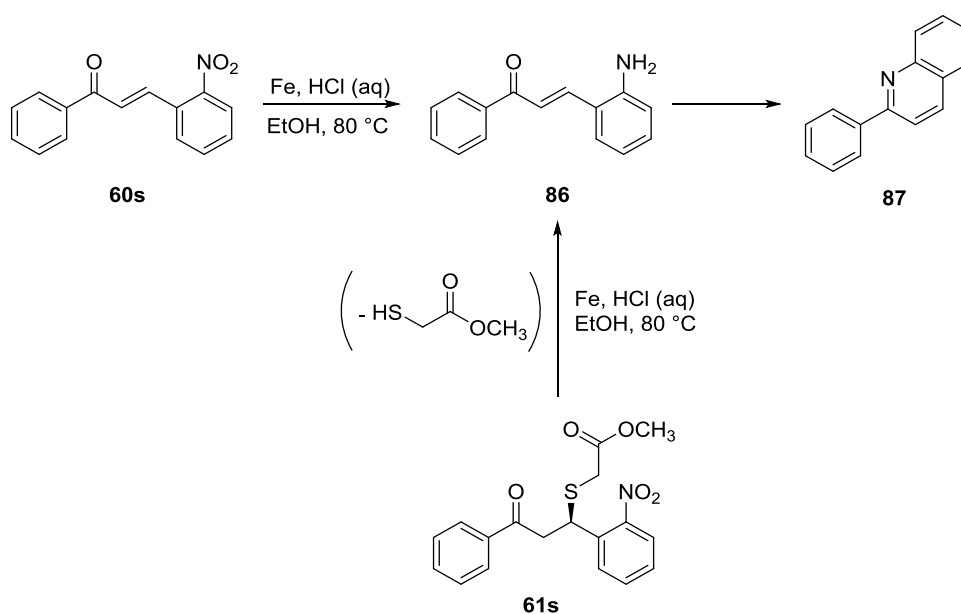
Focusing on the good enantioselectivity attained for the thiol substituted thioester **84**, we carried out the reaction at a milder temperature and increased the methyl thioglycolate ratio to 3 equivalents to ensure complete elimination of benzotriazole moiety. As expected, we obtained **84** with 84% yield and 83% ee (Scheme 2.6).



Scheme 2.6. Updated pathway to obtain **84**

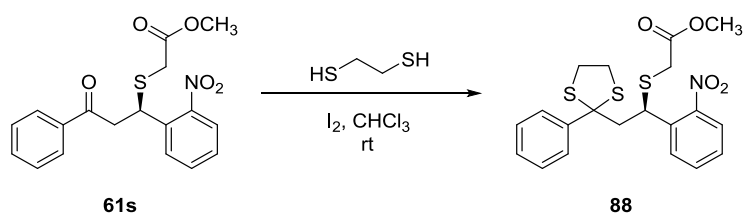
2.3.3 Synthesis of 1,4-Benzothiazepin-2-one Derivative

After obtaining a rather large number of derivatives with success, we focused on the possible further reactions of the enantiomerically enriched sulfa-Michael adducts. For this purpose, 2-nitro substituted adduct **61s** was selected. Our intention was to first reduce the nitro group to amino, and then obtain the intramolecular cyclization product of the amino substituted adduct: the 1,4-benzothiazepin-2-one derivative. However, direct reduction caused the amino chalcone to undergo a *cis*- to *trans*-isomerization, followed by intramolecular cyclization and subsequent condensation, which transformed the substrate into the undesired 2-phenylquinoline **87** slowly. When we proceeded with the sulfa-Michael addition, transformation of amino chalcone to 2-phenylquinoline was almost instantaneous (Scheme 2.7).



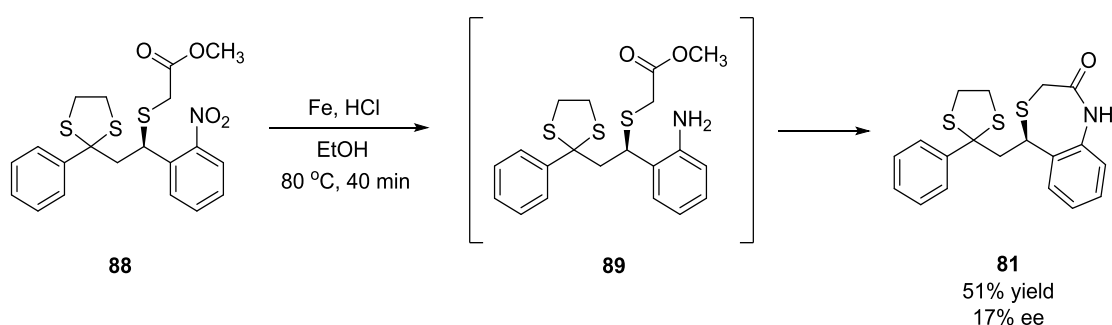
Scheme 2.7. Reduction of amino chalcone and transformation to 2-phenylquinoline

To overcome this problem, we designed a new synthetic route which starts with the dithiolane protection of the carbonyl group of the 2-nitro substituted sulfa-Michael adduct **61s**. **61s** was reacted with 1,2-ethanedithiol in the presence of I_2 , and the desired thioacetal protected product **88** was obtained with 61% yield (Scheme 2.8).



Scheme 2.8. Dithiolane protection of the 2-nitro substituted sulfa-Michael adduct **61s**

With the undesired 2-phenylquinoline formation risk prevented, we proceeded to reduction of the protected adduct with iron in acidic medium, and the desired ring closure was observed without the isolation of the amino-adduct with 51% yield and 17% ee (Scheme 2.9). The loss in the enantiomeric excess is attributed to the unpreventable retro-sulfa-Michael reaction, which was indicated by the appearance of starting material chalcone **60s** on the TLC plates during the course of reduction.



Scheme 2.9. Synthesis of chiral 1,4-benzothiazepin-2-one

2.4 Asymmetric Sulfa-Michael Addition of 1-Thionaphthol to *trans*-Chalcones

2.4.1 Optimization Studies

The chiral organocatalysts synthesized in the first part of the thesis (Figure 2.2) were surveyed also for the asymmetric SMA of 1-thionaphthol to chalcone derivatives.

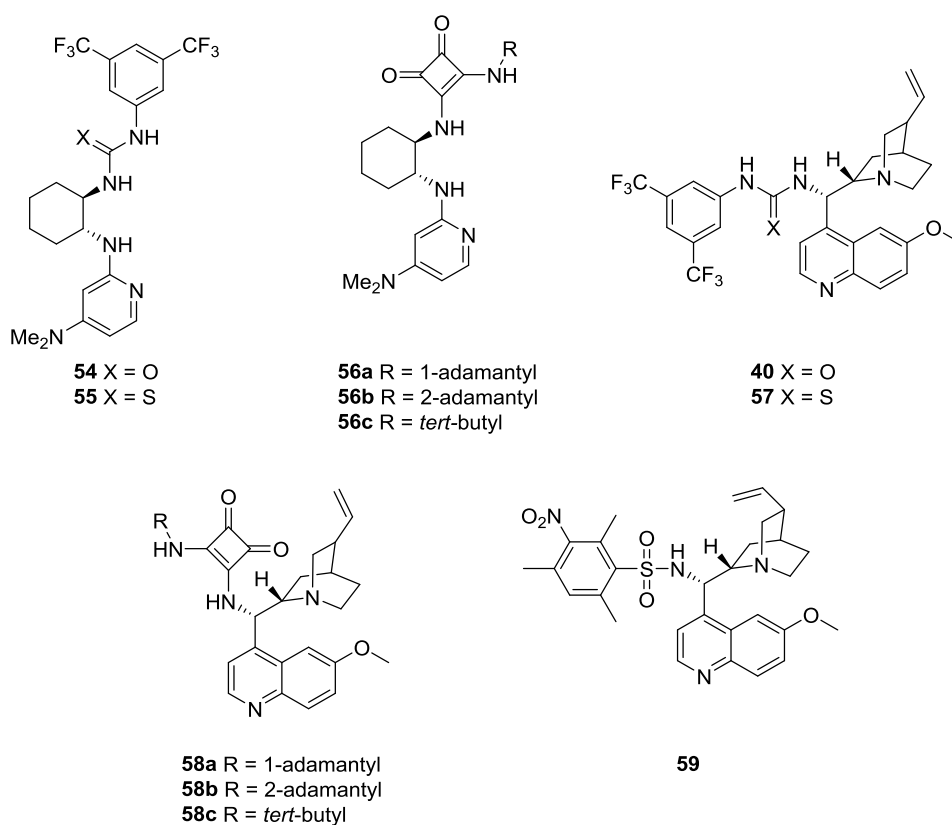
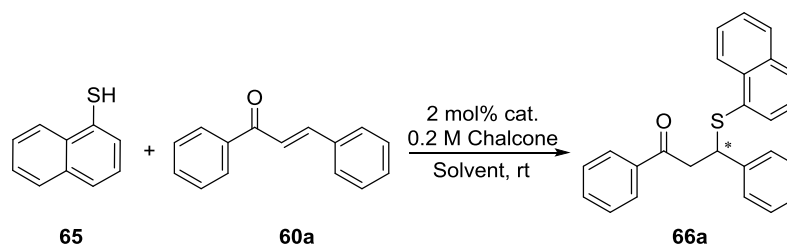


Figure 2.2. Structures of surveyed organocatalysts

The best catalyst for this transformation was quinine derived sulfonamide **59**, which gave the desired product **66a** with 98% yield and 63% ee (Table 2.6, entry 11).

Table 2.6. Catalyst and solvent screening^a



Entry	Cat	Solvent	Time (h)	Yield ^b (%)	ee ^c (%)
1	54	Toluene	0.5	69	8
2	55	Toluene	0.5	73	61

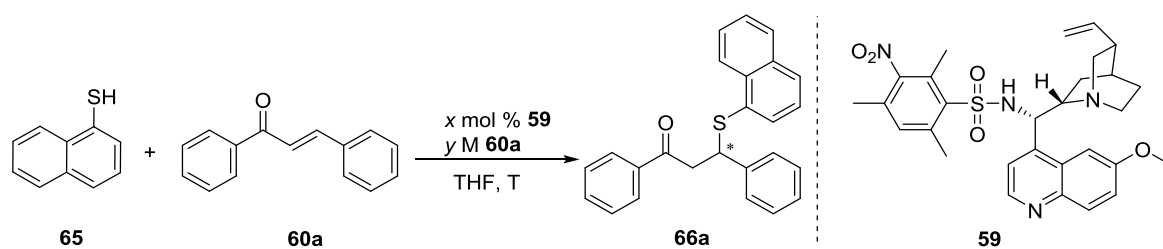
Table 2.6 Continued.^a

Entry	Cat	Solvent	Time (h)	Yield ^b (%)	ee ^c (%)
3	56a	Toluene	0.5	92	46
4	56b	Toluene	0.5	63	40
5	56c	Toluene	0.5	79	52
6	40	Toluene	0.5	97	25
7	57	Toluene	0.5	71	41
8	58a	Toluene	0.5	72	41
9	58b	Toluene	0.5	96	43
10	58c	Toluene	0.5	70	31
11	59	Toluene	1	98	63
12	59	Hexane	1	>99	6
13	59	DCM	2.5	42	65
14	59	THF	4	85	79
15	59	Chloroform	2	50	65
16	59	Dioxane	4	90	75
17	59	MTBE	1	92	57
18	59	EtOAc	2	49	65
19	59	MeCN	1	81	55
20	59	Et ₂ O	3	28	57

^a Unless stated otherwise, all reactions were performed with 0.10 mol *trans*-chalcone and 0.20 mmol 1-thionaphthol in 0.5 mL of solvent, in the presence of 2 mol% organocatalyst at room temperature. ^b Isolated yields. ^c Determined by chiral HPLC analysis, AD-H column, 99:1 Hexane/isopropanol, 0.8 mL/min, 230 nm.

After selecting the best working catalyst, optimization studies were initiated on the model reaction to determine the conditions to achieve the best enantioselectivity. The first parameter screened was the effect of solvent. Using THF and dioxane (Table 2.6, entries 14 and 16, respectively) gave the two highest results, but the use of dioxane is best avoided due to its toxicity. Except for hexane (only 6% ee, entry 12), all other solvents afforded the target SMA adduct with similar moderate ee values. Thus, THF was selected as the best solvent.

Table 2.7. Further screening for SMA of 1-thionaphthol to *trans*-chalcone^a



Entry	Load	Conc. (M)	T (°C)	Time (h)	Yield ^b (%)	ee ^c (%)
1	0.1%	0.2	rt	72	-	-
2	0.5%	0.2	rt	40	81	82
3	1%	0.2	rt	23	93	81
4	2%	0.2	rt	4	85	79
5	5%	0.2	rt	6	95	76
6	10%	0.2	rt	3	83	69
7	1%	0.05	rt	72	-	-
8	1%	0.1	rt	72	-	-
9	1%	0.15	rt	26	>99	79
10	1%	0.25	rt	25	>99	78
11	1%	0.3	rt	20	91	79
12	1%	0.4	rt	19	>99	75
13 ^d	1%	0.2	rt	72	-	-
14 ^e	1%	0.2	rt	41	91	79
15 ^f	1%	0.2	rt	19	90	78
16	1%	0.2	0	40	96	73
17	1%	0.2	-20	41	97	68
18	1%	0.2	-40	49	90	62

^a Unless stated otherwise, all reactions were performed with 1:2 ratio of *trans*-chalcone to 1-thionaphthol in THF, in the presence of organocatalyst **59** at the indicated temperature.

^b Isolated yields. ^c Determined by chiral HPLC analysis, AD-H column, 99:1 hexane / isopropanol, 0.8 mL/min, 230 nm. ^d The reaction was carried out using 1:1 ratio of *trans*-chalcone to 1-thionaphthol.

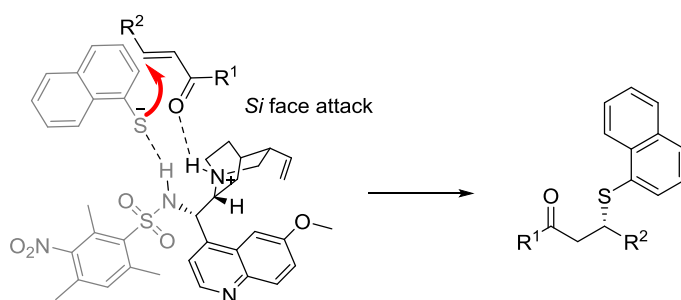
^e The reaction was carried out using 1:1.5 ratio of *trans*-chalcone to 1-thionaphthol. ^f The reaction was carried out using 1:3 ratio of *trans*-chalcone to 1-thionaphthol.

Then, the catalyst loading was varied between 0.1 and 10 mol% to investigate its effect on enantioselectivity (Table 2.7, entries 1-6). At very low catalyst loading as 0.1 mol%, the reaction was too sluggish; amount of the product was too small and

was not isolated. Using 0.5 mol% of **59** gave rise to the best ee value (82%, entry 2), however the outcome of the reaction with 1 mol% of **59** (81%, entry 3) was very close to the former and was completed in a shorter time (40 hours, compared to 23 hours, respectively). Thus, the optimization was continued with 1 mol% catalyst loading. The effect of concentration of the reaction mixture was investigated by changing the chalcone concentration gradually from 0.05 to 0.4 M (Table 2.7, entries 3 and 7-12). The best selectivity (81% ee) was obtained at 0.2 M chalcone concentration (Entry 3). Diluting the reaction mixture further than 0.15 M decreased the rate of reaction considerably and the amounts of products were not appreciable to be isolated. Increasing the concentration led to a small decrease in ee.

Using an equimolar mixture of chalcone and naphthalene-1-thiol had a similar outcome for the progress of the reaction as dilution (Table 2.7, entry 14). Changing the chalcone to naphthalene-1-thiol ratios to 1:1.5 or 1:3 resulted in small losses in enantioselectivity. Hence, the studies were continued with 2 molar equivalents of 1-thionaphthol to *trans*-chalcone. The optimization studies were concluded by investigating the effect of temperature on asymmetric induction (Table 2.7, entries 16-18). Lowering the temperature gradually to -40 °C caused a significant loss in ee, allowing the synthesis of the product **66a** with a final ee of 62% (entry 18). The most enantioenriched product was obtained at room temperature (81% ee). It is thought the matching of the catalyst and substrates required energy to some extent.

Since the enantioenriched product **66a** was unable to form adequate single crystals for XRD analysis, the absolute configuration of the product was assigned as “*S*” by comparing the obtained optical rotation value with the values in the literature for the organocatalytic SMA of thiols to *trans*-chalcone derivatives.^{44b,70} A transition state model to explain the origin of stereoinduction was proposed (Scheme 2.10), according to the Houk’s Brønsted acid–hydrogen bonding model, which was found to be the lowest-energy transition state for the SMA of thiols in the presence of cinchona alkaloid-type organocatalysts in Guo’s work in 2017.⁷¹



Scheme 2.10. Proposed transition state for the SMA of 1-thionaphthol to *trans*-chalcones

2.4.2 Substrate Scope

The substrate scope was extended to substituted chalcones, under the optimized conditions (Table 2.8). Among the chalcone derivatives employed in the model reaction, the best result in terms of enantioselectivity was attained with 4-methyl substituted chalcone, which allowed the synthesis of corresponding SMA adduct **66d** with an excellent ee of 91%. Good to moderate results were obtained with chalcone derivatives possessing electron donating and withdrawing substituents. Compared with the unsubstituted *trans*-chalcone, a drastic decrease in enantioselectivity was observed with chalcone derivative **66c**, however (23% ee, entry 3).

Table 2.8. SMA of 1-thionaphthol to substituted *trans*-chalcones in THF

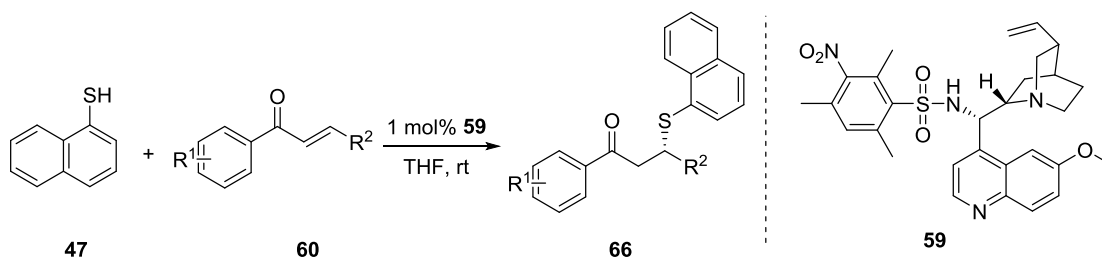


Table 2.8. Continued.^a

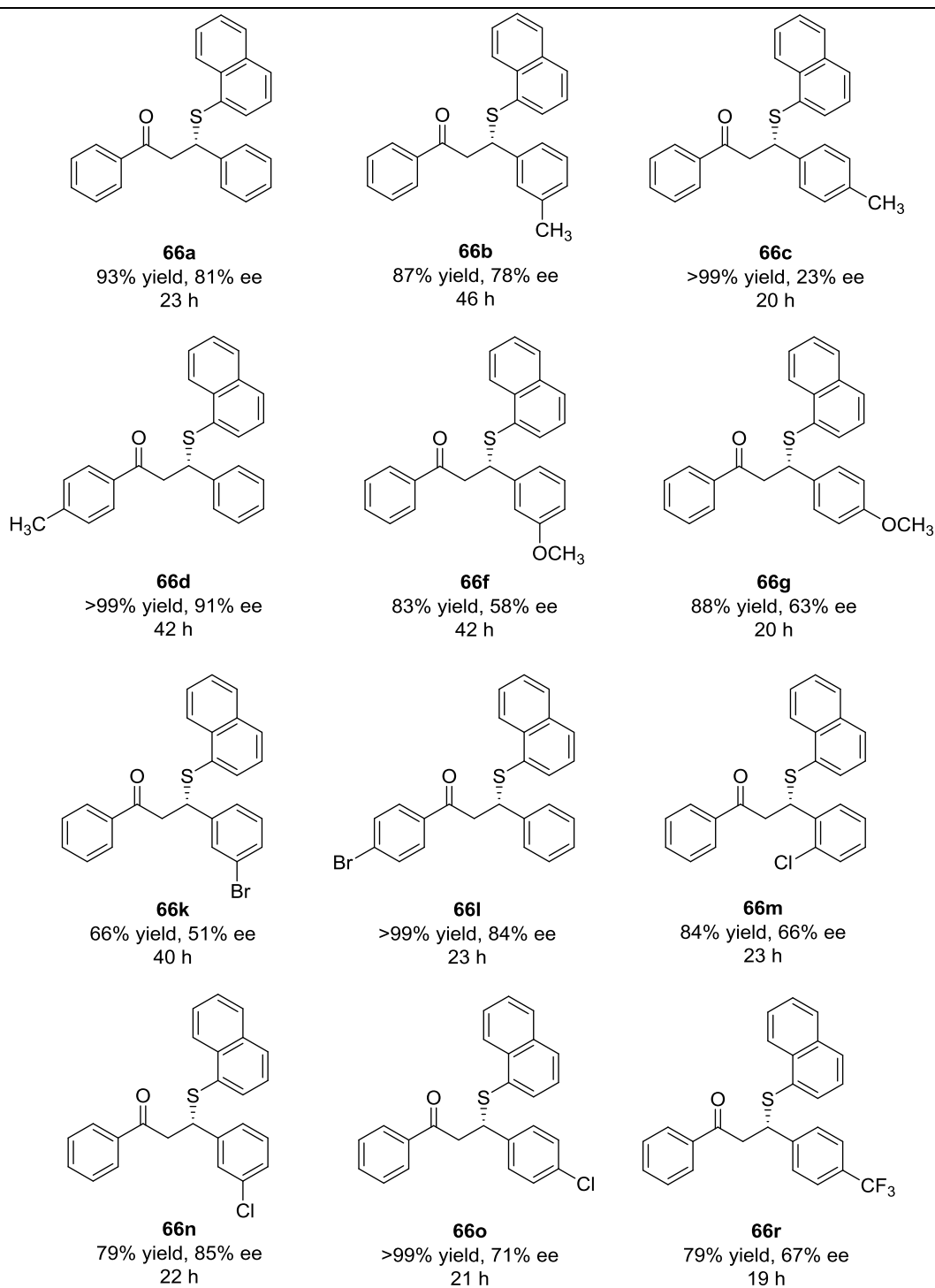
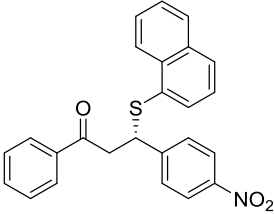
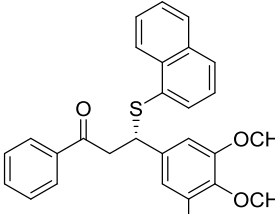
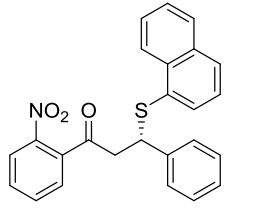
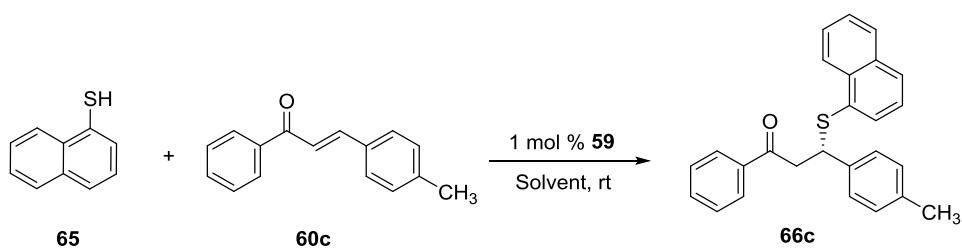


Table 2.8. Continued.^a

		
66u 81% yield, 68% ee 21 h	66w 94% yield, 50% ee 21 h	66x 84% yield, 82% ee 21 h

^a Unless stated otherwise, all reactions were performed with 0.20 mmol *trans*-chalcone derivative and 0.40 mmol 1-thionaphthol in 1.0 mL of THF, in the presence of 1 mol % **59** at room temperature.

Intrigued by this unexpected result, we decided to revisit the solvent screening. For this purpose, the sulfa-Michael addition of 1-thionaphthol to **60c** was carried out again in toluene, dioxane and DCM, in addition to THF (Table 2.9). In DCM, 93% ee was attained for adduct **66c**. In the light of this striking improvement, we decided to repeat the derivatization studies with DCM (Table 2.10).

Table 2.9. Further solvent screening results for the selected derivative **66c**^a

Entry	Solvent	Time (h)	Yield ^b (%)	ee ^c (%)
1	THF	20	>99	23
2	Toluene	6	95	78
3	Dioxane	20	78	76
4	DCM	6	94	93

^a Unless stated otherwise, all reactions were performed with 0.20 mmol **60c** and 0.40 mmol 1-thionaphthol in 1.0 mL of solvent, in the presence of 1 mol % **59** at room temperature. ^b Isolated yields.

^c Determined by chiral HPLC analysis.

Table 2.10. SMA of 1-thionaphthol to substituted *trans*-chalcones in DCM

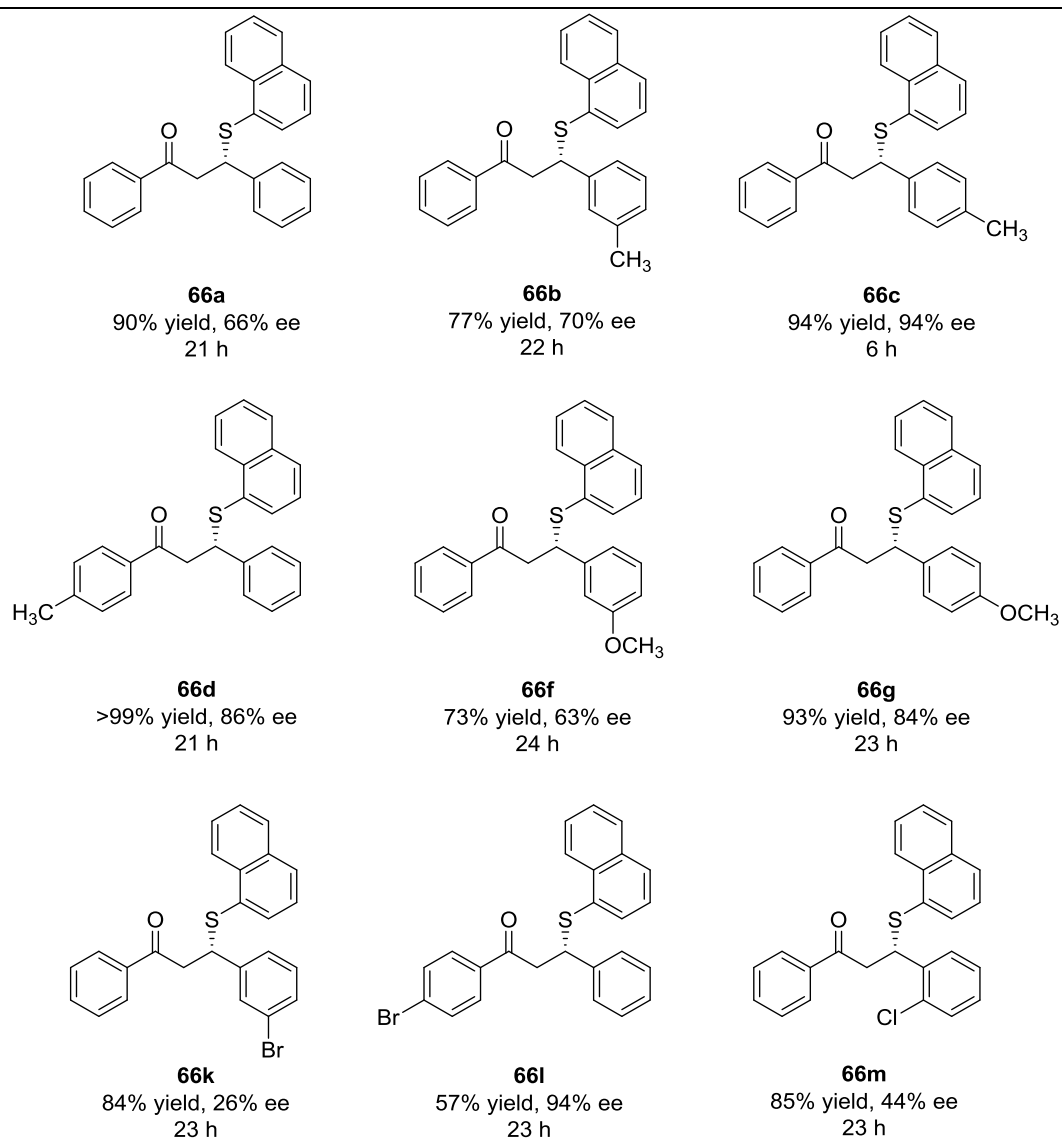
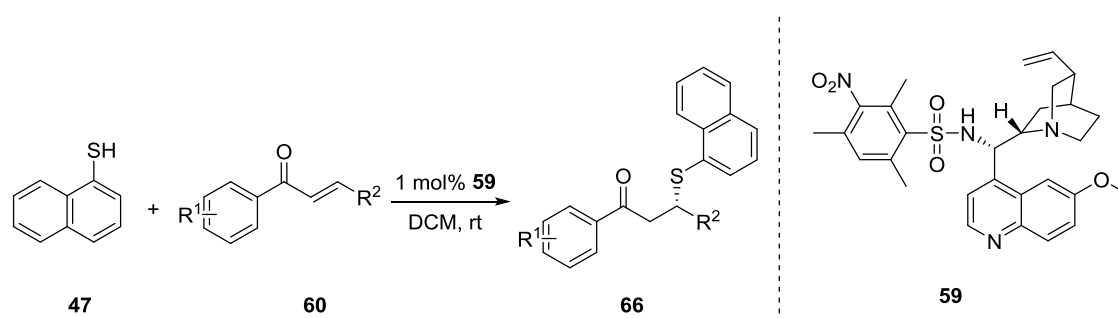
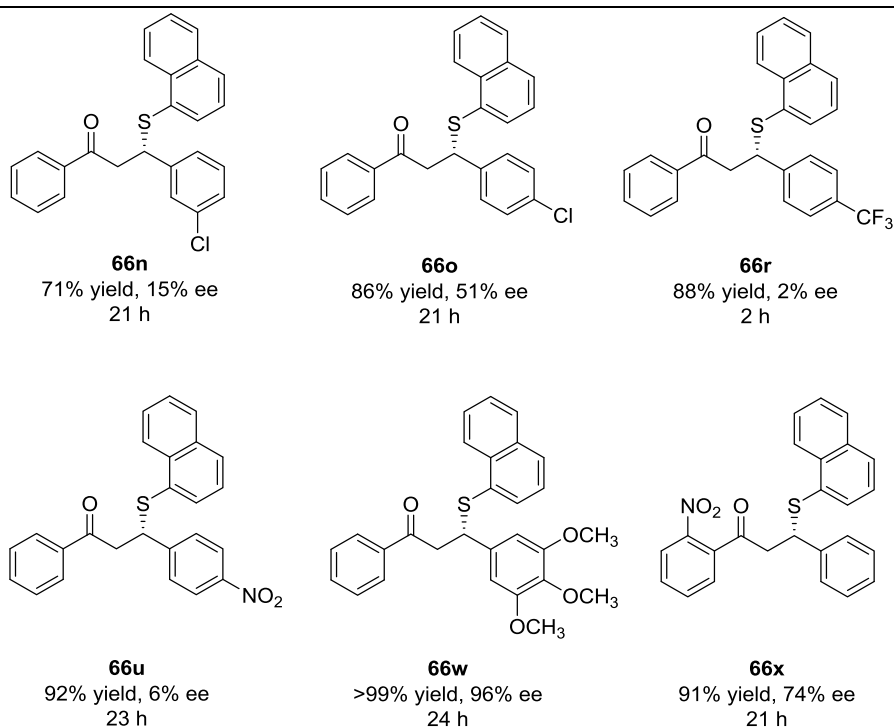


Table 2.10. Continued.^a

^a Unless stated otherwise, all reactions were performed with 0.20 mmol *trans*-chalcone derivative and 0.40 mmol 1-thionaphthol in 1.0 mL of DCM, in the presence of 1 mol % **59** at room temperature.

Employing DCM as the solvent showed significant improvements in the asymmetric induction for chalcone derivatives having electron donating methyl and methoxy substituents (Table 10) especially with 4-methyl and 3,4,5-trimethoxy substituted chalcones (23% to 93% ee and 50% to 96% ee; **66c** and **66w**, respectively.) The two exceptions to this pattern were with 3-methyl substituted adduct **66f**, which was obtained with a small decrease in enantioselectivity (77% to 63% ee) when THF was changed to DCM. In the case of halogens and electron withdrawing substituents, an opposite behavior was observed. The use of DCM instead of THF led to lower ee's for the chalcone derivatives having the aforementioned substituents. The most dramatic decreases in selectivity were observed for derivatives **66r** and **66u**, for which the outcomes of the reactions were almost racemic. Only the bromo derivative **66l** showed a small improvement in DCM. The solvent effects on the SMA of

chalcone derivatives and 1-thionaphthol was summarized in Figure 2. This behavior might be related to the better stabilization of the transition state of substrates containing electron withdrawing substituents or halogens with THF, or vice versa.

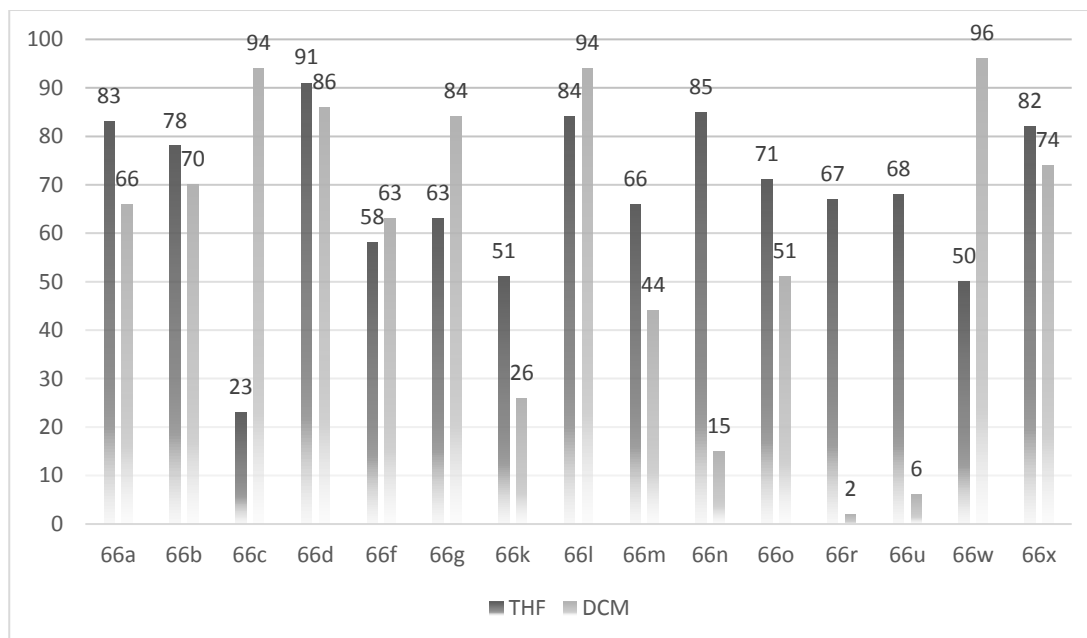


Figure 2.3. Comparison of the ee's of SMA in the presence of THF and DCM as solvent

2.4.3 Synthesis of Sulfones

In order to enhance the potential bioactivity of the obtained enantioenriched products, selected SMA adducts (β -aryl- β -sulfanyl ketones) were subjected to oxidation with *m*-CPBA.⁷² The characterization of the newly formed oxidation product was done by ATR-FTIR, by comparing the FTIR spectra of SMA adduct **66a** with its corresponding oxidation product **67a** (Figure 2.2). The formation of new strong absorption peaks at around 1303 cm^{-1} and 1120 cm^{-1} shows that the oxidation product is a sulfone.³⁷ The results of the oxidation reactions are summarized in Table 2.11.

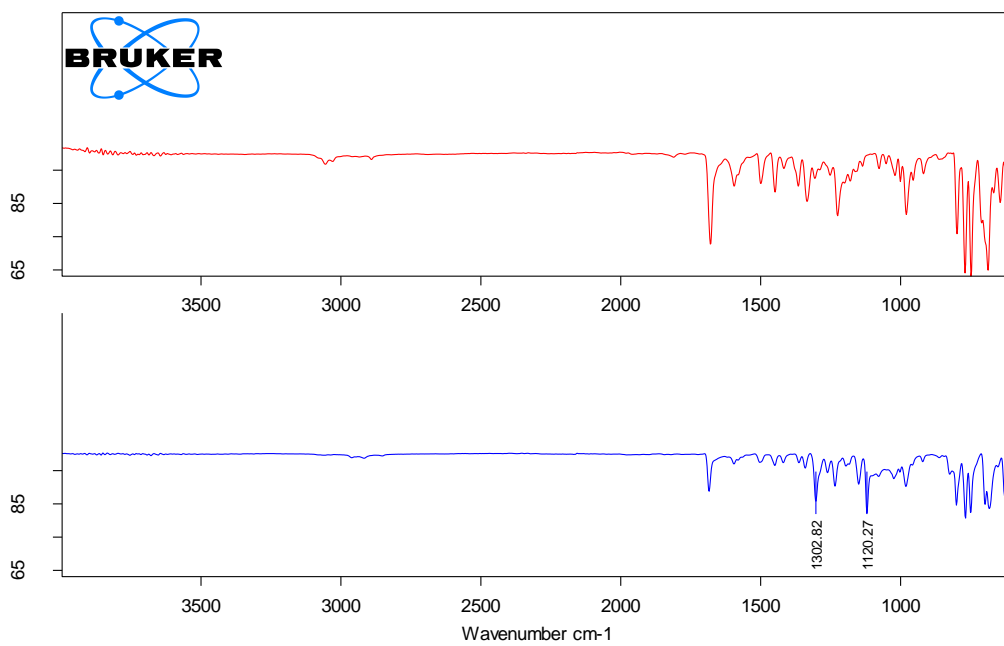


Figure 2.4. Comparison of FTIR spectra of **66a** (red, top) and **67a** (blue, bottom)

Table 2.11. Synthesis of enantioenriched sulfones from β -aryl- β -sulfanyl ketones

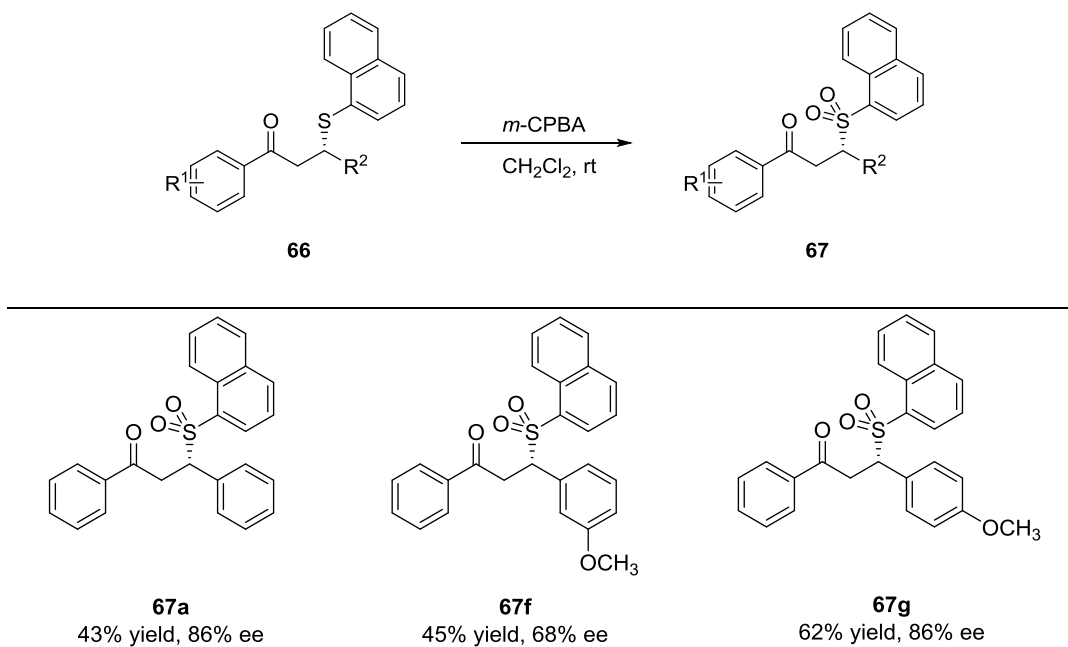
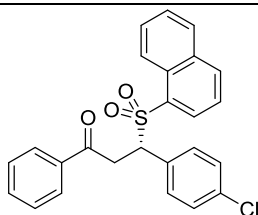


Table 2.11. Continued.^a



67o

28% yield, 66% ee

^a Unless stated otherwise, all reactions were performed with 1 eq β -aryl- β -sulfanyl ketone derivative and 2.2 eq *m*-CPBA in DCM.

Despite all the efforts, the retro sulfa-Michael reaction was inevitable regardless of the nature of the substituent and the target sulfones were obtained with low yields. Small increments in ee were observed when the oxidation was performed to form sulfones **67a**, **67f** and **67g**. However, there was a small loss in enantioselectivity for **67o**.

CHAPTER 3

EXPERIMENTAL

3.1 Materials and Methods

^1H and ^{13}C NMR spectra were recorded on a Bruker Spectrospin Avance DPX 400 spectrometer, at 400 and 100 MHz, respectively and in CDCl_3 . The solvent peaks are observed at δ 7.26 ppm (^1H NMR) and 77.2 ppm (^{13}C NMR); and δ 2.50 ppm (^1H NMR) and 39.5 ppm (^{13}C NMR), respectively. TMS was used as the internal standard and the chemical shifts were reported in ppm. The coupling values (J) are calculated in Hz. The NMR spectra of the previously unknown compounds in the literature can be found in Appendix A.

Enantiometric excess values were determined by Thermo Finnigan and Agilent HPLC systems, using Daicel AD-H, OD-H and IA chiral columns with mixtures of chromatography grade *n*-hexane and *i*-propanol. HPLC chromatograms of chiral products are given in Appendix B.

FTIR analyses were done with a Bruker ATR instrument.

HRMS analyses were done in UNAM, Bilkent University with an Agilent 6224 TOF LC-MS system.

Optical rotation measurements were performed on a Rudolph Scientific Autopol III polarimeter, operating at 589 nm (sodium D-line). Specific rotation values were reported as $[\alpha]_{\text{D}}^{\text{T}}$ with c is in g/100 mL of solvent.

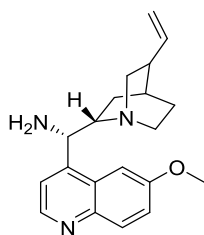
The melting points of solid products that are new to the literature was measured on a MEL-TEMP 1002D apparatus.

The reactions were monitored by thin layer chromatography, using Merck Silica Gel 60 F₂₅₄ plates, pre-coated on aluminum sheets. The TLC plates were visualized by

UV light and phosphomolybdic acid stain. Silica gel 60 F₂₅₄ with mesh size 230-400 was used for flash column chromatography.

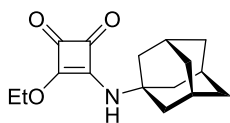
3.2 Synthesis of Bifunctional Quinine-type Organocatalysts

3.2.1 Synthesis of Quinine Amine **77**



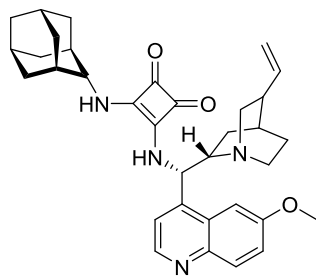
Quinine (10.0 mmol, 3.24 g) and triphenylphosphine (12.0 mmol, 3.15 g) were dissolved in freshly distilled THF (50 mL) and the solution was cooled down to 0 °C. To this cooled solution, diisopropyl azodicarboxylate (12.0 mmol, 2.36 mL) was added all at once, followed by the dropwise addition of a cooled solution of diphenyl phosphoryl azide (12.0 mmol, 2.58 mL) in dry THF (20 mL). After the addition was complete, the solution was allowed to warm up to room temperature. After the reaction mixture was stirred at room temperature for 12 h, it was heated to 50 °C and stirred for an additional 2 h. Then a second portion of triphenylphosphine (13.0 mmol, 3.41 g) was added and the mixture was maintained at 50 °C until the evolution of N₂ gas was ceased (about 2 h). At this point, the mixture was cooled down to room temperature and the reaction was quenched by the addition of 1 mL of distilled water. The solvents were removed in vacuo and the residue was dissolved in a 1:1 mixture of DCM and 10% HCl (aq). Following the extraction, the aqueous phase was washed with DCM (4 x 50 mL). Next, the aqueous phase was made alkaline with concentrated NH₃ and then washed with DCM again (4 x 50 mL). Finally, the organic phases were combined, dried over Na₂SO₄ and concentrated in vacuo. The crude product was purified by column chromatography on silica gel, using EtOAc/MeOH/conc. NH₃ = 50:50:1. The desired product **77** was isolated as an orange-yellow viscous liquid with 75% yield. Analytical data matched previously reported value in the literature.²⁵

Synthesis of 2-Adamantyl Monosquaramide **76b**



Squaric acid (8.8 mmol, 10.0 g) was dissolved in 10 mL of absolute ethanol. The solution was refluxed for 3 h and then the solvent was removed under vacuum. Then 10 mL of ethanol was added once again to the residue and the mixture was heated to reflux again. After 30 minutes, EtOH was evaporated again and the procedure was repeated twice more with 30-minute reflux periods. The final evaporation yields diethyl squarate as a pale-yellow oil. To obtain the 2-adamantyl monosquaramide, the crude diethyl squarate (1.0 mmol, 148 μ L) dissolved in 2 mL of DCM was added to a solution of 2-adamantylamine (1.0 mmol, 151 mg) in 2 mL of DCM at room temperature. The mixture was allowed to stir at room temperature for 24 h. The crude product was purified by column chromatography on silica gel, using 1:4 EtOAc/*n*-hexane as eluent, which afforded the product **76b** as a white solid with 91% yield. Analytical data matched previously reported value in the literature.⁶³

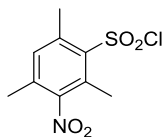
3.2.2 Synthesis of Bifunctional Organocatalyst **58b**



Quinine amine **77** (1.0 mmol, 323.4 mg) was dissolved in MeOH (1 mL) in a screw capped reaction vial. To this mixture, a solution of 2-adamantyl monosquaramide **76b** (1.2 mmol, 330.4 mg) in DCM (2 mL) was added. The resulting reaction mixture was stirred at room temperature for 48 h. The desired organocatalyst **58b** was obtained as an off-white solid with 87% yield after purification with column

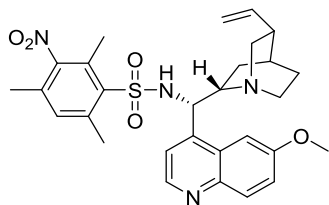
chromatography on silica gel, using 3:1 EtOAc/MeOH as eluent. Analytical data matched previously reported value in the literature.⁶³

3.2.3 Synthesis of 2,4,6-Trimethyl-3-nitrobenzene-1-sulfonyl chloride (**79**)



Fuming nitric acid (47.6 mmol, 2 mL) was added to 2,4,6-trimethylbenzene-1-sulfonyl chloride (**78**) (4 mmol, 874 mg) dropwise in 15 minutes. The reaction mixture was stirred for 1 h at room temperature, then diluted with 20 mL of ice-cold water upon the completion of the reaction. The mixture was extracted with diethyl ether (2 x 25 mL). The organic phases were combined and washed consecutively with 25 mL of cold water, 25 mL of 1% Na₂CO₃ and brine (2 x 25 mL). Combined organic phases were dried on Na₂SO₄ and concentrated in vacuo. The residue was recrystallized from *n*-pentane to yield **79** as white crystals with 43% yield. Analytical data matched previously reported value in the literature.⁶⁷

3.2.4 Synthesis of Bifunctional Catalyst **59**



2,4,6-trimethyl-3-nitrobenzene-1-sulfonyl chloride (**79**) (1.0 mmol, 263.7 mg) was added to a solution of quinine amine **77** (1.0 mmol, 323.4 mg) and triethylamine (1.1 mmol, 140 μ L in DCM (2.5 mL) at 0 °C. The mixture was brought to room temperature and stirred for 48 h. The mixture was then directly loaded onto silica gel column. Elution with EtOAc/MeOH/TEA = 90:10:1 afforded **59** as an off-white solid with 35% yield.

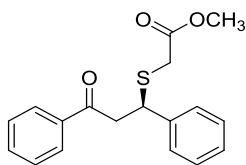
Off-white colored solid, mp 101 °C, 35% yield. $[\alpha]_D^{30} = -135.0$ (*c* 0.780, MeOH). ¹H NMR (400 MHz, CDCl₃) (mixture of rotamers) δ 8.58 (d, *J* = 4.2 Hz, 1H), 8.47 (d,

$J = 4.5$ Hz, 1H), 7.97 (d, $J = 9.1$ Hz, 1H), 7.87 (d, $J = 9.2$ Hz, 1H), 7.74 – 7.53 (m, 1H), 7.50 – 7.45 (m, 1H), 7.44 – 7.31 (m, 1H), 7.20 (d, $J = 4.2$ Hz, 1H), 7.15 (d, $J = 4.5$ Hz, 1H), 6.54 (s, 1H), 6.44 (s, 1H), 5.78 – 5.56 (m, 1H), 5.31 (s, 1H), 5.10 (d, $J = 10.6$ Hz, 1H), 5.04 – 4.85 (m, 1H), 4.46 (d, $J = 10.9$ Hz, 1H), 3.99 (s, 1H), 3.94 (s, 1H), 3.46 (dd, $J = 17.9, 9.4$ Hz, 1H), 3.38 – 3.25 (m, 1H), 3.22 – 3.09 (m, 1H), 3.09 – 2.92 (m, 1H), 2.90 – 2.71 (m, 1H), 2.41 (s, 1H), 2.39 (s, 1H), 2.34 (s, 1H), 2.13 (s, 1H), 2.12 (s, 1H), 1.96 (s, 1H), 1.75 (s, 1H), 1.71 – 1.59 (m, 2H), 1.48 – 1.19 (m, 1H), 1.06 – 0.79 (m, 1H). ^{13}C NMR (100 MHz, CDCl_3) (mixture of rotamers): δ 157.8, 156.8, 151.8, 151.2, 147.0, 146.5, 144.5, 144.2, 141.6, 141.0, 140.9, 140.8, 140.5, 138.9, 135.8, 134.8, 132.6, 132.4, 132.3, 132.1, 132.0, 131.9, 131.8, 131.8, 131.7, 131.3, 130.0, 129.8, 128.4, 128.3, 128.0, 126.3, 123.7, 121.4, 120.2, 119.7, 118.4, 114.7, 103.6, 100.7, 62.9, 61.1, 60.2, 55.8, 55.5, 55.3, 52.8, 40.3, 39.8, 39.4, 39.2, 27.7, 27.5, 27.2, 27.1, 26.1, 24.8, 23.2, 22.5, 16.8, 16.8, 15.9, 15.5, 14.1. IR (neat): 3077, 2934, 2871, 1619, 1589, 1530, 1506, 1475, 1429, 1359, 1262, 1238, 1168, 1138, 1103, 1032, 987, 912, 865, 840, 775, 717, 666, 563, 493 cm^{-1} . HRMS (ESI-TOF) m/z : $[\text{M} + \text{H}]^+$ Calcd. for $\text{C}_{29}\text{H}_{35}\text{N}_4\text{O}_5\text{S}$ 551.2328; Found 551.2339.

3.3 General Procedure for the Synthesis of Products 61a-v

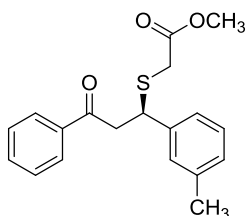
A screw-capped reaction vial was charged with chalcone derivative **60a-v** (0.10 mmol) and organocatalyst **58b** (5.5 mg, 0.010 mmol) and toluene (0.5 mL). The mixture was cooled to -40 °C, then a solution of methyl thioglycolate **47** (18.0 μL , 0.20 mmol) in 0.5 mL of toluene was introduced slowly into the vial with stirring. The mixture was stirred at -40 °C and progress of the reaction was monitored with TLC. Upon the consumption of chalcone derivative, the reaction mixture was directly subjected to flash column chromatography on silica, using *n*-hexanes/ethyl acetate mixture as eluent to yield products **61a-v**.

3.3.1 Methyl 2-((3-oxo-1,3-diphenylpropyl)thio)acetate (61a)



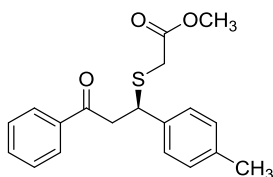
Colorless oil, >99% yield. HPLC (AD-H, 80:20 *n*-Hexane/Isopropanol, 1 mL/min, 254 nm): $t_{\text{minor}} = 10.65$ min, $t_{\text{major}} = 12.90$ min, 97% ee, $[\alpha]_{\text{D}}^{28} = 138.9$ (c 0.567, CHCl_3). Analytical data matched previously reported values in the literature.⁴⁷

3.3.2 Methyl 2-((3-oxo-3-phenyl-1-(*m*-tolyl)propyl)thio)acetate (61b)



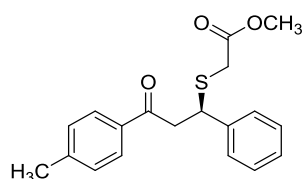
Colorless oil, >99% yield. HPLC (AD-H, 80:20 *n*-Hexane/Isopropanol, 1 mL/min, 254 nm): $t_{\text{minor}} = 9.41$ min, $t_{\text{major}} = 11.25$ min, 95% ee, $[\alpha]_{\text{D}}^{26} = 133.2$ (c 0.547, CHCl_3). Analytical data matched previously reported values in the literature.⁴⁷

3.3.3 Methyl 2-((3-oxo-3-phenyl-1-(*p*-tolyl)propyl)thio)acetate (61c)



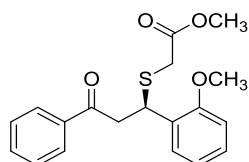
Colorless oil, >99% yield. HPLC (AD-H, 80:20 *n*-Hexane/Isopropanol, 1 mL/min, 254 nm): $t_{\text{minor}} = 13.41$ min, $t_{\text{major}} = 23.05$ min, 96% ee, $[\alpha]_{\text{D}}^{26} = 130.4$ (c 0.547, CHCl_3). Analytical data matched previously reported values in the literature.⁴⁷

3.3.4 Methyl 2-((3-oxo-1-phenyl-3-(p-tolyl)propyl)thio)acetate (61d)



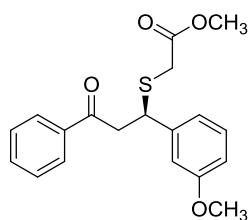
Colorless oil, >99% yield. HPLC (AD-H, 80:20 *n*-Hexane/Isopropanol, 1 mL/min, 254 nm): $t_{\text{minor}} = 18.65$ min, $t_{\text{major}} = 26.65$ min, 97% ee, $[\alpha]_{\text{D}}^{34} = 200.8$ (c 0.520, CHCl_3). Analytical data matched previously reported values in the literature.⁴⁷

3.3.5 Methyl 2-((1-(2-methoxyphenyl)-3-oxo-3-phenylpropyl)thio)acetate (61e)



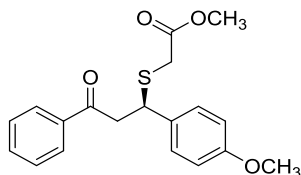
Colorless oil, >99% yield. HPLC (AD-H, 80:20 *n*-Hexane/Isopropanol, 1 mL/min, 254 nm): $t_{\text{minor}} = 10.41$ min, $t_{\text{major}} = 11.95$ min, 82% ee, $[\alpha]_{\text{D}}^{35} = 95.98$ (c 0.835, CHCl_3). Analytical data matched previously reported values in the literature.⁴⁷

3.3.6 Methyl 2-((1-(3-methoxyphenyl)-3-oxo-3-phenylpropyl)thio)acetate (61f)



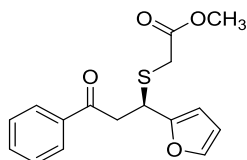
Colorless oil, >99% yield. HPLC (AD-H, 80:20 *n*-Hexane/Isopropanol, 1 mL/min, 254 nm): $t_{\text{minor}} = 13.32$ min, $t_{\text{major}} = 14.84$ min, 96% ee, $[\alpha]_{\text{D}}^{26} = 159.5$ (c 0.574, CHCl_3). Analytical data matched previously reported values in the literature.⁴⁷

3.3.7 Methyl 2-((1-(4-methoxyphenyl)-3-oxo-3-phenylpropyl)thio)acetate (61g)



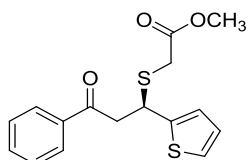
Colorless oil, >99% yield. HPLC (AD-H, 80:20 *n*-Hexane/Isopropanol, 1 mL/min, 254 nm): $t_{\text{minor}} = 29.55$ min, $t_{\text{major}} = 16.05$ min, 99% ee, $[\alpha]_{\text{D}}^{26} = 101.7$ (c 0.574, CHCl_3). Analytical data matched previously reported values in the literature.⁴⁷

3.3.8 Methyl 2-((1-(furan-2-yl)-3-oxo-3-phenylpropyl)thio)acetate (61h)



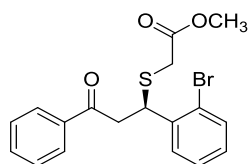
Yellow oil, >99% yield. HPLC (AD-H, 90:10 *n*-Hexane/Isopropanol, 1 mL/min, 254 nm): $t_{\text{minor}} = 19.83$ min, $t_{\text{major}} = 23.21$ min, 91% ee, $[\alpha]_{\text{D}}^{26} = 99.08$ (c 0.476, CHCl_3). ^1H NMR (400 MHz, CDCl_3): δ 7.92 – 7.84 (m, 2H), 7.55 – 7.47 (m, 1H), 7.43 – 7.34 (m, 2H), 7.32 – 7.25 (m, 1H), 6.24 – 6.18 (m, 2H), 4.75 (dd, $J = 7.8, 6.3$ Hz, 1H), 3.71 – 3.64 (m, 1H), 3.63 (s, 3H), 3.53 – 3.45 (m, 1H), 3.13 (s, 2H). ^{13}C NMR (100 MHz, CDCl_3): δ 196.0, 170.6, 152.4, 142.4, 136.5, 133.4, 128.7, 128.1, 110.3, 108.1, 52.5, 41.9, 37.8, 32.9. IR (neat): 2952, 2918, 2850, 1733, 1684, 1596, 1503, 1448, 1436, 1353, 1150, 1011, 761, 741, 689 cm^{-1} . HRMS (ESI-TOF) m/z : $[\text{M} + \text{Na}]^+$ Calcd. for $\text{C}_{16}\text{H}_{16}\text{O}_4\text{SNa}$ 327.0667; Found 327.0677.

3.3.9 Methyl 2-((3-oxo-3-phenyl-1-(thiophen-2-yl)propyl)thio)acetate (61i)



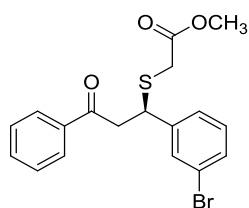
Yellow oil, >99% yield. HPLC (AD-H, 80:20 *n*-Hexane/Isopropanol, 1 mL/min, 254 nm): $t_{\text{minor}} = 13.91$ min, $t_{\text{major}} = 16.13$ min, 95% ee, $[\alpha]_{\text{D}}^{26} = 196.1$ (c 0.487, CHCl_3). ^1H NMR (400 MHz, CDCl_3): δ 7.92 – 7.81 (m, 2H), 7.54 – 7.46 (m, 1H), 7.43 – 7.33 (m, 2H), 7.14 (dd, $J = 5.0, 0.9$ Hz, 1H), 7.03 – 6.95 (m, 1H), 6.82 (dd, $J = 5.1, 3.5$ Hz, 1H), 5.10 – 4.91 (m, 1H), 3.62 (s, 3H), 3.59 – 3.48 (m, 2H), 3.13 (d, $J = 15.1$ Hz, 1H), 3.07 (d, $J = 15.1$ Hz, 1H). ^{13}C NMR (100 MHz, CDCl_3): δ 195.9, 170.6, 145.1, 136.5, 133.4, 128.7, 128.1, 126.6, 126.5, 125.1, 52.5, 45.8, 40.1, 33.0. IR (neat): 2952, 2918, 2850, 1732, 1684, 1608, 1597, 1510, 1448, 1269, 1176, 1129, 1031, 829, 763, 690, 552 cm^{-1} . HRMS (ESI-TOF) m/z : $[\text{M} + \text{Na}]^+$ Calcd. for $\text{C}_{16}\text{H}_{16}\text{O}_3\text{S}_2\text{Na}$ 343.0439; Found 343.0436.

3.3.10 Methyl 2-((1-(2-bromophenyl)-3-oxo-3-phenylpropyl)thio)acetate (61j)



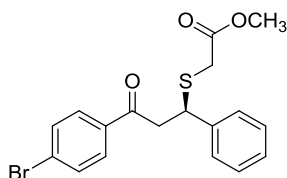
Colorless oil, >99% yield. HPLC (AD-H, 80:20 *n*-Hexane/Isopropanol, 1 mL/min, 254 nm): $t_{\text{minor}} = 12.46$ min, $t_{\text{major}} = 13.47$ min, 81% ee, $[\alpha]_{\text{D}}^{34} = 74.00$ ($c = 0.700$ g/100 mL, CHCl_3). Analytical data matched previously reported value.⁴⁷

3.3.11 Methyl 2-((1-(3-bromophenyl)-3-oxo-3-phenylpropyl)thio)acetate (61k)



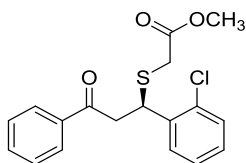
Light yellow oil, >99% yield. HPLC (AD-H, 80:20 *n*-Hexane/Isopropanol, 1 mL/min, 254 nm): $t_{\text{minor}} = 9.83$ min, $t_{\text{major}} = 10.84$ min, 96% ee, $[\alpha]_{\text{D}}^{26} = 149.4$ (c 0.614, CHCl_3). Analytical data matched previously reported value.⁴⁷

3.3.12 Methyl 2-((3-(4-bromophenyl)-3-oxo-1-phenylpropyl)thio)acetate (61l)



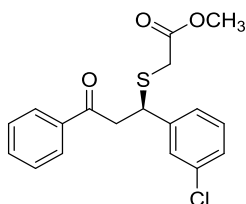
Colorless oil, >99% yield. HPLC (AD-H, 80:20 *n*-Hexane/Isopropanol, 1 mL/min, 254 nm): $t_{\text{minor}} = 21.32$ min, $t_{\text{major}} = 28.58$ min, 96% ee, $[\alpha]_{\text{D}}^{34} = 158.0$ (c 0.775, CHCl_3). Analytical data matched previously reported value.⁴⁷

3.3.13 Methyl 2-((1-(2-chlorophenyl)-3-oxo-3-phenylpropyl)thio)acetate (61m)



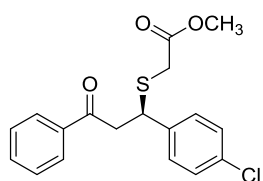
Colorless oil, >99% yield. HPLC (AD-H, 80:20 *n*-Hexane/Isopropanol, 1 mL/min, 254 nm): $t_{\text{minor}} = 11.56$ min, $t_{\text{major}} = 12.73$ min, 95% ee, $[\alpha]_{\text{D}}^{34} = 109.4$ (c 0.633, CHCl_3). Analytical data matched previously reported value.⁴⁷

3.3.14 Methyl 2-((1-(3-chlorophenyl)-3-oxo-3-phenylpropyl)thio)acetate (61n)



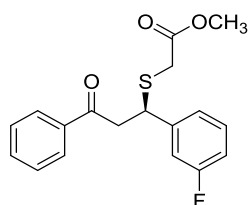
Colorless oil, >99% yield. HPLC (AD-H, 90:10 *n*-Hexane/Isopropanol, 1 mL/min, 254 nm): $t_{\text{minor}} = 12.56$ min, $t_{\text{major}} = 13.78$ min, 96% ee, $[\alpha]_{\text{D}}^{32} = 185.8$ (c 0.483, CHCl_3). Analytical data matched previously reported value.⁴⁷

3.3.15 Methyl 2-((1-(4-chlorophenyl)-3-oxo-3-phenylpropyl)thio)acetate (61o)



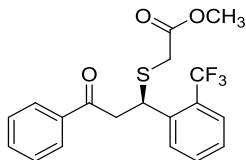
Colorless oil, >99% yield. HPLC (IA, 80:20 *n*-Hexane/Isopropanol, 1 mL/min, 254 nm): $t_{\text{minor}} = 11.34$ min, $t_{\text{major}} = 16.62$ min, 96% ee, $[\alpha]_{\text{D}}^{26} = 182.3$ (c 0.581, CHCl_3). Analytical data matched previously reported value.⁴⁷

3.3.16 Methyl 2-((1-(3-fluorophenyl)-3-oxo-3-phenylpropyl)thio)acetate (61p)



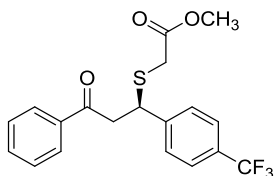
Colorless oil, >99% yield. HPLC (AD-H, 85:15 *n*-Hexane/Isopropanol, 1 mL/min, 254 nm): $t_{\text{minor}} = 11.22$ min, $t_{\text{major}} = 12.36$ min, 95% ee, $[\alpha]_{\text{D}}^{26} = 147.4$ (c 0.554, CHCl_3). ^1H NMR (400 MHz, CDCl_3): δ 7.92 – 7.76 (m, 2H), 7.53 – 7.45 (m, 1H), 7.44 – 7.33 (m, 2H), 7.24 – 7.17 (m, 1H), 7.17 – 7.11 (m, 1H), 7.12 – 7.04 (m, 1H), 6.96 – 6.76 (m, 1H), 4.67 (t, $J = 7.0$ Hz, 1H), 3.61 (s, 3H), 3.51 – 3.49 (m, 2H), 3.05 (d, $J = 15.1$ Hz, 1H), 2.95 (d, $J = 15.1$ Hz, 1H). ^{13}C NMR (100 MHz, CDCl_3): δ 195.9, 170.5, 143.5, 133.4, 130.1, 130.0, 128.7, 128.1, 124.0, 115.1, 114.8, 114.5, 52.4, 44.6, 44.2, 32.9. IR (neat): 3058, 2952, 1727, 1679, 1586, 1482, 1447, 1433, 1295, 1223, 1134, 1001, 981, 890, 791, 757, 680 cm^{-1} . HRMS (ESI-TOF) m/z : $[\text{M} + \text{Na}]^+$ Calcd. for $\text{C}_{18}\text{H}_{17}\text{FO}_3\text{SNa}$ 355.0780; Found 355.0771.

3.3.17 Methyl 2-((3-oxo-3-phenyl-1-(2-(trifluoromethyl)phenyl)propyl)thio)acetate (61q)



Colorless oil, >99% yield. HPLC (AD-H, 80:20 *n*-Hexane/Isopropanol, 1 mL/min, 254 nm): $t_{\text{minor}} = 15.78$ min, $t_{\text{major}} = 19.52$ min, 79% ee, $[\alpha]_{\text{D}}^{32} = 117.2$ (c 0.607, CHCl_3). ^1H NMR (400 MHz, CDCl_3): δ 7.90 – 7.85 (m, 2H), 7.83 (d, $J = 7.9$ Hz, 1H), 7.57 (d, $J = 7.9$ Hz, 1H), 7.54 – 7.47 (m, 2H), 7.42 – 7.36 (m, 2H), 7.30 (t, $J = 7.6$ Hz, 1H), 5.06 (dd, $J = 9.0, 4.7$ Hz, 1H), 3.61 – 3.54 (m, 1H), 3.50 (s, 3H), 3.35 – 3.27 (m, 1H), 3.18 (s, 2H). ^{13}C NMR (100 MHz, CDCl_3): δ 195.6, 170.1, 140.8, 136.5, 133.4, 132.4, 129.7, 128.7, 128.2, 128.2, 127.5, 125.9, 125.8, 52.3, 46.3, 40.9, 34.1. IR (neat): 2953, 2920, 2851, 1739, 1685, 1598, 1581, 1451, 1376, 1312, 1155, 1121, 1061, 1035, 769, 691 cm^{-1} . HRMS (ESI-TOF) m/z : $[\text{M} + \text{Na}]^+$ Calcd. for $\text{C}_{19}\text{H}_{17}\text{F}_3\text{O}_3\text{SNa}$ 405.0748; Found 405.0726.

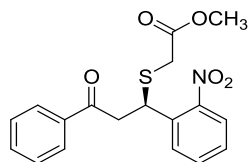
3.3.18 Methyl 2-((3-oxo-3-phenyl-1-(4-(trifluoromethyl)phenyl)propyl)thio)acetate (61r)



Colorless oil, >99% yield. HPLC (AD-H, 80:20 *n*-Hexane/Isopropanol, 1 mL/min, 254 nm): $t_{\text{minor}} = 10.88$ min, $t_{\text{major}} = 22.90$ min, 95% ee, $[\alpha]_{\text{D}}^{25} = 119.3$ (c 0.637, CHCl_3). ^1H NMR (400 MHz, CDCl_3): δ 7.91 – 7.76 (m, 2H), 7.56 – 7.45 (m, 5H), 7.43 – 7.32 (m, 2H), 4.72 (t, $J = 7.1$ Hz, 1H), 3.59 (s, 3H), 3.53 (d, $J = 7.1$ Hz, 2H), 3.08 – 2.87 (m, 2H). ^{13}C NMR (100 MHz, CDCl_3): δ 194.7, 169.3, 144.1, 135.4, 132.5, 128.8, 128.6, 127.7, 127.6, 127.03, 124.6, 51.4, 43.4, 43.2, 31.8. IR (neat): 2954, 2920, 2850, 1730, 1680, 1616, 1596, 1540, 1424, 1364, 1364, 1324, 1273,

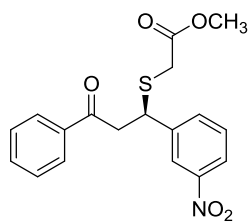
1229, 1155, 1108, 1069, 1001, 822, 689 cm^{-1} . HRMS (ESI-TOF) m/z : $[\text{M} + \text{Na}]^+$
Calcd. for $\text{C}_{19}\text{H}_{17}\text{F}_3\text{O}_3\text{SNa}$ 405.0748; Found 405.0763.

3.3.19 Methyl 2-((1-(2-nitrophenyl)-3-oxo-3-phenylpropyl)thio)acetate (61s)



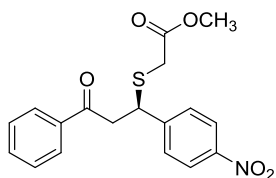
Yellow oil, >99% yield. HPLC (AD-H, 80:20 *n*-Hexane/Isopropanol, 1 mL/min, 254 nm): $t_{\text{minor}} = 25.37$ min, $t_{\text{major}} = 27.70$ min, 68% ee, $[\alpha]_{\text{D}}^{34} = 79.61$ (*c* 0.467, CHCl_3). ^1H NMR (400 MHz, CDCl_3): δ 7.87 – 7.81 (m, 2H), 7.87 – 7.68 (m, 2H), 7.54 – 7.46 (m, 2H), 7.41 – 7.35 (m, 2H), 7.34 – 7.27 (m, 1H), 5.28 (t, $J = 7.1$ Hz, 1H), 3.60 – 3.56 (m, 2H), 3.53 (s, 3H), 3.22 (d, $J = 15.3$ Hz, 1H), 3.16 (d, $J = 15.3$ Hz, 1H). ^{13}C NMR (100 MHz, CDCl_3): δ 195.6, 170.1, 149.9, 136.7, 136.2, 133.5, 133.0, 130.0, 128.7, 128.1, 128.1, 124.3, 77.3, 77.0, 76.7, 52.4, 45.6, 39.7, 33.8. IR (neat): 2953, 2919, 2851, 1730, 1684, 1525, 1458, 1376, 1354, 1261, 1179, 1095, 1047, 1022, 801, 722, 698 cm^{-1} . HRMS (ESI-TOF) m/z : $[\text{M} + \text{Na}]^+$ Calcd. for $\text{C}_{18}\text{H}_{17}\text{NO}_5\text{SNa}$ 382.0725; Found 382.0717.

3.3.20 Methyl 2-((1-(3-nitrophenyl)-3-oxo-3-phenylpropyl)thio)acetate (61t)



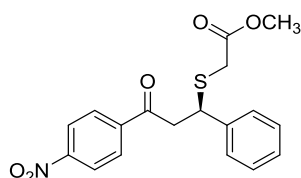
Colorless oil, >99% yield. HPLC (AD-H, 80:20 *n*-Hexane/Isopropanol, 1 mL/min, 254 nm): $t_{\text{minor}} = 17.44$ min, $t_{\text{major}} = 18.82$ min, 76% ee, $[\alpha]_{\text{D}}^{34} = 160.9$ (*c* 0.800, CHCl_3). Analytical data matched previously reported value.⁴⁷

3.3.21 Methyl 2-((1-(4-nitrophenyl)-3-oxo-3-phenylpropyl)thio)acetate (61u)



Yellow oil, >99% yield. HPLC (AD-H, 80:20 *n*-Hexane/Isopropanol, 1 mL/min, 254 nm): $t_{\text{minor}} = 26.03$ min, $t_{\text{major}} = 43.03$ min, 95% ee, $[\alpha]_{\text{D}}^{25} = 161.5$ (*c* 0.559, CHCl₃). Analytical data matched previously reported value.⁴⁷

3.3.22 Methyl 2-((3-(4-nitrophenyl)-3-oxo-1-phenylpropyl)thio)acetate (61v)

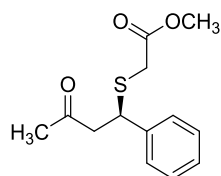


Yellow oil, >99% yield. HPLC (IA, 80:20 *n*-Hexane/Isopropanol, 1 mL/min, 254 nm): $t_{\text{minor}} = 25.82$ min, $t_{\text{major}} = 29.67$ min, 95% ee, $[\alpha]_{\text{D}}^{25} = 100.7$ (*c* 0.562, CHCl₃). Analytical data matched previously reported value.⁴⁷

3.4 General Procedure for the Synthesis of Products 63a-d

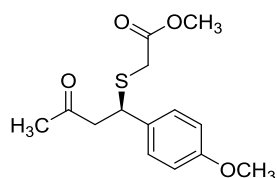
A screw-capped reaction vial was charged with chalcone derivative **62a-d** (0.10 mmol) and organocatalyst **58b** (5.5 mg, 0.010 mmol) and toluene (0.5 mL). Then a solution of methyl thioglycolate **47** (18.0 μ L, 0.20 mmol) in 0.5 mL of toluene was introduced slowly into the vial with stirring at room temperature. The mixture was stirred at ambient temperature and progress of the reaction was monitored with TLC. Upon the consumption of chalcone derivative, the reaction mixture was directly subjected to flash column chromatography on silica, using *n*-hexanes/ethyl acetate mixture as eluent to yield products **63a-d**

3.4.1 Methyl 2-((3-oxo-1-phenylbutyl)thio)acetate (63a)



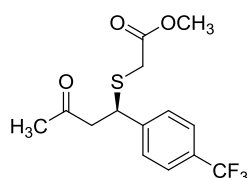
Light yellow oil, 60% yield. HPLC (AD-H, 90:10 *n*-Hexane/Isopropanol, 1 mL/min, 254 nm): $t_{\text{minor}} = 8.26$ min, $t_{\text{major}} = 8.88$ min, 60% ee, $[\alpha]_{\text{D}}^{29} = 139.0$ (c 0.507, CHCl_3). Analytical data matched previously reported value.⁴⁷

3.4.2 Methyl 2-((1-(4-methoxyphenyl)-3-oxobutyl)thio)acetate (63b)



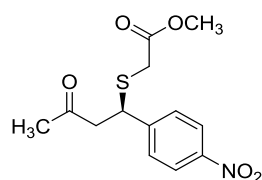
Light yellow oil, 50% yield. HPLC (AD-H, 80:20 *n*-Hexane/Isopropanol, 1 mL/min, 254 nm): $t_{\text{minor}} = 7.33$ min, $t_{\text{major}} = 8.65$ min, 73% ee, $[\alpha]_{\text{D}}^{29} = 116.4$ (c 0.473, CHCl_3). ¹H NMR (400 MHz, CDCl_3): δ 7.23 – 7.16 (m, 2H), 6.84 – 6.72 (m, 2H), 4.41 (t, $J = 7.3$ Hz, 1H), 3.71 (s, 3H), 3.61 (s, 3H), 3.01 – 2.84 (m, 4H), 2.01 (s, 3H). ¹³C NMR (100 MHz, CDCl_3): δ 204.8, 170.6, 158.9, 132.2, 129.0, 113.9, 55.1, 52.2, 49.5, 43.8, 32.5, 30.3. IR (neat): 3000, 2950, 2915, 2838, 1715, 1608, 1583, 1511, 1460, 1436, 1361, 1280, 1248, 1174, 1152, 1132, 1024, 1009, 831, 756, 704, 587, 544 cm^{-1} . HRMS (ESI-TOF) m/z : $[\text{M} + \text{Na}]^+$ Calcd. for $\text{C}_{14}\text{H}_{18}\text{NaO}_4\text{S}$ 305.0823; Found 305.0824.

3.4.3 Methyl 2-((3-oxo-1-(4-(trifluoromethyl)phenyl)butyl)thio)acetate (63c)



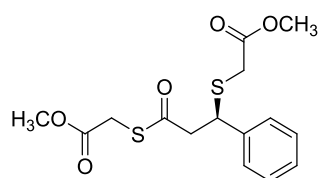
Orange oil, 70% yield. HPLC (AD-H, 90:10 *n*-Hexane/Isopropanol, 1 mL/min, 254 nm): $t_{\text{minor}} = 7.65$ min, $t_{\text{major}} = 9.83$ min, 80% ee, $[\alpha]_{\text{D}}^{29} = 90.22$ (*c* 0.733, CHCl₃). ¹H NMR (400 MHz, CDCl₃): δ 7.47 (dd, *J* = 33.4, 8.2 Hz, 4H), 4.50 (dd, *J* = 7.8, 6.7 Hz, 1H), 3.59 (s, 3H), 3.02 – 2.83 (m, 4H), 2.04 (s, 3H). ¹³C NMR (100 MHz, CDCl₃): δ 204.1, 170.3, 145.0, 128.5, 125.6, 125.6, 125.6, 52.4, 49.2, 43.8, 32.7, 30.3. IR (neat): 2956, 2929, 1719, 1618, 1435, 1420, 1361, 1323, 1281, 1160, 1111, 1068, 1016, 837, 799, 604 cm⁻¹. HRMS (ESI-TOF) *m/z*: [M + Na]⁺ Calcd. for C₁₄H₁₅F₃NaO₃S 343.0592; Found 343.0583.

3.4.4 Methyl 2-((1-(4-nitrophenyl)-3-oxobutyl)thio)acetate (**63d**)



Yellow oil, 68% yield. HPLC (AD-H, 80:20 *n*-Hexane/Isopropanol, 1 mL/min, 254 nm): $t_{\text{minor}} = 12.82$ min, $t_{\text{major}} = 16.07$ min, 74% ee, $[\alpha]_{\text{D}}^{29} = 173.8$ (*c* 0.673, CHCl₃). ¹H NMR (400 MHz, CDCl₃): δ 8.15 – 8.05 (m, 2H), 7.53 – 7.42 (m, 2H), 4.55 (dd, *J* = 8.2, 6.2 Hz, 1H), 3.62 (s, 3H), 3.05 – 2.83 (m, 4H), 2.05 (s, 3H). ¹³C NMR (100 MHz, CDCl₃): δ 203.8, 170.1, 148.5, 147.2, 129.0, 123.8, 52.5, 49.0, 43.5, 32.6, 30.3. IR (neat): 3298, 2956, 2915, 2850, 1730, 1603, 1520, 1468, 1418, 1392, 1348, 1290, 1257, 1215, 1194, 1177, 1100, 1047, 1027, 992, 944, 804, 720 cm⁻¹. HRMS (ESI-TOF) *m/z*: [M - H]⁻ Calcd. For C₁₃H₁₄NO₅S 296.0593; Found 296.0584.

3.5 Procedure for the Synthesis of Product **84**

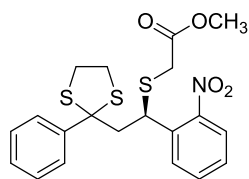


A screw-capped reaction vial was charged with cinnamoyl benzotriazole **82** (0.20 mmol) and organocatalyst **58b** (11.1 mg, 0.020 mmol) and toluene (1.0 mL). Then a solution of methyl thioglycolate **47** (36.0 μ L, 0.40 mmol) in 0.5 mL of toluene

was introduced slowly into the vial with stirring at room temperature. The mixture was stirred at ambient temperature and progress of the reaction was monitored with TLC. Upon the consumption of chalcone derivative, an additional 18.0 μL portion of methyl thioglycolate **47** was added to the reaction mixture and the increment in the relative amount of **84** was observed via regular TLC monitoring. When the reaction reached a plateau in terms of the amount of **84** (2 days), the reaction mixture was directly subjected to flash column chromatography on silica, using *n*-hexane/EtOAc mixture as eluent to yield the pure product.

Light yellow oil, 84% yield. HPLC (AD-H, 80:20 *n*-Hexane/Isopropanol, 1 mL/min, 254 nm): $t_{\text{minor}} = 11.557$ min, $t_{\text{major}} = 13.003$ min, 83% ee, $[\alpha]_{\text{D}}^{23} = 139.7$ (*c* 0.470, CHCl_3). ^1H NMR (400 MHz, CDCl_3): 7.33 – 7.23 (m, 4H), 7.22 – 7.15 (m, 1H), 4.59 – 4.34 (m, 1H), 3.61 (s, 3H), 3.60 (s, $J = 4.2$ Hz, 3H), 3.58 (s, 2H), 3.18 – 3.05 (m, 2H), 3.00 (d, $J = 15.1$ Hz, 1H), 2.89 (d, $J = 15.1$ Hz, 1H). ^{13}C NMR (100 MHz, CDCl_3): δ 194.0, 170.4, 168.8, 139.4, 131.6, 128.7, 128.0, 52.7, 52.4, 49.3, 45.5, 32.7, 31.1. IR (neat): 2952, 2920, 2850, 1936, 1692, 1493, 1453, 1435, 1406, 1379, 1296, 1157, 1135, 1049, 1005, 886, 801, 770, 585, 529 cm^{-1} . HRMS (ESI-TOF) m/z : $[\text{M} + \text{Na}]^+$ Calcd. for $\text{C}_{15}\text{H}_{18}\text{NaO}_5\text{S}_2$ 365.0493; Found 365.0493.

3.6 Procedure for the Dithiolane Protection of Sulfa-Michael Adduct **88**

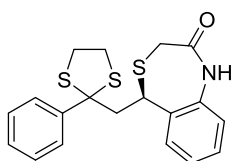


To a solution of the sulfa-Michael product **61s** (0.790 mmol, 284 mg) and 1,2-ethanedithiol (0.96 mmol, 79.5 μL) in 4.5 mL CHCl_3 , I_2 (0.079 mmol, 20 mg) was added and the resulting mixture was stirred at room temperature until the starting material was consumed (5h). The progress of reaction was monitored with TLC. After completion, the reaction was quenched by adding 4 mL of 0.1 M Na_2SO_4 (aq) and 4 mL of 10% NaOH (aq), then extracted with CHCl_3 . The organic layer was washed with H_2O , then dried over MgSO_4 and concentrated in vacuo. The crude

product was purified by flash column chromatography with *n*-hexane/EtOAc = 5:1 as eluent to yield the protected adduct, **88**.

Dark yellow oil, 61% yield. ¹H NMR (400 MHz, CDCl₃) δ 7.62 (dd, *J* = 8.1, 1.2 Hz, 1H), 7.57 (d, *J* = 7.9 Hz, 1H), 7.54 – 7.49 (m, 2H), 7.45 – 7.38 (m, 1H), 7.26 – 7.20 (m, 1H), 7.20 – 7.06 (m, 3H), 4.75 – 4.53 (m, 1H), 3.47 (s, 3H), 3.31 – 3.20 (m, 2H), 3.17 – 2.98 (m, 5H), 2.92 (dd, *J* = 14.9, 5.3 Hz, 1H). δ ¹³C NMR (100 MHz, CDCl₃): δ 169.9, 149.5, 142.9, 136.6, 133.0, 131.0, 130.7, 129.0, 128.0, 124.2, 121.4, 72.3, 52.4, 51.4, 39.8, 39.2, 33.4. IR (neat): 3057, 3027, 3000, 2949, 2922, 2841, 1733, 1604, 1577, 1524, 1489, 1434, 1350, 1275, 1191, 1154, 1126, 1081, 1004, 979, 877, 855, 784, 762, 699, 666, 638, 562, 429 cm⁻¹. MS (MALDI-TOF) *m/z*: [M + Na]⁺ Calcd. For C₂₀H₂₁NNaO₄S₃ 458.0530; Found 458.0537.

3.7 Procedure for Synthesis of Benzothiazepinone Derivative **81**



To a solution of nitro compound **88** (0.295 mmol, 128.5 mg) in 1.5 mL EtOH, Fe powder (0.885 mmol, 49.4 mg) and 0.1 N HCl solution (0.3 mL) was added consecutively. The resulting mixture was stirred vigorously at 80 °C until the completion of reaction (40 min), which was monitored by TLC. After completion, the reaction mixture was cooled down to room temperature, diluted with 2 mL EtOAc and filtered through a celite pad. The filtrate was then washed with saturated NaHCO₃ (1.5 mL). The aqueous phase was back-extracted with EtOAc (2x1 mL). Then the organic phases were combined and dried over MgSO₄ and concentrated. The crude product was purified by column chromatography (1:10 EtOAc/*n*-hexanes) to yield **81**.

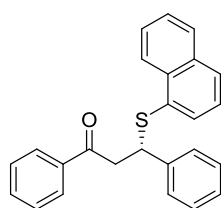
Dark yellow oil, 51% yield. HPLC (AD-H, 80:20 *n*-Hexane/Isopropanol, 1 mL/min, 254 nm): *t*_{minor} = 22.955 min, *t*_{major} = 25.613 min, 17% ee, [α]_D²³ = 13.18 (*c* 0.565, CHCl₃). ¹H NMR (400 MHz, CDCl₃): δ 7.69 – 7.54 (m, 2H), 7.24 – 7.18 (m, 2H),

7.16 – 7.09 (m, 1H), 6.96 (td, $J = 7.8, 1.5$ Hz, 1H), 6.83 (s, $J = 72.3$ Hz, 1H), 6.83 (s, 1H), 6.60 – 6.44 (m, 2H), 3.95 (dd, $J = 7.5, 4.6$ Hz, 1H), 3.49 (s, 2H), 3.31 – 3.15 (m, 3H), 3.12 – 3.01 (m, 2H), 2.93 – 2.78 (m, 2H). ^{13}C NMR (100 MHz, CDCl_3): δ 170.7, 145.2, 144.2, 128.5, 128.1, 128.0, 127.3, 127.2, 118.4, 117.0, 73.5, 52.3, 39.3, 38.9, 32.8, 29.7. IR (neat): 3425, 3413, 3345, 3055, 3021, 2948, 2921, 2850, 1730, 1675, 1619, 1600, 1580, 1491, 1454, 1441, 1434, 1380, 1274, 1194, 1156, 1130, 1081, 1031, 1001, 979, 851, 748, 697, 638, 573, 543, 531, 495, 480, 467 cm^{-1} . MS (MALDI-TOF) m/z : $[\text{M} + \text{Na}]^+$ Calcd. For $\text{C}_{19}\text{H}_{19}\text{NNaOS}_3$ 396.0526; Found 396.0531.

3.8 General Procedure for the Synthesis of Products 66a-x

A screw-capped reaction vial was charged with *trans*-chalcone derivative (0.20 mmol) and organocatalyst **59** (1.1 mg, 0.0020 mmol) and 0.5 mL of THF or DCM. Then a solution of 1-thionaphthol **47** (55. μL , 0.40 mmol) in 0.5 mL of the selected solvent was introduced slowly into the vial with stirring. The mixture was stirred at room temperature and progress of the reaction was monitored with TLC. Upon the consumption of the chalcone derivative, the reaction mixture was directly subjected to flash column chromatography, using *n*-hexane/EtOAc as eluent to yield β -aryl- β -sulfanyl ketones **66a-x**.

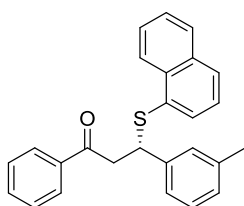
3.8.1 3-(Naphthalen-1-ylthio)-1,3-diphenylpropan-1-one (66a)



White solid, mp 99 $^{\circ}\text{C}$, 93% yield. HPLC (AD-H, 99:1 *n*-Hexane/Isopropanol, 0.8 mL/min, 220 nm): $t_{\text{minor}} = 33.445$ min, $t_{\text{major}} = 35.736$ min, 83% ee, $[\alpha]_{\text{D}}^{23} = -70.25$ (c 1.785, CHCl_3). ^1H NMR (400 MHz, CDCl_3): δ 8.42 (d, $J = 8.6$ Hz, 1H), 7.77 – 7.71 (m, 3H), 7.68 (d, $J = 8.2$ Hz, 1H), 7.48 – 7.38 (m, 4H), 7.31 (t, $J = 7.7$ Hz, 2H), 7.21 – 7.15 (m, 3H), 7.15 – 7.04 (m, 3H), 4.88 (dd, $J = 7.9, 6.3$ Hz, 1H), 3.61 (dd, $J =$

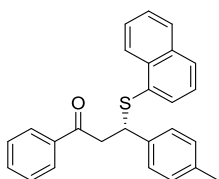
17.2, 8.0 Hz, 1H), 3.53 (dd, $J = 17.2, 6.2$ Hz, 1H). ^{13}C NMR (100 MHz, CDCl_3): δ 197.0, 141.2, 136.7, 134.5, 134.1, 133.3, 133.2, 131.3, 129.1, 128.6, 128.6, 128.5, 128.1, 127.8, 127.4, 126.8, 126.3, 125.8, 125.5, 48.9, 44.7. δ IR (neat): 3053, 3027, 2891, 2878, 1678, 1595, 1501, 1449, 1418, 1368, 1340, 1251, 1225, 1078, 1019, 1002, 981, 921, 801, 769, 750, 711, 689, 667, 642, 624, 599, 565, 549, 530, 419 cm^{-1} . MS (MALDI-TOF) m/z : $[\text{M} + \text{Na}]^+$ Calcd. for $\text{C}_{25}\text{H}_{20}\text{NaOS}$ 391.113; Found 391.133.

3.8.2 3-(Naphthalen-1-ylthio)-1-phenyl-3-(m-tolyl)propan-1-one (66b)



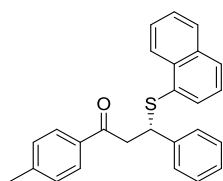
White solid, mp 56 °C, 87% yield. HPLC (OD-H, 99:1 *n*-Hexane/Isopropanol, 0.8 mL/min, 220 nm): $t_{\text{minor}} = 16.063$ min, $t_{\text{major}} = 14.139$ min, 78% ee, $[\alpha]_{\text{D}}^{24} = -111.4$ (c 1.660, CHCl_3). ^1H NMR (400 MHz, CDCl_3): δ 8.42 (d, $J = 8.2$ Hz, 1H), 7.75 (d, $J = 7.4$ Hz, 3H), 7.69 (d, $J = 8.2$ Hz, 1H), 7.54 – 7.38 (m, 4H), 7.31 (t, $J = 7.6$ Hz, 2H), 7.23 (t, $J = 7.7$ Hz, 1H), 7.02 (dd, $J = 15.1, 7.7$ Hz, 3H), 6.90 (d, $J = 6.6$ Hz, 1H), 4.95 – 4.76 (m, 1H), 3.62 (dd, $J = 17.2, 8.1$ Hz, 1H), 3.51 (dd, $J = 17.2, 6.0$ Hz, 1H), 2.17 (s, 3H). ^{13}C NMR (100 MHz, CDCl_3): δ 197.1, 140.9, 138.0, 136.7, 134.4, 134.0, 133.2, 133.1, 131.5, 129.0, 128.6, 128.5, 128.3, 128.2, 128.1, 126.7, 126.2, 125.8, 125.4, 124.7, 48.3, 44.7, 21.4. IR (neat): 3054, 3022, 2920, 2852, 1681, 1594, 1502, 1448, 1415, 1363, 1334, 1249, 1216, 1055, 1019, 1000, 979, 877, 801, 784, 768, 754, 727, 713, 684, 638, 624, 602, 573, 534, 510, 443, 421 cm^{-1} . MS (MALDI-TOF) m/z : $[\text{M} + \text{Na}]^+$ Calcd. for $\text{C}_{26}\text{H}_{22}\text{NaOS}$ 405.129; Found 405.147.

3.8.3 3-(Naphthalen-1-ylthio)-1-phenyl-3-(p-tolyl)propan-1-one (66c)



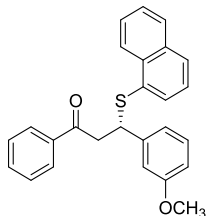
White solid, mp 102 °C, 94% yield. HPLC (AD-H, 98:2 *n*-Hexane/Isopropanol, 0.8 mL/min, 254 nm): $t_{\text{minor}} = 15.832$ min, $t_{\text{major}} = 14.441$ min, 94% ee, $[\alpha]_{\text{D}}^{23} = -91.42$ (*c* 0.480, CHCl₃). ¹H NMR (400 MHz, CDCl₃): δ 8.43 (d, *J* = 8.3 Hz, 1H), 7.77 – 7.70 (m, 3H), 7.68 (d, *J* = 8.2 Hz, 1H), 7.51 – 7.39 (m, 4H), 7.30 (t, *J* = 7.7 Hz, 2H), 7.26 – 7.19 (m, 1H), 7.14 – 7.06 (m, 2H), 6.95 (d, *J* = 7.9 Hz, 2H), 4.87 (dd, *J* = 8.3, 5.9 Hz, 1H), 3.60 (dd, *J* = 17.1, 8.3 Hz, 1H), 3.49 (dd, *J* = 17.1, 5.9 Hz, 1H), 2.19 (s, 3H). ¹³C NMR (100 MHz, CDCl₃): δ 197.2, 138.1, 137.1, 136.7, 134.4, 134.1, 133.2, 132.9, 131.6, 129.2, 129.0, 128.6, 128.1, 127.7, 126.8, 126.3, 125.8, 125.5, 48.1, 44.9, 21.2. IR (neat): 3053, 3030, 2944, 2922, 2892, 2861, 1681, 1595, 1515, 1502, 1449, 1417, 1361, 1334, 1307, 1251, 1226, 1155, 1113, 1062, 1019, 1001, 978, 954, 918, 801, 770, 759, 733, 701, 684, 649, 623, 583, 564, 534, 521, 435, 417 cm⁻¹. MS (MALDI-TOF) *m/z*: [M + Na]⁺ Calcd. for C₂₆H₂₂NaOS 405.129; Found 405.190.

3.8.4 3-(Naphthalen-1-ylthio)-3-phenyl-1-(*p*-tolyl)propan-1-one (66d)



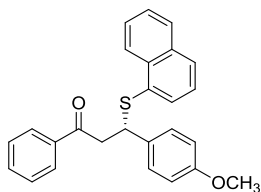
White solid, mp 110-112 °C, >99% yield. HPLC (AD-H, 98:2 *n*-Hexane/Isopropanol, 0.8 mL/min, 254 nm): $t_{\text{minor}} = 22.531$ min, $t_{\text{major}} = 20.044$ min, 91% ee, $[\alpha]_{\text{D}}^{24} = -74.25$ (*c* 1.910, CHCl₃). ¹H NMR (400 MHz, CDCl₃): δ 8.41 (d, *J* = 8.3 Hz, 1H), 7.79 – 7.57 (m, 4H), 7.42 (dq, *J* = 15.4, 6.8 Hz, 3H), 7.27 – 6.98 (m, 8H), 4.88 (dd, *J* = 7.7, 6.4 Hz, 1H), 3.53 (qd, *J* = 17.1, 7.1 Hz, 2H), 2.26 (s, 3H). ¹³C NMR (100 MHz, CDCl₃): δ 196.6, 144.1, 141.3, 134.4, 134.3, 134.1, 133.1, 131.4, 129.3, 129.0, 128.5, 128.4, 128.2, 127.8, 127.4, 126.8, 126.2, 125.8, 125.4, 48.5, 44.6, 21.7. IR (neat): 3053, 3029, 2962, 2894, 1666, 1604, 1498, 1456, 1421, 1362, 1328, 1307, 1230, 118, 1019, 972, 942, 815, 800, 767, 698, 666, 594, 559, 524, 491, 456, 416 cm⁻¹. MS (MALDI-TOF) *m/z*: [M + Na]⁺ Calcd. for C₂₆H₂₂NaOS 405.129; Found 405.147.

**3.8.5 3-(3-Methoxyphenyl)-3-(naphthalen-1-ylthio)-1-phenylpropan-1-one
(66f)**



White solid, mp 46-47 °C, >99% yield. HPLC (OD-H, 90:10 *n*-Hexane/Isopropanol, 1 mL/min, 230 nm): $t_{\text{minor}} = 10.575$ min, $t_{\text{major}} = 9.406$ min, 63% ee, $[\alpha]_{\text{D}}^{24} = -92.87$ (*c* 2.100, CHCl₃). ¹H NMR (400 MHz, CDCl₃): δ 8.42 (d, *J* = 8.2 Hz, 1H), 7.75 (t, *J* = 7.3 Hz, 3H), 7.69 (d, *J* = 8.2 Hz, 1H), 7.52 – 7.38 (m, 4H), 7.32 (t, *J* = 7.6 Hz, 2H), 7.26 – 7.19 (m, 1H), 7.05 (t, *J* = 7.9 Hz, 1H), 6.79 (d, *J* = 7.6 Hz, 1H), 6.67 (d, *J* = 17.9 Hz, 1H), 6.62 (dd, *J* = 8.1, 2.0 Hz, 1H), 4.93 – 4.79 (m, 1H), 3.68 – 3.48 (m, 5H). ¹³C NMR (100 MHz, CDCl₃): δ 195.5, 158.0, 141.3, 135.3, 133.0, 132.6, 131.8, 131.7, 129.9, 128.0, 127.6, 127.1, 127.0, 126.6, 125.3, 124.8, 124.3, 124.0, 118.6, 111.9, 111.5, 53.7, 46.9, 43.2. IR (neat): 3055, 3001, 2959, 2918, 2836, 1710, 1685, 1597, 1489, 1448, 1359, 1260, 1221, 1157, 1090, 1042, 981, 873, 774, 692, 530 cm⁻¹. MS (MALDI-TOF) *m/z*: [M + Na]⁺ Calcd. for C₂₆H₂₂NaO₂S 421.124; Found 421.137.

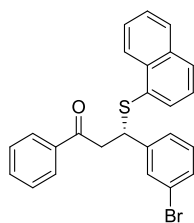
**3.8.6 3-(4-Methoxyphenyl)-3-(naphthalen-1-ylthio)-1-phenylpropan-1-one
(66g)**



White solid, mp 102 °C, 93% yield. HPLC (AD-H, 90:10 *n*-Hexane/Isopropanol, 1 mL/min, 220 nm): $t_{\text{minor}} = 15.595$ min, $t_{\text{major}} = 13.816$ min, 84% ee, $[\alpha]_{\text{D}}^{23} = -120.0$ (*c* 1.845, CHCl₃). ¹H NMR (400 MHz, CDCl₃): δ 8.42 (d, *J* = 8.3 Hz, 1H), 7.79 – 7.69 (m, 3H), 7.67 (d, *J* = 8.2 Hz, 1H), 7.51 – 7.37 (m, 4H), 7.29 (t, *J* = 7.7 Hz, 2H), 7.21

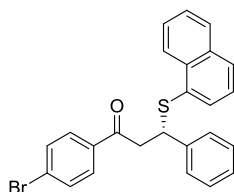
(dd, $J = 8.0, 7.4$ Hz, 1H), 7.13 – 7.07 (m, 2H), 6.73 – 6.60 (m, 2H), 4.86 (dd, $J = 8.3, 5.9$ Hz, 1H), 3.63 (s, $J = 6.0$ Hz, 3H), 3.58 (dd, $J = 17.1, 8.4$ Hz, 1H), 3.47 (dd, $J = 17.1, 5.9$ Hz, 1H). ^{13}C NMR (100 MHz, CDCl_3): δ 197.2, 158.8, 136.8, 134.4, 133.2, 133.1, 133.0, 131.6, 129.0, 128.9, 128.6, 128.5, 128.1, 126.7, 126.2, 125.8, 125.5, 113.8, 55.2, 47.9, 44.9. IR (neat): 3051, 3006, 2953, 2931, 2891, 2834, 1681, 1609, 1594, 1512, 1448, 1415, 1363, 1334, 1293, 1247, 1223, 1176, 1107, 1060, 1029, 1000, 977, 954, 918, 850, 813, 800, 767, 736, 723, 699, 684, 667, 647, 621, 588, 564, 529, 427, 414 cm^{-1} . MS (MALDI-TOF) m/z : $[\text{M} + \text{Na}]^+$ Calcd. for $\text{C}_{26}\text{H}_{22}\text{NaO}_2\text{S}$ 421.124; Found 421.154.

3.8.7 3-(3-Bromophenyl)-3-(naphthalen-1-ylthio)-1-phenylpropan-1-one (66k)



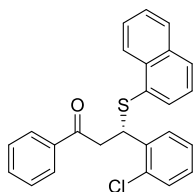
White solid, mp 84 °C, 66% yield. HPLC (OD-H, 90:10 *n*-Hexane/Isopropanol, 1 mL/min, 254 nm): $t_{\text{minor}} = 8.699$ min, $t_{\text{major}} = 7.584$ min, 51% ee, $[\alpha]_{\text{D}}^{24} = -145.1$ (c 1.480, CHCl_3). ^1H NMR (400 MHz, CDCl_3): δ 8.39 (d, $J = 8.2$ Hz, 1H), 7.82 – 7.63 (m, 4H), 7.43 (dd, $J = 15.1, 7.6$ Hz, 4H), 7.37 – 7.27 (m, 3H), 7.29 – 7.11 (m, 2H), 7.03 (d, $J = 7.6$ Hz, 1H), 6.94 (t, $J = 7.8$ Hz, 1H), 4.80 (t, $J = 7.0$ Hz, 1H), 3.55 (d, $J = 7.0$ Hz, 2H). ^{13}C NMR (100 MHz, CDCl_3): δ 195.5, 142.6, 135.4, 133.4, 133.0, 132.7, 132.3, 129.7, 129.5, 129.3, 128.8, 128.4, 127.6, 127.5, 127.0, 125.8, 125.5, 125.3, 124.6, 124.3, 121.3, 46.8, 43.3. IR (neat): 3056, 3041, 2927, 2892, 1680, 1594, 1565, 1501, 1475, 1448, 1429, 1415, 1357, 1329, 1219, 1151, 1061, 983, 953, 918, 878, 811, 795, 768, 753, 716, 685, 667, 638, 604, 570, 533, 508, 445, 433, 419 cm^{-1} . MS (MALDI-TOF) m/z : $[\text{M} + \text{Na}]^+$ Calcd. for $\text{C}_{25}\text{H}_{19}\text{BrNaOS}$ 469.024; Found 469.024.

3.8.8 1-(4-Bromophenyl)-3-(naphthalen-1-ylthio)-3-phenylpropan-1-one (66l)



White solid, mp 162-163 °C, >99% yield. HPLC (AD-H, 98:2 *n*-Hexane/Isopropanol, 1 mL/min, 254 nm): $t_{\text{minor}} = 16.944$ min, $t_{\text{major}} = 17.723$ min, 82% ee, $[\alpha]_{\text{D}}^{24} = -53.21$ (*c* 1.260, CHCl₃). ¹H NMR (400 MHz, CDCl₃): δ 8.40 (d, *J* = 8.2 Hz, 1H), 7.70 (dd, *J* = 23.8, 8.0 Hz, 2H), 7.56 (d, *J* = 8.4 Hz, 2H), 7.51 – 7.31 (m, 5H), 7.27 – 6.99 (m, 6H), 4.84 (t, *J* = 7.0 Hz, 1H), 3.65 – 3.31 (m, 2H). ¹³C NMR (100 MHz, CDCl₃): δ 194.3, 139.1, 133.6, 132.6, 132.3, 131.5, 130.1, 129.4, 127.8, 127.4, 126.8, 126.7, 126.7, 126.0, 125.7, 125.1, 124.5, 123.9, 123.7, 46.6, 42.9. IR (neat): 3055, 3030, 2899, 1682, 1583, 1500, 1452, 1396, 1365, 1331, 1220, 1177, 1070, 1007, 983, 823, 799, 774, 721, 699, 661, 626, 601, 557, 524, 470, 448, 419 cm⁻¹. MS (MALDI-TOF) *m/z*: [M + Na]⁺ Calcd. for C₂₅H₁₉BrNaOS 469.024; Found 469.058.

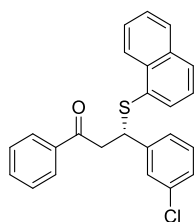
3.8.9 3-(2-Chlorophenyl)-3-(naphthalen-1-ylthio)-1-phenylpropan-1-one (66m)



White solid, mp 54-55 °C, 84% yield. HPLC (OD-H, 90:10 *n*-Hexane/Isopropanol, 1 mL/min, 254 nm): $t_{\text{minor}} = 7.968$ min, $t_{\text{major}} = 9.813$ min, 66% ee, $[\alpha]_{\text{D}}^{24} = -4.622$ (*c* 1.350, CHCl₃). ¹H NMR (400 MHz, CDCl₃): δ 8.73 – 8.41 (m, 1H), 7.97 – 7.79 (m, 4H), 7.68 – 7.52 (m, 4H), 7.50 – 7.32 (m, 5H), 7.18 (dd, *J* = 8.8, 5.1 Hz, 2H), 5.54 (t, *J* = 7.1 Hz, 1H), 3.72 (qd, *J* = 17.3, 7.2 Hz, 2H). ¹³C NMR (100 MHz, CDCl₃): δ 196.6, 138.5, 136.5, 134.7, 134.0, 133.9, 133.5, 133.3, 130.7, 129.8, 129.3, 128.6, 128.4, 128.4, 128.1, 126.9, 126.7, 126.2, 125.8, 125.4, 44.7, 44.2. IR (neat): 3052,

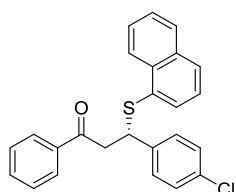
2916, 2894, 1687, 1581, 1502, 1472, 1447, 1357, 1312, 1264, 1243, 1202, 1160, 1061, 1032, 981, 911, 797, 770, 749, 732, 679, 650, 588, 557, 538, 503, 459, 418 cm^{-1} . MS (MALDI-TOF) m/z : $[\text{M} + \text{Na}]^+$ Calcd. for $\text{C}_{25}\text{H}_{19}\text{ClNaOS}$ 425.074; Found 425.131.

3.8.10 3-(3-Chlorophenyl)-3-(naphthalen-1-ylthio)-1-phenylpropan-1-one (66n)



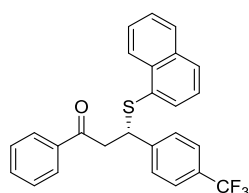
White solid, mp 85 °C, 79% yield. HPLC (OD-H, 95:5 *n*-Hexane/Isopropanol, 1 mL/min, 220 nm): $t_{\text{minor}} = 9.514$ min, $t_{\text{major}} = 8.199$ min, 85% ee, $[\alpha]_{\text{D}}^{23} = -132.7$ (c 1.590, CHCl_3). ^1H NMR (400 MHz, CDCl_3): δ 8.39 (d, $J = 8.3$ Hz, 1H), 7.88 – 7.64 (m, 4H), 7.54 – 7.38 (m, 4H), 7.33 (t, $J = 7.7$ Hz, 2H), 7.26 – 7.19 (m, 1H), 7.17 (s, 1H), 7.10 – 6.92 (m, 3H), 4.82 (t, $J = 7.1$ Hz, 1H), 3.67 – 3.45 (m, 2H). ^{13}C NMR (100 MHz, CDCl_3): δ 196.6, 143.4, 136.5, 134.5, 134.2, 134.1, 133.7, 133.4, 130.7, 129.6, 129.5, 128.7, 128.6, 128.1, 127.9, 127.5, 126.9, 126.3, 126.1, 125.7, 125.4, 47.9, 44.4. IR (neat): 3054, 3029, 2951, 2920, 2851, 1681, 1593, 1570, 1500, 1431, 1412, 1364, 1333, 1254, 1226, 1185, 1163, 1076, 1001, 984, 904, 834, 798, 769, 752, 729, 683, 64, 625, 604, 533, 508, 436, 419 cm^{-1} . MS (MALDI-TOF) m/z : $[\text{M} + \text{Na}]^+$ Calcd. for $\text{C}_{25}\text{H}_{19}\text{ClNaOS}$ 425.074; Found 425.087.

3.8.11 3-(4-Chlorophenyl)-3-(naphthalen-1-ylthio)-1-phenylpropan-1-one (66o)



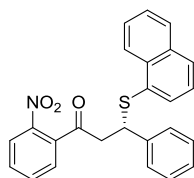
White solid, mp 121-122 °C, >99% yield. HPLC (AD-H, 90:10 *n*-Hexane/Isopropanol, 1 mL/min, 220 nm): $t_{\text{minor}} = 11.144$ min, $t_{\text{major}} = 9.939$ min, 71 ee, $[\alpha]_{\text{D}}^{24} = -125.2$ (c 2.090, CHCl_3). $^1\text{H NMR}$ (400 MHz, CDCl_3): δ 8.40 (d, $J = 8.2$ Hz, 1H), 7.88 – 7.72 (m, 3H), 7.70 (d, $J = 8.2$ Hz, 1H), 7.55 – 7.38 (m, 4H), 7.33 (t, $J = 7.7$ Hz, 2H), 7.21 (dd, $J = 14.7, 6.8$ Hz, 1H), 7.13 – 7.03 (m, 4H), 4.83 (dd, $J = 7.7, 6.5$ Hz, 1H), 3.70 – 3.42 (m, 2H). $^{13}\text{C NMR}$ (100 MHz, CDCl_3): δ 196.7, 139.9, 136.6, 134.5, 134.1, 133.5, 133.4, 133.0, 130.8, 129.4, 129.1, 128.7, 128.6, 128.5, 128.1, 126.9, 126.3, 125.7, 125.5, 77.4, 77.1, 76.8, 47.8, 44.5. IR (neat): 3050, 3028, 2926, 2897, 1679, 1595, 1493, 1450, 1418, 1359, 1332, 1226, 1154, 1091, 1015, 976, 954, 917, 853, 815, 799, 769, 751, 732, 683, 656, 619, 571, 531, 505, 430 cm^{-1} . MS (MALDI-TOF) m/z : $[\text{M} + \text{Na}]^+$ Calcd. for $\text{C}_{25}\text{H}_{19}\text{ClNaOS}$ 425.074; Found 425.086.

3.8.12 3-(Naphthalen-1-ylthio)-1-phenyl-3-(4-(trifluoromethyl)phenyl)propan-1-one (66r)



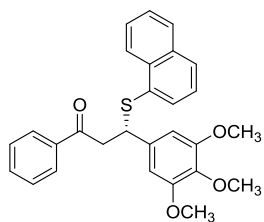
White solid, mp 118 °C, 91% yield. HPLC (AD-H, 90:10 *n*-Hexane/Isopropanol, 1 mL/min, 254 nm): $t_{\text{minor}} = 8.847$ min, $t_{\text{major}} = 7.195$ min, 67% ee, $[\alpha]_{\text{D}}^{23} = -74.02$ (c 1.730, CHCl_3). $^1\text{H NMR}$ (400 MHz, CDCl_3): δ 8.37 (d, $J = 7.8$ Hz, 1H), 7.88 – 7.68 (m, 4H), 7.54 – 7.30 (m, 8H), 7.28 – 7.16 (m, 3H), 4.89 (t, $J = 7.1$ Hz, 1H), 3.78 – 3.50 (m, 2H). $^{13}\text{C NMR}$ (100 MHz, CDCl_3): δ 195.4, 144.3, 135.4, 133.4, 133.0, 132.7, 132.4, 129.3, 128.6, 128.3 (q, $J = 32.3$ Hz), 127.6, 127.5, 127.0, 127.0, 125.9, 125.3, 124.5, 124.3, 124.3 (dd, $J = 7.5, 3.8$ Hz), 46.9, 43.5. IR (neat): 3050, 2939, 2902, 1677, 1618, 1596, 1503, 1450, 1426, 1365, 1328, 1226, 1157, 1123, 1072, 1018, 986, 954, 918, 860, 821, 797, 769, 758, 708, 684, 647, 634, 620, 601, 563, 529, 425 cm^{-1} . MS (MALDI-TOF) m/z : $[\text{M} + \text{Na}]^+$ Calcd. for $\text{C}_{26}\text{H}_{19}\text{F}_3\text{NaOS}$ 459.101; Found 459.123.

3.8.13 3-(Naphthalen-1-ylthio)-3-(4-nitrophenyl)-1-phenylpropan-1-one (66u)



Yellow solid, mp 129-130 °C, 81% yield. HPLC (AD-H, 90:10 *n*-Hexane/Isopropanol, 1 mL/min, 210 nm): $t_{\text{minor}} = 26.461$ min, $t_{\text{major}} = 24.532$ min, 68% ee, $[\alpha]_{\text{D}}^{23} = -153.6$ (*c* 1.665, CHCl_3). $^1\text{H NMR}$ (400 MHz, CDCl_3): δ 8.37 (d, $J = 8.1$ Hz, 1H), 7.92 (d, $J = 8.7$ Hz, 2H), 7.83 – 7.68 (m, 4H), 7.54 – 7.40 (m, 3H), 7.37 (t, $J = 7.6$ Hz, 3H), 7.26 – 7.15 (m, 3H), 4.90 (t, $J = 7.1$ Hz, 1H), 3.74 – 3.55 (m, 2H). $^{13}\text{C NMR}$ (100 MHz, CDCl_3): δ 195.1, 148.0, 145.8, 135.2, 133.4, 133.1, 133.1, 132.6, 128.9, 128.8, 127.7, 127.7, 127.5, 127.0, 126.1, 125.4, 124.5, 124.4, 122.5, 46.8, 42.9. IR (neat): 3073, 3048, 2962, 2900, 2851, 1673, 1595, 1515, 1449, 1260, 1227, 1107, 1016, 975, 956, 918, 857, 798, 796, 751, 716, 682, 647, 618, 566, 536, 514, 427 cm^{-1} . MS (MALDI-TOF) m/z : $[\text{M} + \text{Na}]^+$ Calcd. for $\text{C}_{25}\text{H}_{19}\text{NNaO}_3\text{S}$ 436.098; Found 436.151.

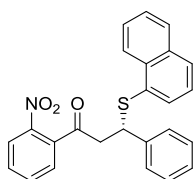
3.8.14 3-(Naphthalen-1-ylthio)-1-phenyl-3-(3,4,5-trimethoxyphenyl) propan-1-one (66w)



White solid, mp 115-116 °C, >99% yield. HPLC (AD-H, 90:10 *n*-Hexane/Isopropanol, 1 mL/min, 230 nm): $t_{\text{minor}} = 22.490$ min, $t_{\text{major}} = 16.387$ min, 96% ee, $[\alpha]_{\text{D}}^{23} = -123.30$ (*c* 2.410, CHCl_3). $^1\text{H NMR}$ (400 MHz, CDCl_3): δ 8.36 (d, $J = 8.1$ Hz, 1H), 7.84 – 7.76 (m, 2H), 7.76 – 7.66 (m, 2H), 7.52 – 7.37 (m, 4H), 7.34 (t, $J = 7.6$ Hz, 2H), 7.23 (t, $J = 7.7$ Hz, 1H), 6.27 (s, 2H), 4.80 (t, $J = 7.1$ Hz, 1H), 3.66 (s, 3H), 3.63 – 3.48 (m, 8H). $^{13}\text{C NMR}$ (100 MHz, CDCl_3): δ 195.7, 151.6,

135.8, 135.4, 135.3, 133.3, 132.7, 132.4, 132.0, 129.8, 127.9, 127.3, 127.1, 126.8, 125.4, 124.9, 124.5, 124.1, 103.5, 59.5, 54.7, 47.6, 43.1. IR (neat): 3057, 3001, 2970, 2934, 2899, 2838, 2827, 1682, 1590, 1513, 1454, 1430, 1366, 1335, 1320, 1254, 1223, 1182, 1125, 1008, 899, 805, 768, 754, 722, 688, 647, 557, 522, 416 cm^{-1} . MS (MALDI-TOF) m/z : $[\text{M} + \text{Na}]^+$ Calcd. for $\text{C}_{28}\text{H}_{26}\text{NaO}_4\text{S}$ 481.145; Found 481.137.

3.8.15 3-(Naphthalen-1-ylthio)-1-(2-nitrophenyl)-3-phenylpropan-1-one (66x)



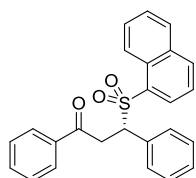
White solid, mp 112 °C, 89% yield. HPLC (AD-H, 99:1 *n*-Hexane/Isopropanol, 0.8 mL/min, 254 nm): $t_{\text{minor}} = 64.775$ min, $t_{\text{major}} = 68.571$ min, 82% ee, $[\alpha]_{\text{D}}^{24} = -1.545$ (c 1.165, CHCl_3). ^1H NMR (400 MHz, CDCl_3): δ 8.52 – 8.22 (m, 1H), 8.07 – 7.82 (m, 1H), 7.78 – 7.60 (m, 2H), 7.55 – 7.31 (m, 5H), 7.20 (t, $J = 7.7$ Hz, 1H), 7.16 – 7.00 (m, 5H), 6.94 – 6.81 (m, 1H), 4.75 (t, $J = 7.3$ Hz, 1H), 3.41 (t, $J = 8.7$ Hz, 2H). ^{13}C NMR (100 MHz, CDCl_3): 198.2, 143.9, 139.0, 136.1, 132.8, 132.7, 132.5, 131.6, 129.4, 129.1, 127.1, 127.0, 126.3, 126.1, 126.1, 125.3, 124.7, 124.1, 123.9, 122.7, 47.2, 46.9. IR (neat): 3058, 3029, 2923, 2910, 2856, 1709, 1573, 1529, 1499, 1455, 1403, 1367, 1343, 1218, 1142, 1019, 987, 935, 856, 790, 767, 747, 732, 715, 697, 668, 634, 618, 572, 547, 508, 451, 420 cm^{-1} . (MALDI-TOF) m/z : $[\text{M} + \text{Na}]^+$ Calcd. for $\text{C}_{25}\text{H}_{19}\text{NNaO}_3\text{S}$ 436.098; Found 436.139.

3.9 General Procedure for the Synthesis of Sulfones

A solution of β -aryl- β -sulfanyl ketone (0.1 mmol) in 0.8 mL DCM was cooled to 0°C. *m*-CPBA (0.22 mmol, 38.0 mg) was added to this stirred solution portionwise over 15 minutes. After the addition was complete, the mixture was allowed to warm up to room temperature and stirred for a total of 30 minutes. When all the β -aryl- β -sulfanyl ketone was consumed, the reaction mixture was diluted with 0.8 mL of DCM, then washed with 3 x 0.8 mL of 5% K_2CO_3 (aq) and 3 x 1 mL of 5% NaHCO_3 (aq) to remove the excess *m*-CPBA. The aqueous layer was extracted three times

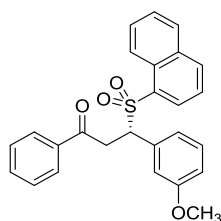
with DCM (1 mL). The organic layers were then combined, dried over Na₂SO₄ and concentrated in vacuo. The crude product was purified by column chromatography on silica, using *n*-hexane/ethyl acetate as eluent to afford the desired sulfones.

3.9.1 3-(Naphthalen-1-ylsulfonyl)-1,3-diphenylpropan-1-one (67a)



White solid, mp 135 °C, 43% yield. HPLC (IA, 95:5 *n*-Hexane/Isopropanol, 1 mL/min, 220 nm): $t_{\text{minor}} = 44.650$ min, $t_{\text{major}} = 47.501$ min, 86% ee, $[\alpha]_{\text{D}}^{22} = -156.9$ (*c* 1.140, CHCl₃). ¹H NMR (400 MHz, CDCl₃): δ 8.74 (d, *J* = 8.6 Hz, 1H), 7.92 (dd, *J* = 28.8, 7.8 Hz, 4H), 7.75 (d, *J* = 7.3 Hz, 1H), 7.69 – 7.62 (m, 1H), 7.59 – 7.48 (m, 2H), 7.44 – 7.36 (m, 2H), 7.25 (t, *J* = 7.8 Hz, 1H), 7.13 – 6.90 (m, 5H), 5.22 (dd, *J* = 9.2, 3.8 Hz, 1H), 4.15 (dd, *J* = 17.9, 3.8 Hz, 1H), 3.94 (dd, *J* = 18.0, 9.3 Hz, 1H). ¹³C NMR (100 MHz, CDCl₃): δ 198.0, 136.2, 135.3, 133.9, 133.7, 132.6, 132.0, 129.4, 129.4, 139.1, 128.8, 128.8, 128.7, 128.3, 128.2, 127.0, 124.3, 123.9, 65.7, 36.8. IR (neat): 3034, 2957, 2915, 2852, 1685, 1596, 1505, 1449, 1420, 1363, 1341, 1303, 1235, 1196, 1150, 1025, 981, 921, 826, 801, 768, 750, 699, 686, 629, 594, 573, 555, 525, 506, 476 cm⁻¹. HRMS (ESI-TOF) *m/z*: [M + Na]⁺ Calcd. for C₂₅H₂₀NaO₃S 423.1031; Found 423.1022.

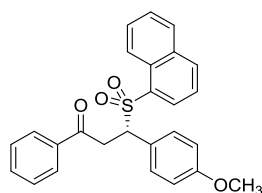
3.9.2 3-(3-Methoxyphenyl)-3-(naphthalen-1-ylsulfonyl)-1-phenylpropan-1-one (67f)



White solid, mp 93 °C, 45% yield. HPLC (IA, 95:5 *n*-Hexane/Isopropanol, 1 mL/min, 254 nm): $t_{\text{minor}} = 18.229$ min, $t_{\text{major}} = 20.872$ min, 68% ee, $[\alpha]_{\text{D}}^{23} = -115.5$ (*c*

1.313, CHCl₃). ¹H NMR (400 MHz, CDCl₃): δ. ¹³C NMR (100 MHz, CDCl₃): δ 8.74 (d, *J* = 8.7 Hz, 1H), 7.96 (d, *J* = 8.2 Hz, 1H), 7.88 (t, *J* = 7.5 Hz, 3H), 7.80 (d, *J* = 7.4 Hz, 1H), 7.65 (t, *J* = 7.8 Hz, 1H), 7.58 – 7.48 (m, 2H), 7.40 (t, *J* = 7.6 Hz, 2H), 7.28 (t, *J* = 7.8 Hz, 1H), 6.91 (t, *J* = 8.0 Hz, 1H), 6.65 – 6.51 (m, 2H), 6.41 (s, *J* = 9.9 Hz, 1H), 5.18 (dd, *J* = 9.3, 3.8 Hz, 1H), 4.12 (dd, *J* = 17.9, 3.9 Hz, 1H), 3.93 (dd, *J* = 18.0, 9.3 Hz, 1H), 3.42 (s, *J* = 10.6 Hz, 3H). ¹³C NMR (100 MHz, CDCl₃): δ 192.9, 157.2, 134.1, 133.1, 131.8, 131.7, 131.5, 130.0, 129.9, 127.3, 127.2, 126.9, 126.7, 126.6, 126.1, 124.8, 122.2, 121.9, 119.5, 112.6, 112.6, 63.7, 52.9, 34.6. IR (neat): 3053, 2960, 2918, 2849, 1726, 1685, 1594, 1493, 1447, 1362, 1305, 1258, 1231, 1149, 1121, 1035, 883, 792, 770, 688, 679, 633, 619, 593, 552, 528, 504, 486 cm⁻¹. HRMS (ESI-TOF) *m/z*: [M]⁺ Calcd. for C₂₆H₂₂O₄S 430.1239; Found 439.1239.

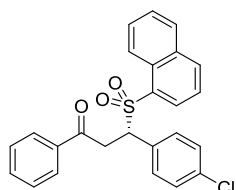
3.9.3 3-(3-Methoxyphenyl)-3-(naphthalen-1-ylsulfonyl)-1-phenylpropan-1-one (67g)



White solid, mp 146 °C, 62% yield. HPLC (IA, 90:10 *n*-Hexane/Isopropanol, 1 mL/min, 254 nm): *t*_{minor} = 40.307 min, *t*_{major} = 45.189 min, 86% ee, [α]_D²² = -173.1 (c 1.773, CHCl₃). ¹H NMR (400 MHz, CDCl₃): δ 8.73 (d, *J* = 8.6 Hz, 1H), 7.96 (d, *J* = 8.2 Hz, 1H), 7.87 (d, *J* = 7.7 Hz, 3H), 7.78 (d, *J* = 7.3 Hz, 1H), 7.66 (t, *J* = 7.8 Hz, 1H), 7.59 – 7.49 (m, 2H), 7.39 (t, *J* = 7.6 Hz, 2H), 7.29 (t, *J* = 7.8 Hz, 1H), 6.88 (d, *J* = 8.6 Hz, 2H), 6.53 (d, *J* = 8.7 Hz, 2H), 5.16 (dd, *J* = 9.4, 3.7 Hz, 1H), 4.09 (dd, *J* = 17.9, 3.8 Hz, 1H), 3.90 (dd, *J* = 17.9, 9.5 Hz, 1H), 3.61 (s, 3H), 1.51 (s, *J* = 19.6 Hz, 3H). ¹³C NMR (100 MHz, CDCl₃): δ 194.1, 158.8, 135.2, 134.1, 132.9, 132.6, 131.1, 130.9, 129.6, 128.4, 128.1, 127.7, 127.7, 127.1, 125.9, 123.4, 123.3, 123.0, 112.8, 64.2, 54.1, 35.8. IR (neat): 3061, 3004, 2962, 2916, 2850, 1684, 1610, 1580, 1511, 1457, 1421, 1361, 1303, 1254, 1229, 1179, 1154, 1120, 1025, 979, 910, 852,

800, 768, 729, 711, 679, 639, 621, 600, 572, 552, 529, 505, 484, 440 cm^{-1} . HRMS (ESI-TOF) m/z : $[\text{M} + \text{Na}]^+$ Calcd. for; $\text{C}_{26}\text{H}_{22}\text{NaO}_4\text{S}$ 453.1136; Found 453.1164.

3.9.4 3-(4-Chlorophenyl)-3-(naphthalen-1-ylsulfonyl)-1-phenylpropan-1-one (67o)



White solid, mp 134 °C, 28% yield. HPLC (IA, 90:10 *n*-Hexane/Isopropanol, 1 mL/min, 254 nm): $t_{\text{minor}} = 25.206$ min, $t_{\text{major}} = 31.435$ min, 66% ee, $[\alpha]_{\text{D}}^{23} = -135.7$ (c 1.040, CHCl_3). ^1H NMR (400 MHz, CDCl_3): δ 8.71 (d, $J = 8.7$ Hz, 1H), 8.00 – 7.93 (m, 1H), 7.90 – 7.82 (m, 3H), 7.77 (d, $J = 7.4$ Hz, 1H), 7.71 – 7.64 (m, 1H), 7.64 – 7.42 (m, 3H), 7.40 (t, $J = 7.7$ Hz, 2H), 7.35 – 7.27 (m, 1H), 6.93 (dd, $J = 35.0, 8.5$ Hz, 4H), 5.17 (dd, $J = 9.6, 3.6$ Hz, 1H), 4.01 (ddd, $J = 27.6, 18.0, 6.6$ Hz, 2H). ^{13}C NMR (100 MHz, CDCl_3): δ 193.6, 134.9, 134.3, 133.7, 132.8, 132.7, 130.9, 130.6, 130.1, 129.5, 128.4, 128.1, 127.8, 127.6, 127.4, 127.0, 125.9, 123.0, 122.9, 64.0, 49.3, 35.6. IR (neat): 3059, 2917, 2849, 1681, 1658, 1593, 1492, 1447, 1420, 1363, 1329, 1142, 1119, 1094, 1015, 979, 924, 858, 798, 772, 775, 707, 689, 631, 620, 598, 564, 533, 507, 481, 456 cm^{-1} . HRMS (ESI-TOF) m/z : $[\text{M} + \text{Na}]^+$ Calcd. for $\text{C}_{25}\text{H}_{19}\text{ClNaO}_3\text{S}$ 457.0641; Found 457.0666.

CHAPTER 4

CONCLUSION

In this work, the activities of chiral bifunctional organocatalysts developed in our research group on the enantioselectivity of sulfa-Michael addition to *trans*-chalcone derivatives were surveyed.

In the first half of the study, the enantioselective SMA of methyl thioglycolate to *trans*-chalcone derivatives was carried out in the presence of 10 mol% of 2-adamantyl/quinine organocatalyst **58b**. A total of 27 enantiomerically enriched sulfa-Michael adducts were obtained, with ee values ranging between 60-99%. The selected derivative **61s** was subjected to further transformations to afford the benzothiazepinone derivative **81**, which is a potential drug core against type II diabetes. The drop in enantioselectivity from 68% ee to 17% ee at the end of the transformation was attributed to the unavoidable retro-sulfa-Michael reaction.

The second half of the work employed 1-thionaphthol as the sulfa-Michael donor, newly developed quinine derived sulfonamide organocatalyst **59** in the SMA to *trans*-chalcones. 15 enantiomerically enriched β -aryl- β -sulfanyl ketones were obtained with moderate to excellent enantioselectivities (51-96% ee) with a very low catalyst loading (1 mol%) at ambient temperature, using two different solvent systems. Different extents of asymmetric induction were achieved with each solvent-substrate pair, presumably due to different levels of stabilization of transition state for each. Four of the β -aryl- β -sulfanyl ketones were oxidized via a simple single-step route to form corresponding chiral sulfones without any appreciable loss in enantioselectivities.

REFERENCES

1. Feng, H.; Tang, B.; Liangi S. H.; Jiang, X. *Curr. Top. Med. Chem.* **2016**, *16*, 1200-1216.
2. Fleming, A. *Br. J. Exp. Pathol.* **1929**, *10*, 226-236.
3. Colebrook, L.; Kenny, M. *The Lancet*, **1936**, 1279-1281.
4. Furr, B. J. A. *Eur. Urol.* **1996**, *29*, 83-95.
5. Chaffman, M.; Brogden, R. N. *Drugs*, **1985**, *29*, 387-454.
6. Markham, A.; Faulds, D. *Drugs*, **1998**, *56*, 251-256.
7. Bentley, R. *Chem. Rev.* **2006**, *106*, 4099-4112.
8. Mayer, J. M.; Testa, B. *Drugs Fut.* **1997**, *22*, 1347-1366.
9. Eichelbaum M. Side Effects and Toxic Reactions of Chiral Drugs: A Clinical Perspective. In: *Toxicology in Transition. Archives of Toxicology (Supplement), vol 17*, Degen G.H., Seiler J.P., Bentley P., Eds.; Springer; Berlin, Heidelberg, **1985**.
10. Nguyen, L. A.; He, H.; Pham-Huy, C. *Int. J. Biomed. Sci.*, **2006**, *2*, 85–100.
11. Calcaterra, A.; D'Acquerica, I. *J. Pharm. Biomed. Anal.*, **2018**, *147*, 323-340.
12. Shimazawa, R.; Nagai, N.; Toyoshima, S.; Okuda, H. *J. Health. Sci.* **2008**, *54*, 23-29.
13. Zhan, G.; Du, W.; Chen, Y.-C. *Chem. Soc. Rev.* **2017**, *46*, 1675-1692.
14. Ojima, I. *Catalytic Asymmetric Synthesis*; Wiley-VCH: USA, 2000.
15. Berkessel, A.; Gröger, H. *Asymmetric Organocatalysis – From Biomimetic Concepts to Applications in Asymmetric Synthesis*; Wiley-VCH: Weinheim, Germany, 2005.
16. Ahrendt, K. A.; Borths, C. J.; MacMillan, D. W. C. *J. Am. Chem. Soc.* **2000**, *122*, 4243-4244
17. Langenbeck, W. *Die Organischen Katalysatoren und ihre Beziehungen zu den Fermenten*, **1935**.
18. Bredig, G.; Fiske, W. S. *Biochem. Z.* **1912**, *7*.
19. List, B.; Lerner, R. A.; Barbas, C. F. *J. Am. Chem. Soc.* **2000**, *122*, 2395-2396.
20. Jacobsen, E N.; MacMillan, D. W. C. *Proc. Natl. Acad. Sci.* **2010**, *107*, 20618-20619.
21. Ma, J.-A.; Cahard, D. *Angew. Chem. Int. Ed.* **2004**, *43*, 4566-4583.
22. McCooey, S. H.; Connon, S. J. *Angew. Chem. Int. Ed.* **2005**, *44*, 6367-6370.
23. Okino, T.; Hoashi, Y.; Takemoto, Y. *J. Am. Chem. Soc.* **2003**, *125*, 12672-12673.
24. Yu, Z.; Liu, X.; Zhou, L.; Lin, L.; Feng, X. *Angew. Chem. Int. Ed.* **2009**, *48*, 5195-5198.
25. Vakulya, B.; Varga, S.; Csámpai, A.; Soós, T. *Org. Lett.* **2005**, *7*, 1967-1969.
26. Chauhan, P.; Mahajan, S.; Kaya, U.; Hack, D.; Enders, D. *Adv. Synth. Catal.* **2015**, *17*, 6890-6899.
27. Rabalakos, C.; Wulff, W. D. *J. Am. Chem. Soc.* **2008**, *130*, 13524-13525.
28. Mei, K.; Jin, M.; Zhang, S.; Li, P.; Liu, W.; Chen, X.; Xue, F.; Duan, W.; Wang, W. *Org. Lett.* **2009**, *11*, 2864-2867.

29. Wu, F.; Hong, R.; Khan, J.; Liu, X.; Deng, L. *Angew. Chem. Int. Ed.* **2006**, *45*, 4301-4305.
30. Kacprzak KM. *Chemistry and Biology of Cinchona Alkaloids*; Springer: 2013, 605-641.
31. Hiemstra, H.; Wynberg, H. *J. Am. Chem. Soc.* **1981**, *103*, 417-430.
32. Malerich, J. P.; Hagihara, K.; Rawal, V. H. *J. Am. Chem. Soc.* **2008**, *130*, 14416-14417.
33. Alemán, J.; Parra, A.; Jiang, H.; Jørgensen, K. A. *Chem. Eur. J.* **2011**, *17*, 6890-6899.
34. For selected works regarding cinchona alkaloid derived squaramide type organocatalysts, see: a) Jarava-Barrera, C.; Esteban, F.; Navarro-Ranninger, C.; Parra, A.; Alemán, J. *Chem. Commun.* **2013**, *49*, 2001-2003; b) Nair, D. K.; Menna-Barreto, R. F. S.; da Silva Júnior, E. N.; Mobin, S. M.; Namboothiri, I. N. N. *Chem. Commun.* **2014**, *50*, 6973-6976; c) Zhu, Y.; Malerich, J. P.; Rawal, V. H. *Angew. Chem. Int. Ed.*, **2010**, *49*, 153-156; d) Han, X.; Zhou, H.-B.; Dongi C. *Chem. Rec.* **2016**, *16*, 897-906; e) Blümel, M.; Chauhan, P.; Hahn, R.; Raabe, G.; Enders, D. *Org. Lett.* **2014**, *16*, 6012-6015.
35. Oh, S. H.; Rho, H. S.; Lee, J. W.; Lee, J. E.; Youk, S. H.; Chin, J.; Song, C. E. *Angew. Chem. Int. Ed.* **2008**, *47*, 7872-7875
36. For selected works regarding cinchona alkaloid derived sulfonamide type organocatalysts, see: a) Bae, H. Y.; Sim, J. H.; Lee, J.-W.; List, B.; Song, C. E. *Angew. Chem. Int. Ed.* **2013**, *52*, 12143-12147; b) Luo, J.; Xu, L.-W.; Hay, R. A. S.; Lu, Y. *Org. Lett.* **2009**, *11*, 437-440; c) Park, S. E.; Nam, E. N.; Jang, H. B.; Oh, J. S.; Some, S.; Lee, Y. S.; Song, C. E. *Adv. Synth. Catal.*, **2010**, *352*, 2211-2217; d) Blise, K.; Cvitkovic, M. W.; Gibbs, N. J.; Roberts, S. F.; Whitaker, R.M. Hofmeister, G. E.; Kohen, D. *J. Org. Chem.* **2017**, *82*, 1347-1355.
37. Pine, S. H. *Organic Chemistry*; McGraw-Hill: Singapore, 1987.
38. Clayden, J.; Greeves, N.; Warren, S.; Wothers, P. *Organic Chemistry*; Oxford University Press: New York, USA, 2001.
39. For an early comprehensive review on SMA, see: Enders, D.; Lüttgen, K.; Narine, A. *Synthesis*, **2007**, *7*, 959-980.
40. Inoue, S.; Ohashi, S.; Tabata, A.; Tsuruta, T. *Makromol. Chem.* **1968**, *112*, 66-72.
41. Pracejus, H.; Wilcke, F. -W.; Hanemann, K. *J. Prakt. Chem.* **1977**, *319*, 219-229.
42. Helder, R.; Arends, R.; Bolt, W.; Hiemstra, H.; Wynberg, H. *Tetrahedron Letters*, **1977**, *25*, 2181-2182.
43. a) Marigo, M.; Shulte, T.; Franzén, J.; Jørgensen, K. A. *J. Am. Chem. Soc.* **2005**, *127*, 15710-15711; b) Liu, Y.; Sun, B.; Wang, B.; Wakem, M.; Deng, L. *J. Am. Chem. Soc.*, **2009**, *131*, 418-419; c) Fang, X.; Li, J.; Wang, C.-J. *Org. Lett.*, **2013**, *15*, 3448-3451; d) Pei, Q.; Han, W.; Wu, Z.; Zhang, X.; Yuan, W., *Tetrahedron*, **2013**, *69*, 5367-5373

44. a) McDaid, P.; Chen, Y.; Deng, L. *Angew. Chem. Int. Ed.*, **2012**, *41*, 338-340; b) Rana, N. K.; Selvakumar, S.; Singh, V. K. *J. Org. Chem.* **2010**, *75*, 2089-2091; c) Dai, L.; Wang, S.; Chen, F. *Adv. Synth. Catal.* **2010**, *352*, 2137-2141.
45. Singh, P.; Anand, A.; Kumar, V. *Eur. J. Med. Chem.* **2014**, *85*, 758-777.
46. Allgäuer, D. S.; Jangra, H.; Asahara, H.; Li, Z.; Chen, Q.; Zipse, H.; Ofial, A. R.; Mayr, H. *J. Am. Chem. Soc.* **2017**, *139*, 13318-13329.
47. a) Hui, Y.; Jiang, J.; Wang, W.; Chen, W.; Cai, Y.; Lin, L.; Liu, X.; Feng, X. *Angew. Chem. Int. Ed.* **2010**, *49*, 4290-4293; b) Chakka, S. K.; Cele, Z. E. D.; Sosibo, S. C.; Francis, V.; Arvidsson, P. I.; Kruger, H. G.; Maguire, G. E. H.; Govender, T. *Tetrahedron: Asymmetry*, **2012**, *23*, 616-622.
48. Thu, L. T.; Ahn, J. R.; Woo, S. -R. *Eur. J. Pharmacol.*, **2006**, *552*, 15-19.
49. García-Casas, P.; Arias-del-Val, J.; Alvarez-Illera, P.; Wojnicz, A.; de los Rios, C.; Fonteriz, R. I.; Montero, M.; Alvarez, J. *Front. Aging Neurosci.* **2019**, *10*:440.
50. Pei, Y.; Lilly, M. J.; Owen, D. J.; D'Souza, L. J.; Tang, X.; Yu, J.; Nazarbaghi, R.; Hunter, A.; Anderson, C. M.; Glasco, S.; Ede, N. J.; James, I. W.; Maitra, U.; Chandrasekhan, S.; Moos, W. H.; Ghosh, S. S., *J. Org. Chem.*, **2003**, *68*, 92-103.
51. Perin, G.; Mesquita, K.; Calheiro, T. P.; Silva, M. S.; Lenardão, E. J.; Alves, D.; Jacob, R. G. *Synth. Commun.*, **2014**, *44*, 49-58.
52. Kopel, L. C.; Ahmed, M. S.; Halaweish, F. T. *Steroids*, **2013**, *78*, 1119-1125.
53. Kumar, A.; Tripathi, V. D.; Kumar, P.; Gupta, L. P.; Trivedi, A. R.; Bid, H.; Nayak, V. L.; Siddiqui, J. A.; Chakravarti, B.; Saxena, R.; Dwivedi, A.; Siddiquee, M. I.; Siddiqui, U.; Konwar, R.; Chattopadhyay, N. *Bioorg. Med. Chem.* **2011**, *19*, 5409-5419.
54. Ahari-Mostafavi, M. M.; Sharifi, A.; Mirzaei, M.; Amanlou, M. *J. Iran. Chem. Soc.* **2014**, *11*, 1113-1119.
55. Zuidema, J.; Hilbers-Modderman, E. S. M.; Merkus, F. W. H. M. *Clin. Pharmacokinet.* **1986**, *11*, 299-315.
56. Meadows, D. C.; Sanchez, T.; Neamati, N.; North, T. W.; Gervay-Hague, J. *Bioorg. Med. Chem.*, **2007**, *15*, 1127-1137.
57. Velázquez, F.; Sannigrahi, M.; Bennett, F.; Lovey, R. G.; Arasappan, A.; Bogen, S.; Nair, L.; Venkatraman, S.; Blackman, M.; Hendrata, S.; Huang, Y.; Huelgas, R.; Pinto, P.; Cheng, K.-C.; Tong, X.; McPhail, A. T.; Njoroge, F. G. *J. Med. Chem.*, **2010**, *53*, 3075-3085.
58. Otzen, T.; Wempe, E. G.; Kunz, B.; Bartels, R.; Lehwarz-Yvetot, G.; Hänsel, W.; Schaper, K.-J.; Seydel, J. K. *J. Med. Chem.* **2004**, *47*, 240-253.
59. Yu, X.; Liu, Y.; Li, Y.; Wang, Q. *J. Agric. Food Chem.*, **2016**, *64*, 3034-3040.
60. Liu, N.-W.; Liang, S.; Manolikakes, G. *Synthesis*, **2016**, *48*, 1939-1973.
61. Konduru, N. K.; Dey, S.; Sajid, M.; Owais, M.; Ahmed, N. *Eur. J. Med. Chem.* **2013**, *59*, 23-30.
62. Işık, M.; Unver, M. Y.; Tanyeli, C. *J. Org. Chem.* **2015**, *80*, 828-835.
63. Kanberoğlu, E.; Tanyeli, C. *Asian J. Org. Chem.* **2016**, *5*, 114-119.

64. Susam, D.; Tanyeli, C. *New. J. Chem.* **2017**, *41*, 3555-3561.
65. Karahan, S.; Tanyeli, C. *New. J. Chem.* **2017**, *41*, 9192-9202.
66. Vakulya, B.; Varga, S.; Csámpai, A.; Soós, T.; *Org. Lett.* **2013**, *7(10)*, 1967-1969.
67. Işık, M.; Tanyeli, C. *J. Org. Chem.* **2013**, *78*, 1604-1611.
68. Wattanasin, S.; Murphy, W. S. *Synthesis*, **1980**, *8*, 647-650.
69. Katritzky, A. R.; Zhang, Y.; Singh, S. K. *Synthesis*, **2003**, *18*, 2795-2798.
70. Ricci, P.; Carlone, A.; Bartoli, G.; Bosco, M.; Sambri, L.; Melchiorre, P. *Adv. Synth. Catal.* **2008**, *350*, 49-53.
71. Guo, J.; Wong, M. W. *J. Org. Chem.* **2017**, *82*, 4362-4368.
72. Konduru, N. K.; Dey, S.; Sajid, M.; Owais, M.; Ahmed, N. *Eur. J. Med. Chem.* **2013**, *59*, 23-30.

APPENDICES

A. NMR SPECTRA

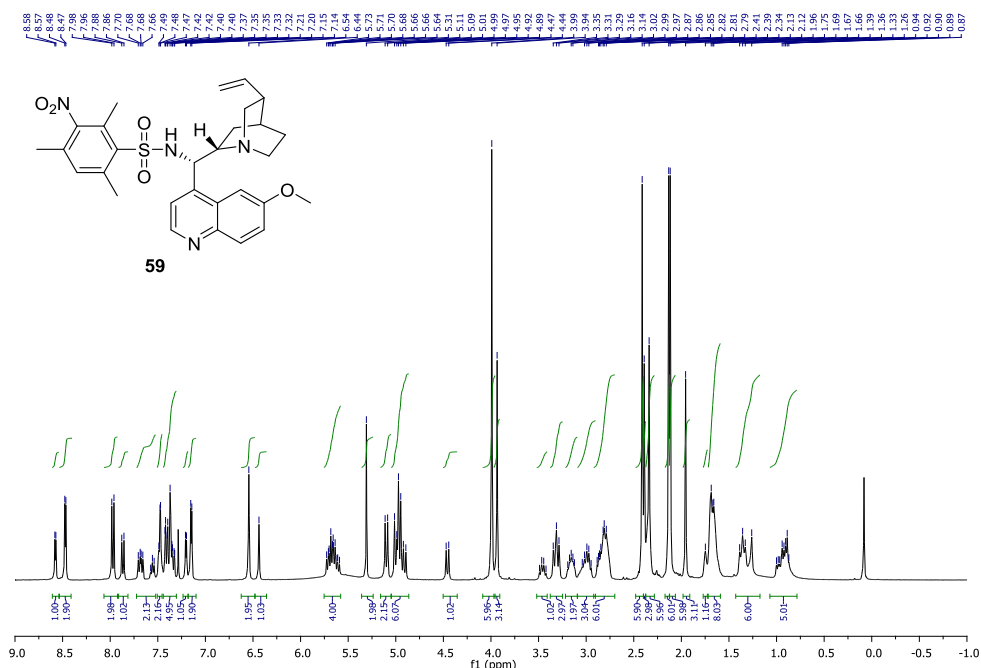


Figure A. 1 ^1H NMR spectrum of **59**

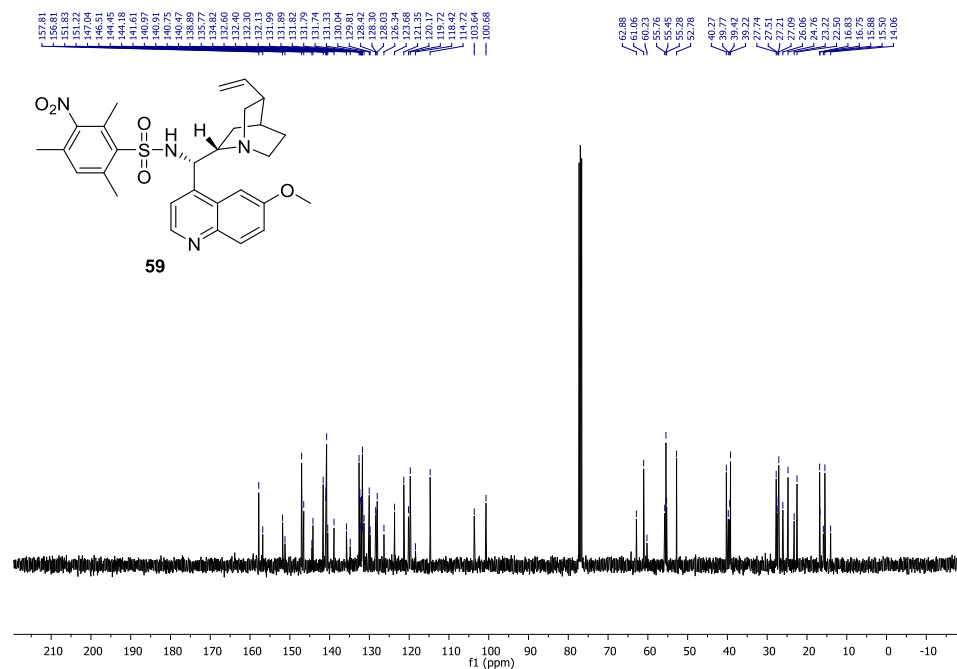


Figure A. 2 ^{13}C NMR spectrum of **59**

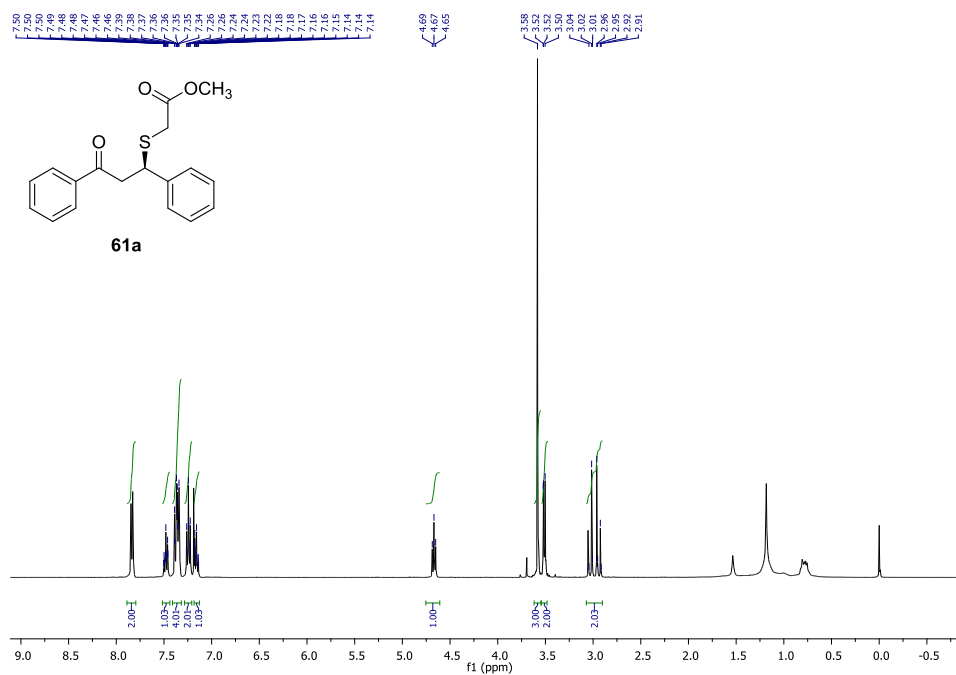


Figure A. 3 ¹H NMR spectrum of **61a**

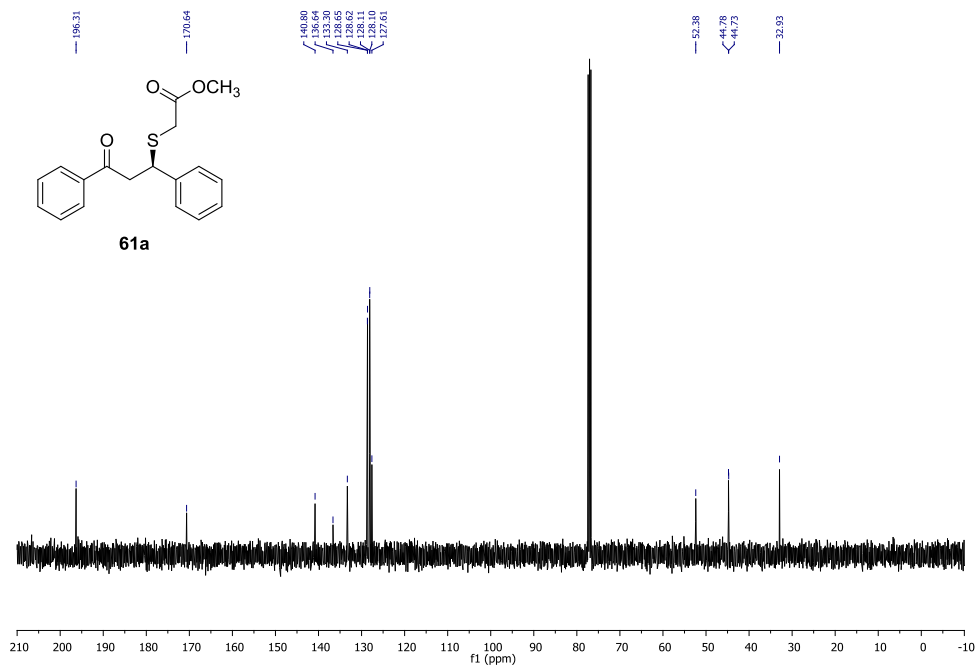


Figure A. 4 ¹³C NMR spectrum of **61a**

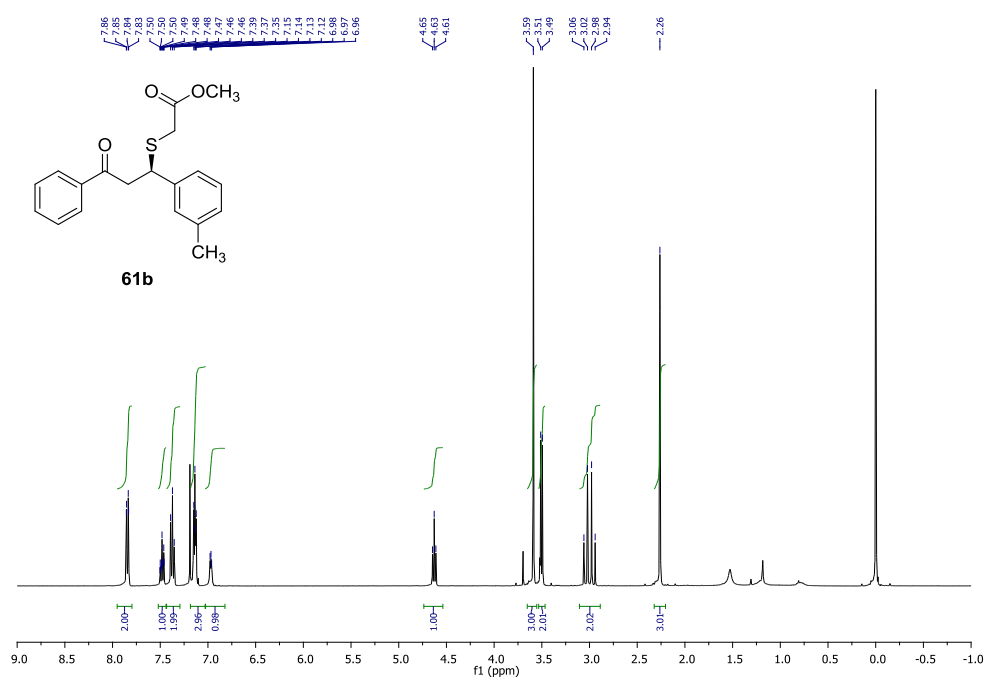


Figure A. 5 ^1H NMR spectrum of **61b**

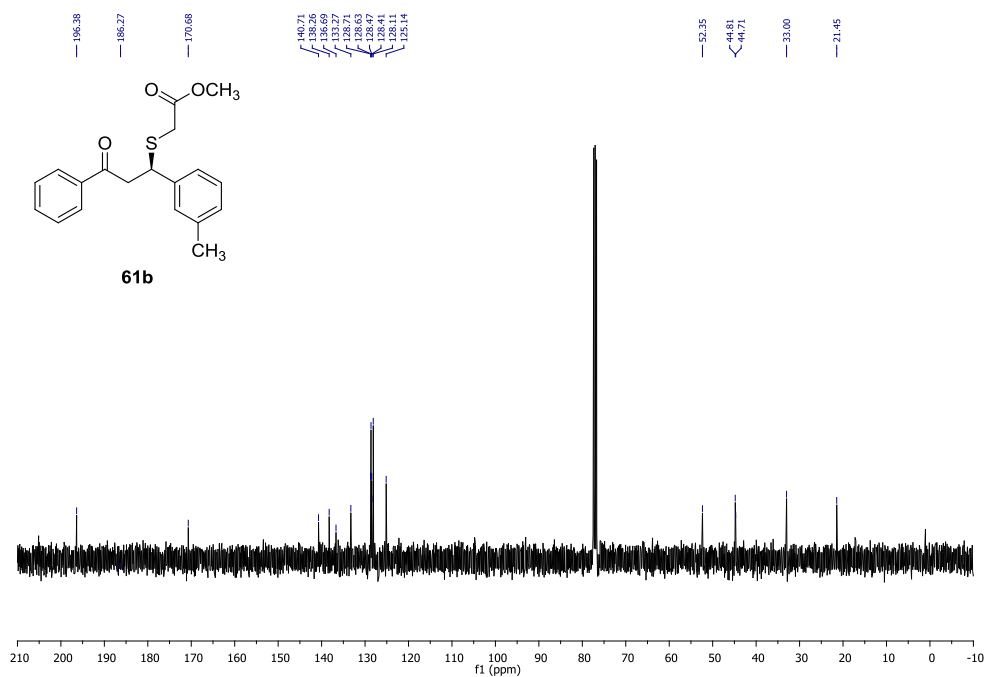


Figure A. 6 ^{13}C NMR spectrum of **61b**

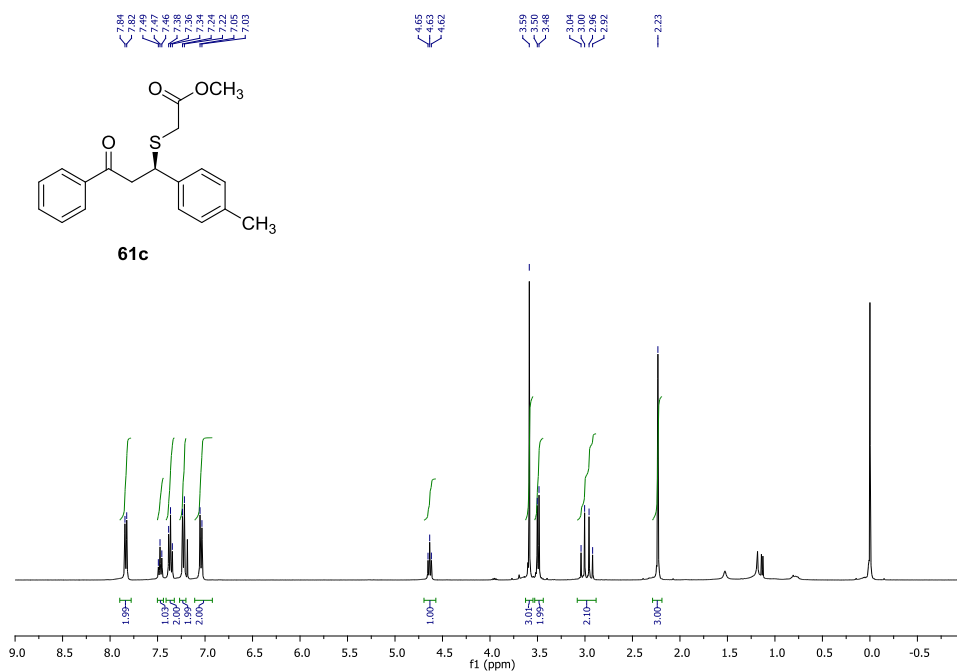


Figure A. 7 ¹H NMR spectrum of **61c**

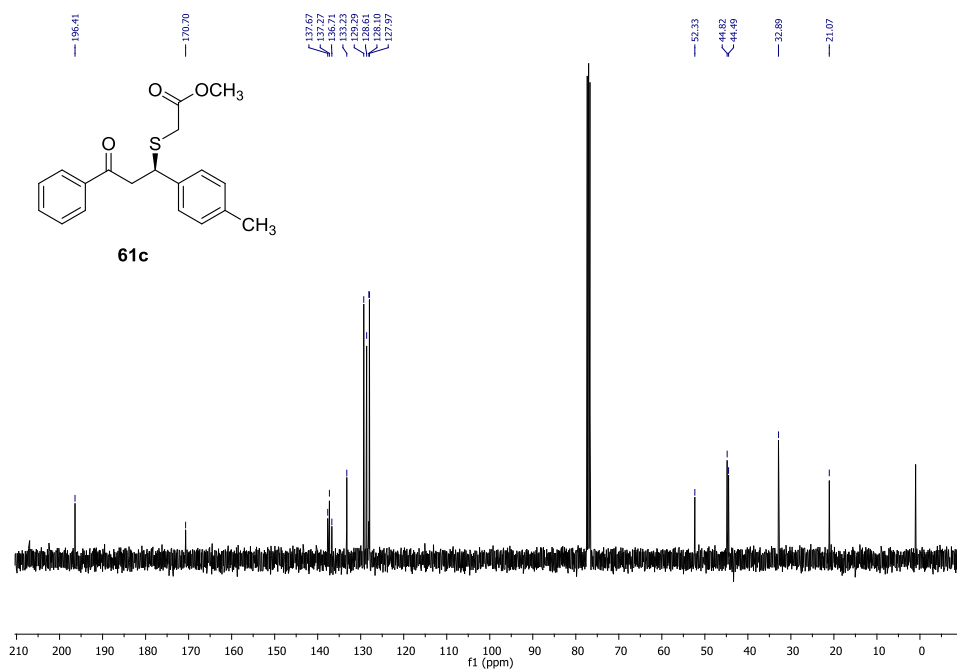


Figure A. 8 ¹³C NMR spectrum of **61c**

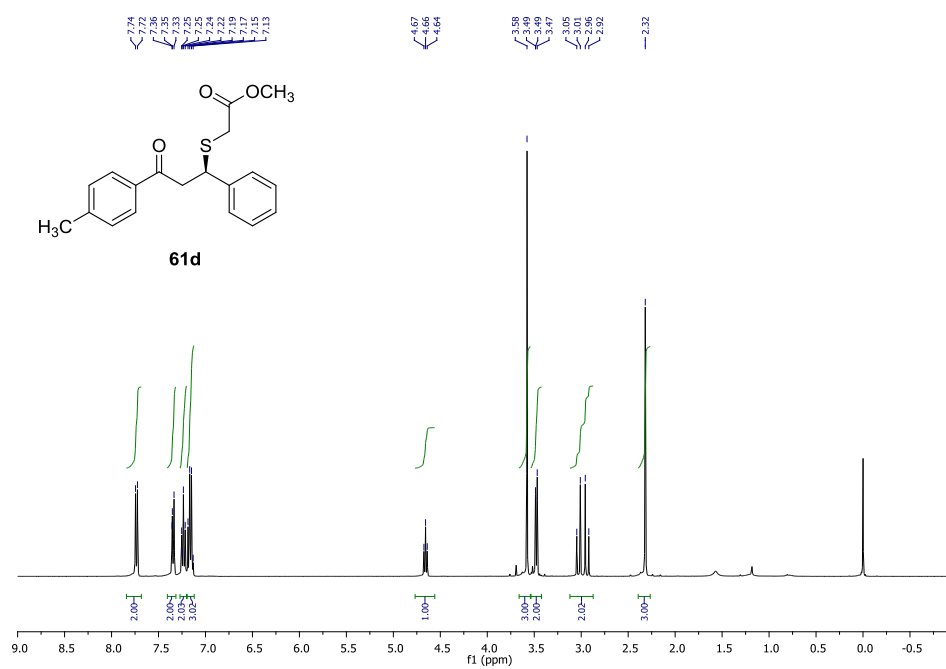


Figure A. 9 ¹H NMR spectrum of **61d**

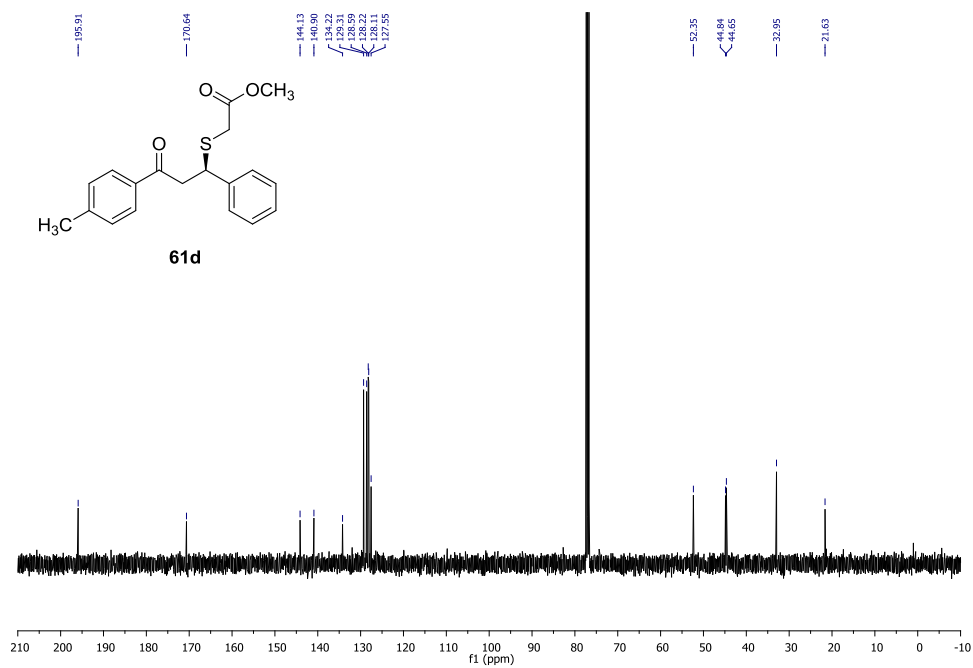


Figure A. 10 ¹³C NMR spectrum of **61d**

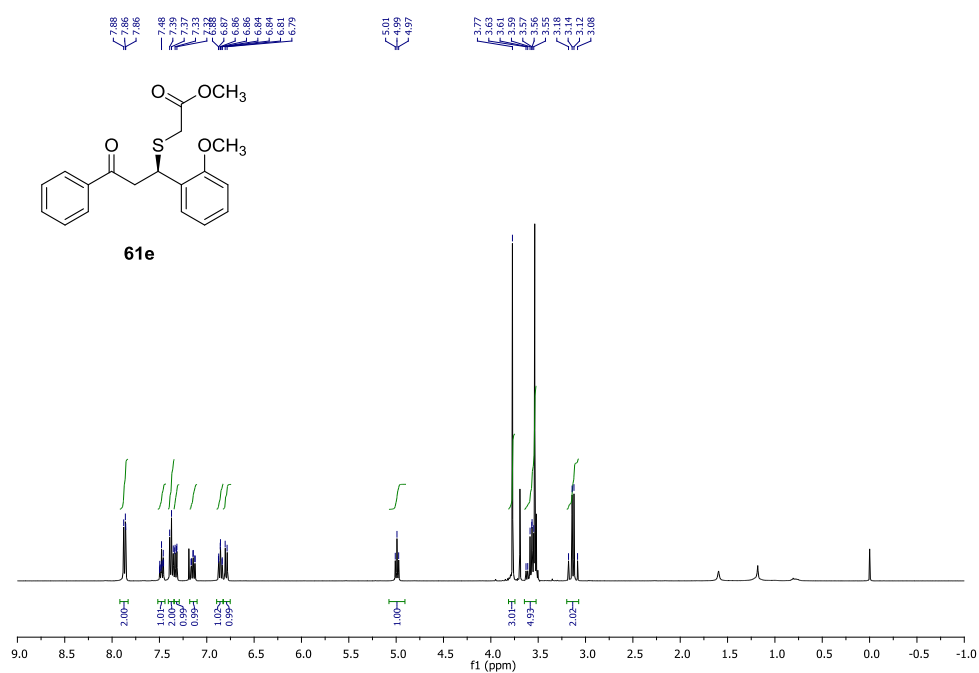


Figure A. 11 ^1H NMR spectrum of **61e**

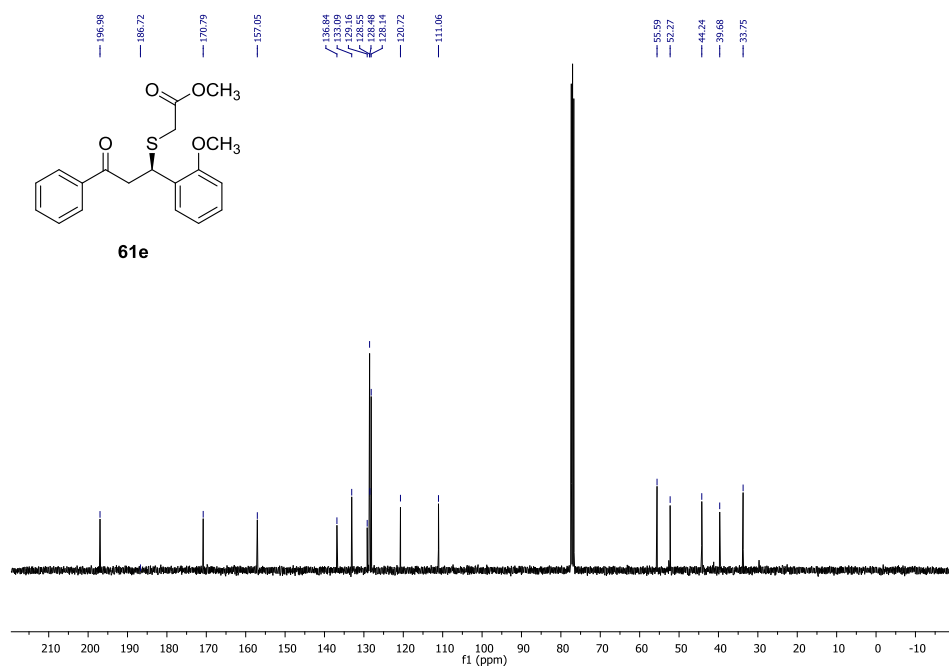


Figure A. 12 ^{13}C NMR spectrum of **61e**

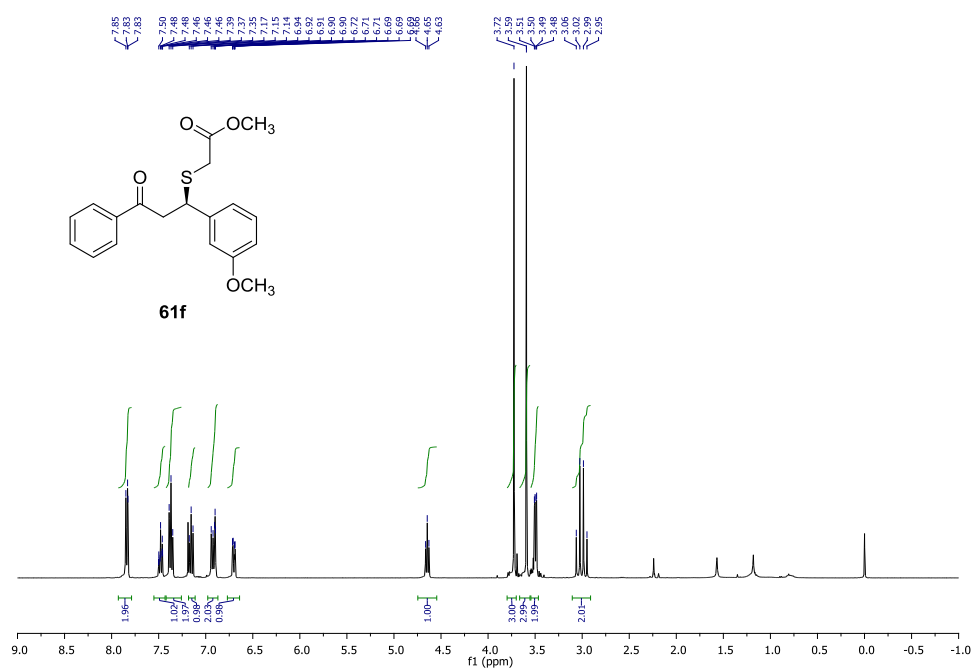


Figure A. 13 ^1H NMR spectrum of **61f**

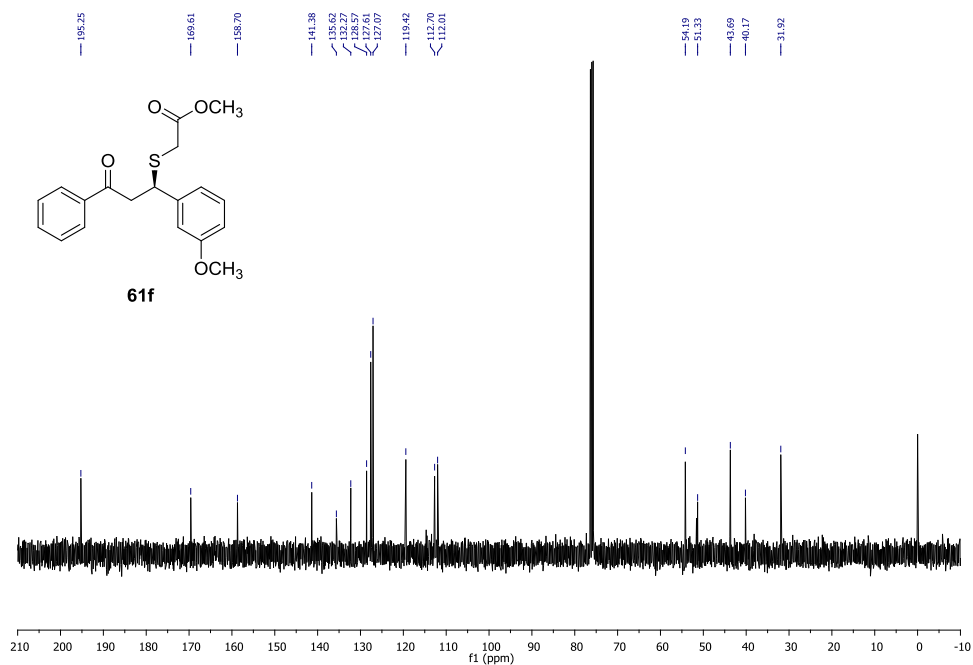


Figure A. 14 ^{13}C NMR spectrum of **61f**

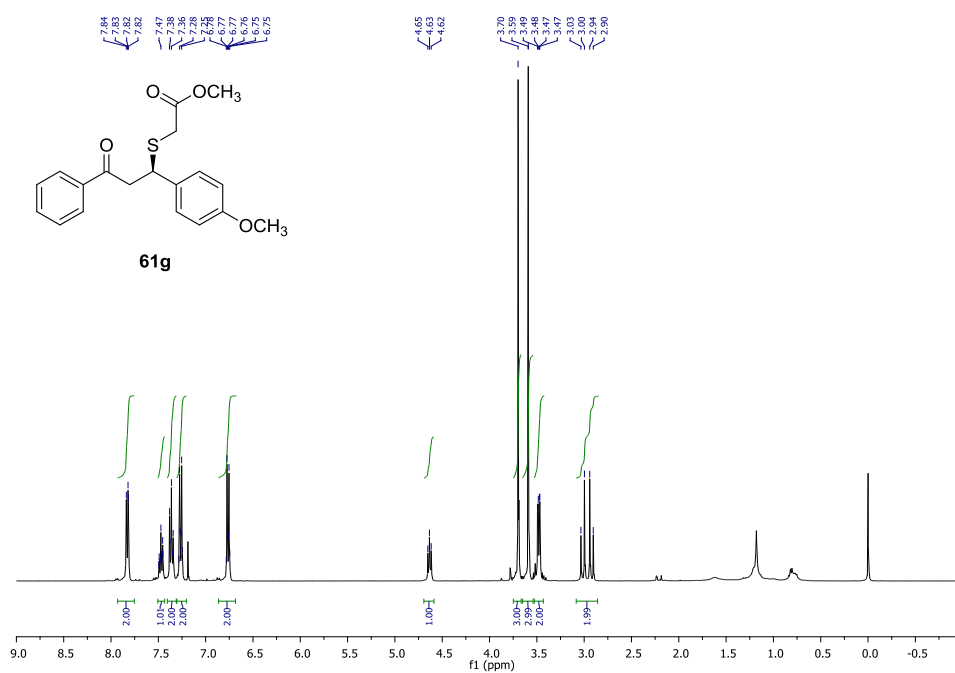


Figure A. 15 ¹H NMR spectrum of **61g**

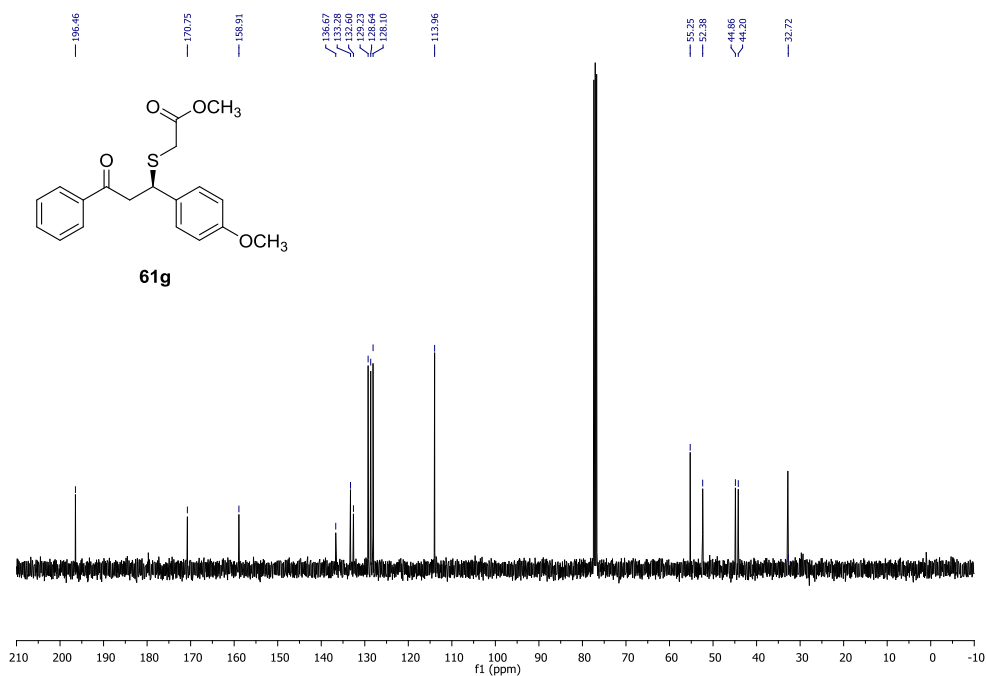


Figure A. 16 ¹³C NMR spectrum of **61g**

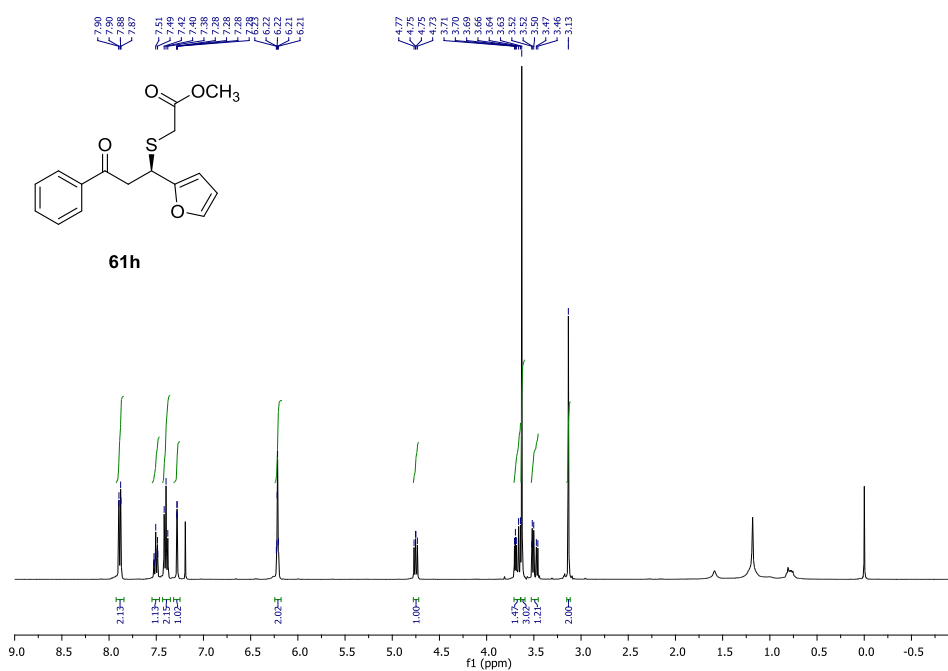


Figure A. 17 ^1H NMR spectrum of **61h**

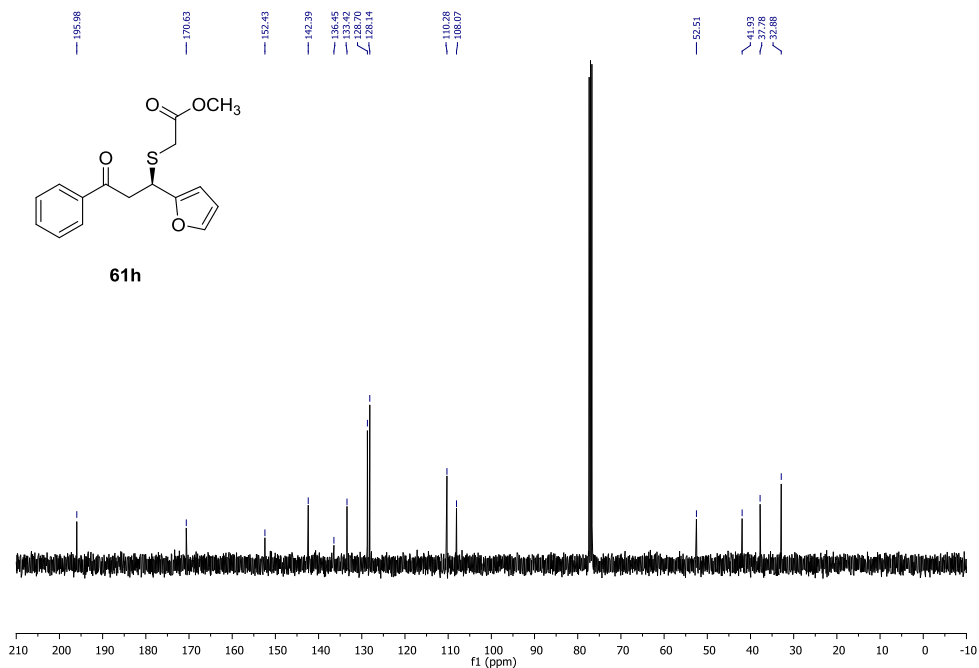


Figure A. 18 ^{13}C NMR spectrum of **61h**

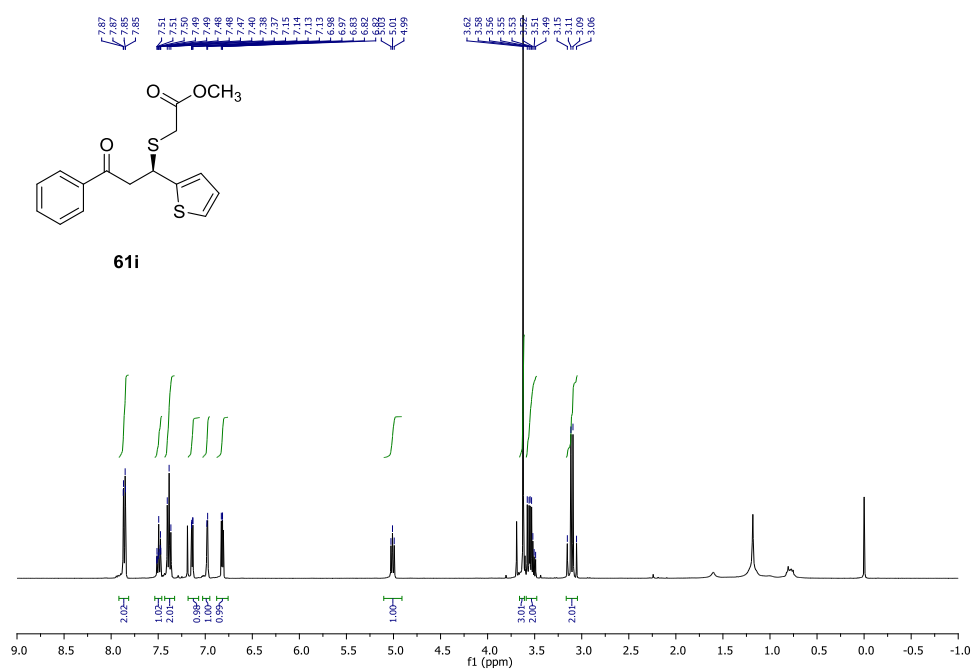


Figure A. 19 ^1H NMR spectrum of **61i**

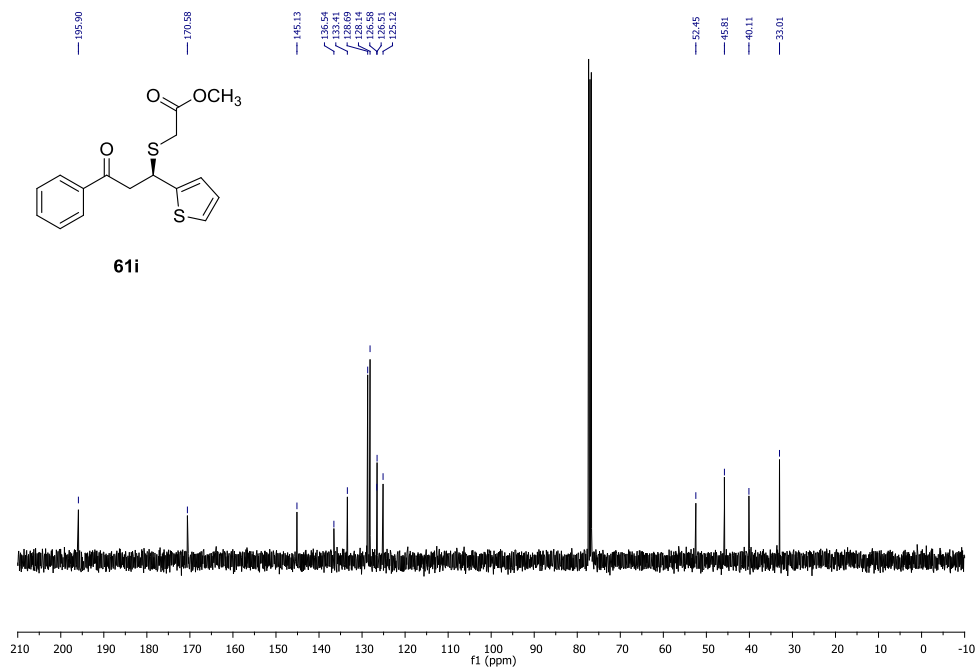


Figure A. 20 ^{13}C NMR spectrum of **61i**

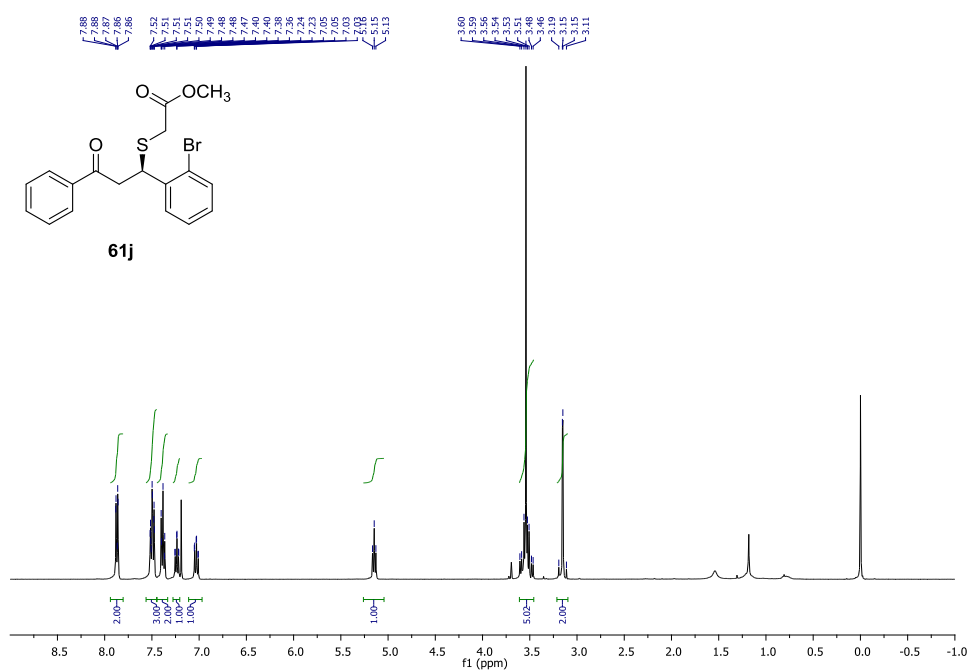


Figure A. 21 ¹H NMR spectrum of **61j**

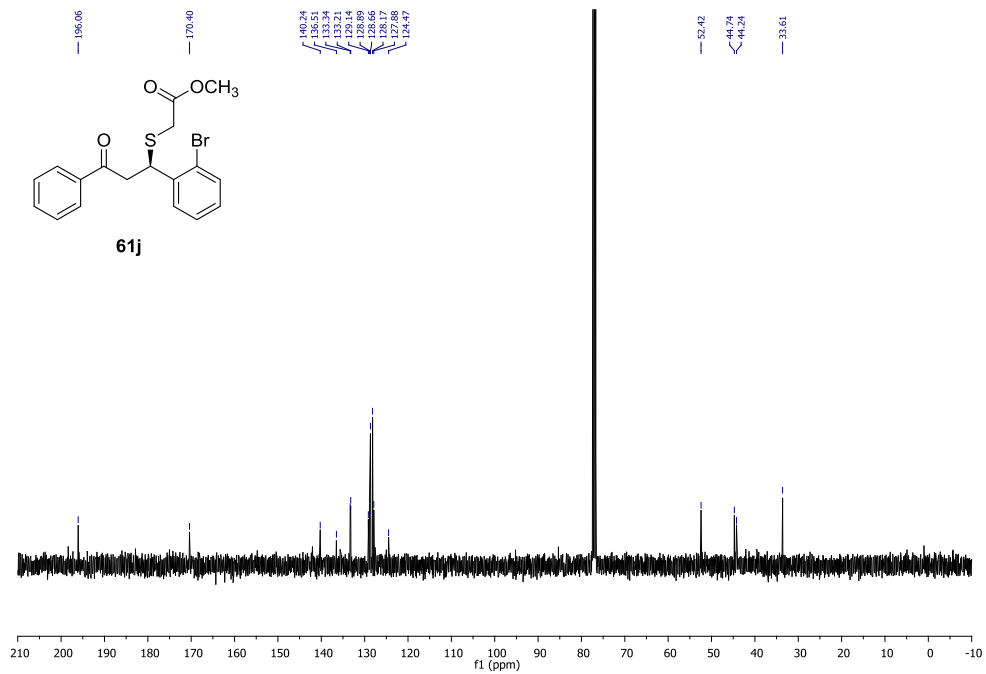


Figure A. 22 ¹³C NMR spectrum of **61j**

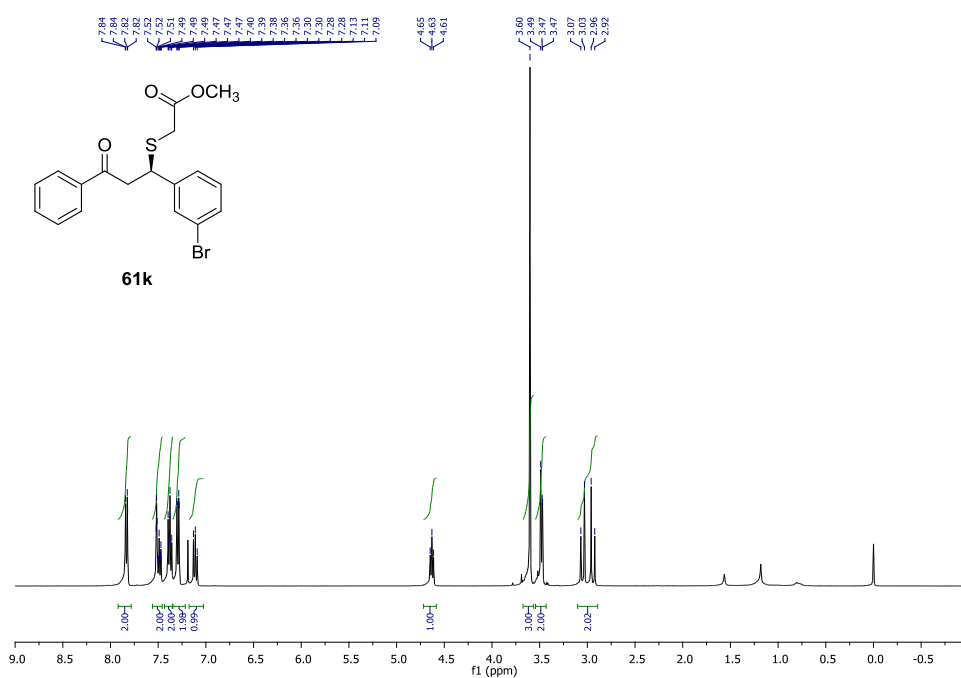


Figure A. 23 ^1H NMR spectrum of **61k**

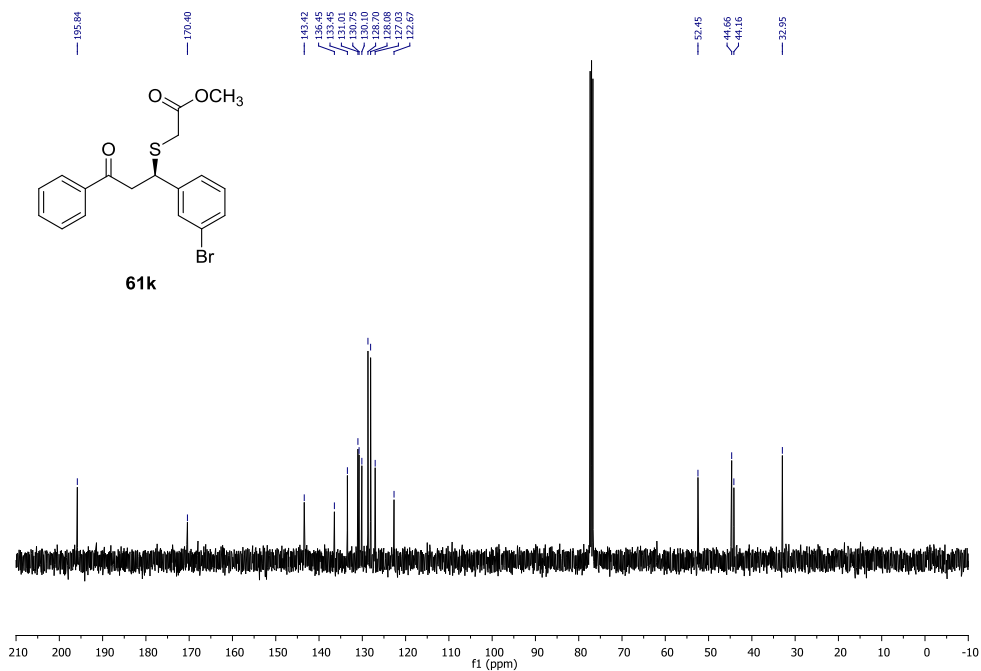


Figure A. 24 ^{13}C NMR spectrum of **61k**

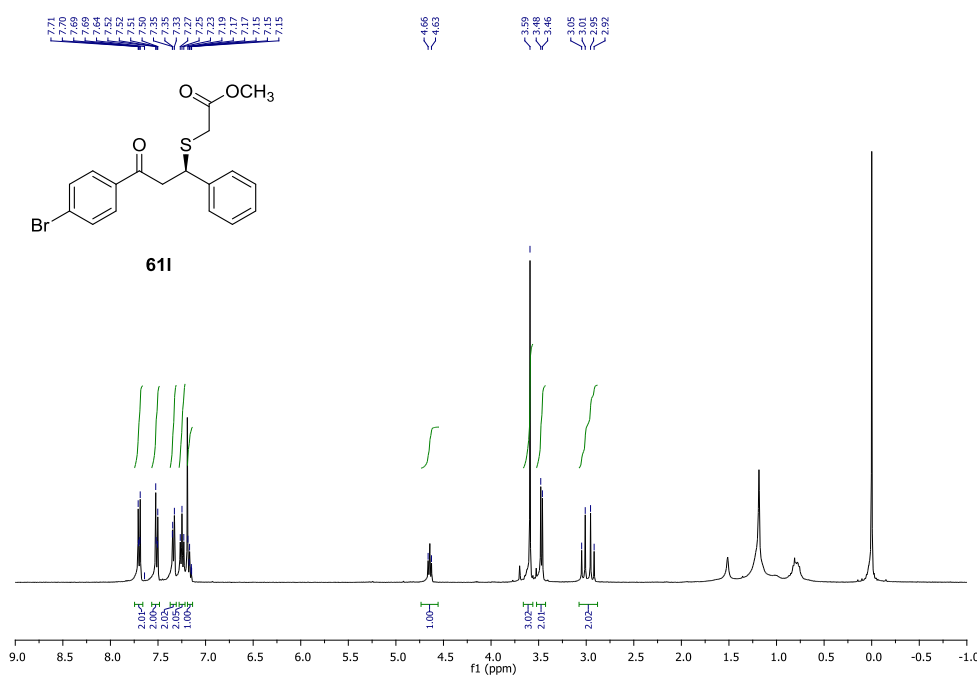


Figure A. 25 ¹H NMR spectrum of **611**

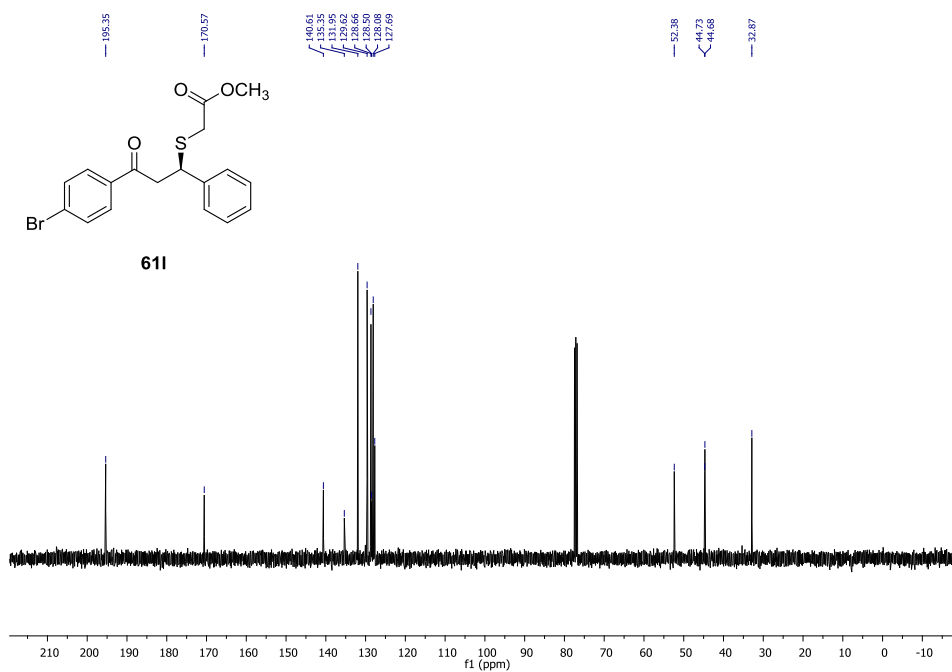


Figure A. 26 ¹³C NMR spectrum of **611**

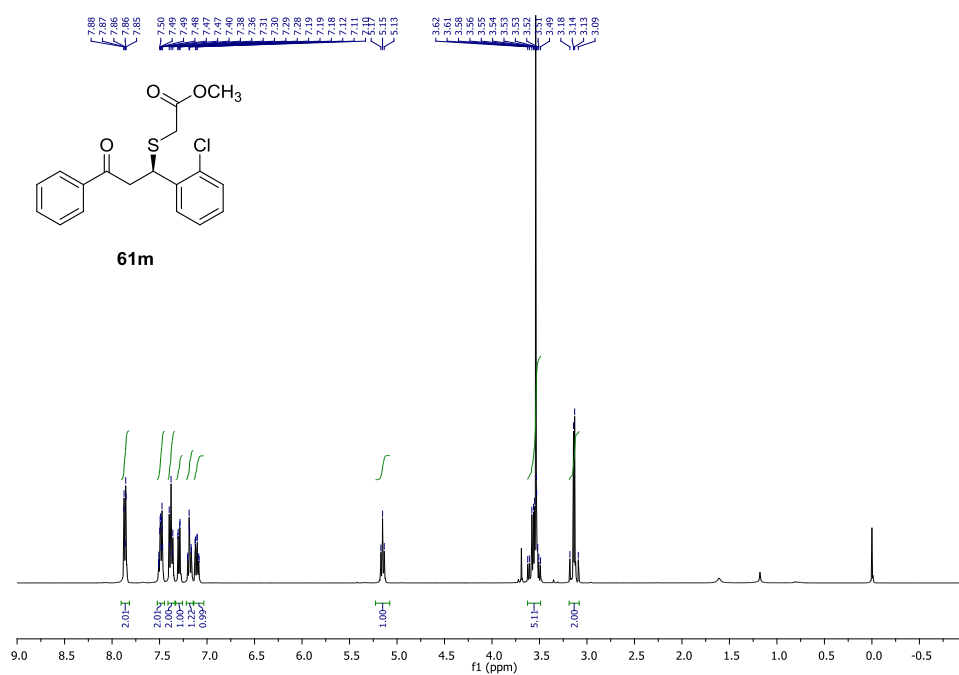


Figure A. 27 ^1H NMR spectrum of **61m**

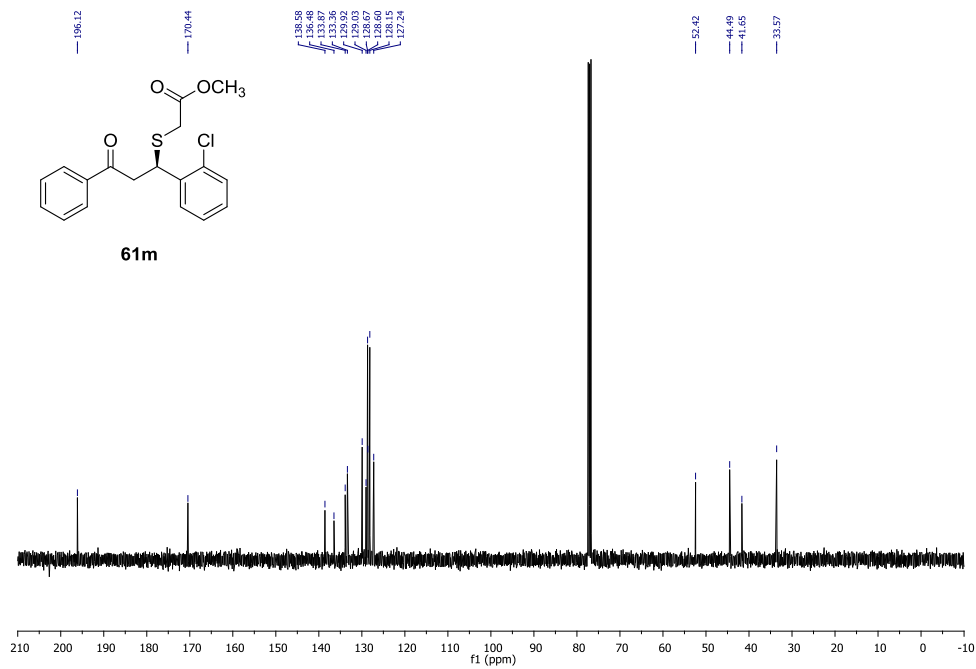


Figure A. 28 ^{13}C NMR spectrum of **61m**

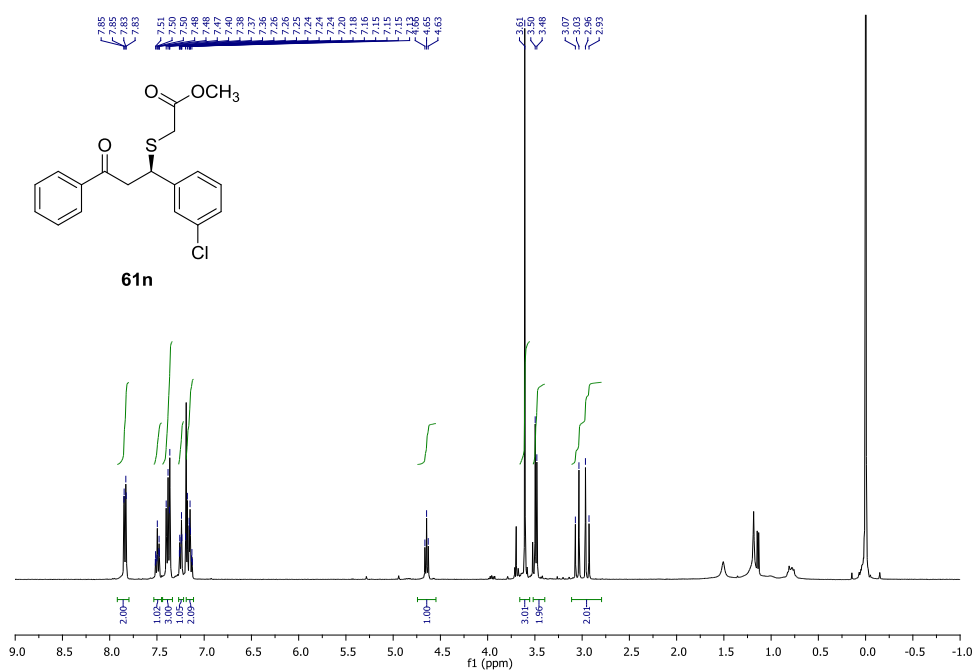


Figure A. 29 $^1\text{H NMR}$ spectrum of **61n**

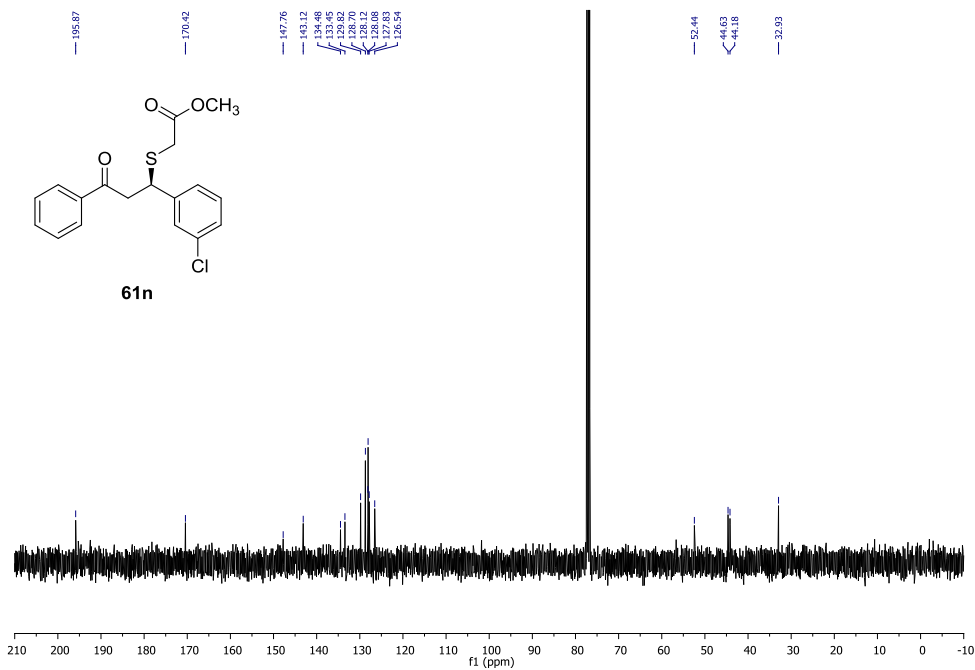


Figure A. 30 $^{13}\text{C NMR}$ spectrum of **61n**

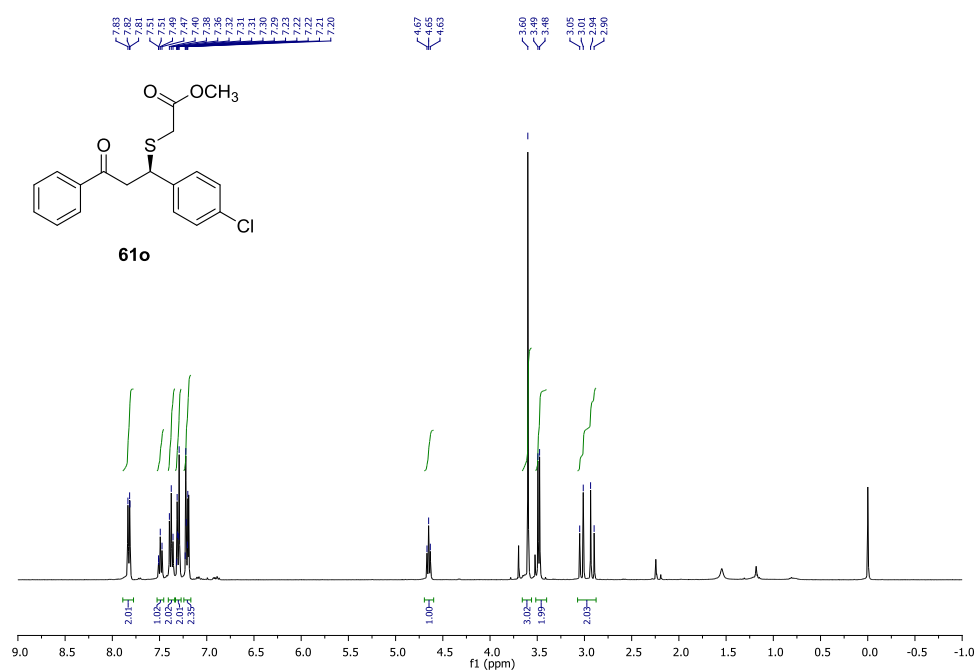


Figure A. 31 ¹H NMR spectrum of **61o**

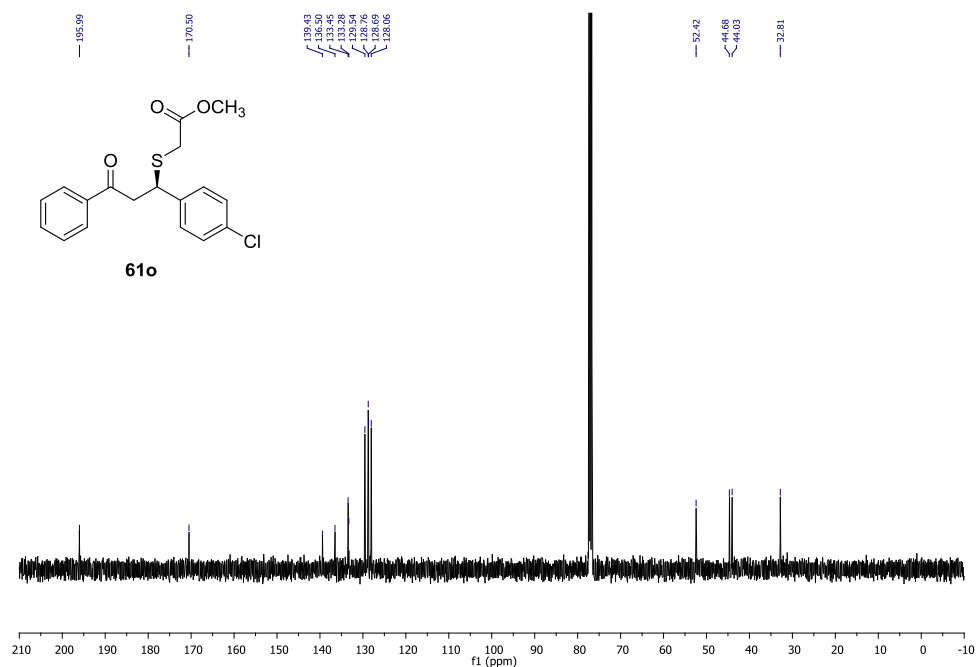


Figure A. 32 ¹³C NMR spectrum of **61o**

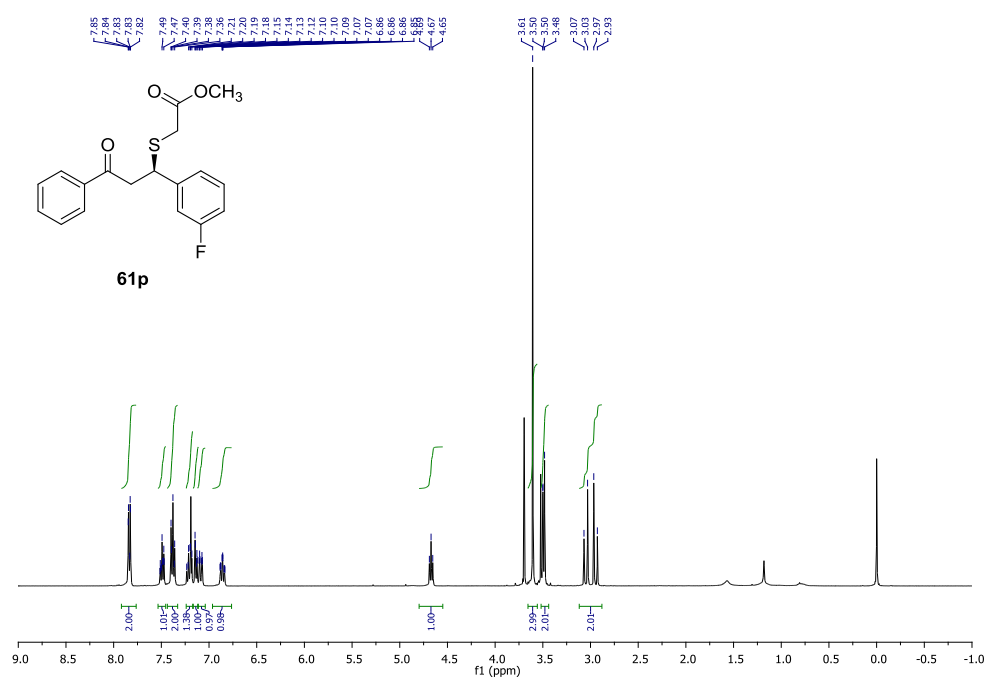


Figure A. 33 ¹H NMR spectrum of **61p**

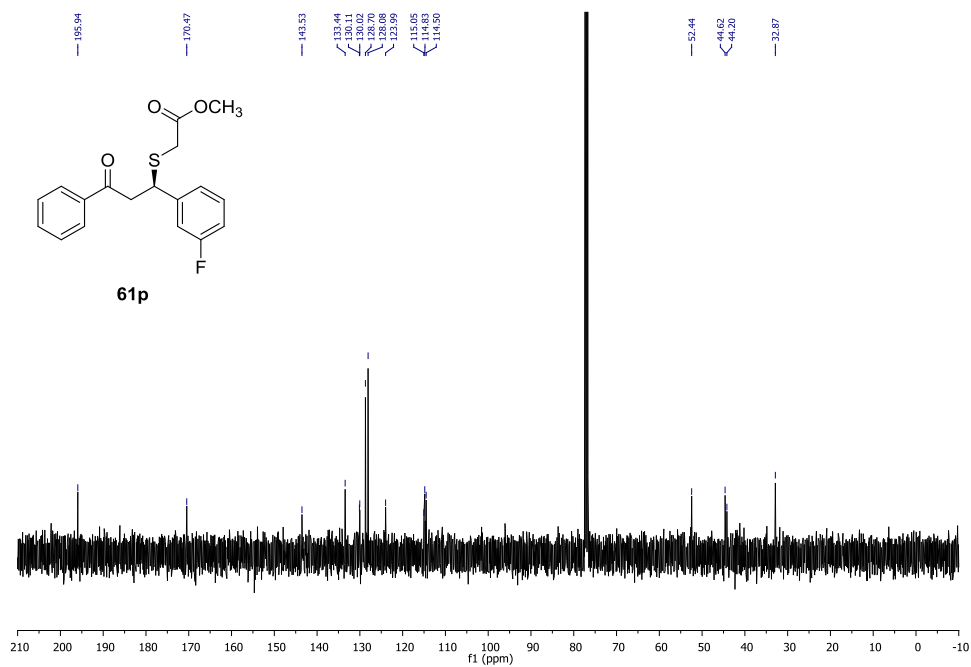


Figure A. 34 ¹³C NMR spectrum of **61p**

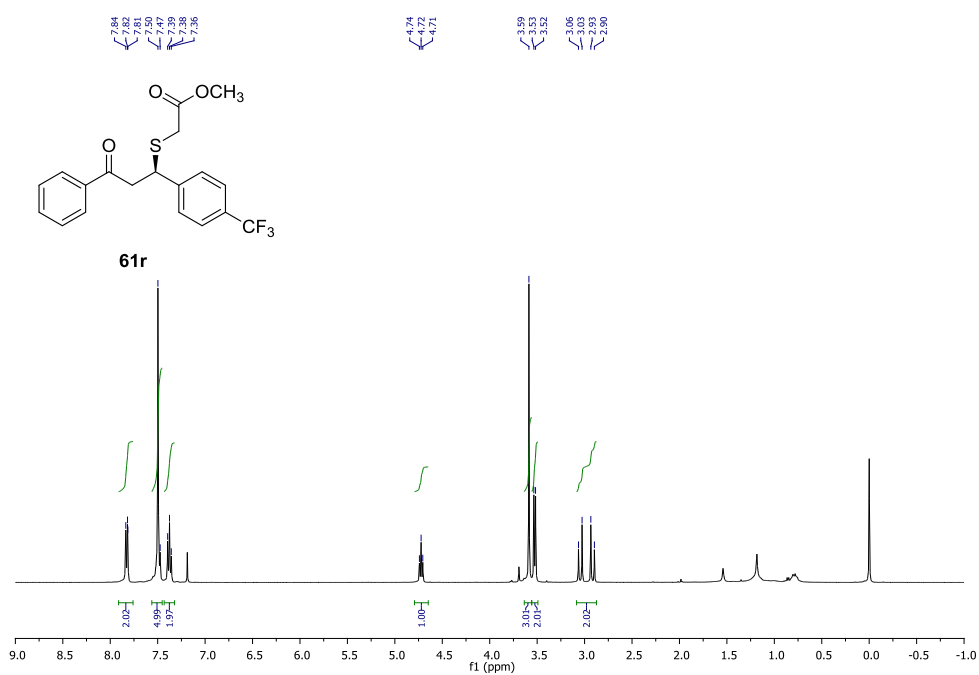


Figure A. 37 ¹H NMR spectrum of **61r**

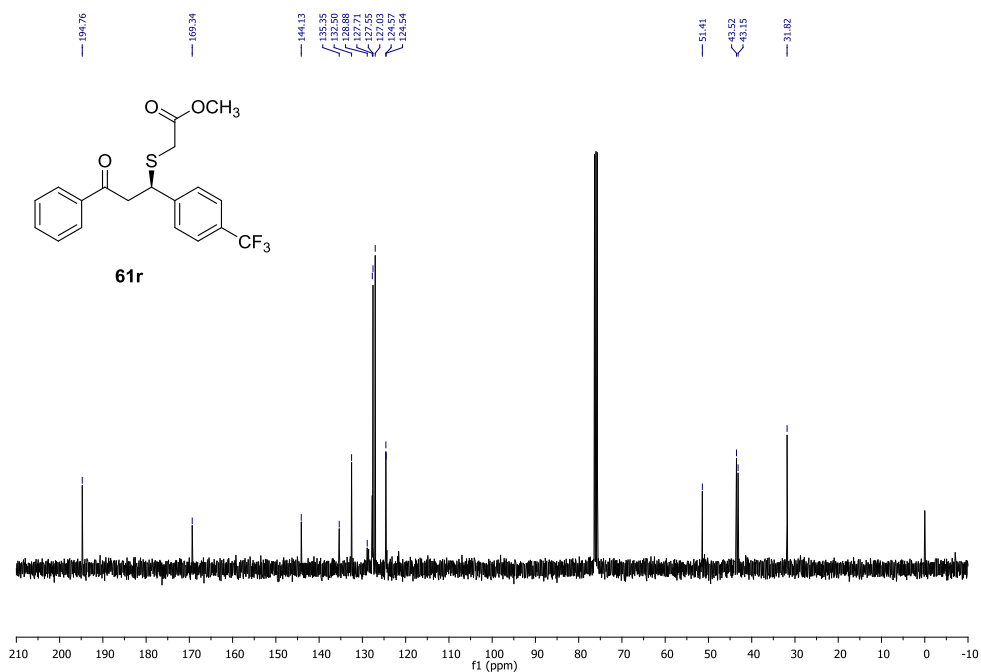


Figure A. 38 ¹³C NMR spectrum of **61r**

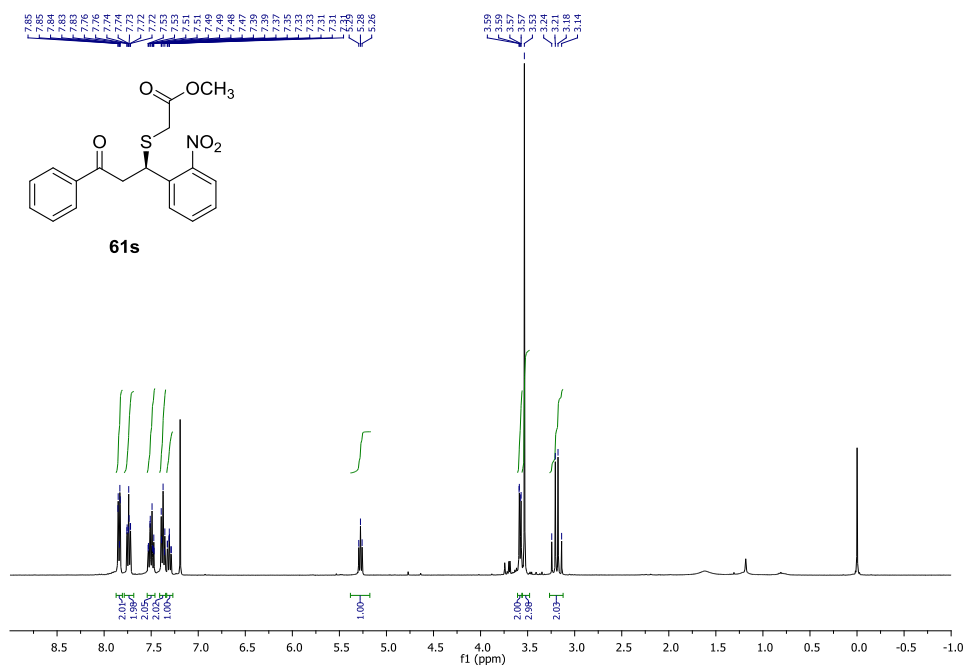


Figure A. 39 ^1H NMR spectrum of **61s**

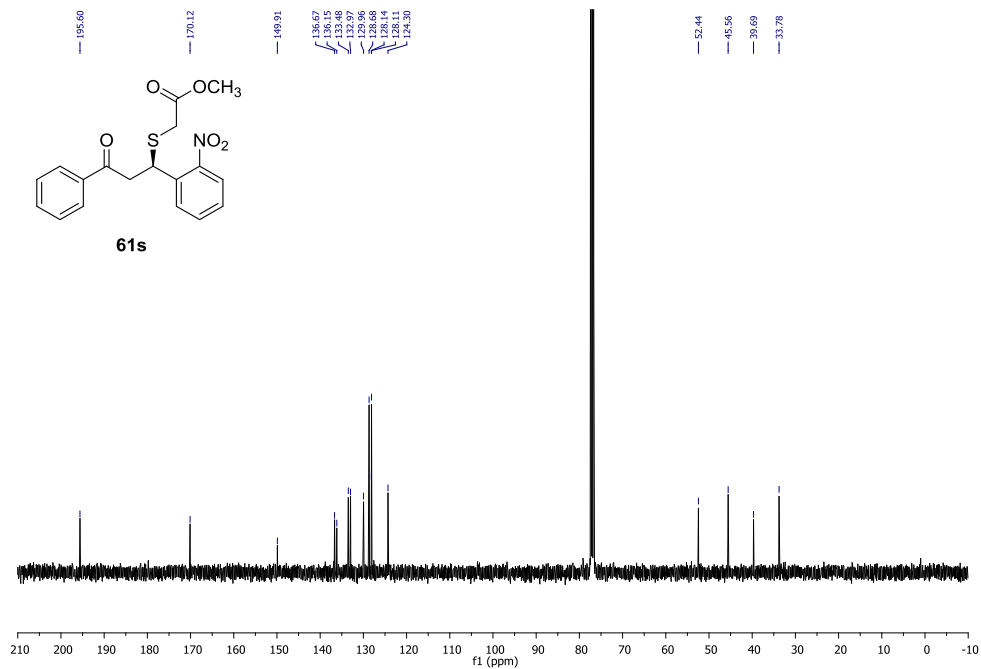


Figure A. 40 ^{13}C NMR spectrum of **61s**

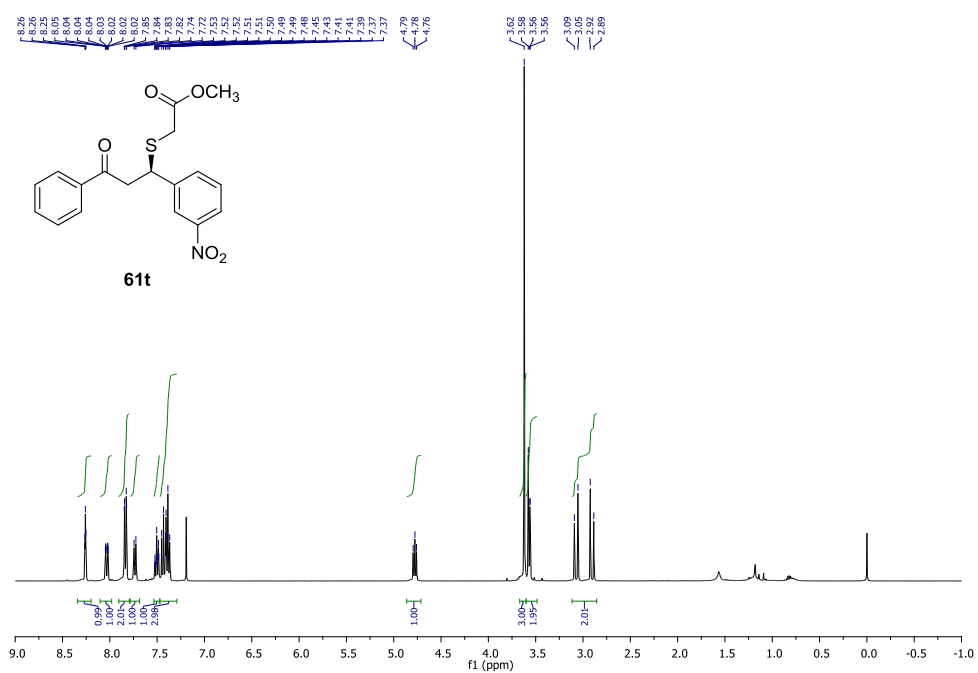


Figure A. 41 ¹H NMR spectrum of **61t**

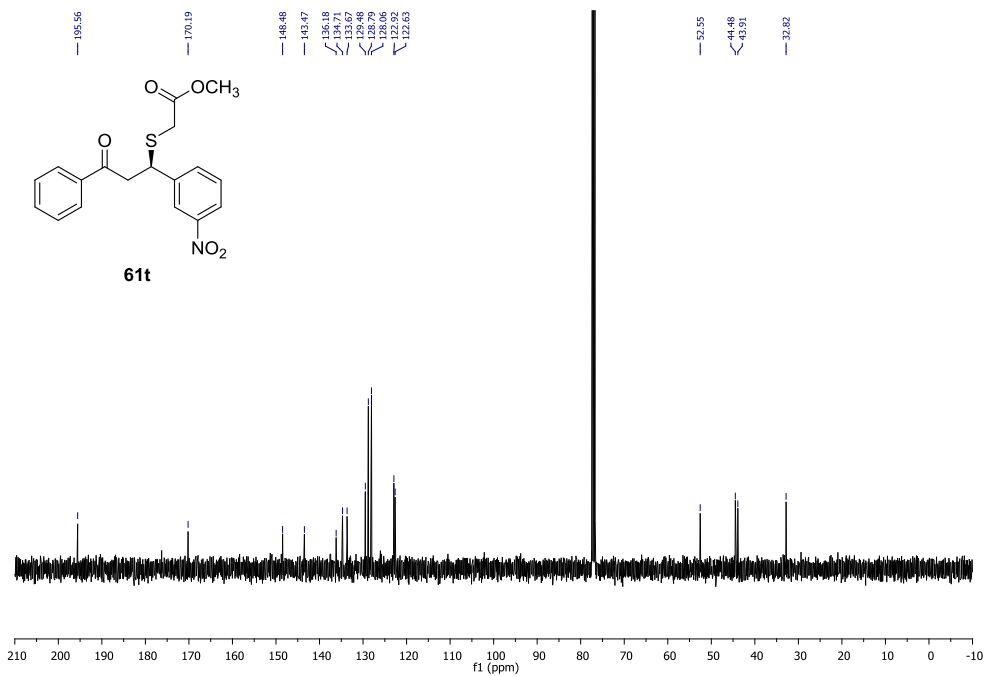


Figure A. 42 ¹³C NMR spectrum of **61t**

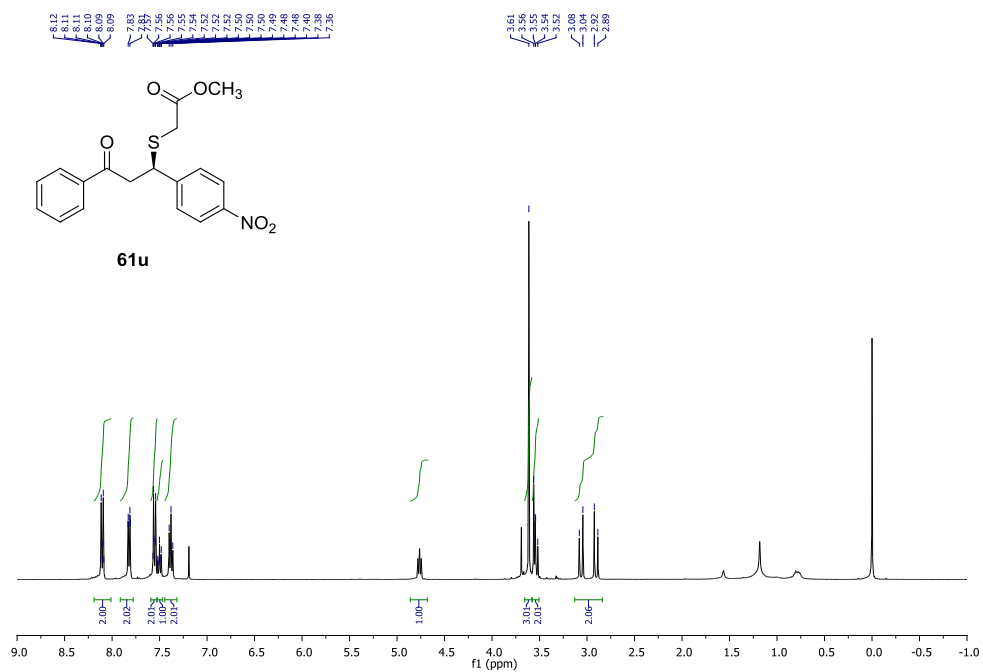


Figure A. 43 ¹H NMR spectrum of **61u**

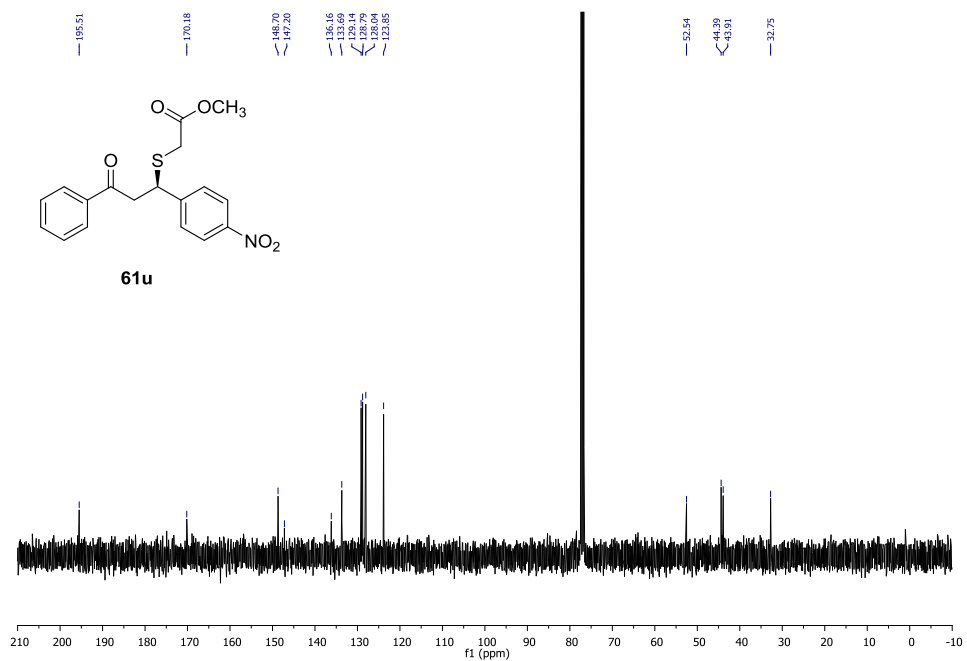


Figure A. 44 ¹³C NMR spectrum of **61u**

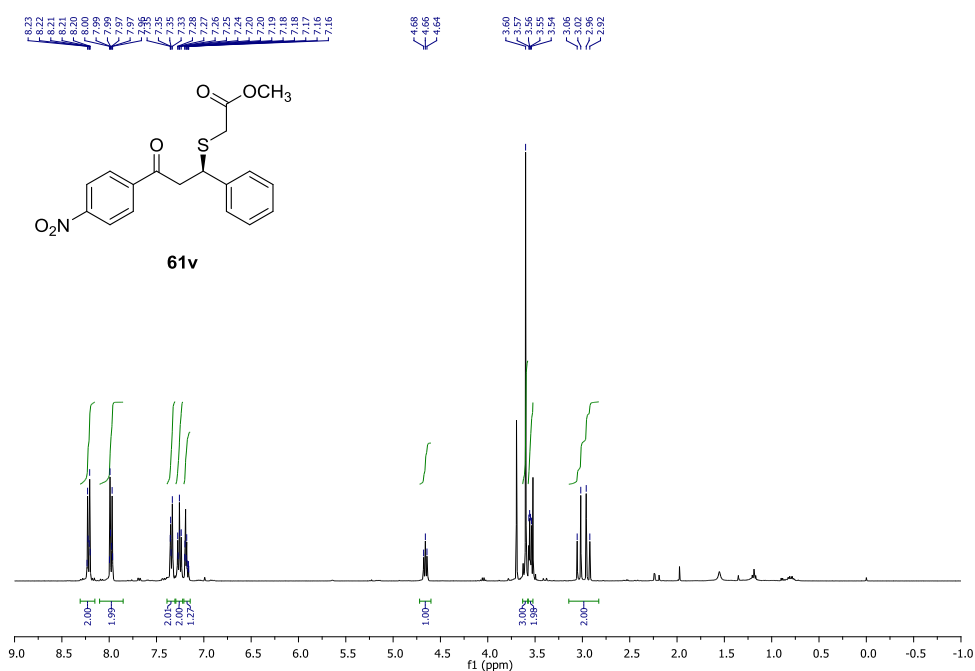


Figure A. 45 $^1\text{H NMR}$ spectrum of **61v**

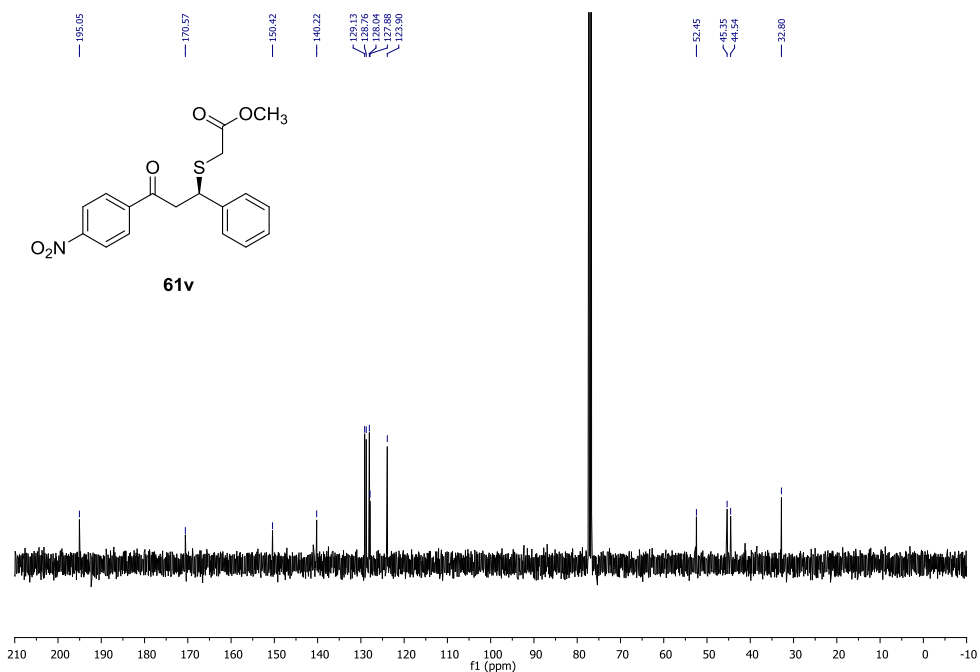


Figure A. 46 $^{13}\text{C NMR}$ spectrum of **61v**

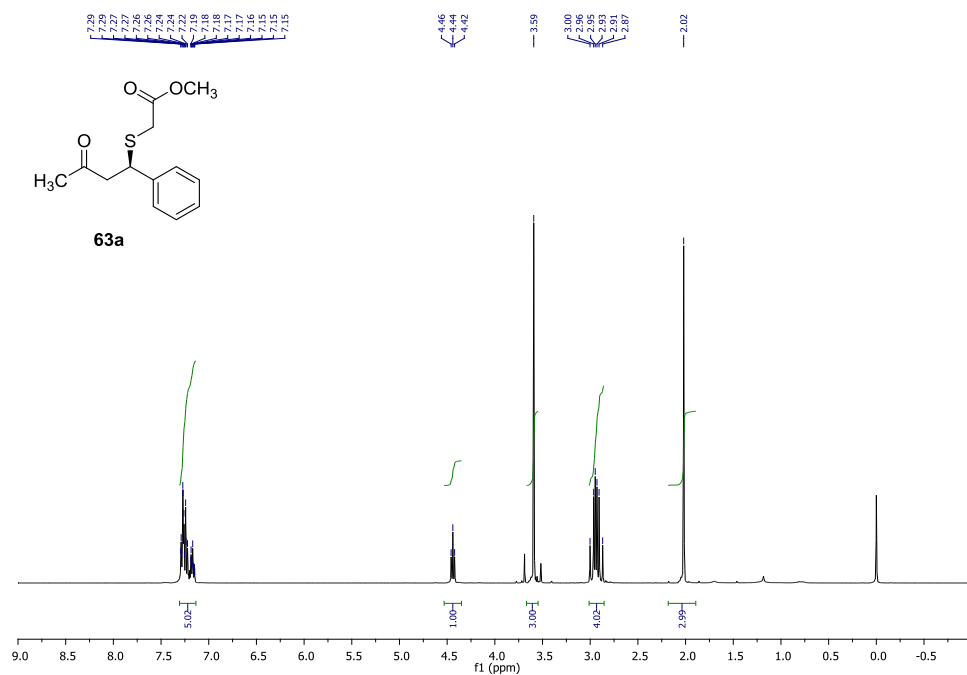


Figure A. 47 ¹H NMR spectrum of **63a**

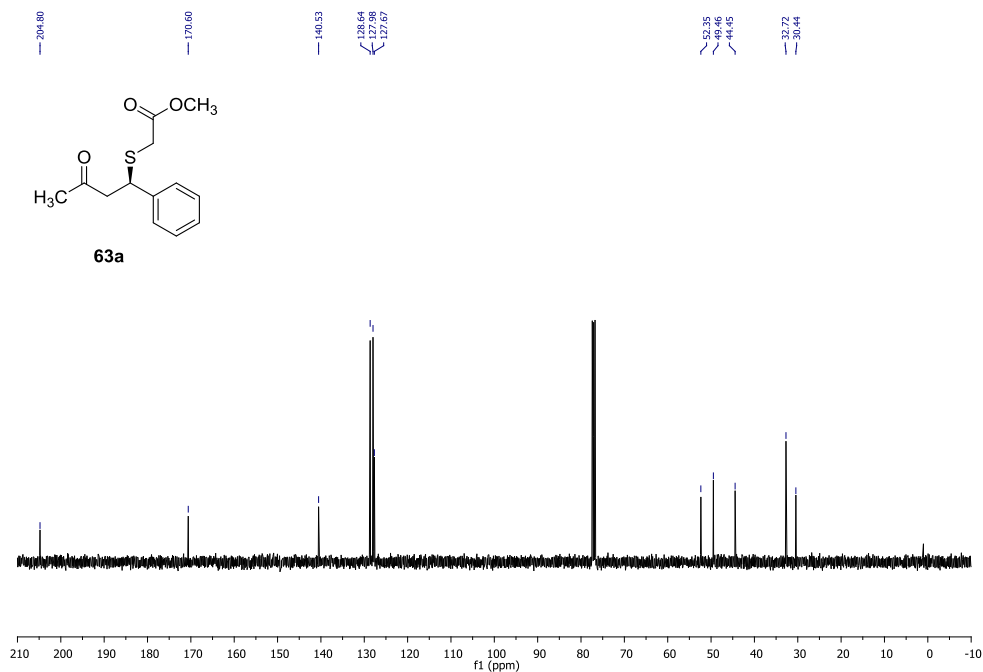


Figure A. 48 ¹³C NMR spectrum of **63a**

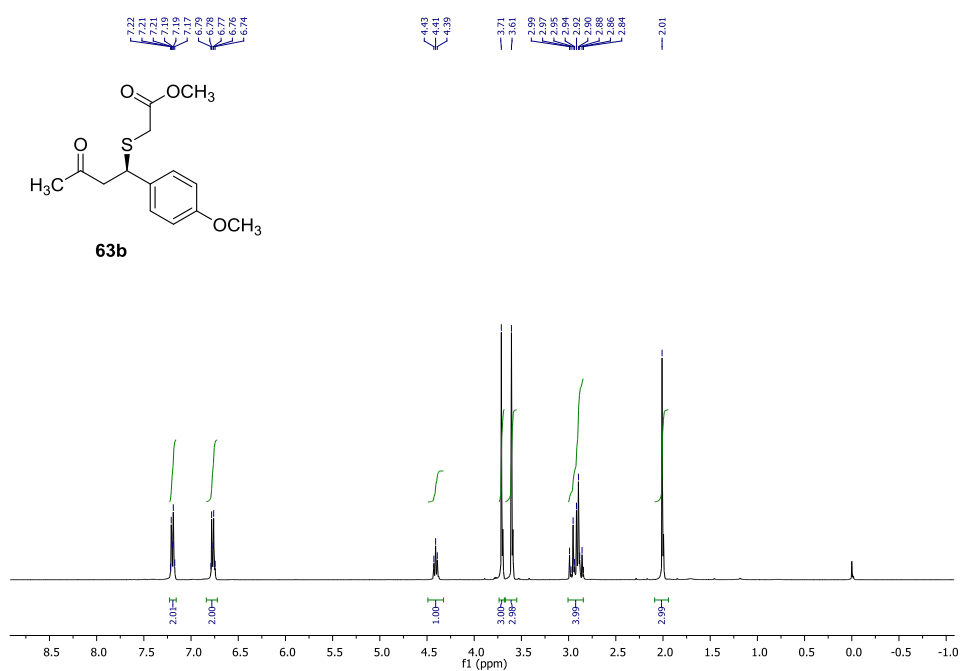


Figure A. 49 ¹H NMR spectrum of **63b**

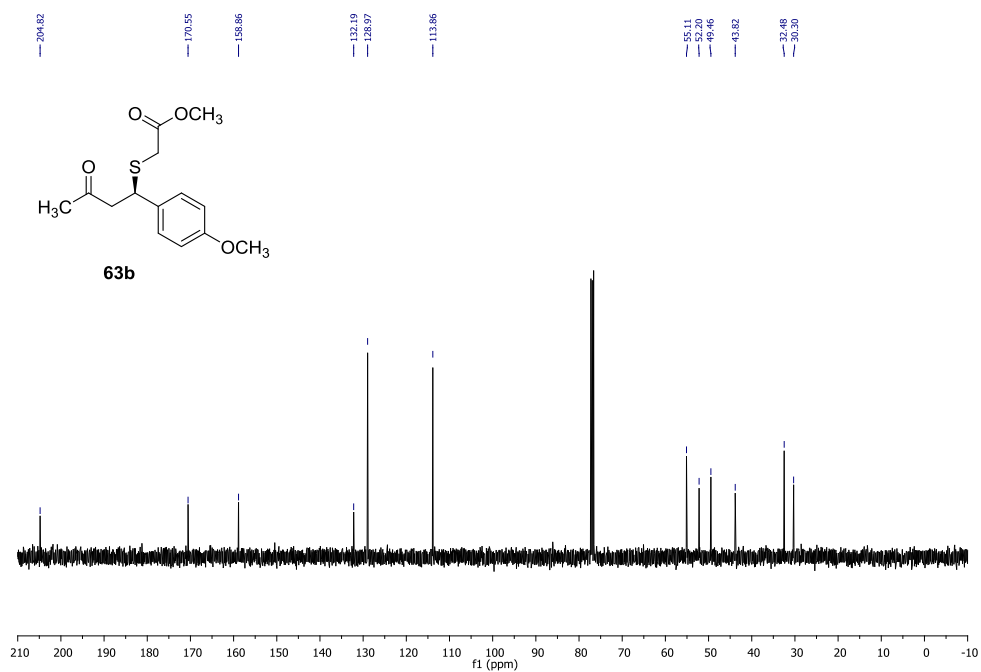


Figure A. 50 ¹³C NMR spectrum of **63b**

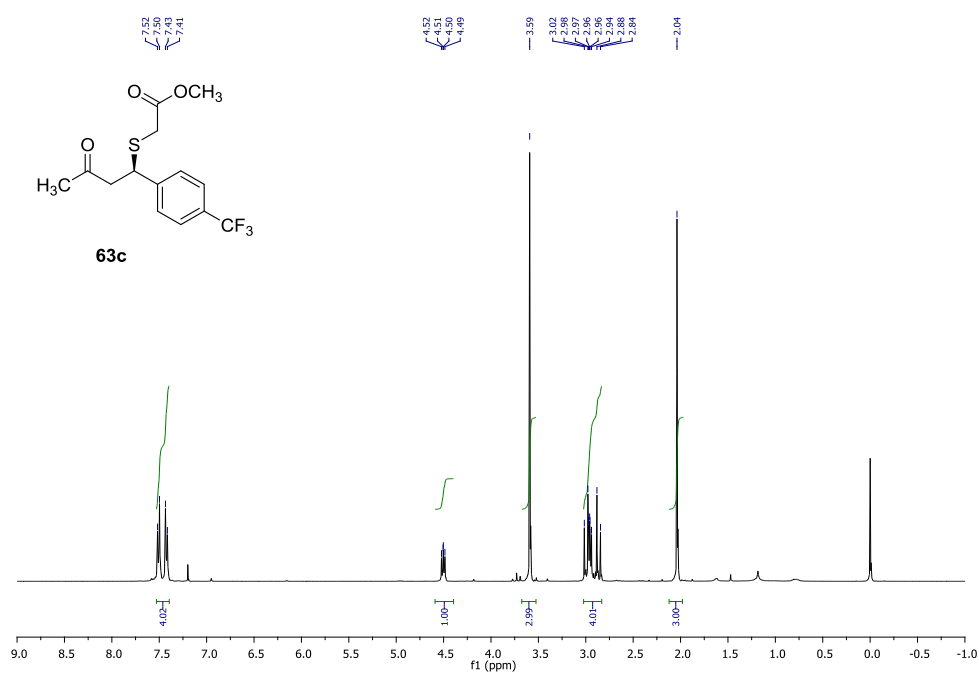


Figure A. 51 ¹H NMR spectrum of **63c**

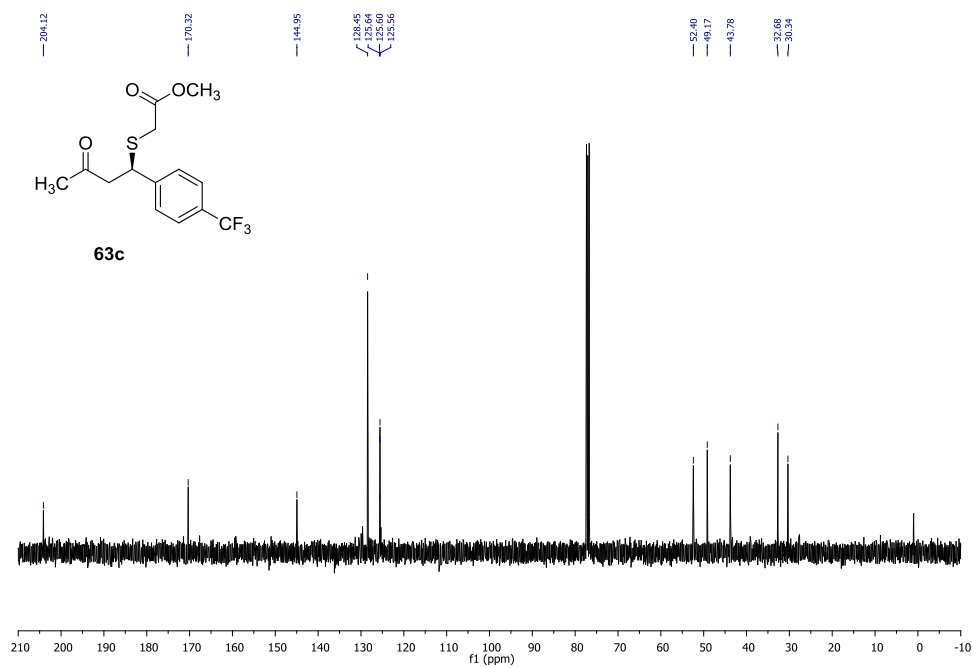


Figure A. 52 ¹³C NMR spectrum of **63c**

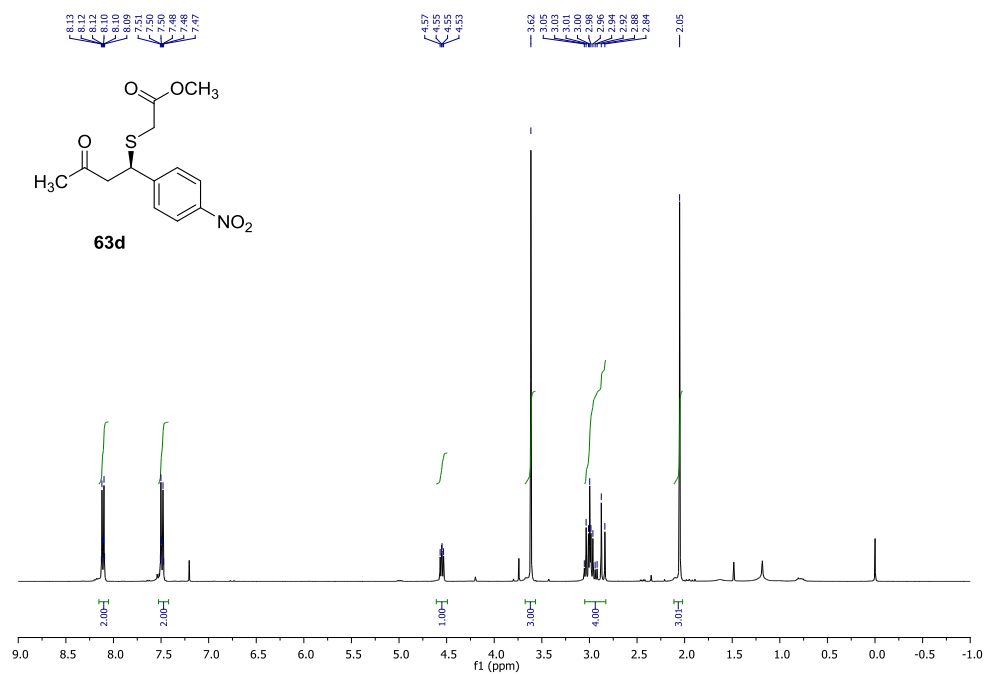


Figure A. 53 $^1\text{H NMR}$ spectrum of **63d**

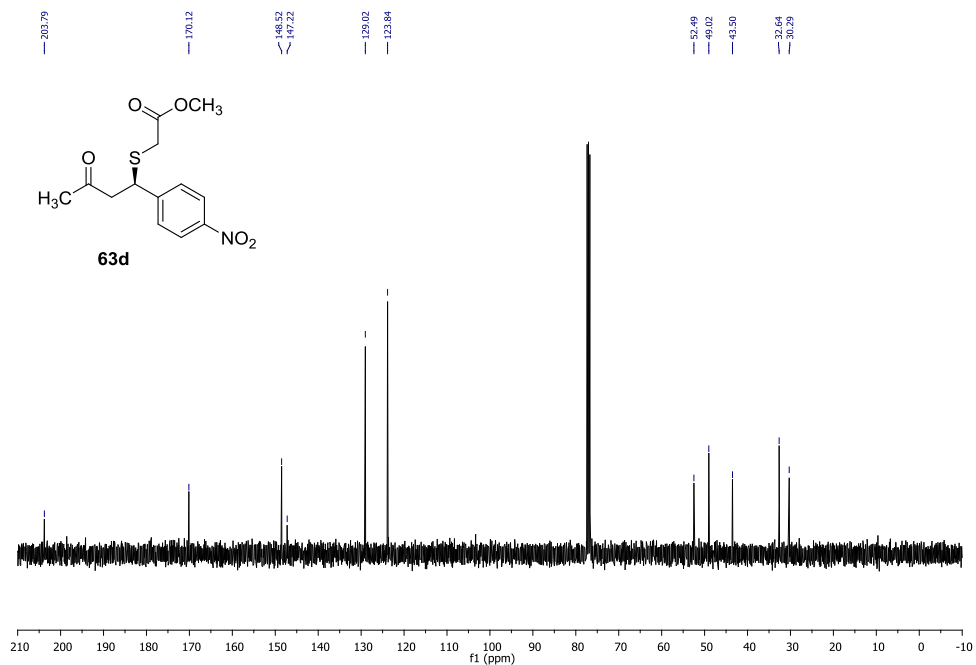


Figure A. 54 $^{13}\text{C NMR}$ spectrum of **63d**

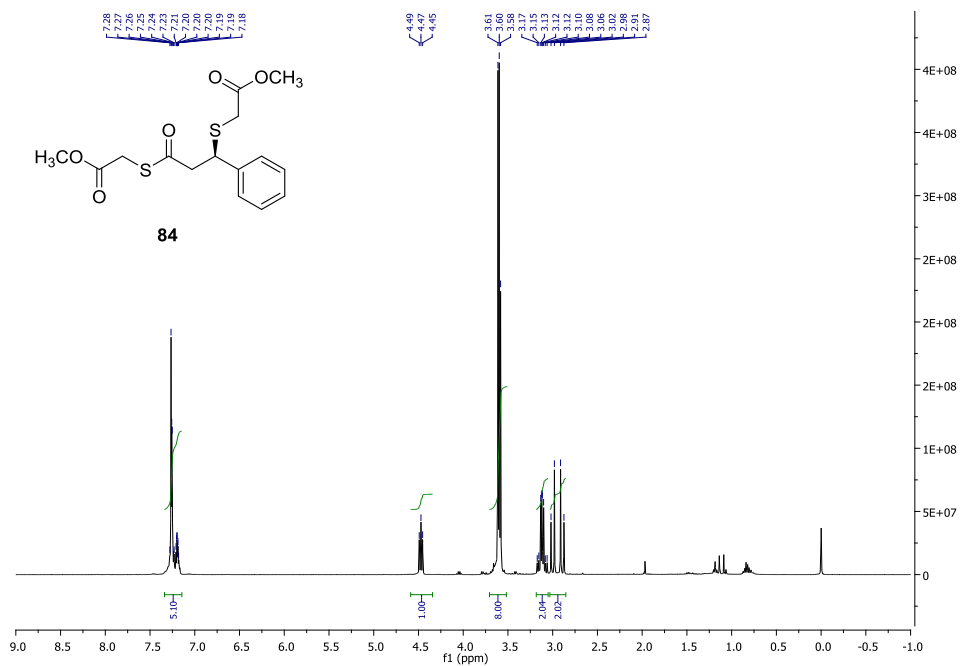


Figure A. 55 ¹H NMR spectrum of **84**

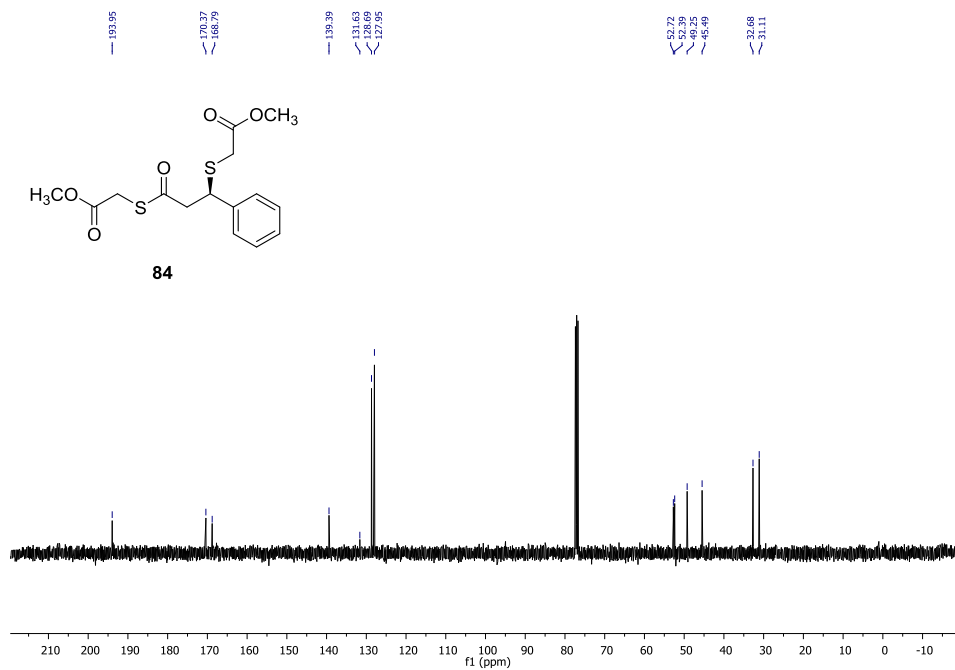


Figure A. 56 ¹³C NMR spectrum of **84**

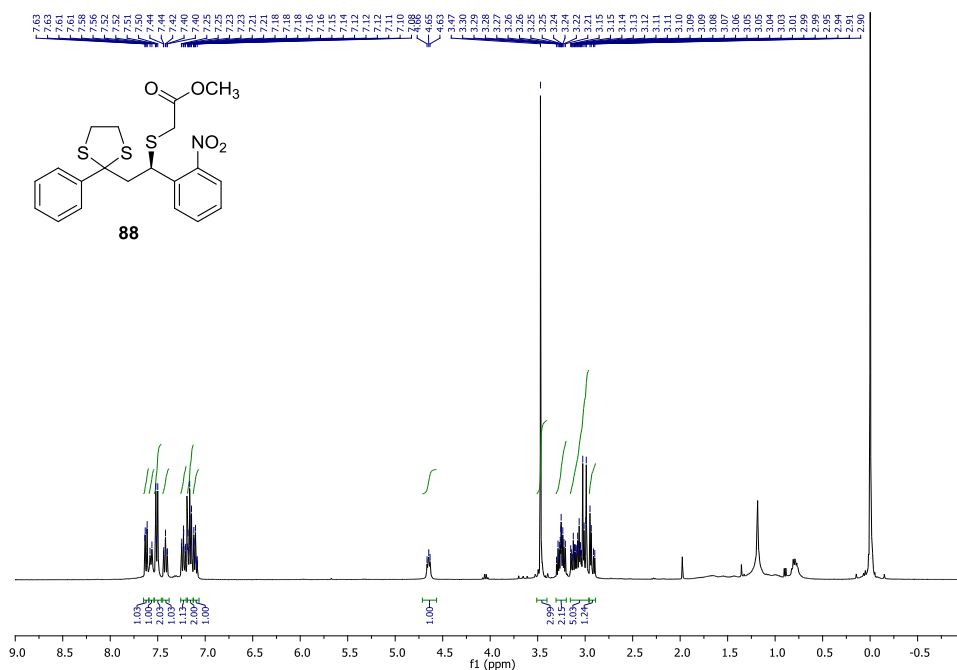


Figure A. 57 ¹H NMR spectrum of **88**

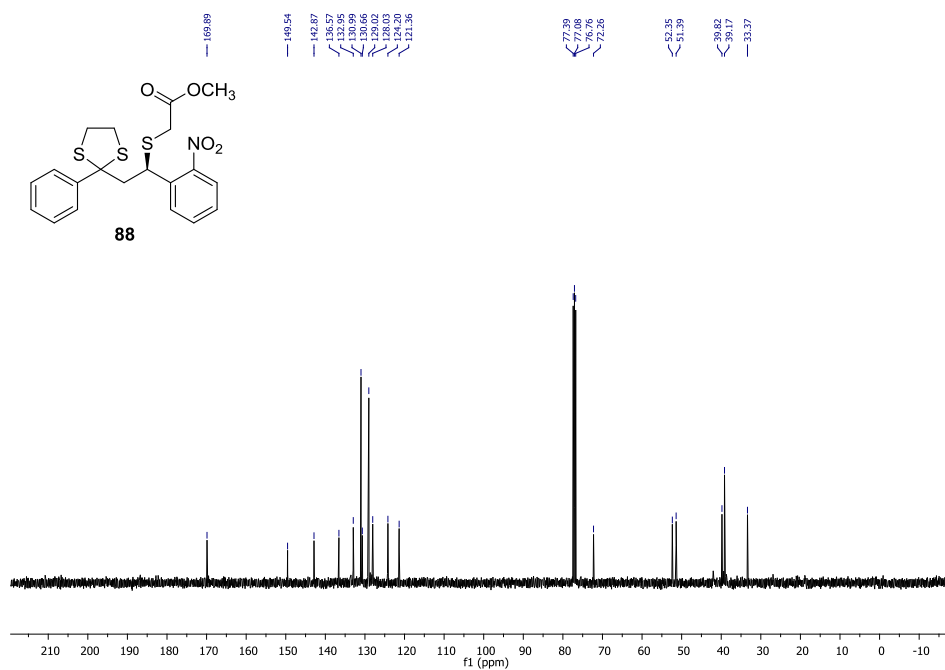


Figure A. 58 ¹³C NMR spectrum of **88**

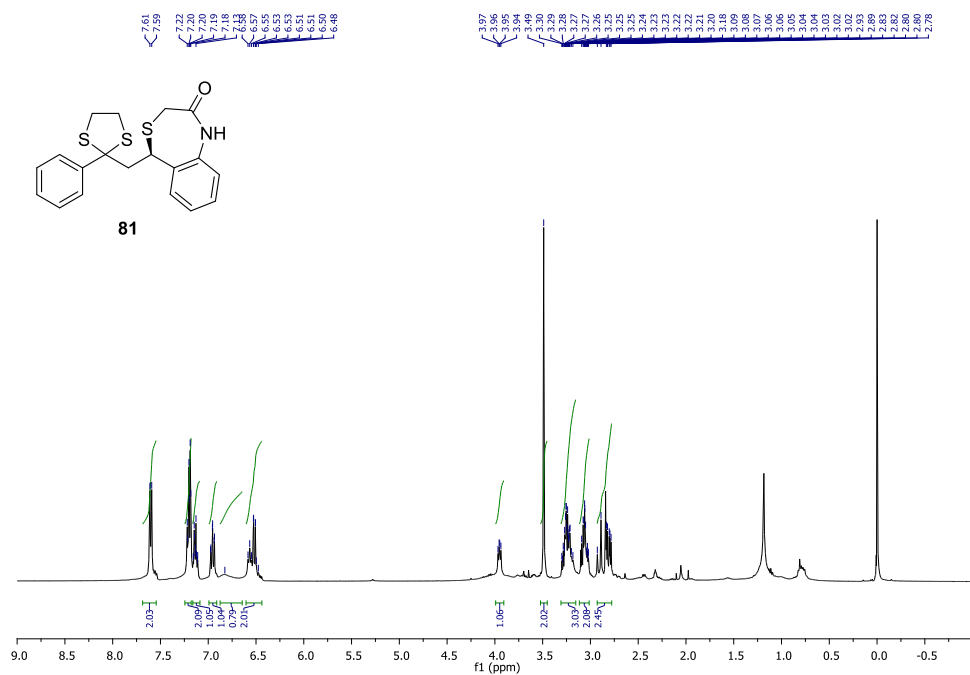


Figure A. 59 ^1H NMR spectrum of **81**

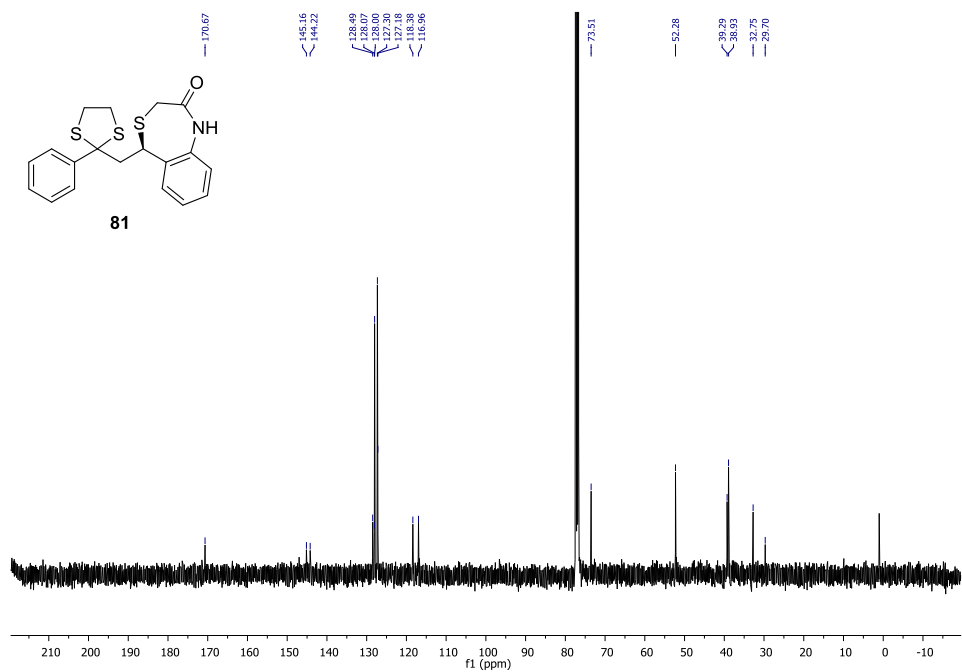


Figure A. 60 ^{13}C NMR spectrum of **81**

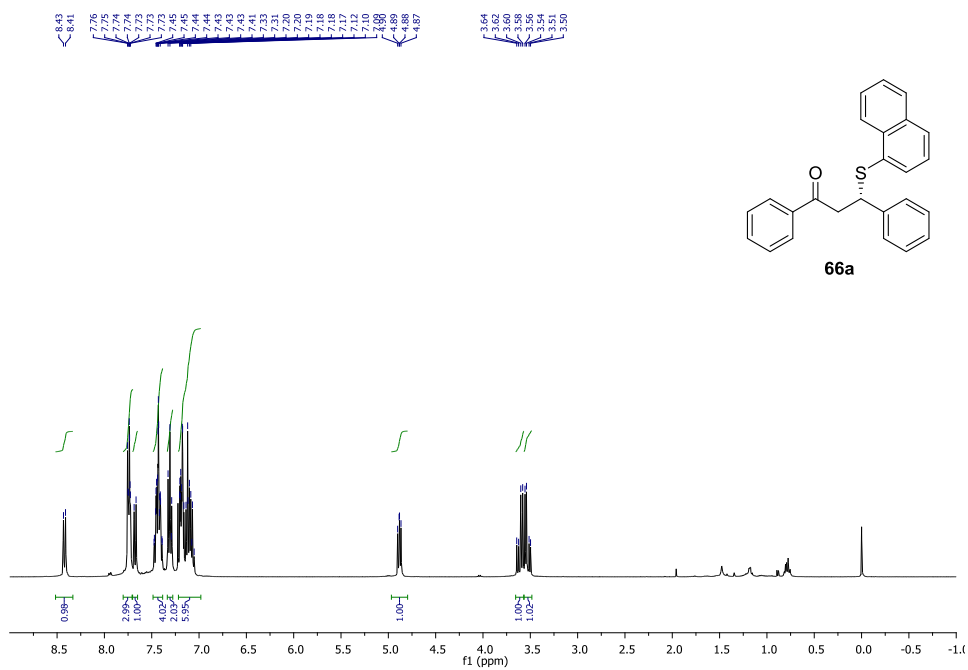


Figure A. 61 ¹H NMR spectrum of **66a**

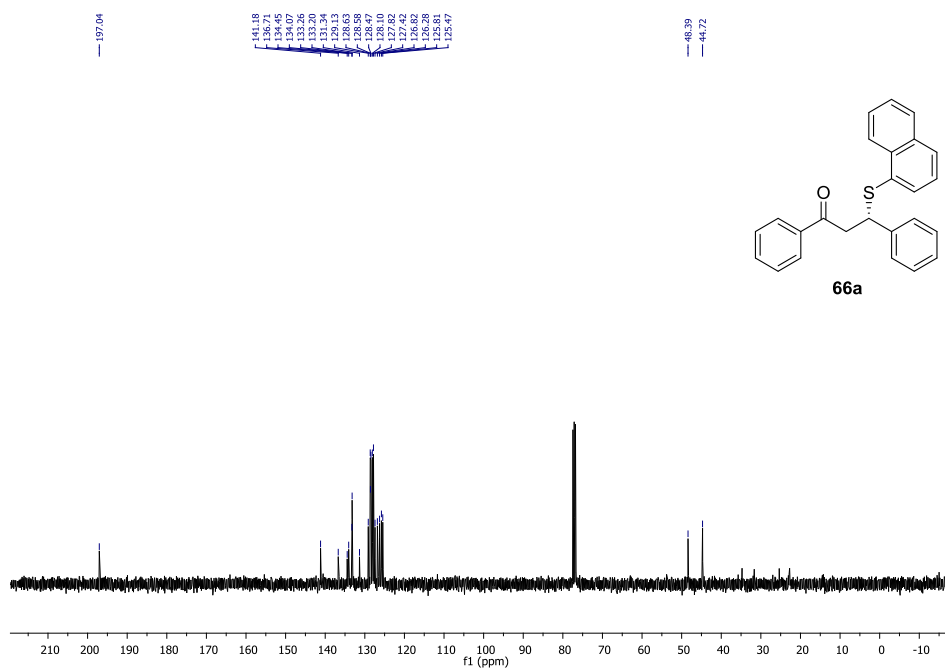


Figure A. 62 ¹³C NMR spectrum of **66a**

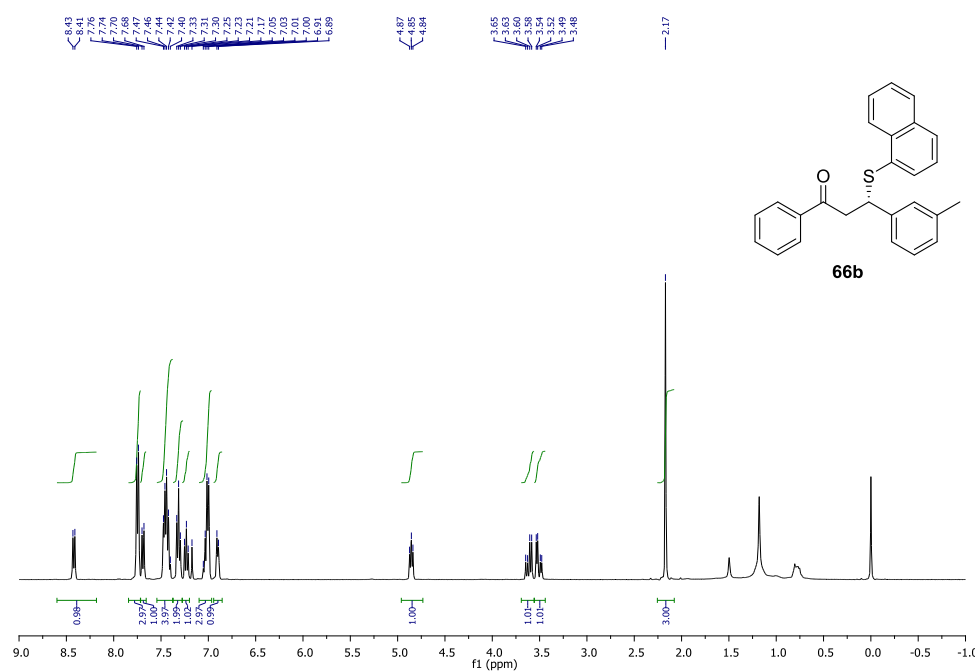


Figure A. 63 ¹H NMR spectrum of **66b**

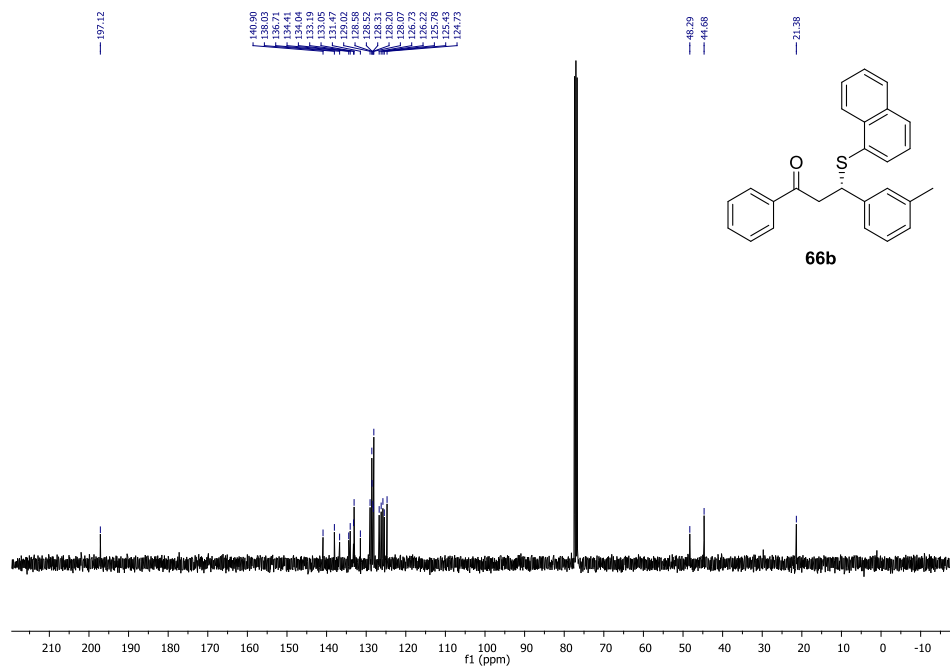


Figure A. 64 ¹³C NMR spectrum of **66b**

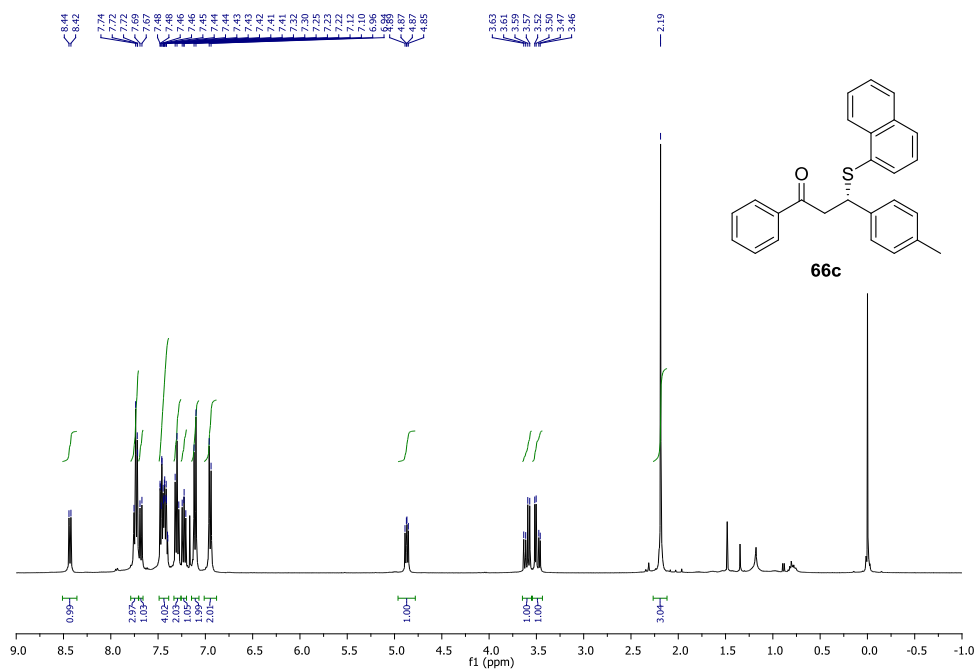


Figure A. 65 ¹H NMR spectrum of **66c**

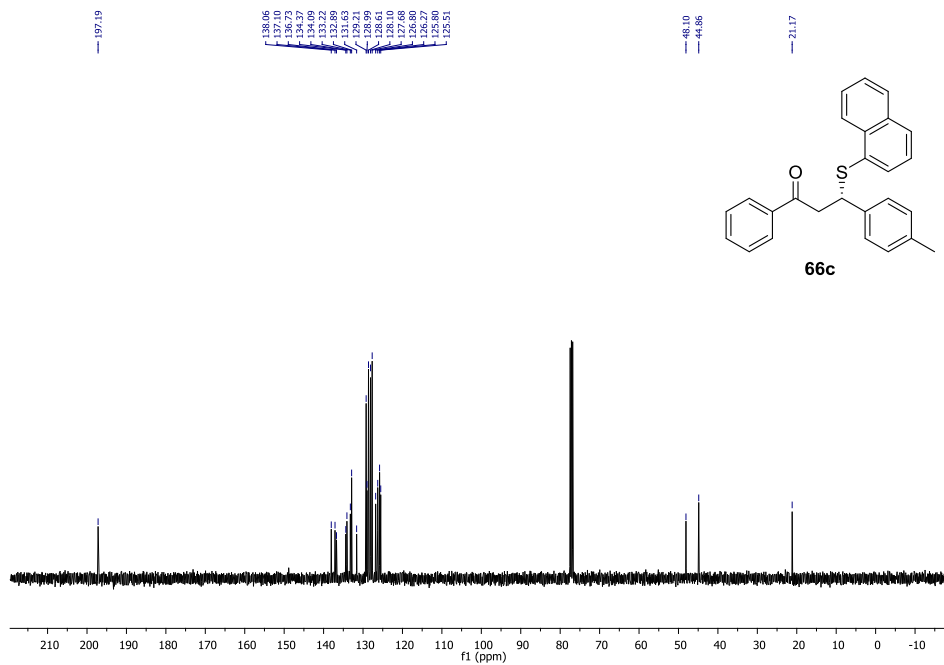


Figure A. 66 ¹³C NMR spectrum of **66c**

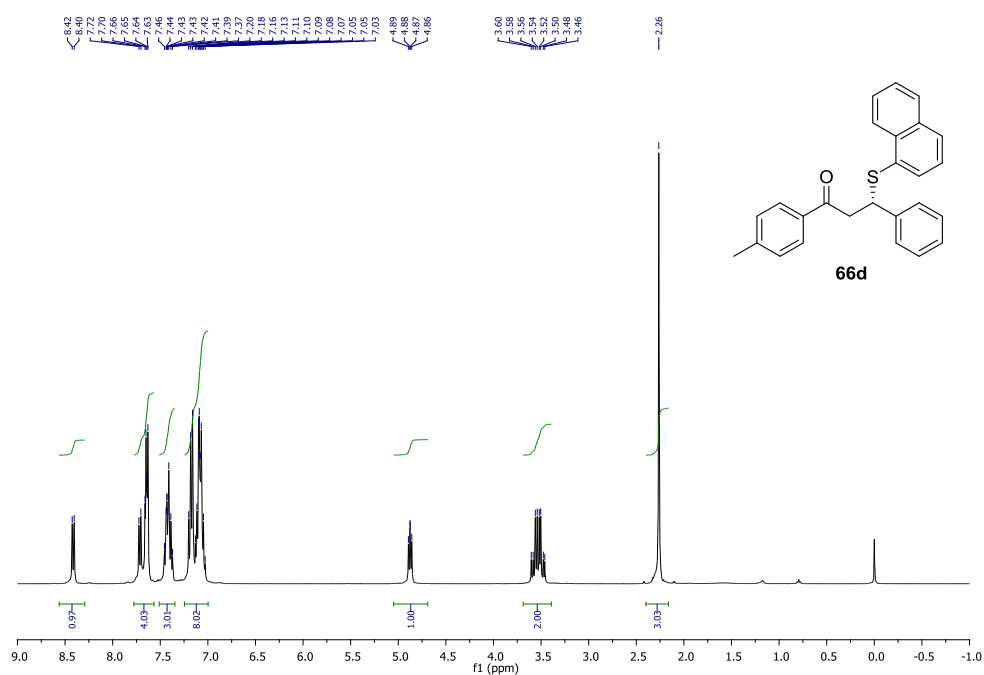


Figure A. 67 ^1H NMR spectrum of **66d**

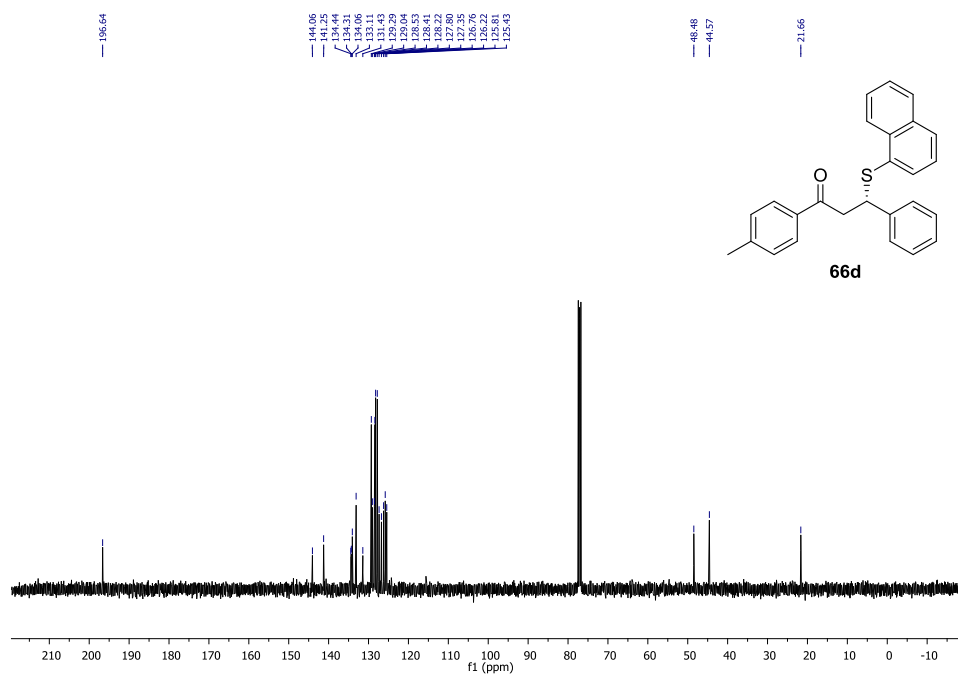


Figure A. 68 ^{13}C NMR spectrum of **66d**

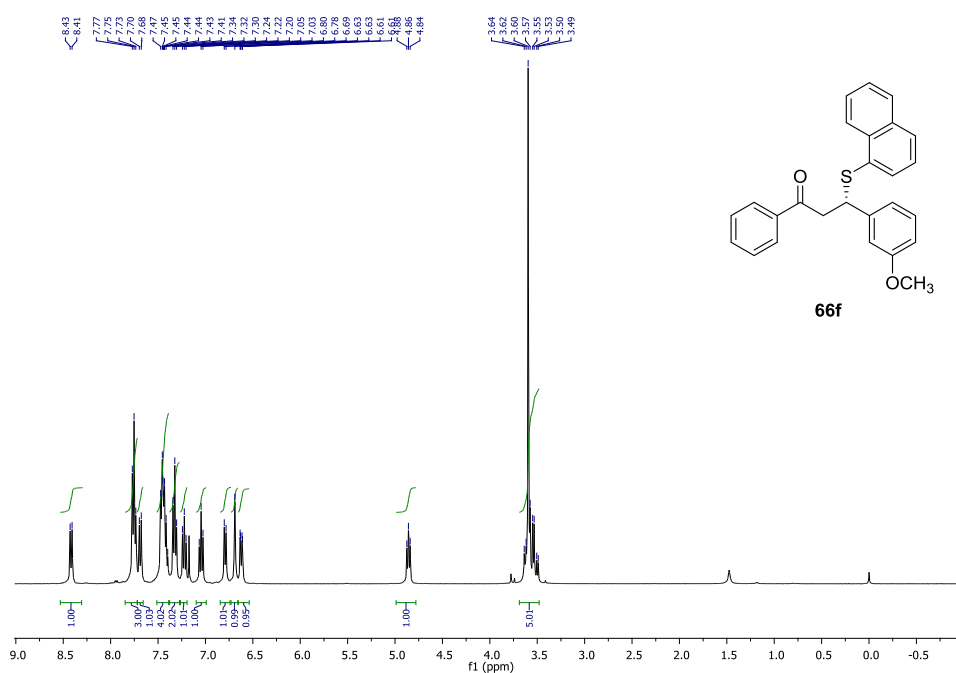


Figure A. 69 ¹H NMR spectrum of **66f**

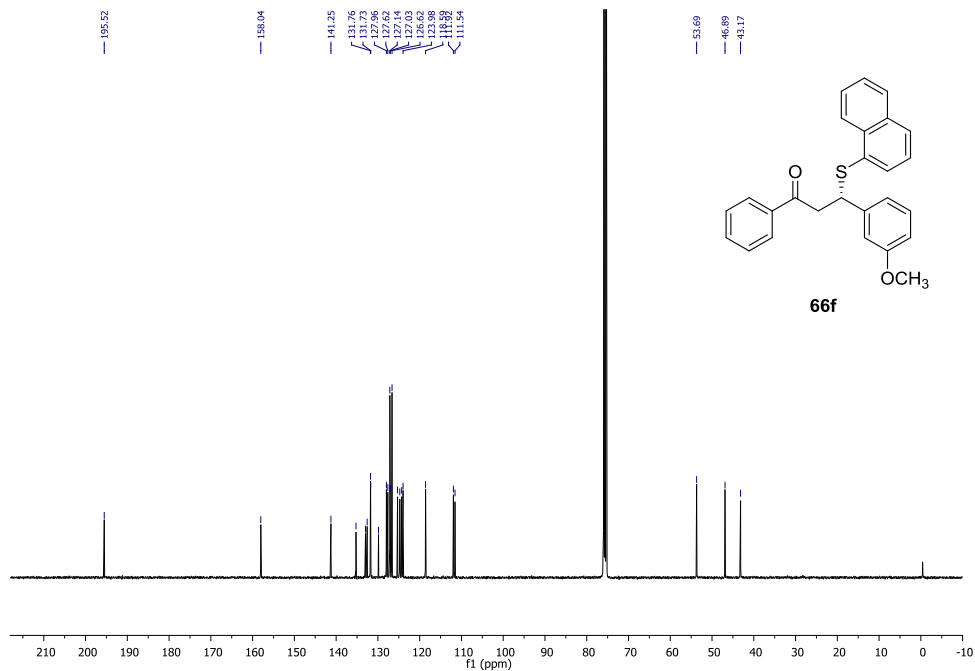


Figure A. 70 ¹³C NMR spectrum of **66f**

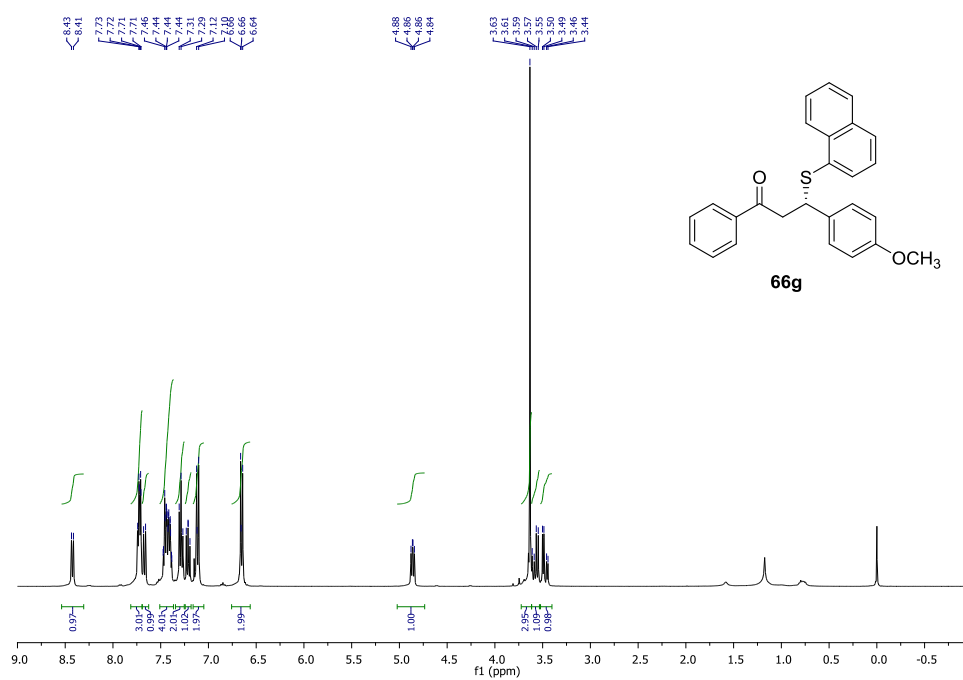


Figure A. 71 ¹H NMR spectrum of **66g**

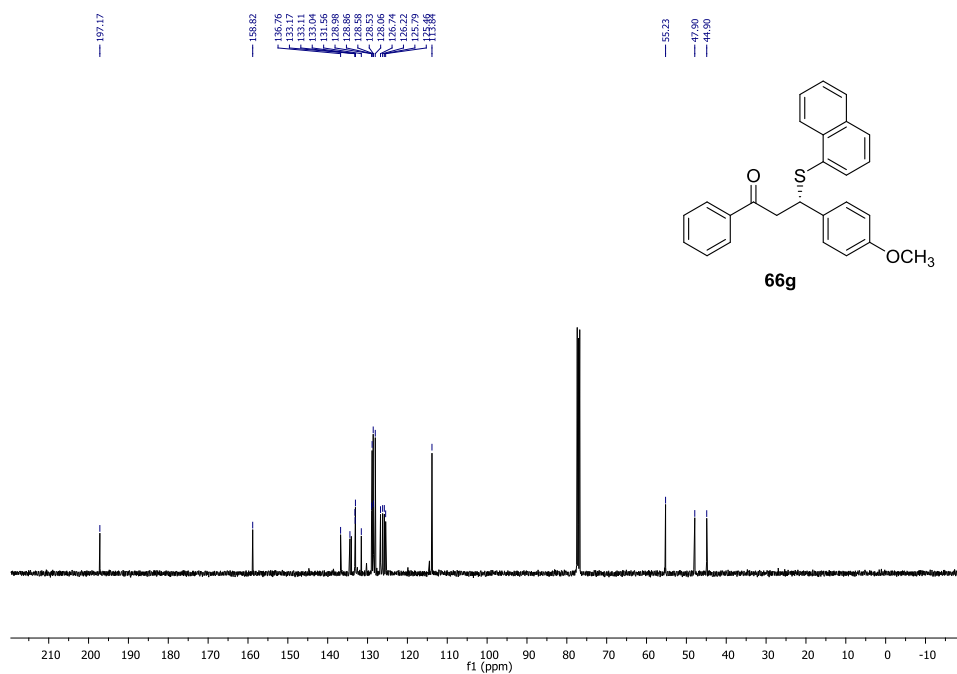


Figure A. 72 ¹³C NMR spectrum of **66g**

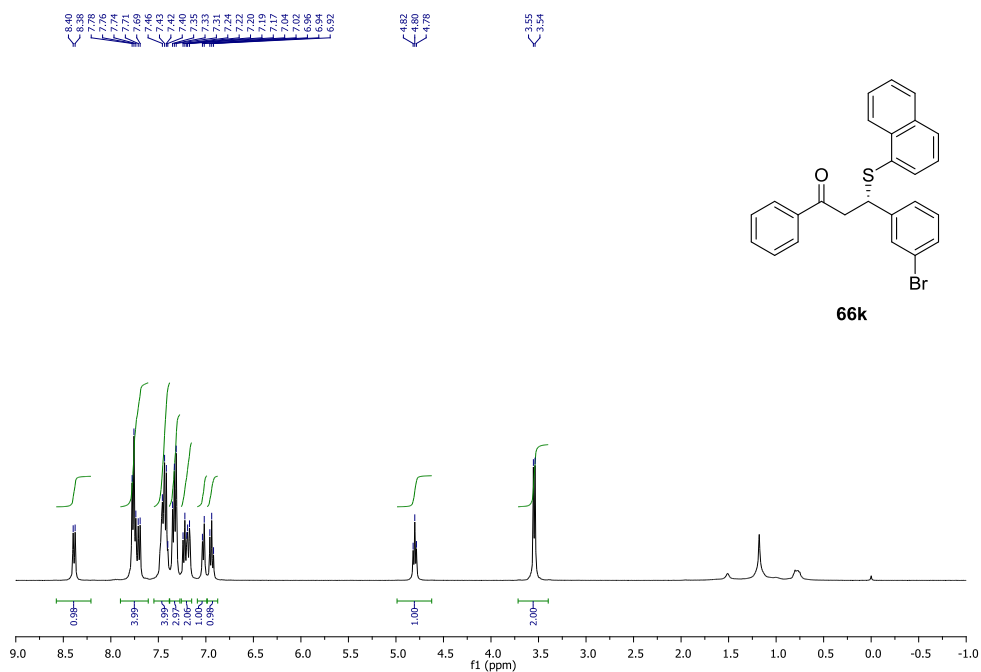


Figure A. 73 ¹H NMR spectrum of **66k**

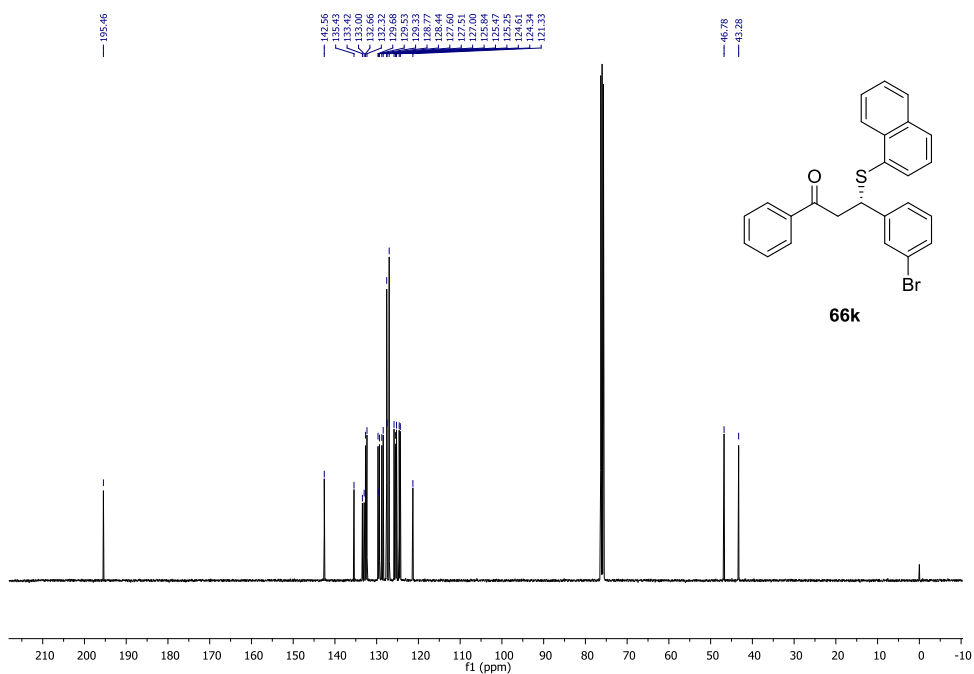


Figure A. 74 ¹³C NMR spectrum of **66k**

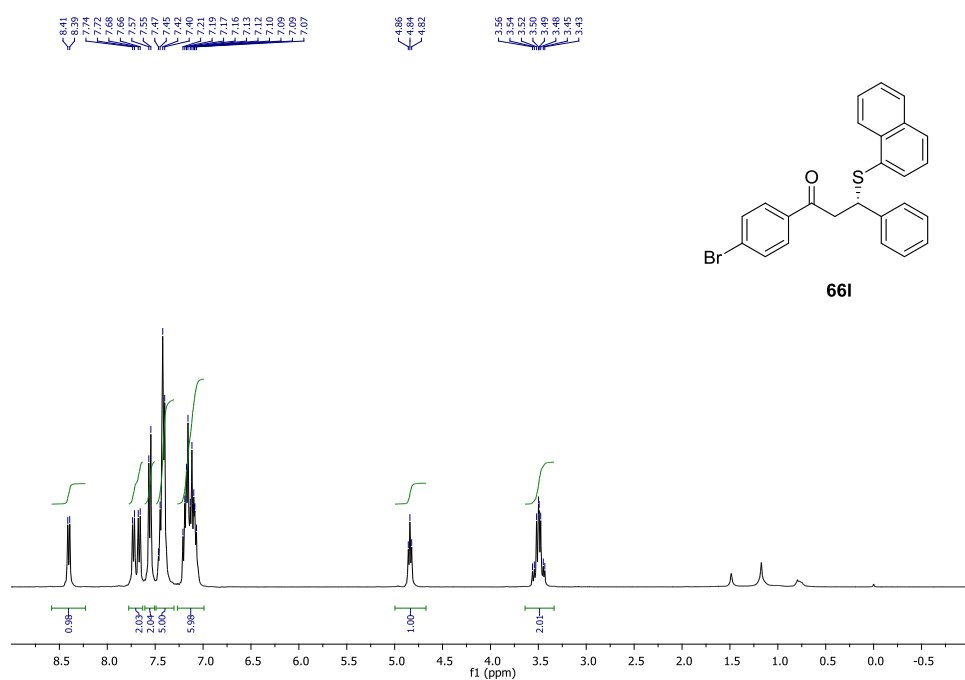


Figure A. 75 ^1H NMR spectrum of **661**

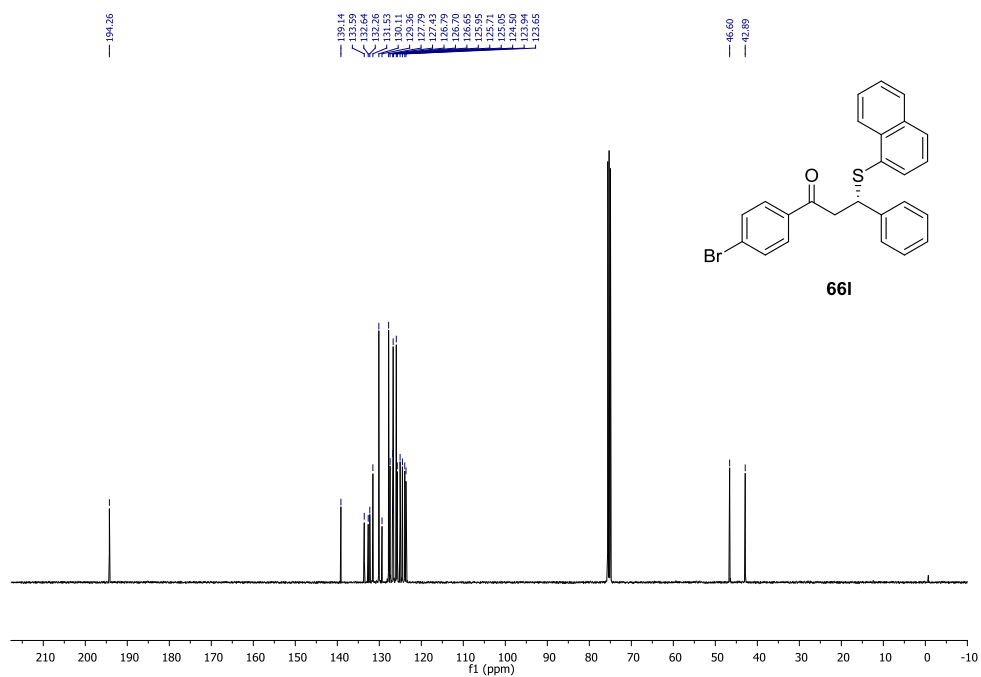


Figure A. 76 ^{13}C NMR spectrum of **661**

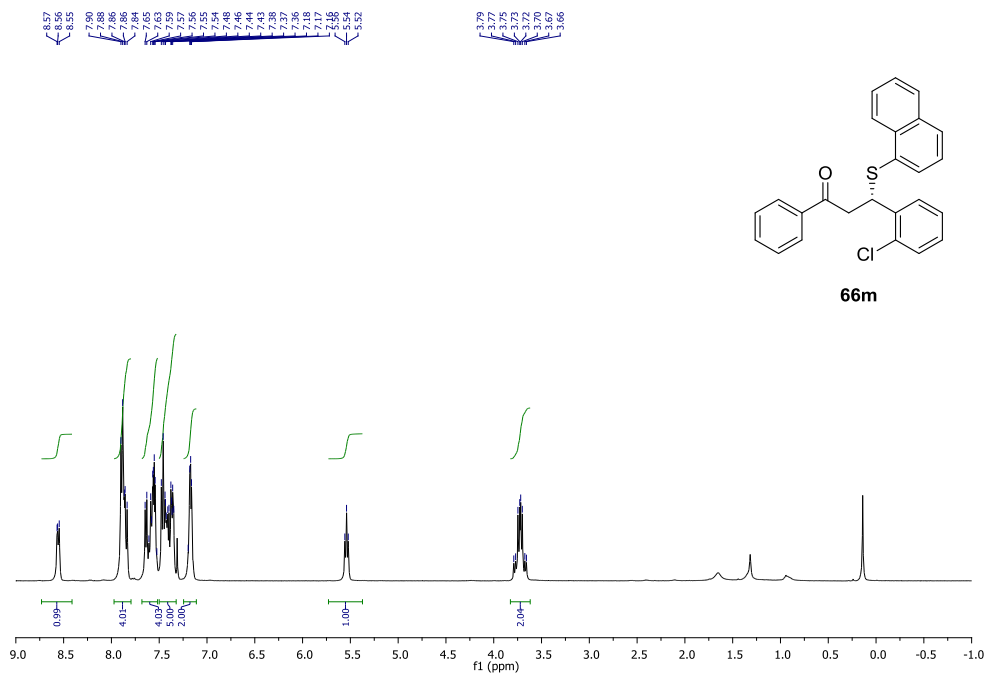


Figure A. 77 ¹H NMR spectrum of **66m**

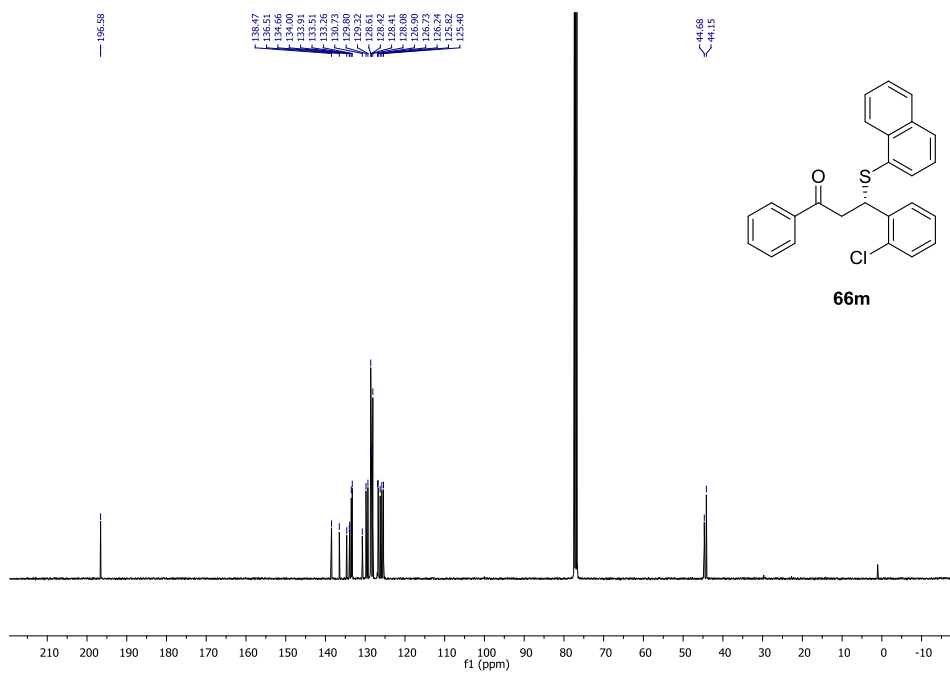


Figure A. 78 ¹³C NMR spectrum of **66m**

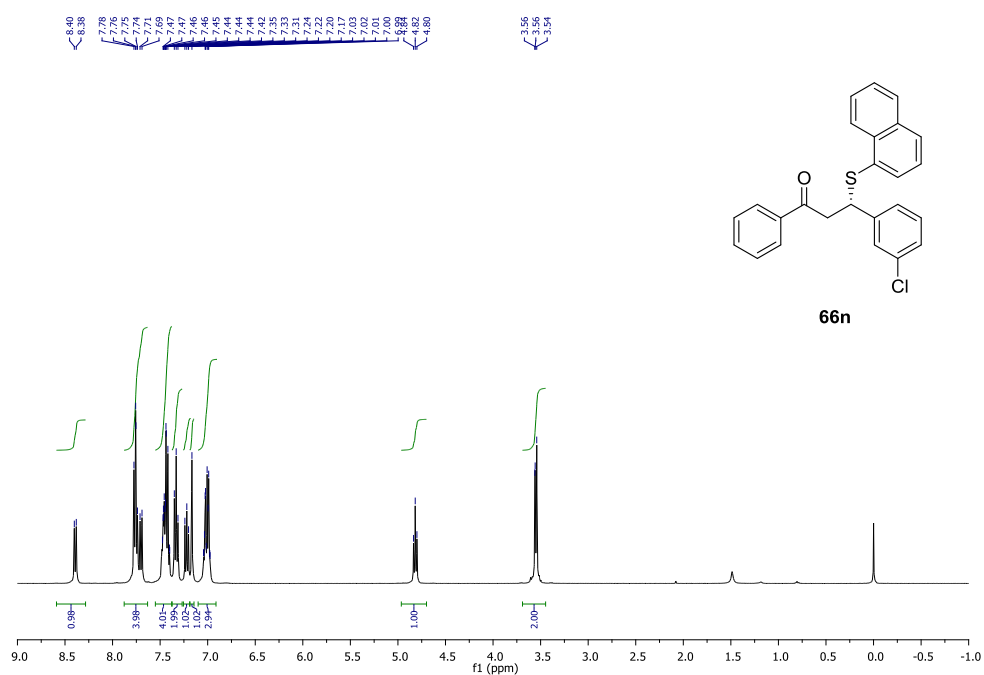


Figure A. 79 ^1H NMR spectrum of **66n**

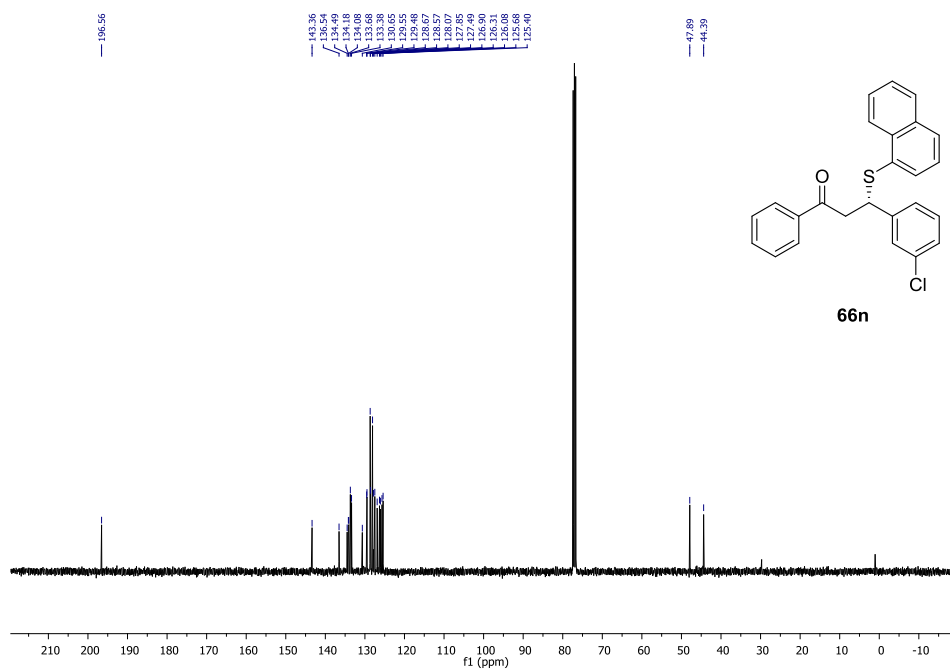


Figure A. 80 ^{13}C NMR spectrum of **66n**

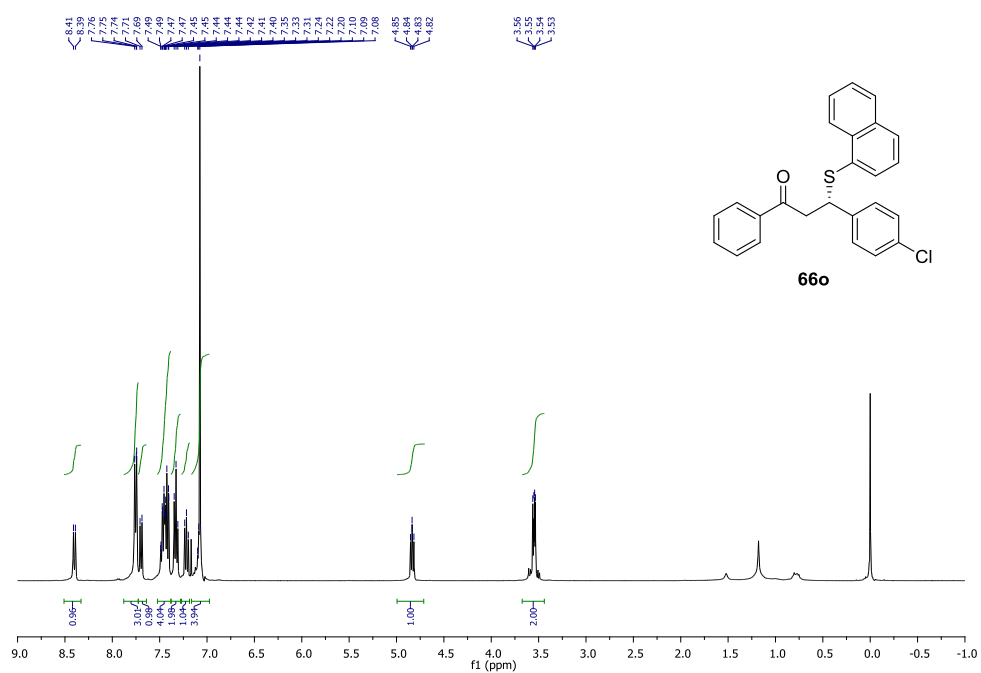


Figure A. 81 ¹H NMR spectrum of **66o**

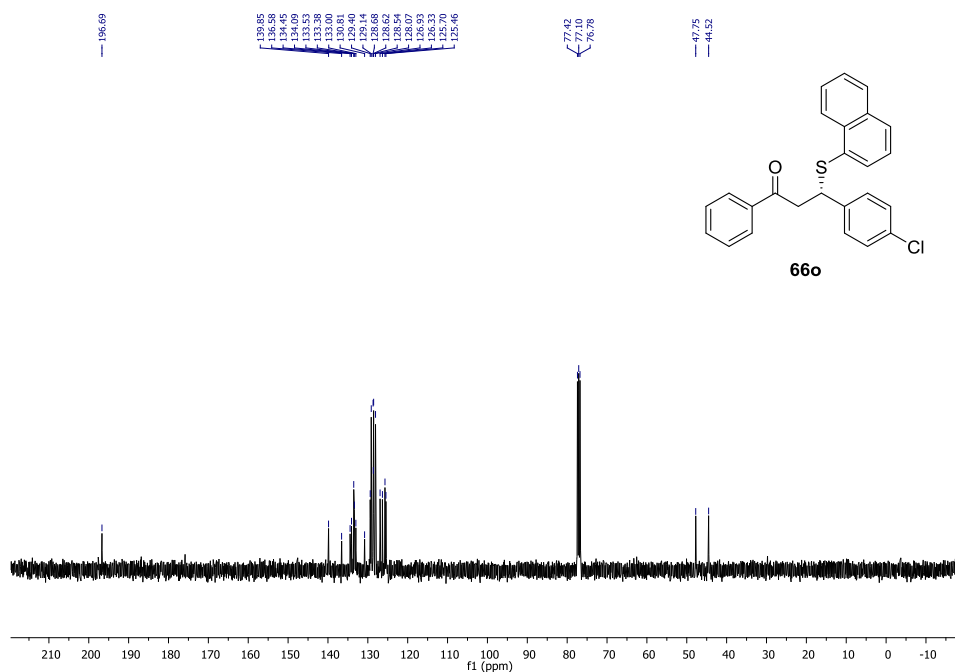


Figure A. 82 ¹³C NMR spectrum of **66o**

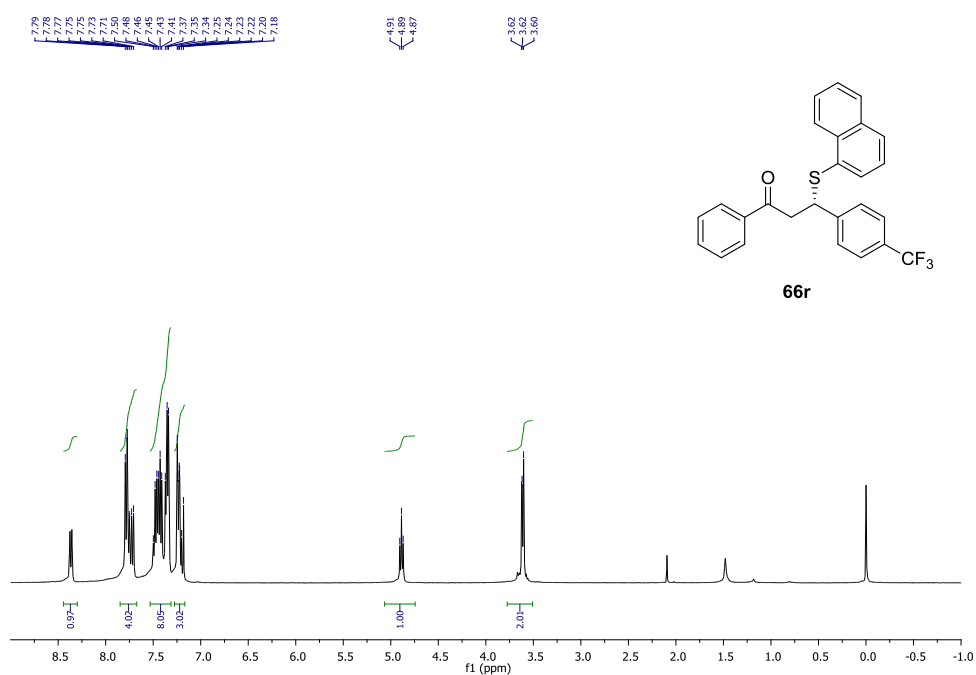


Figure A. 83 $^1\text{H NMR}$ spectrum of **66r**

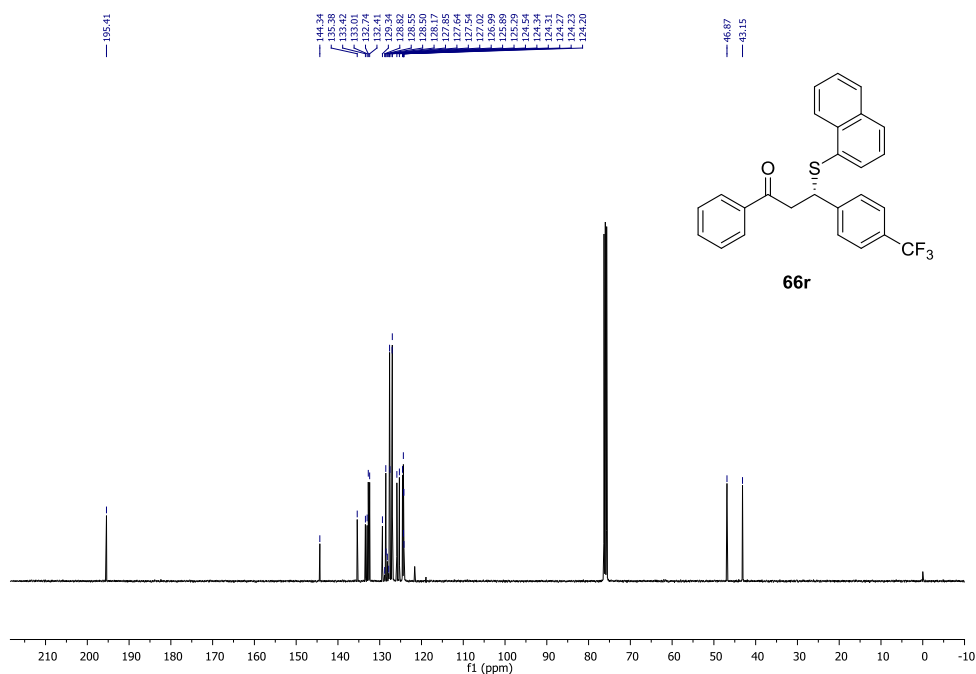


Figure A. 84 $^{13}\text{C NMR}$ spectrum of **66r**

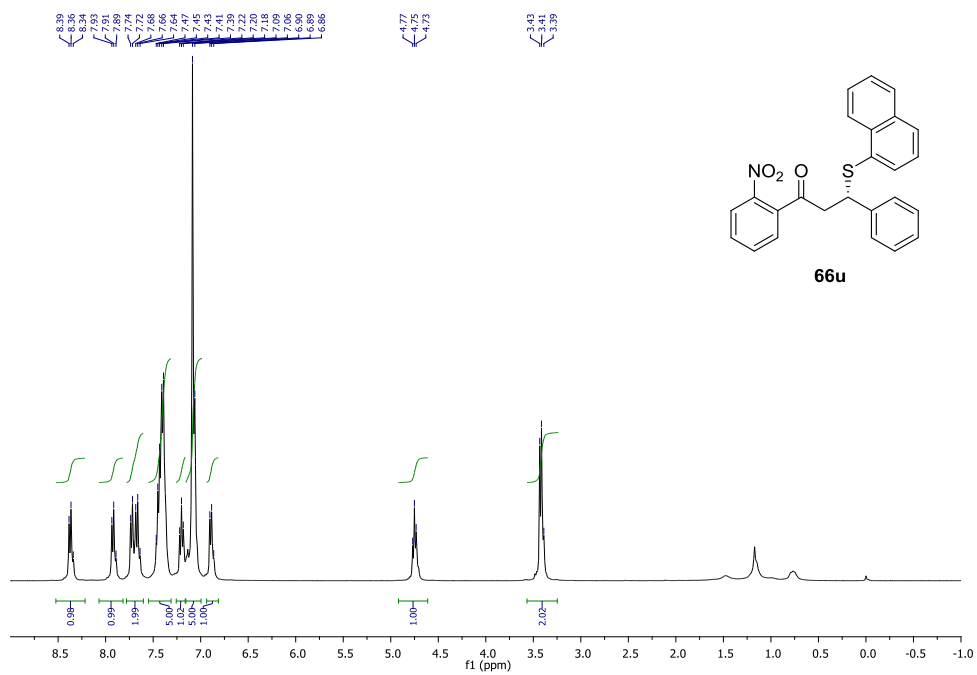


Figure A. 85 $^1\text{H NMR}$ spectrum of **66u**

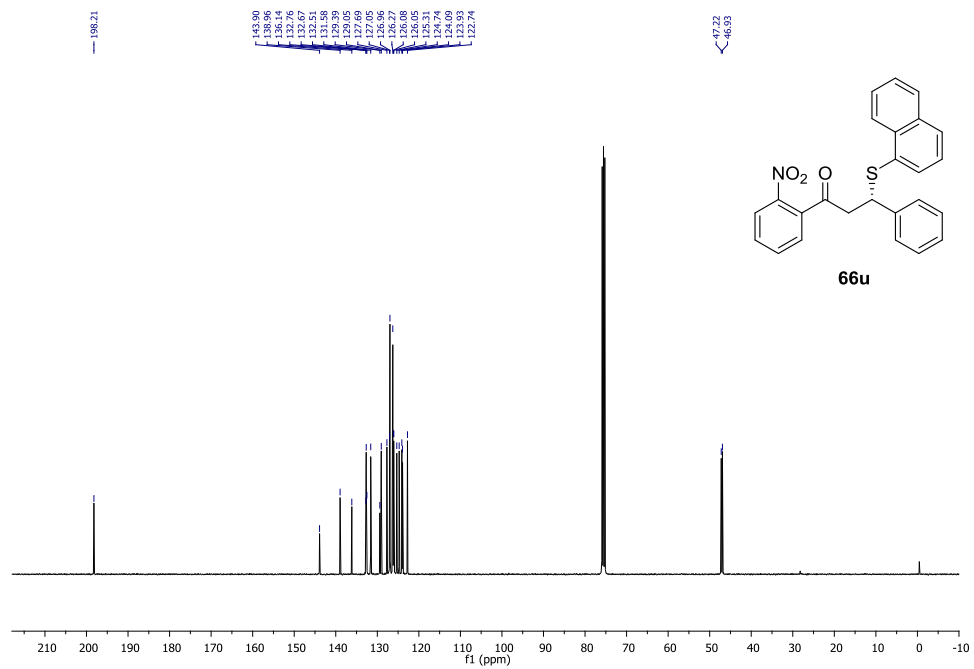


Figure A. 86 $^{13}\text{C NMR}$ spectrum of **66u**

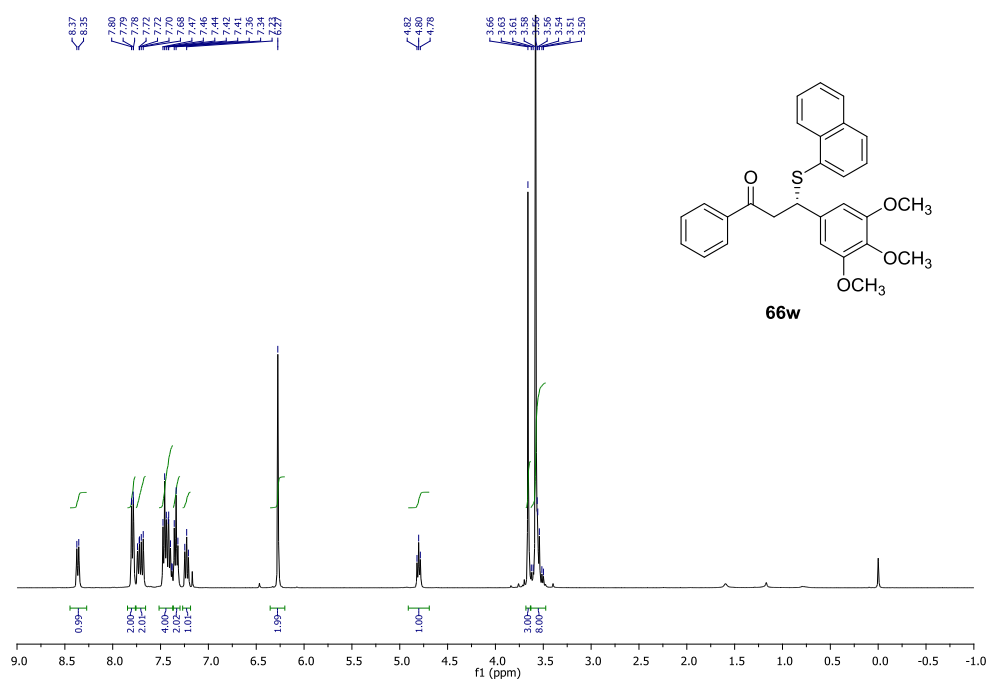


Figure A. 87 ¹H NMR spectrum of **66w**

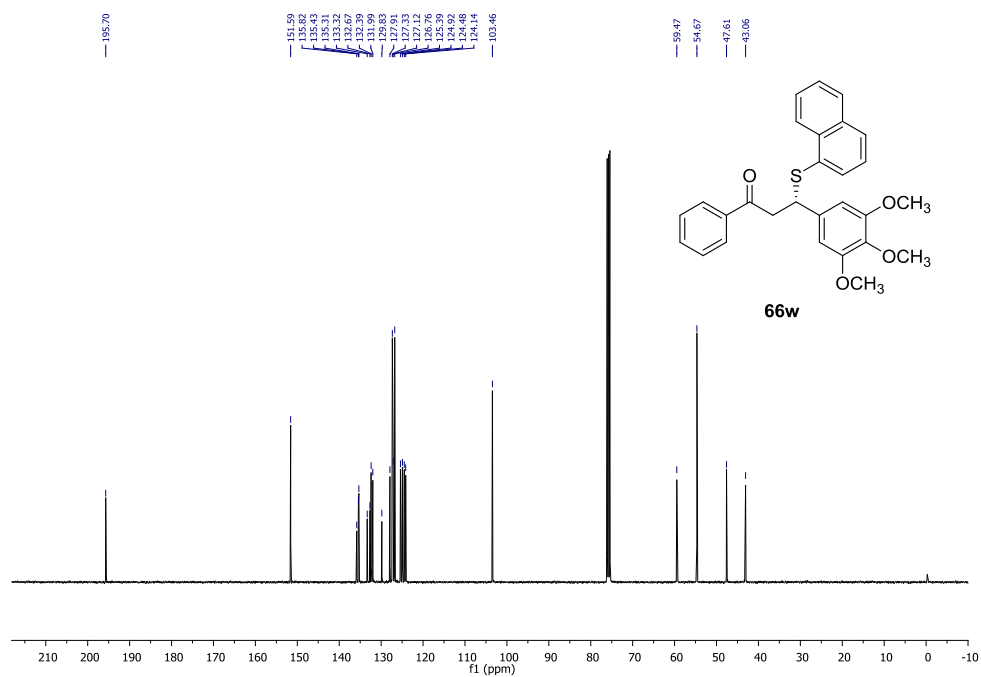


Figure A. 88 ¹³C NMR spectrum of **66w**

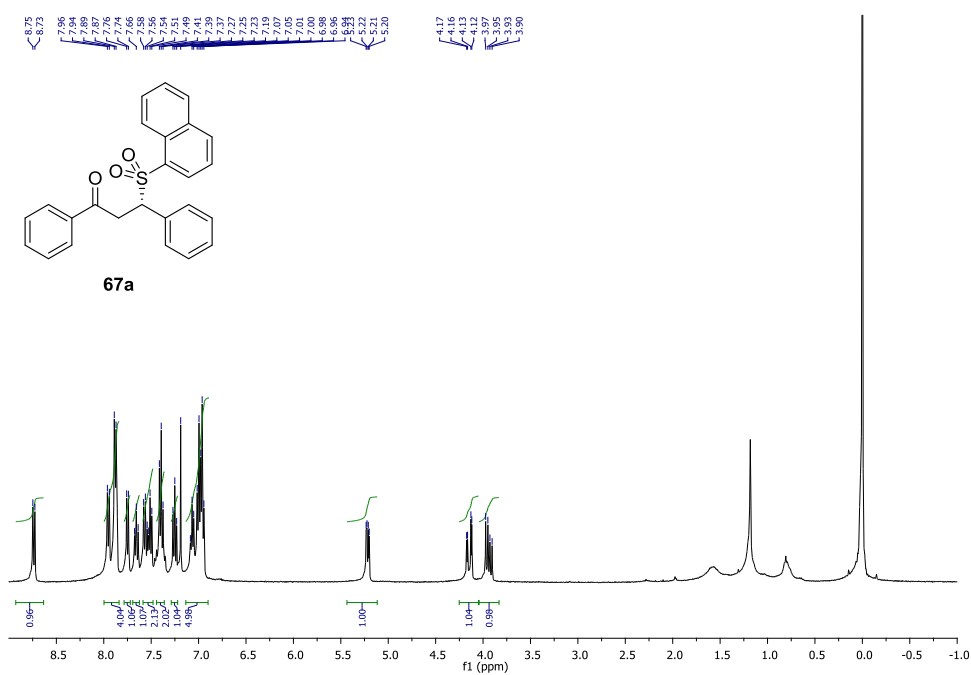


Figure A. 91 ^1H NMR spectrum of **67a**

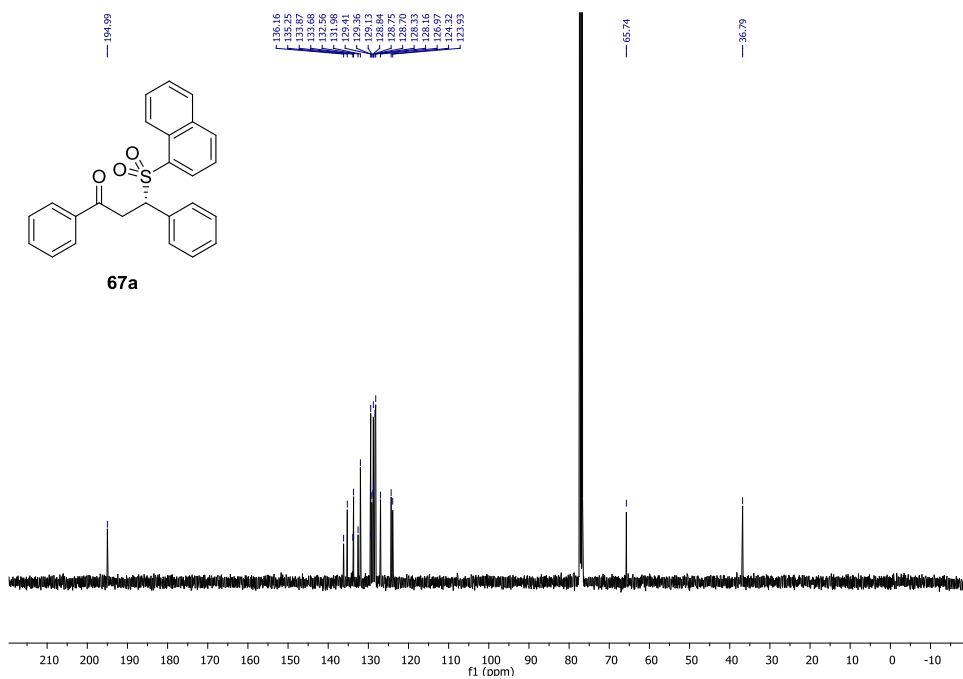


Figure A. 92 ^{13}C NMR spectrum of **67a**

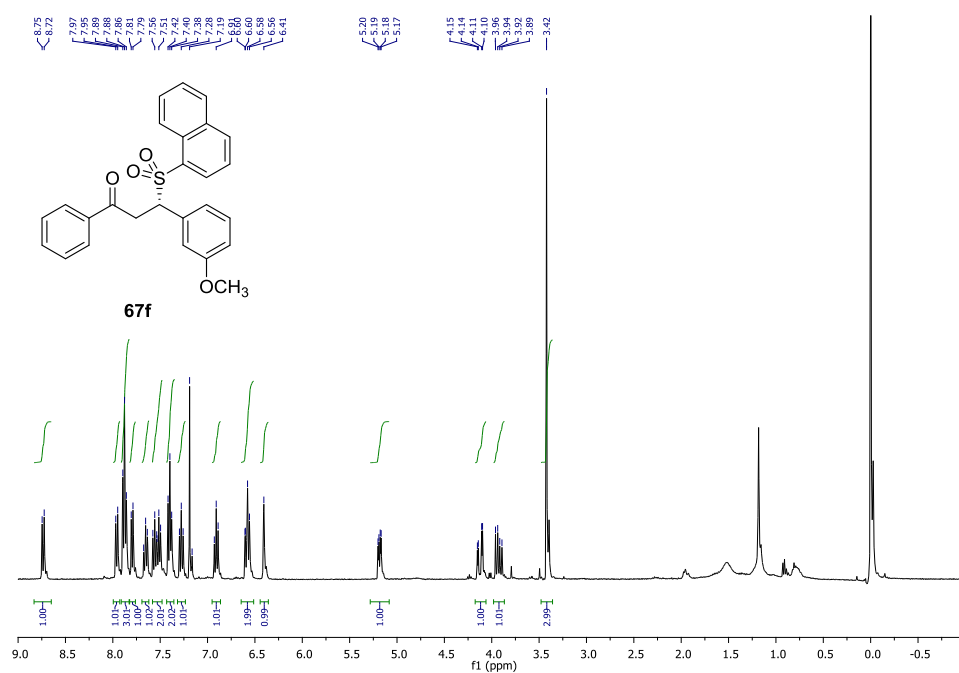


Figure A. 93 ¹H NMR spectrum of **67f**

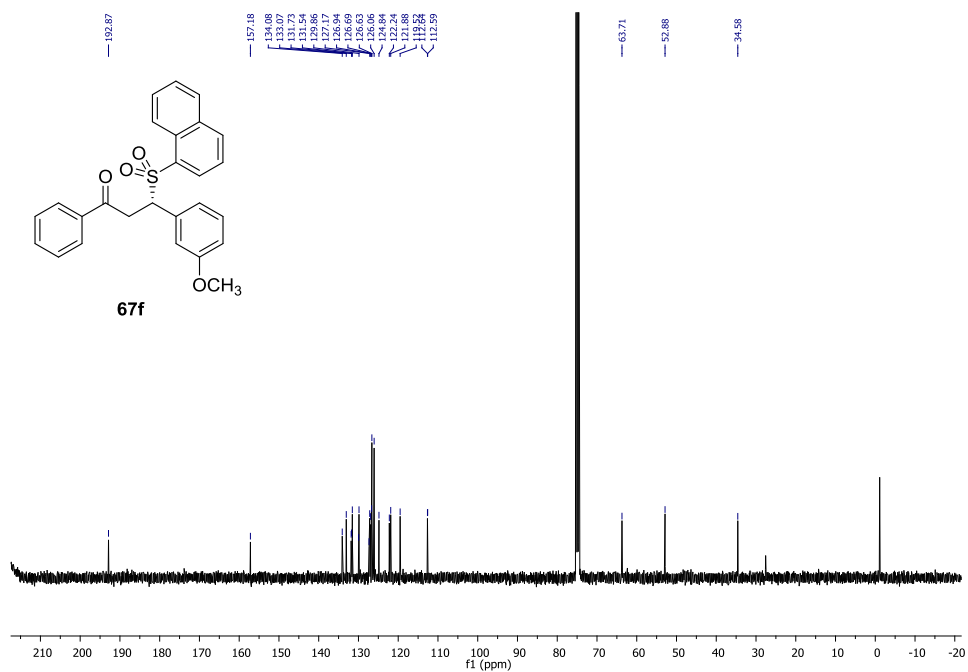


Figure A. 94 ¹³C NMR spectrum of **67f**

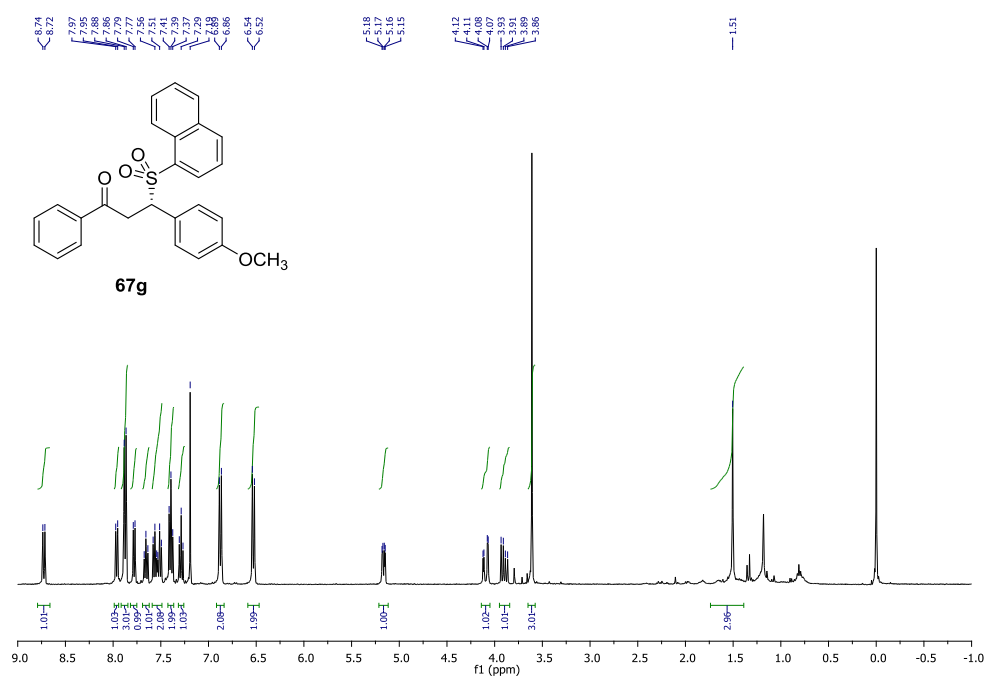


Figure A. ^1H NMR spectrum of **67g**

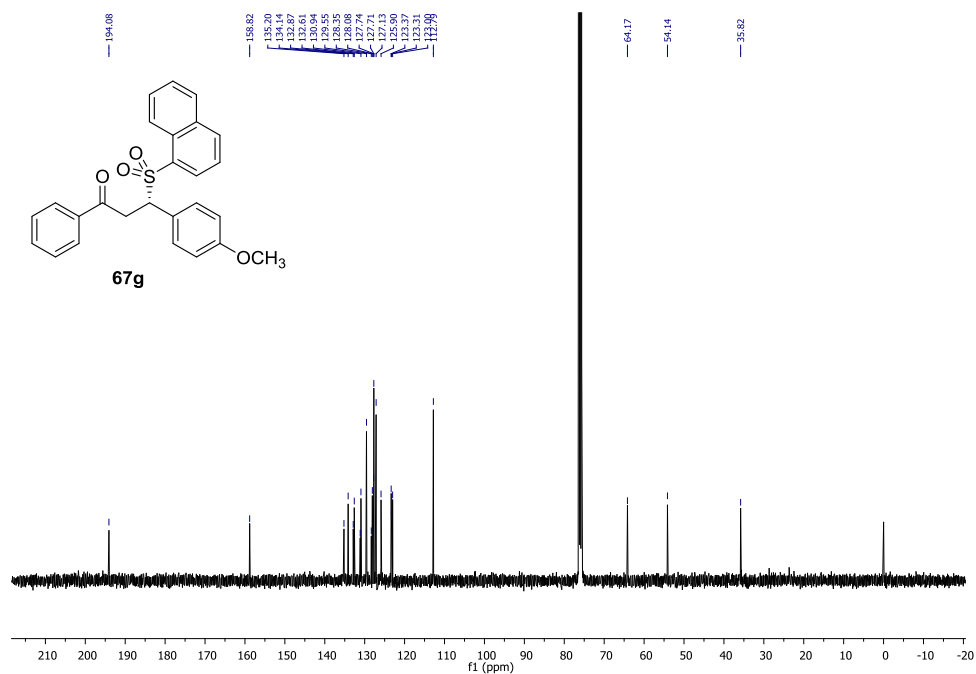


Figure A. ^{13}C NMR spectrum of **67g**

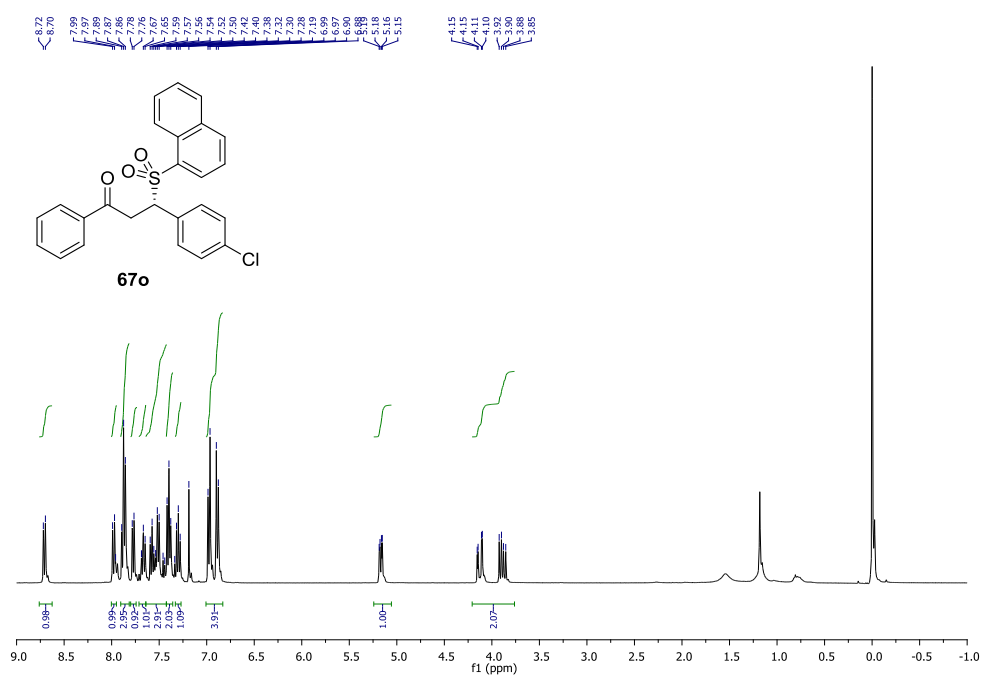


Figure A. 97 ¹H NMR spectrum of **67o**

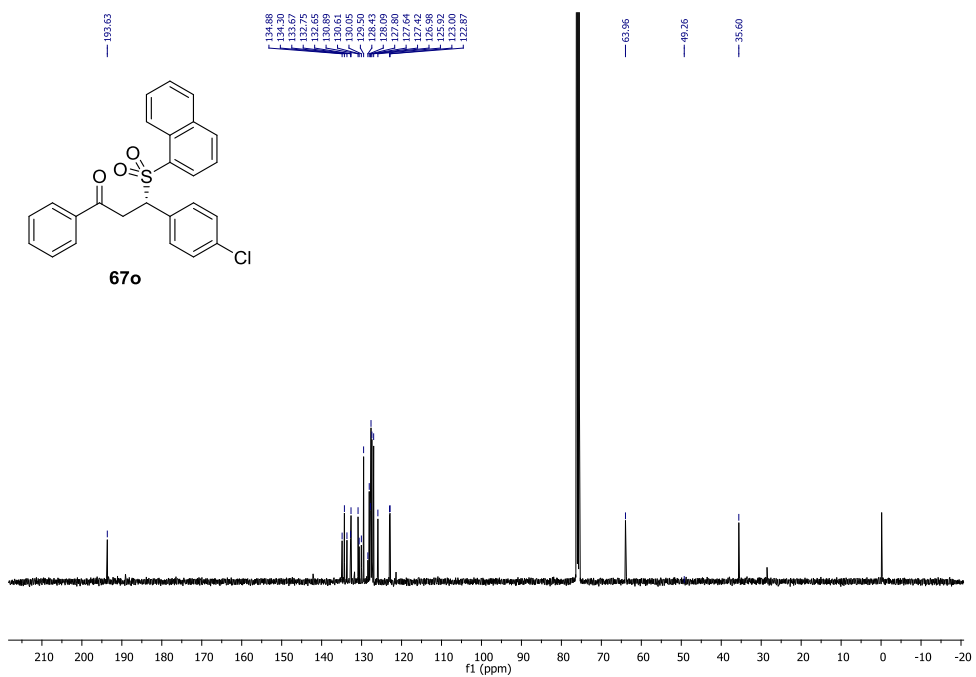


Figure A. 98 ¹³C NMR spectrum of **67o**

B. HPLC CHROMATOGRAMS

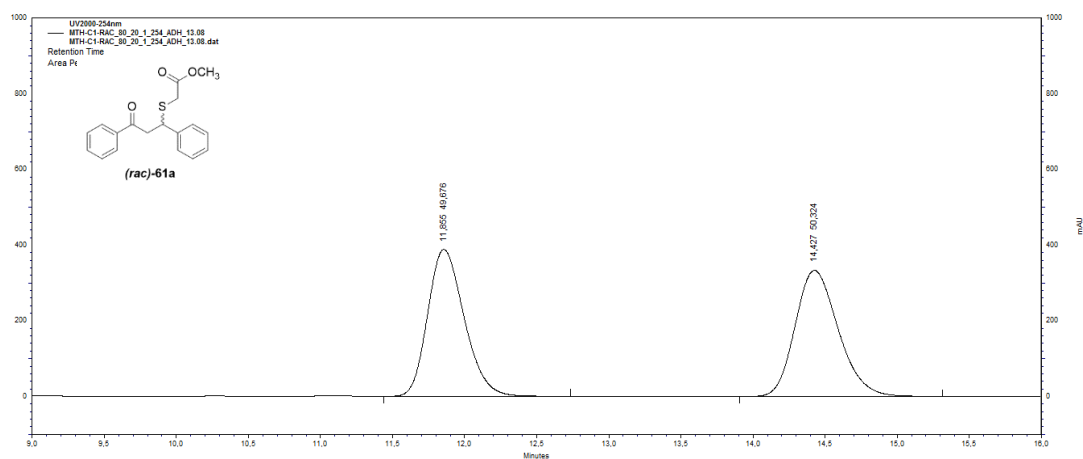


Figure B. 1 HPLC chromatogram of *rac*-61a

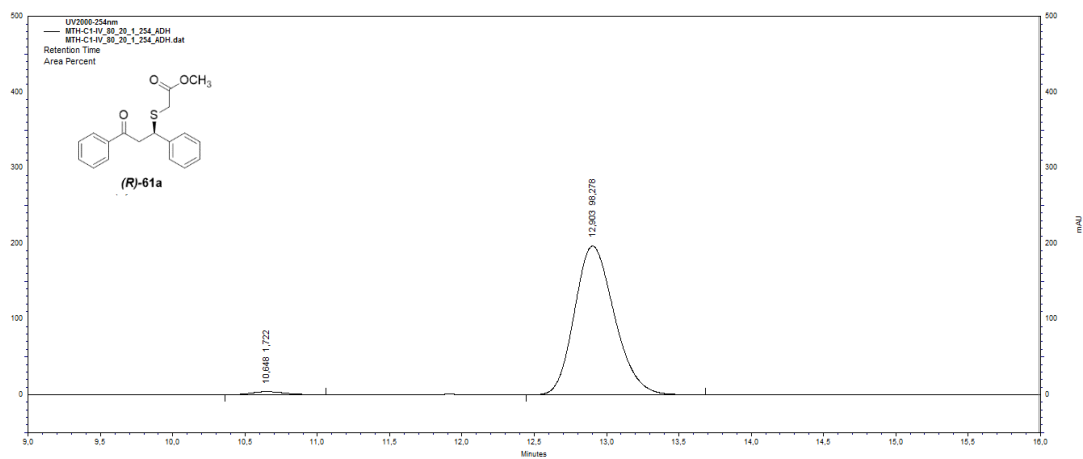


Figure B. 2 HPLC chromatogram of enantiomerically enriched **61a**

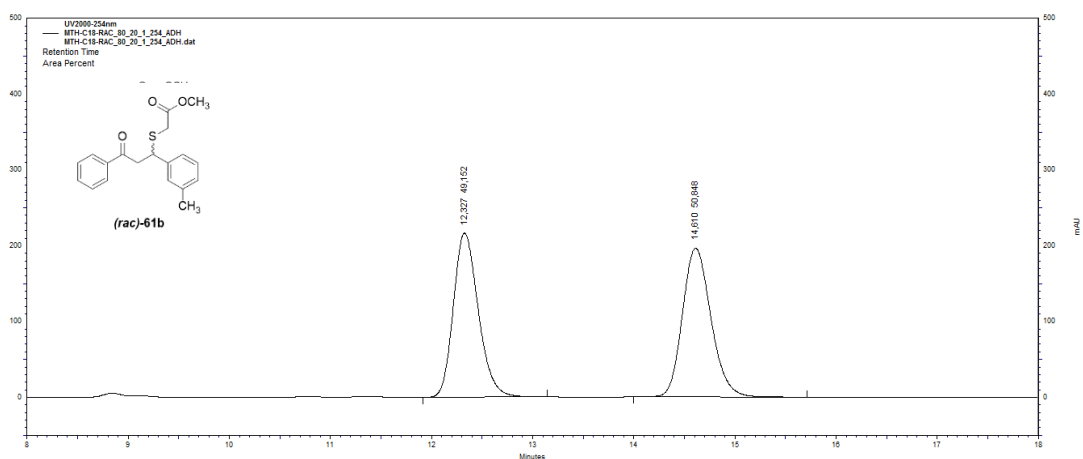


Figure B. 3 HPLC chromatogram of *rac*-**61b**

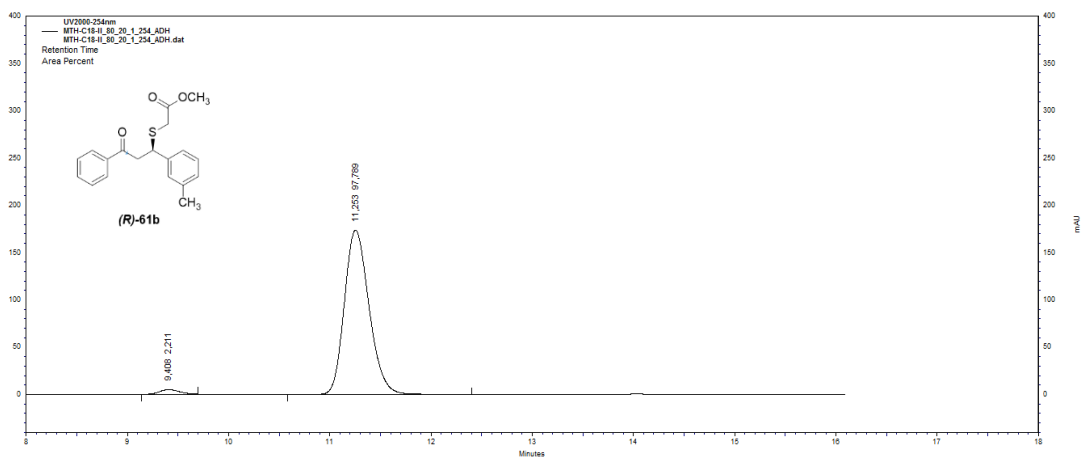


Figure B. 4 HPLC chromatogram of enantiomerically enriched **61b**

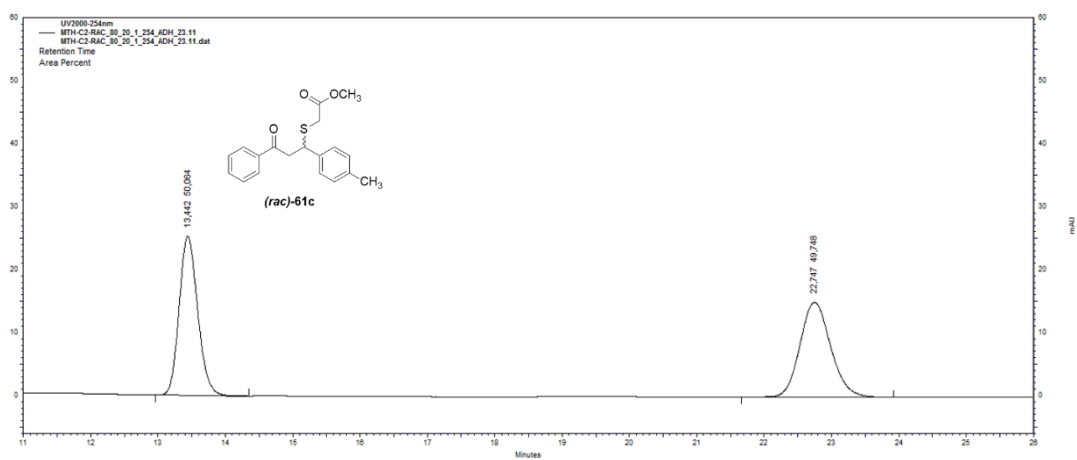


Figure B. 5 HPLC chromatogram of *rac*-**61c**

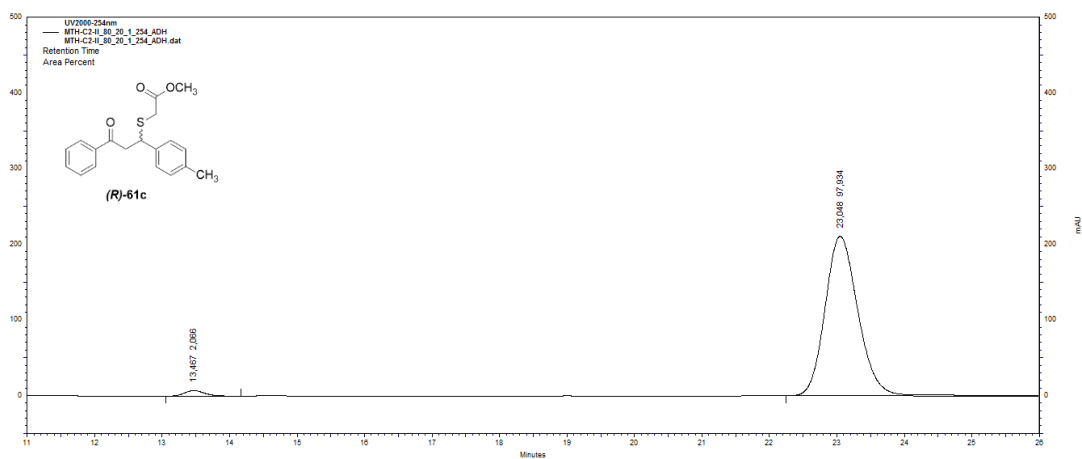


Figure B. 6 HPLC chromatogram of enantiomerically enriched **61c**

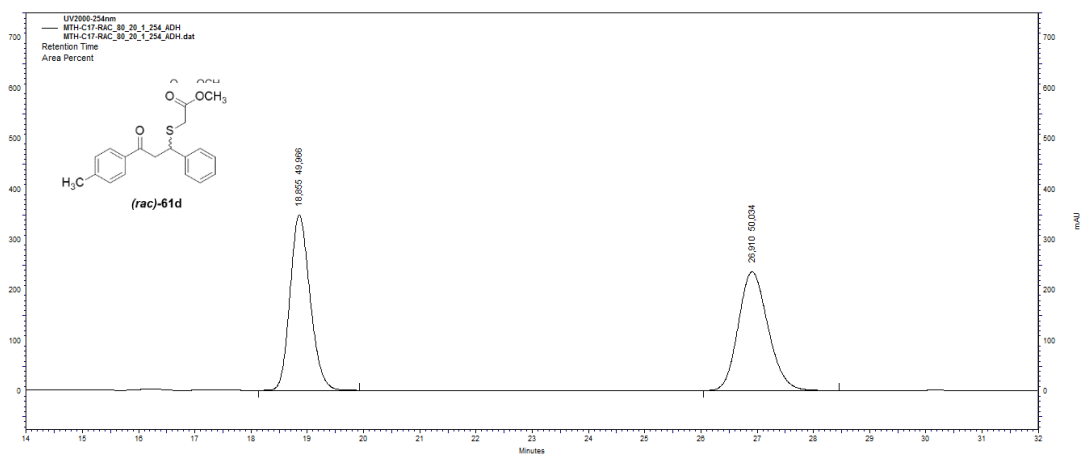


Figure B. 7 HPLC chromatogram of *rac*-**61d**

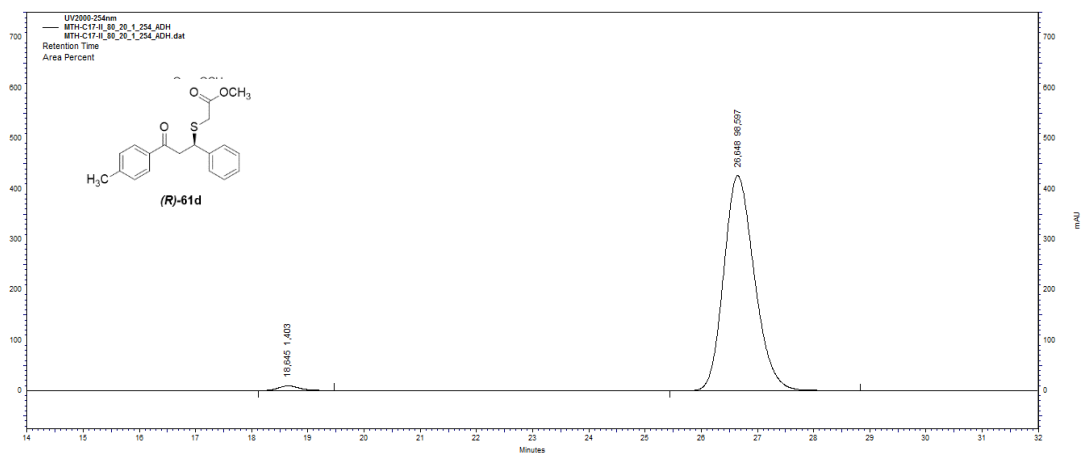


Figure B. 8 HPLC chromatogram of enantiomerically enriched **61d**

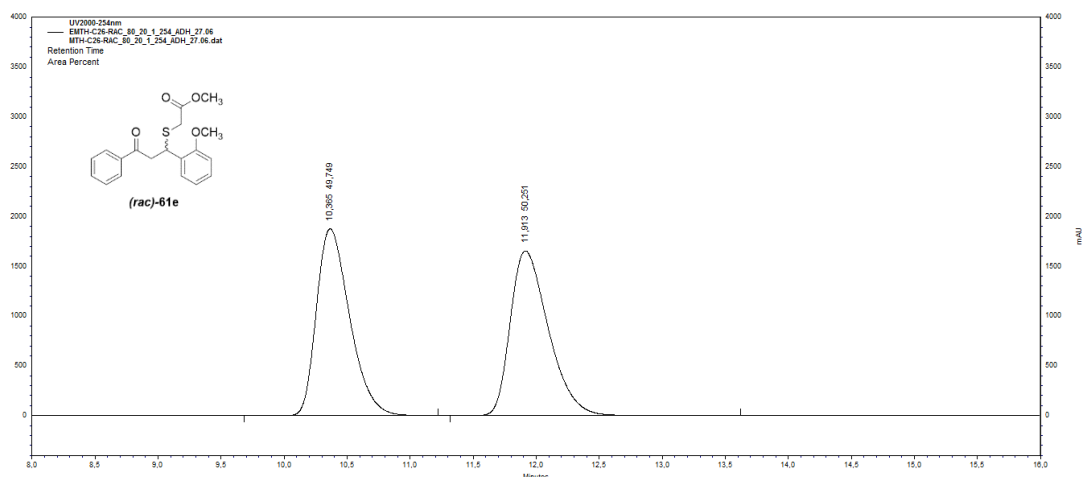


Figure B. 9 HPLC chromatogram of *rac*-61e

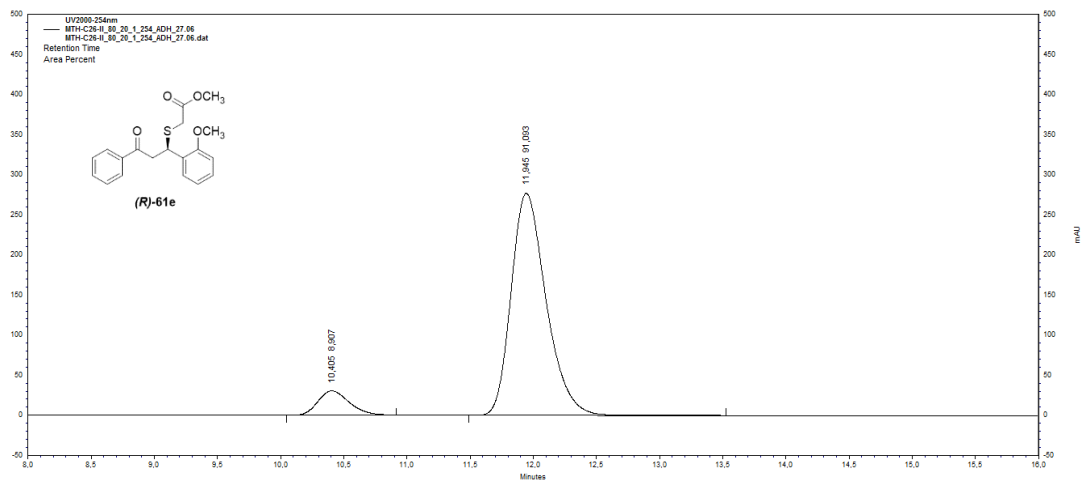


Figure B. 10 HPLC chromatogram of enantiomerically enriched 61e

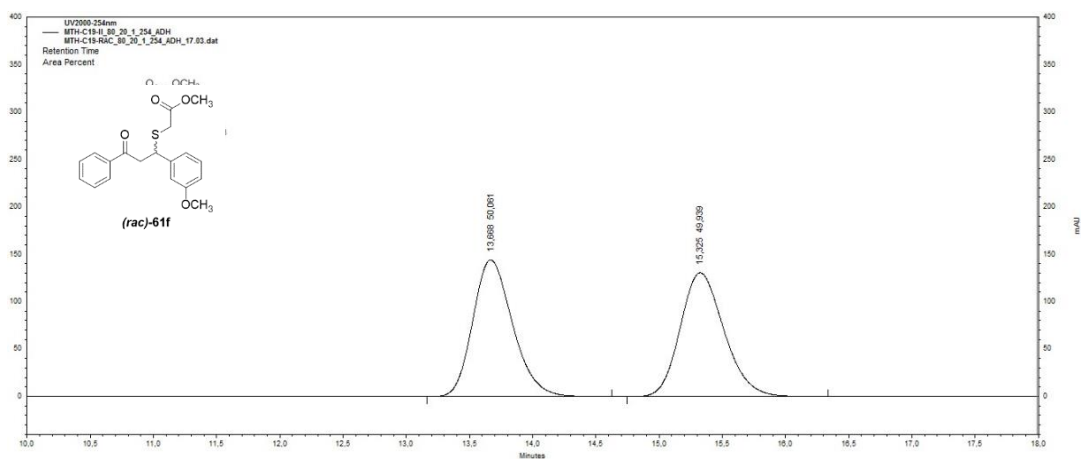


Figure B. 11 HPLC chromatogram of *rac*-**61f**

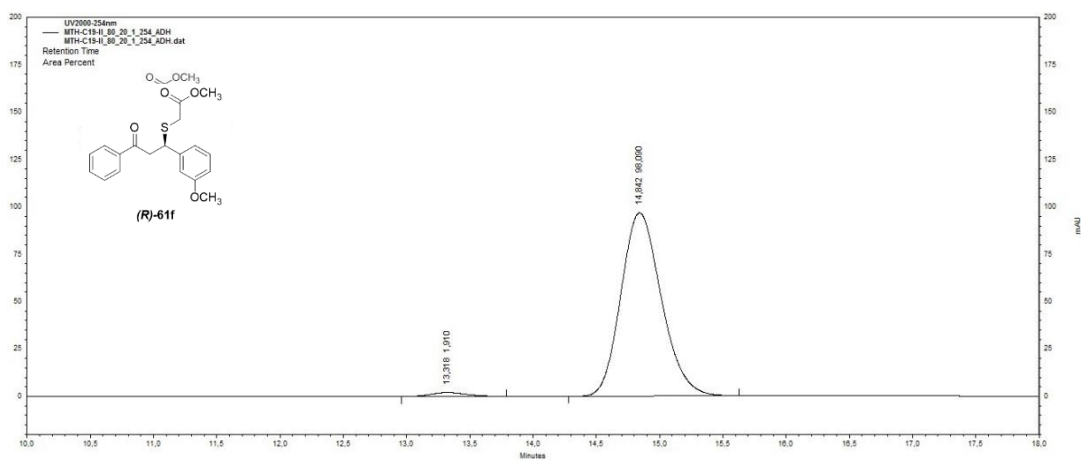


Figure B. 12 HPLC chromatogram of enantiomerically enriched **61f**

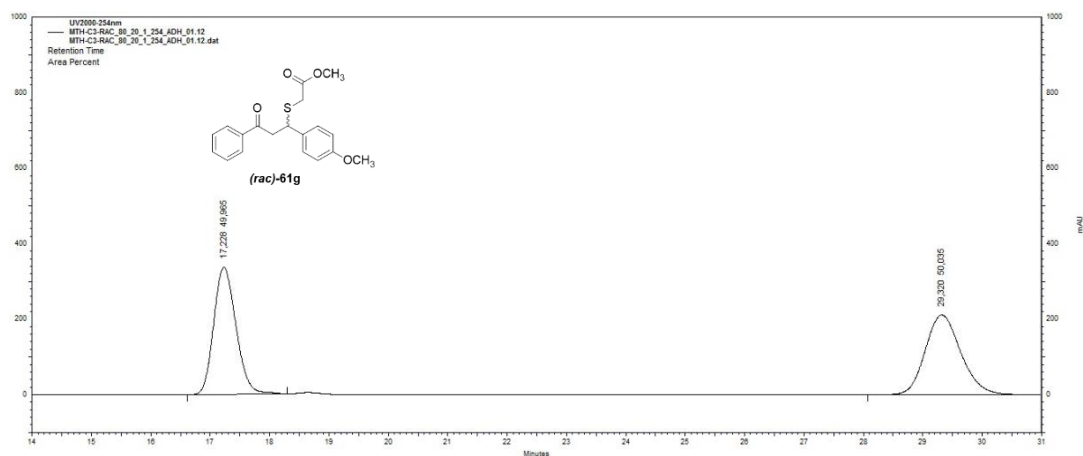


Figure B. 13 HPLC chromatogram of *rac*-**61g**

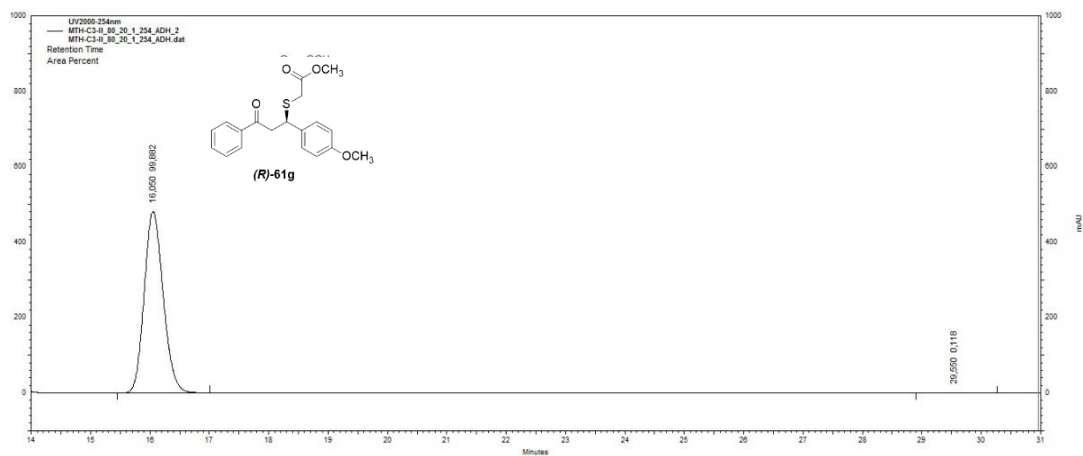


Figure B. 14 HPLC chromatogram of enantiomerically enriched **61g**

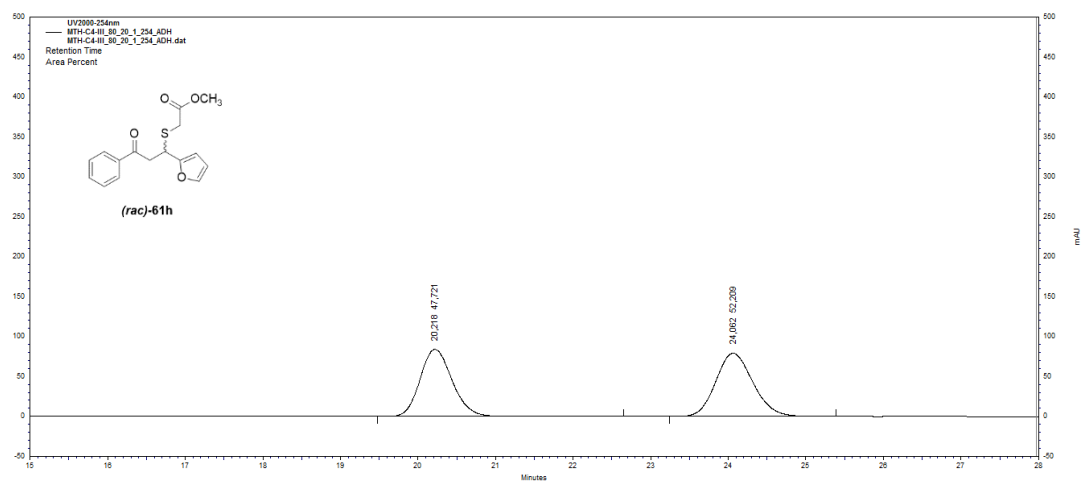


Figure B. 15 HPLC chromatogram of *rac*-**61h**

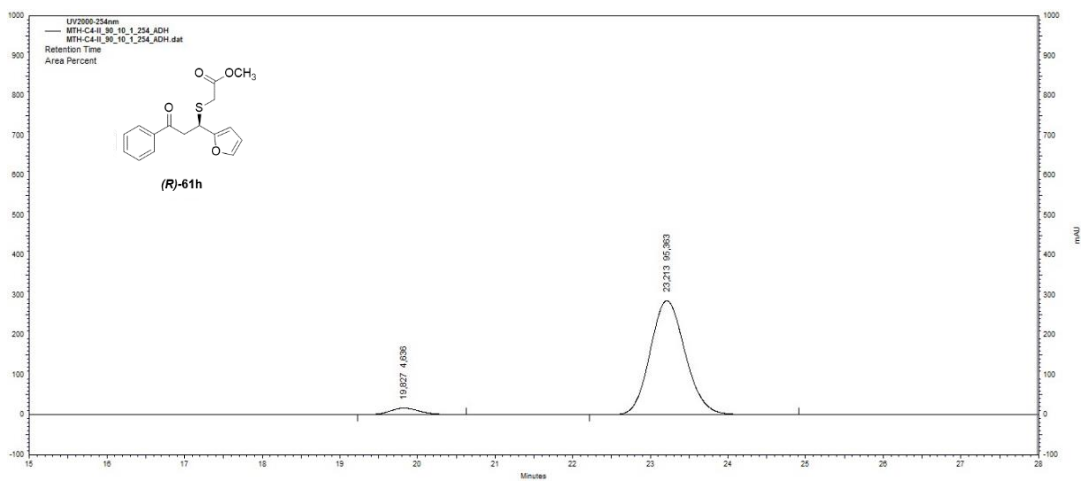


Figure B. 16 HPLC chromatogram of enantiomerically enriched **61h**

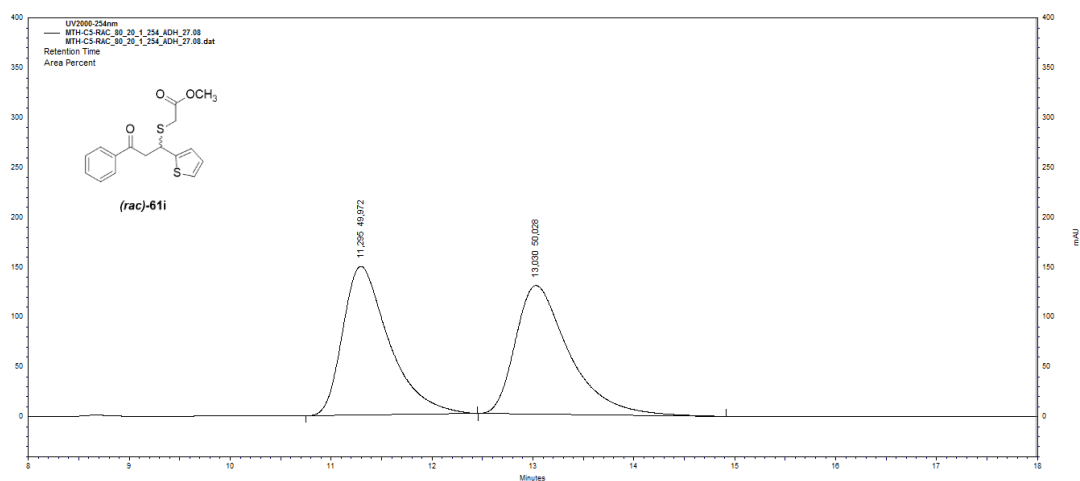


Figure B. 17 HPLC chromatogram of *rac*-**61i**

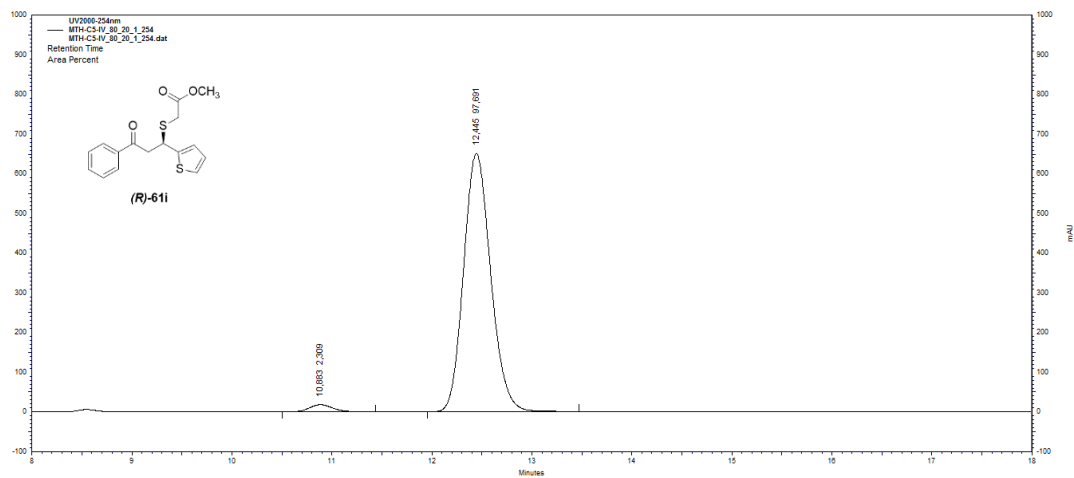


Figure B. 18 HPLC chromatogram of enantiomerically enriched **61i**

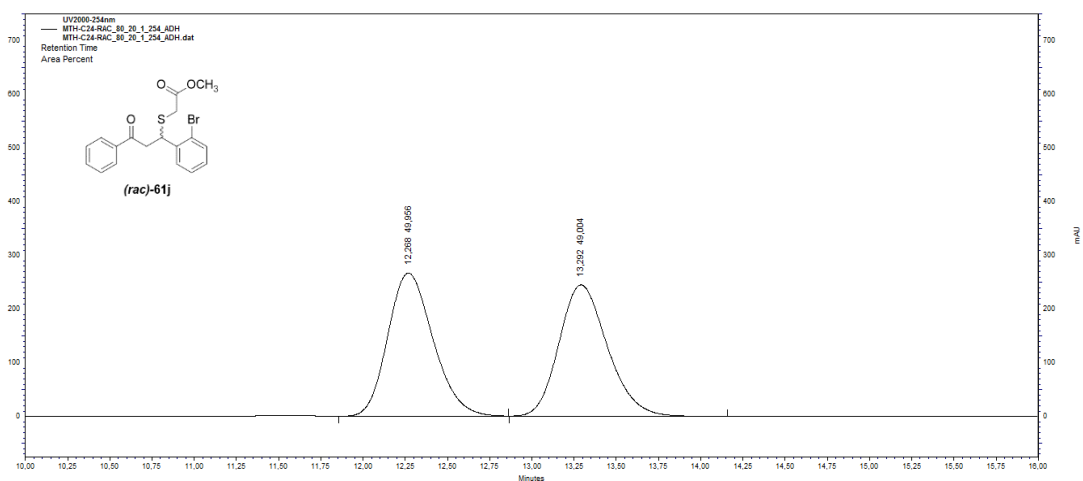


Figure B. 19 HPLC chromatogram of *rac*-**61j**

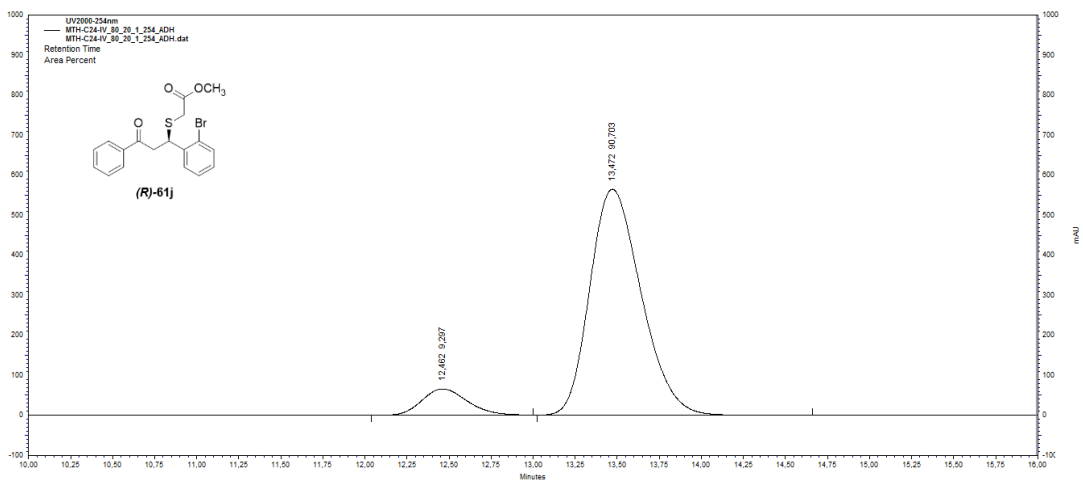


Figure B. 20 HPLC chromatogram of enantiomerically enriched **61j**

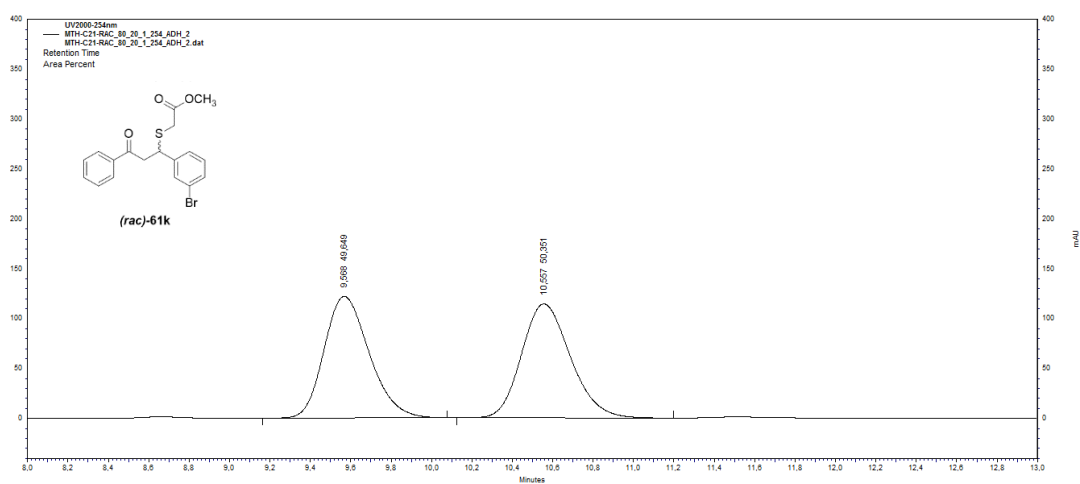


Figure B. 21 HPLC chromatogram of *rac*-**61k**

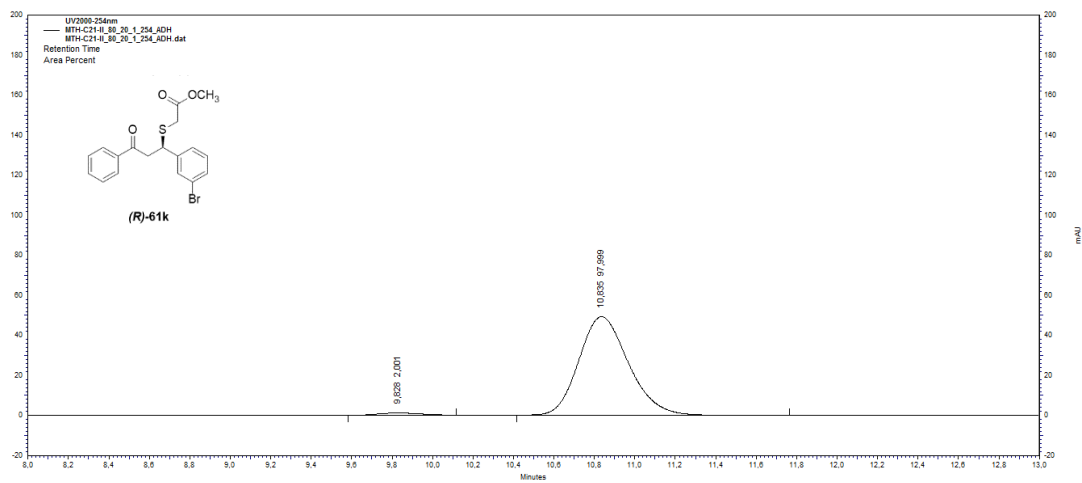


Figure B. 22 HPLC chromatogram of enantiomerically enriched **61k**

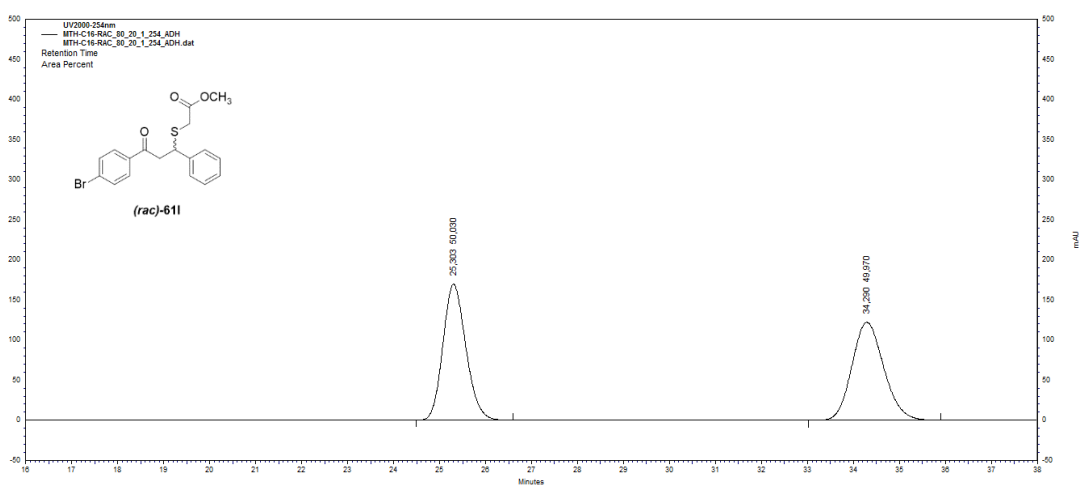


Figure B. 23 HPLC chromatogram of *rac*-**611**

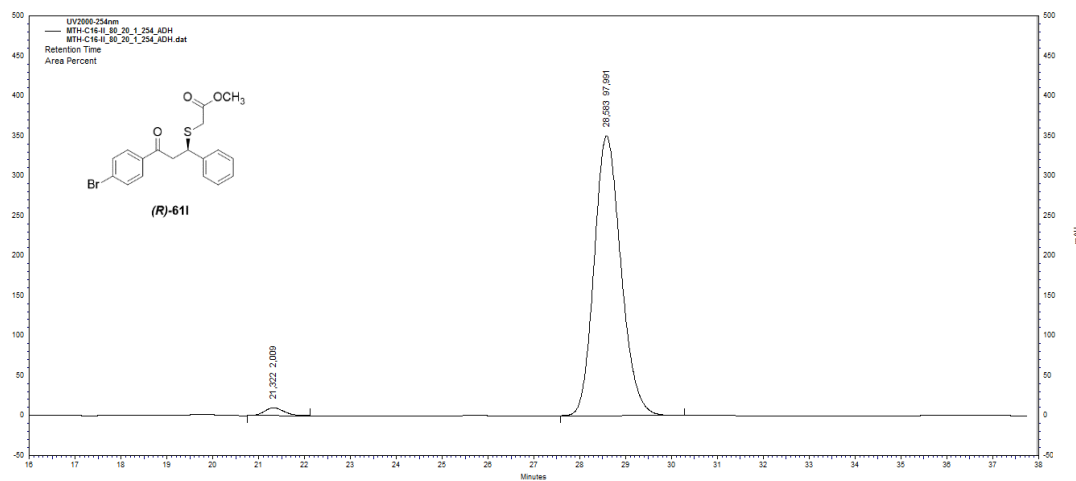


Figure B. 24 HPLC chromatogram of enantiomerically enriched **611**

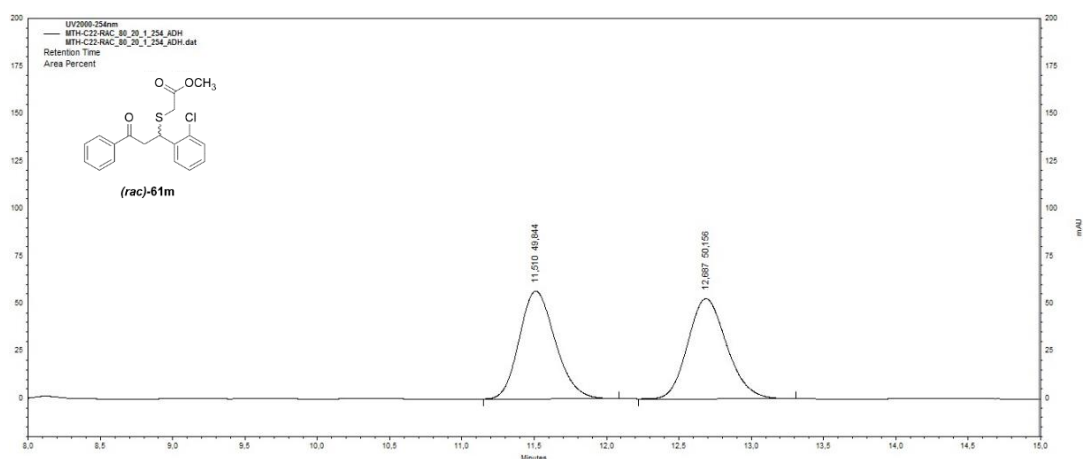


Figure B. 25 HPLC chromatogram of *rac*-**61m**

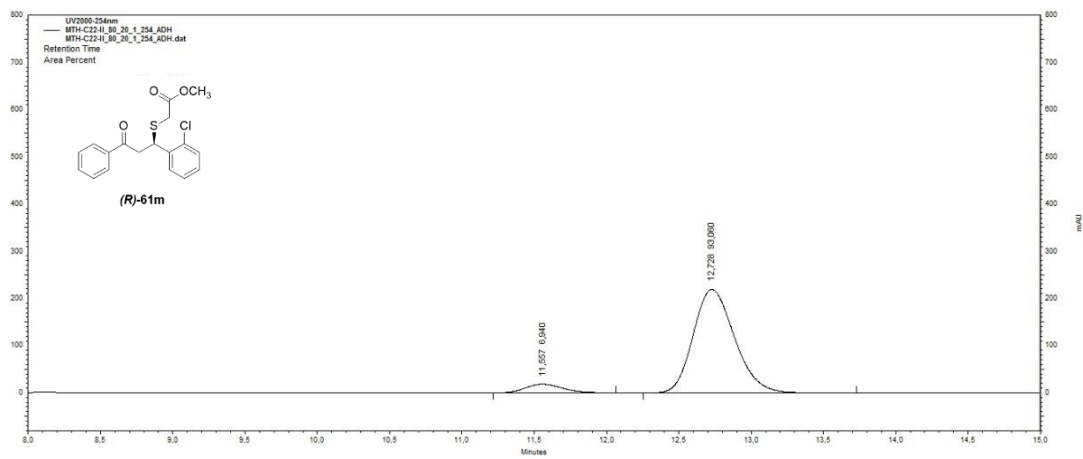


Figure B. 26 HPLC chromatogram of enantiomerically enriched **61m**

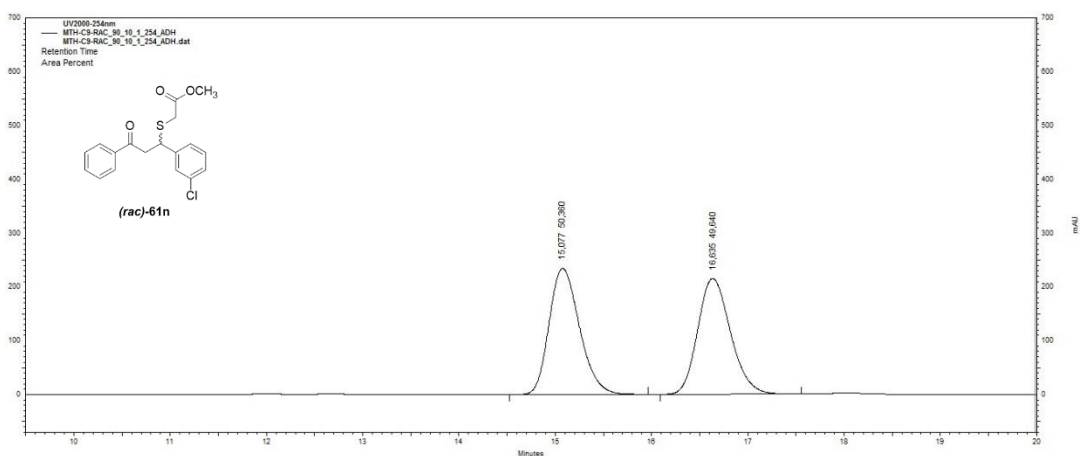


Figure B. 27 HPLC chromatogram of *rac*-**61n**

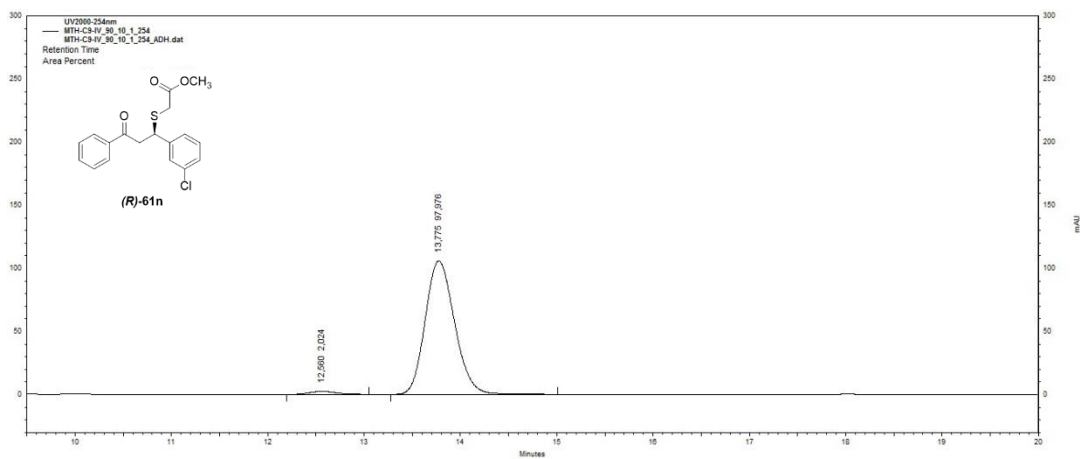


Figure B. 28 HPLC chromatogram of enantiomerically enriched **61n**

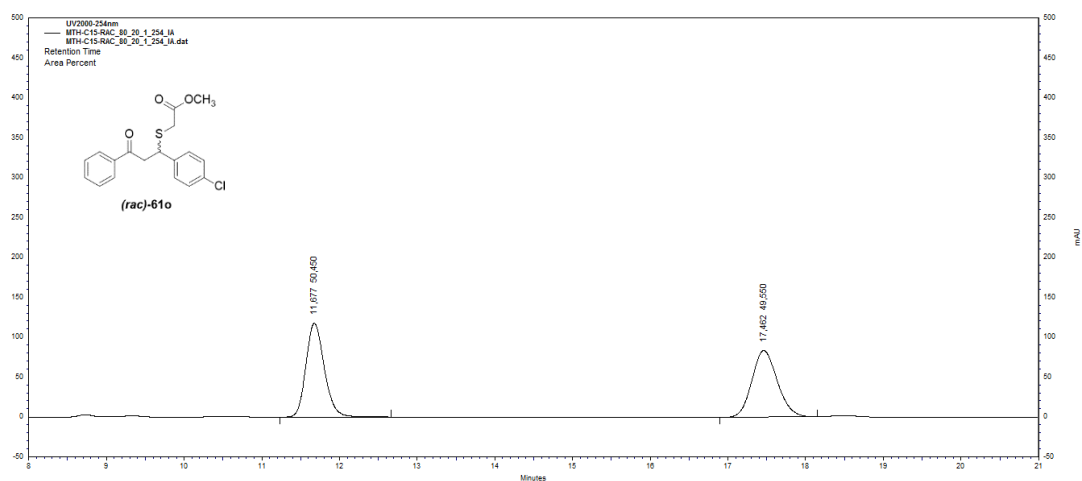


Figure B. 29 HPLC chromatogram of *rac*-**61o**

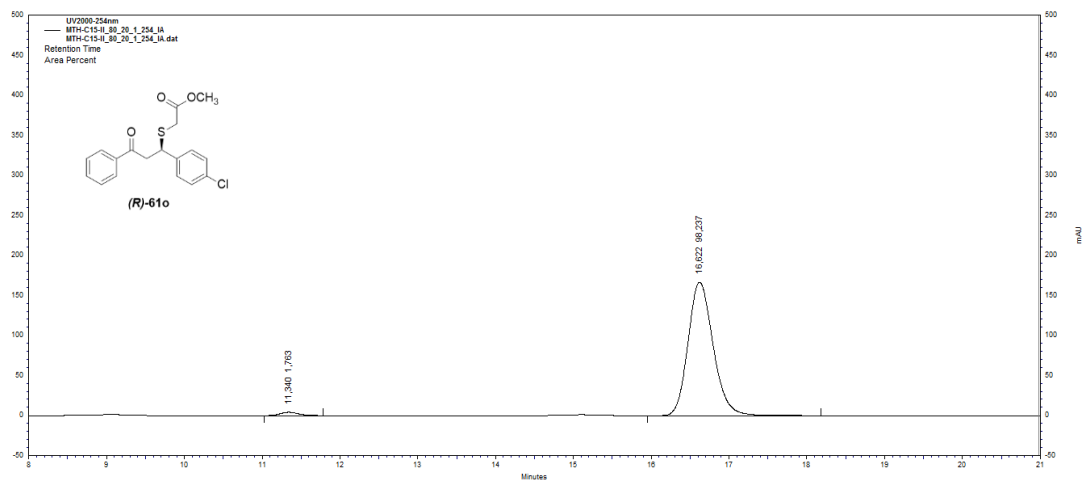


Figure B. 30 HPLC chromatogram of enantiomerically enriched **61o**

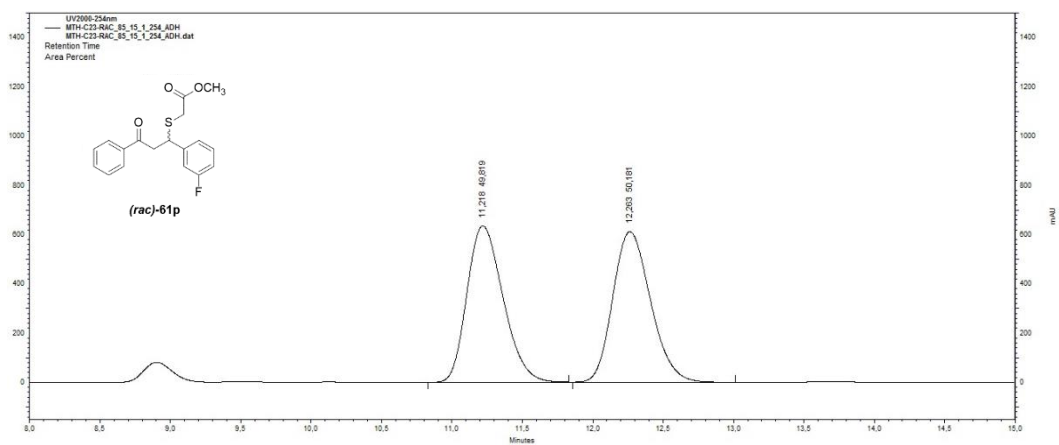


Figure B. 31 HPLC chromatogram of *rac*-**61p**

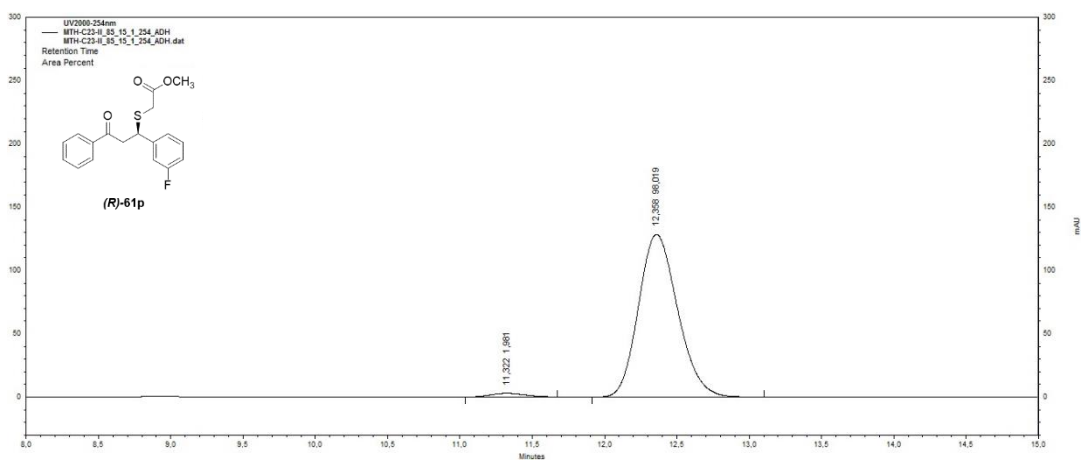


Figure B. 32 HPLC chromatogram of enantiomerically enriched **61p**

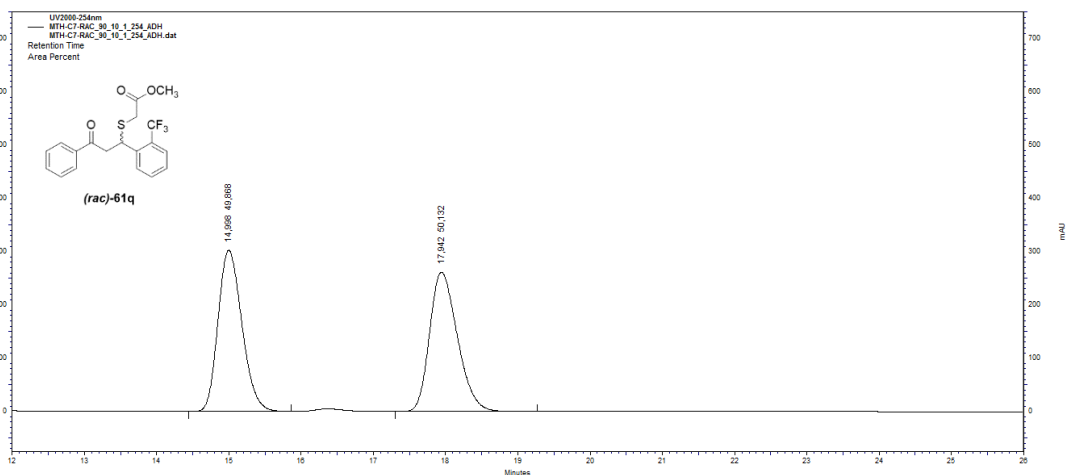


Figure B. 33 HPLC chromatogram of *rac*-**61q**

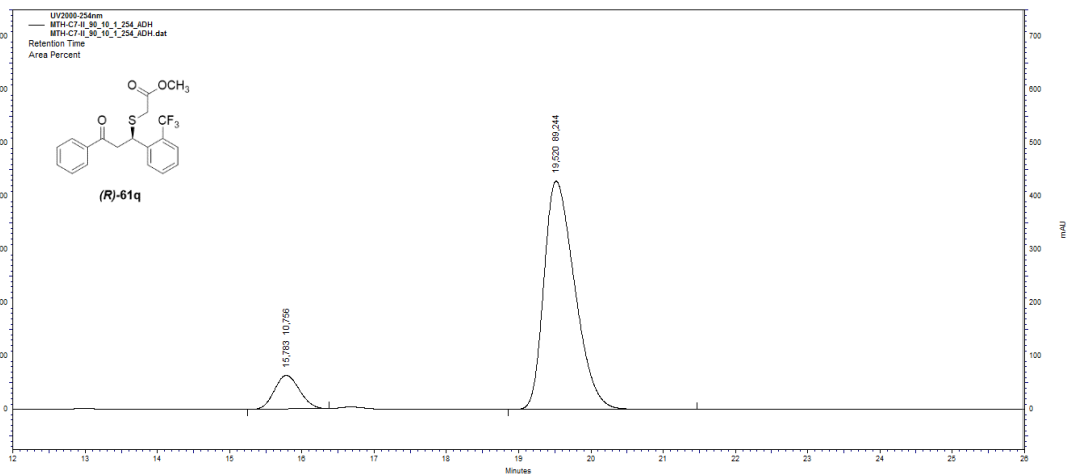


Figure B. 34 HPLC chromatogram of enantiomerically enriched **61q**

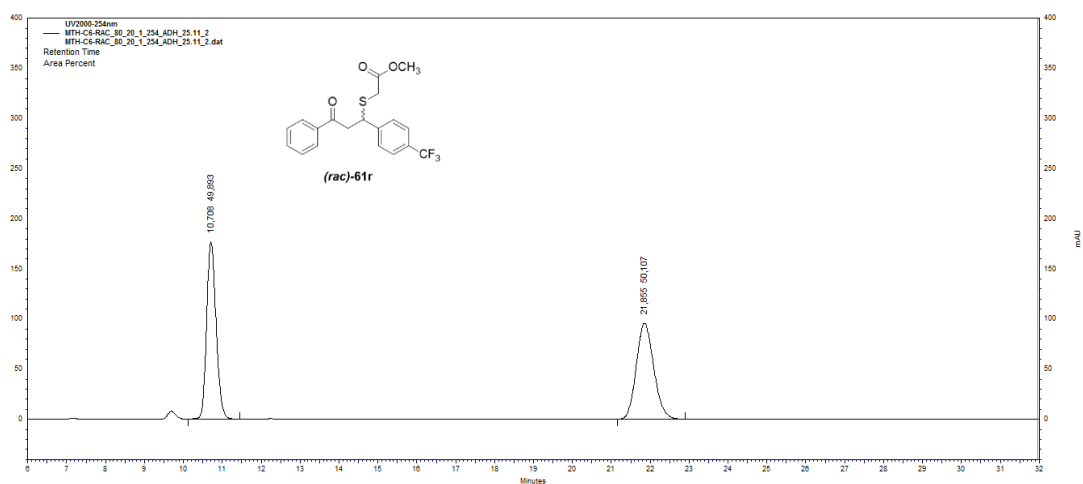


Figure B. 35 HPLC chromatogram of *rac*-**61r**

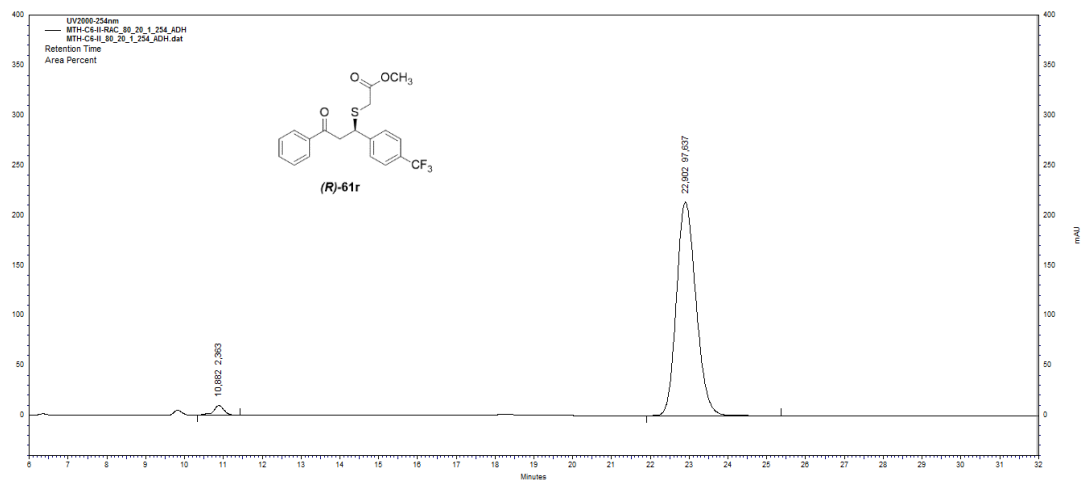


Figure B. 36 HPLC chromatogram of enantiomerically enriched **61r**

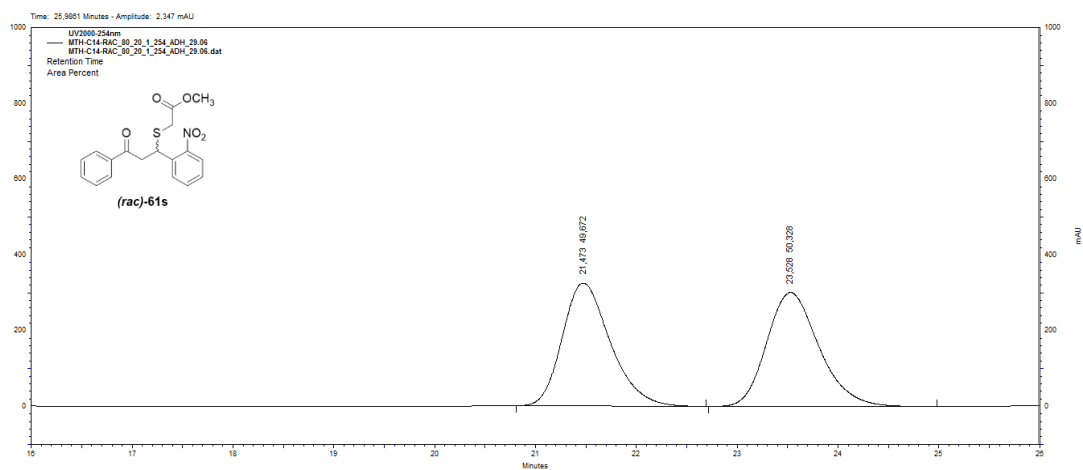


Figure B. 37 HPLC chromatogram of *rac*-**61s**

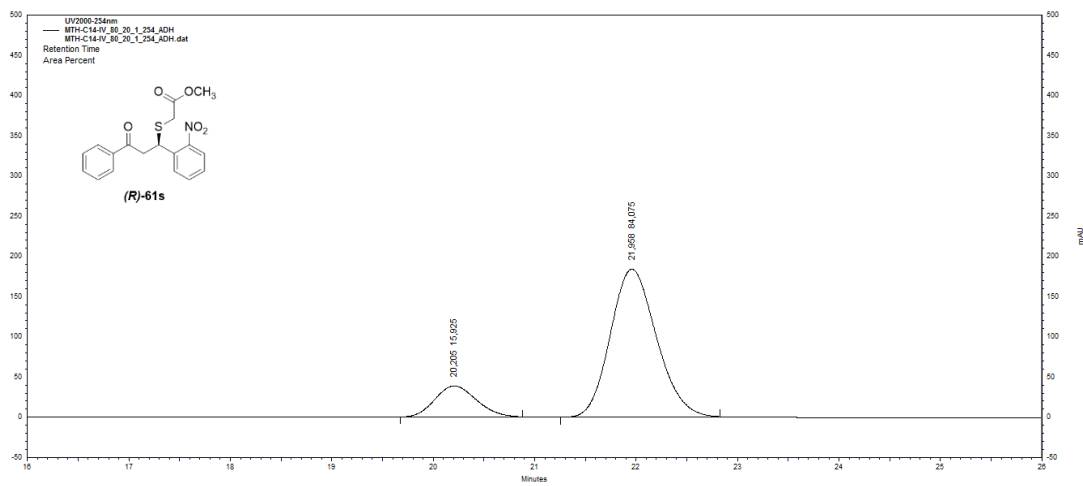


Figure B. 38 HPLC chromatogram of enantiomerically enriched **61s**

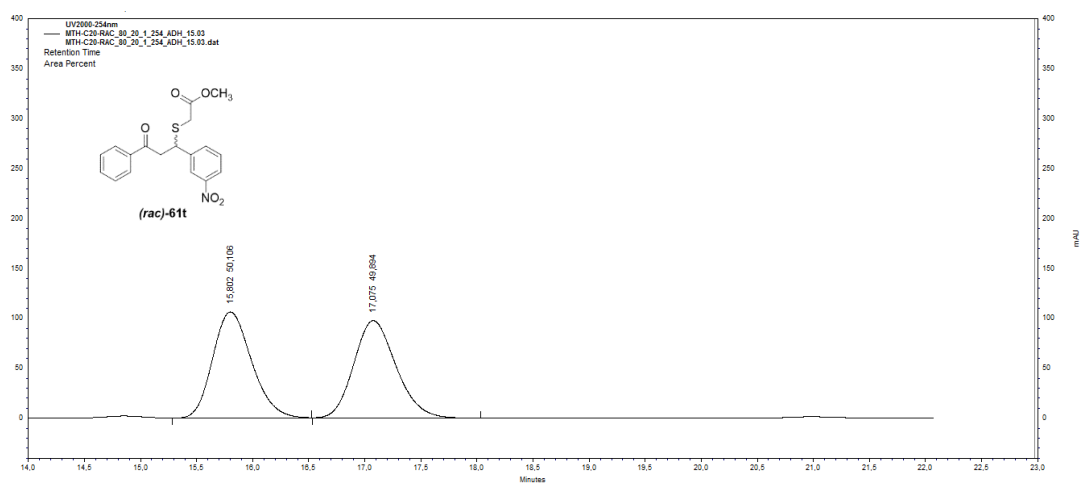


Figure B. 39 HPLC chromatogram of *rac*-**61t**

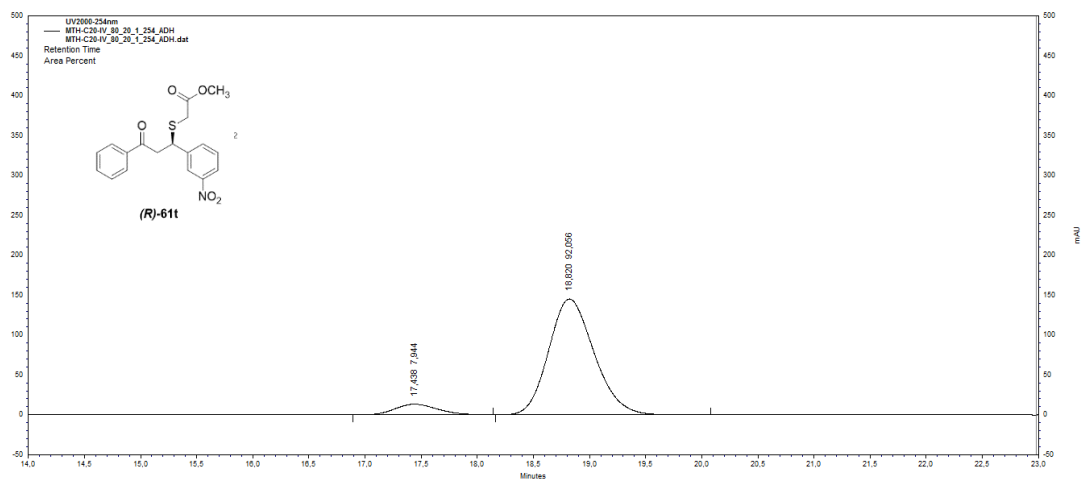


Figure B. 40 HPLC chromatogram of enantiomerically enriched **61t**

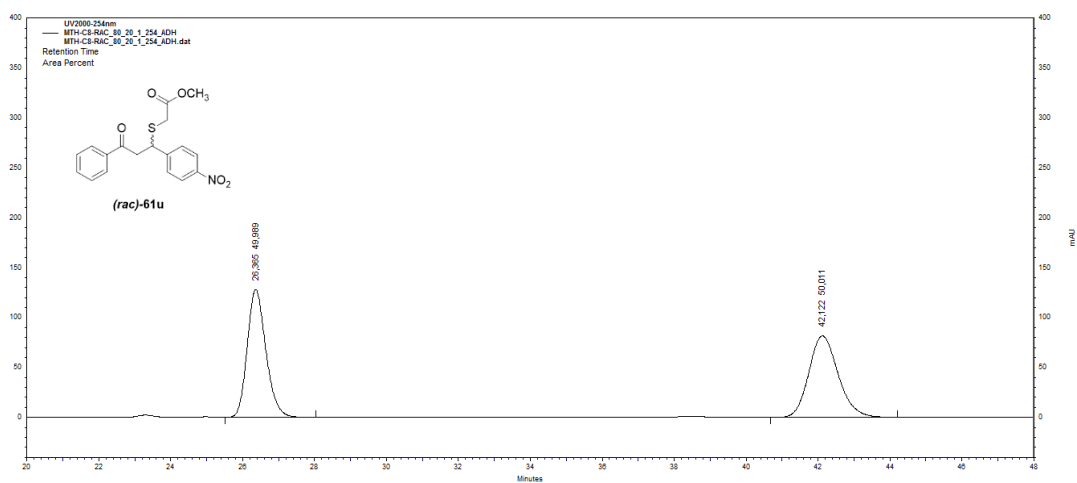


Figure B. 41 HPLC chromatogram of *rac*-**61u**

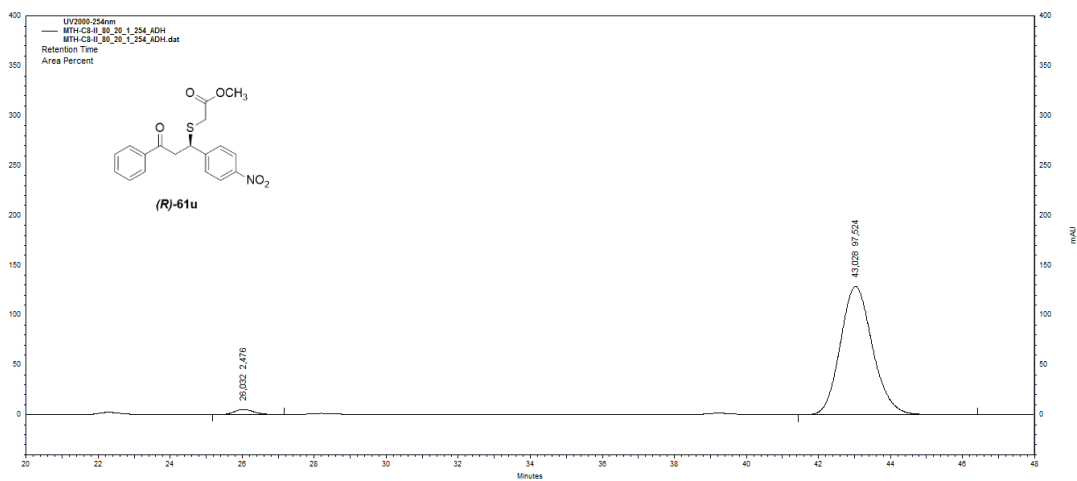


Figure B. 42 HPLC chromatogram of enantiomerically enriched **61u**

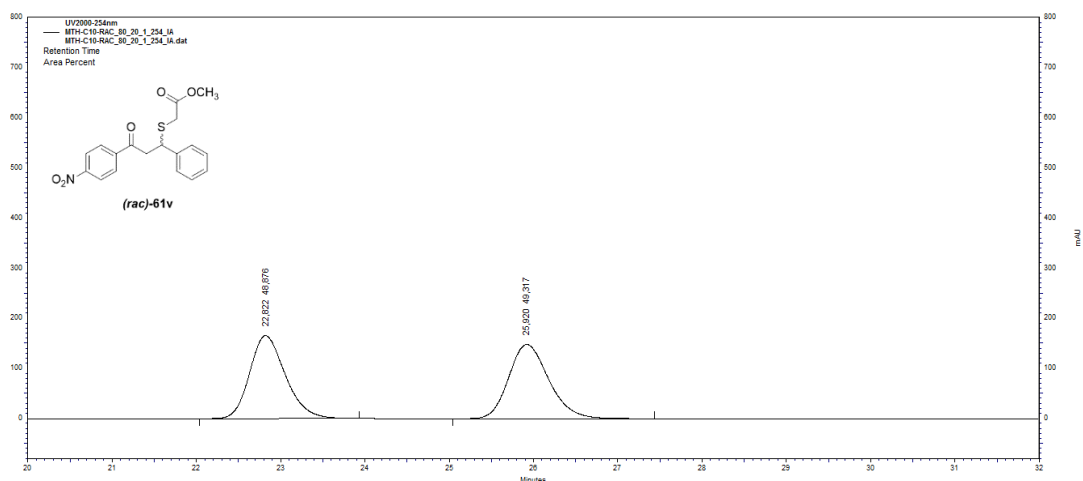


Figure B. 43 HPLC chromatogram of *rac*-**61v**

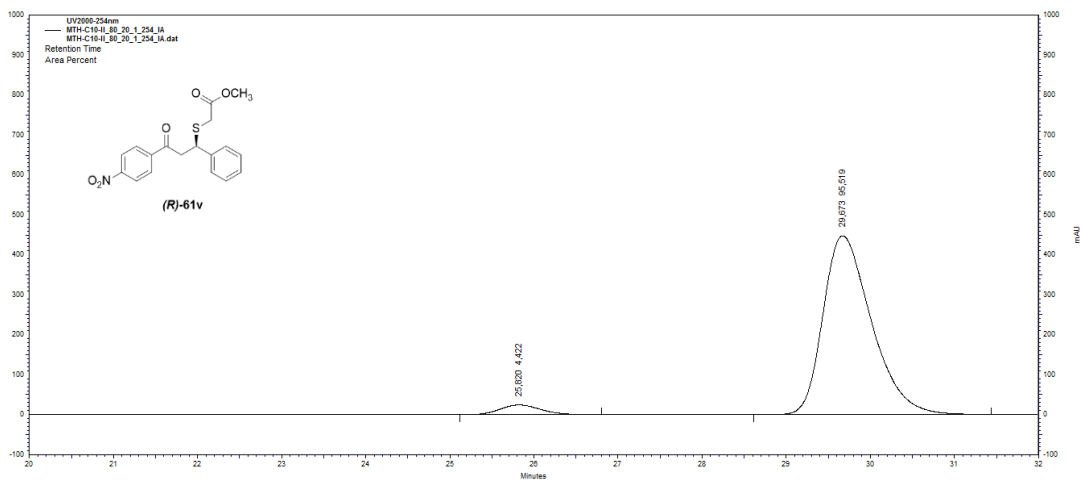


Figure B. 44 HPLC chromatogram of enantiomerically enriched **61v**

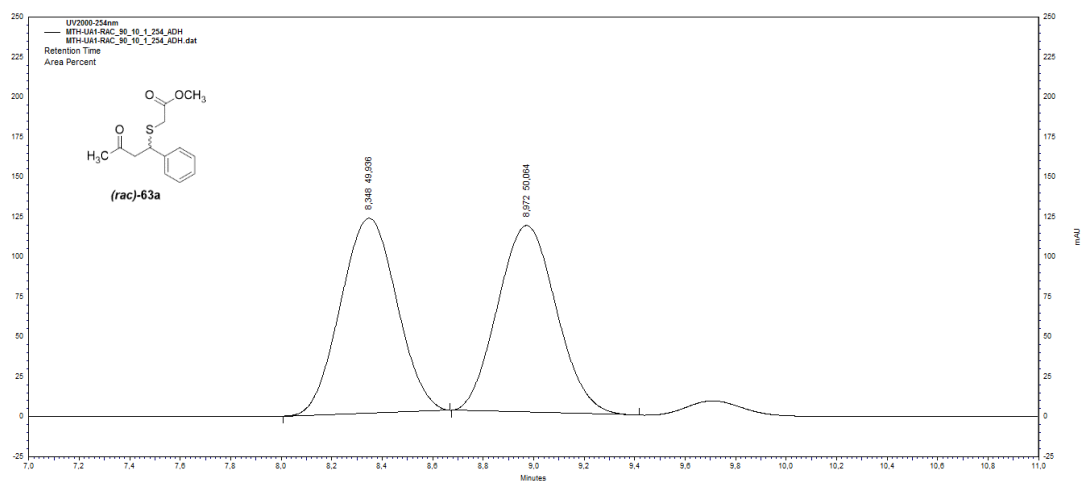


Figure B. 45 HPLC chromatogram of *rac*-**63a**

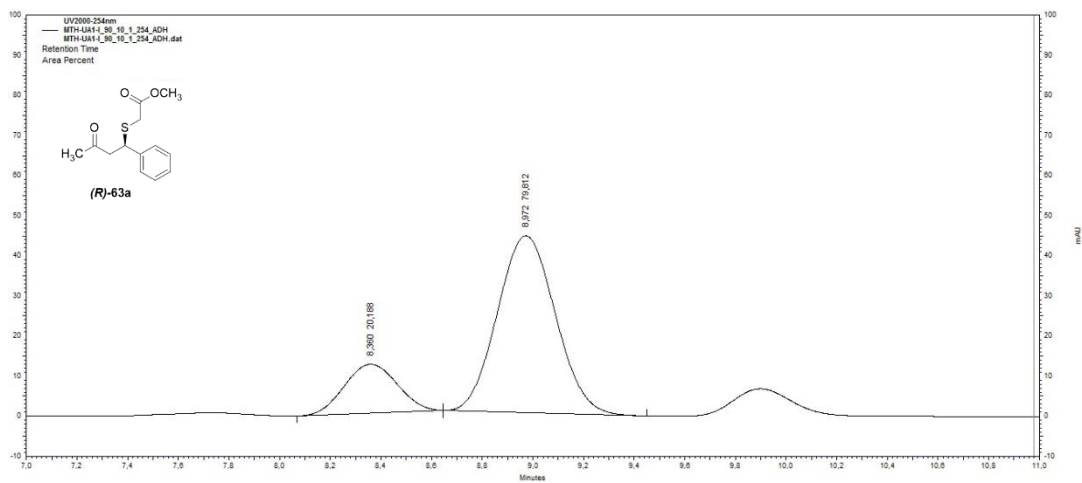


Figure B. 46 HPLC chromatogram of enantiomerically enriched **63a**

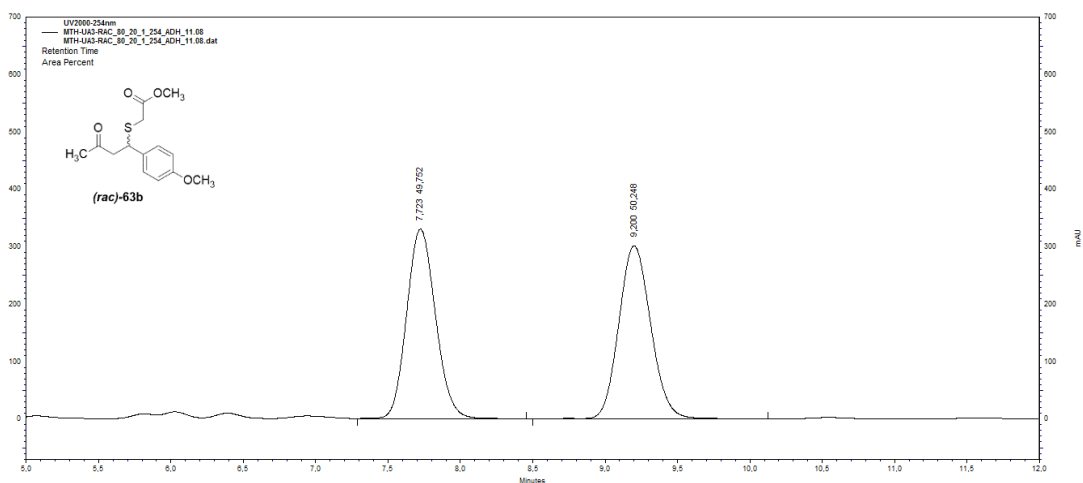


Figure B. 47 HPLC chromatogram of *rac*-**63b**

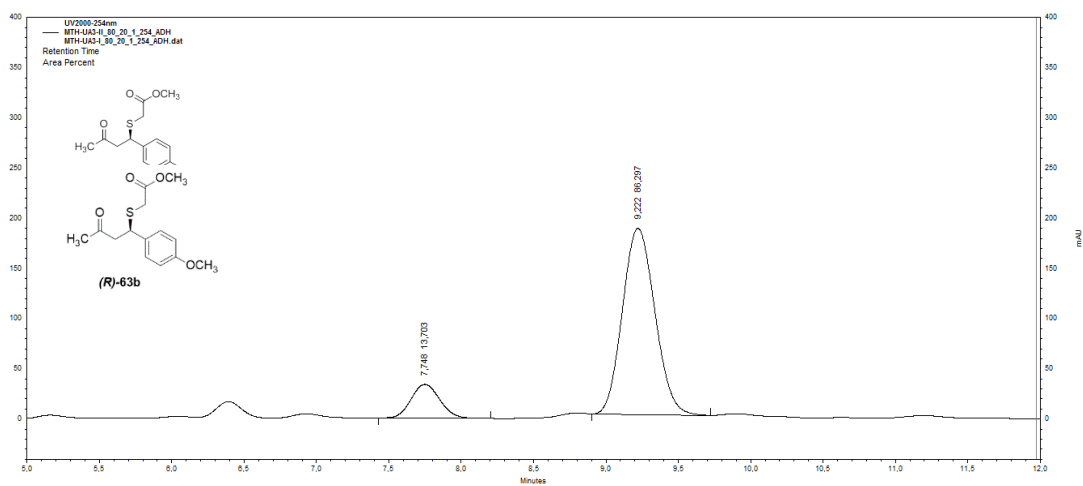


Figure B. 48 HPLC chromatogram of enantiomerically enriched **63b**

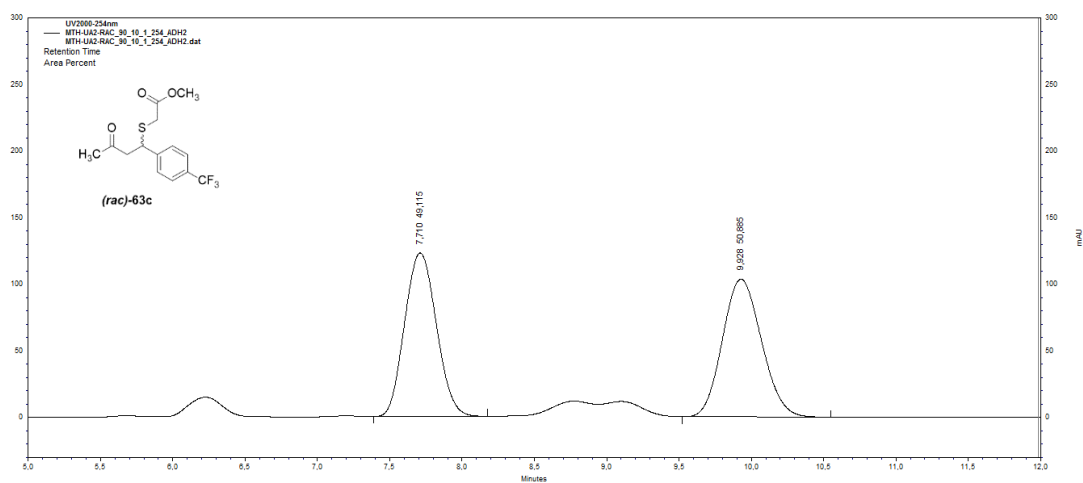


Figure B. 49 HPLC chromatogram of *rac*-**63c**

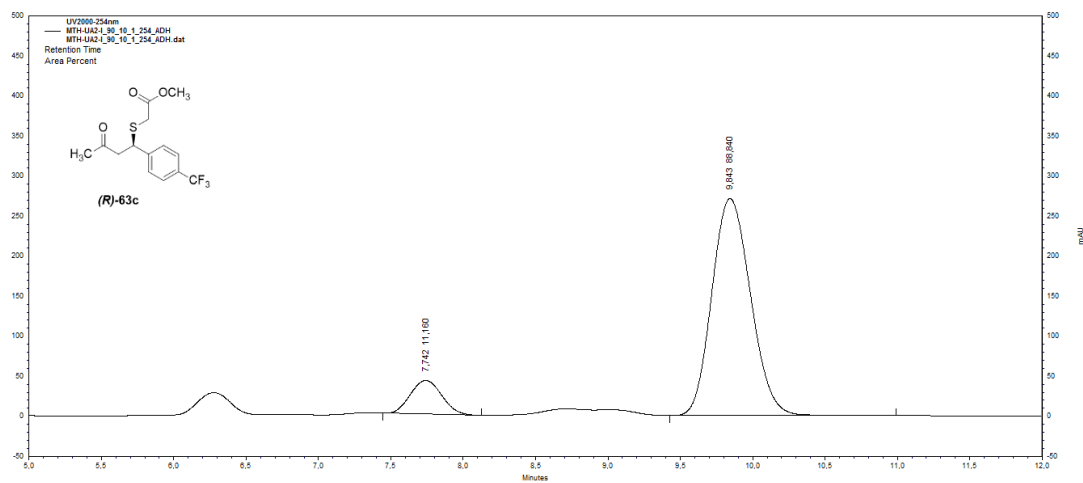


Figure B. 50 HPLC chromatogram of enantiomerically enriched **63c**

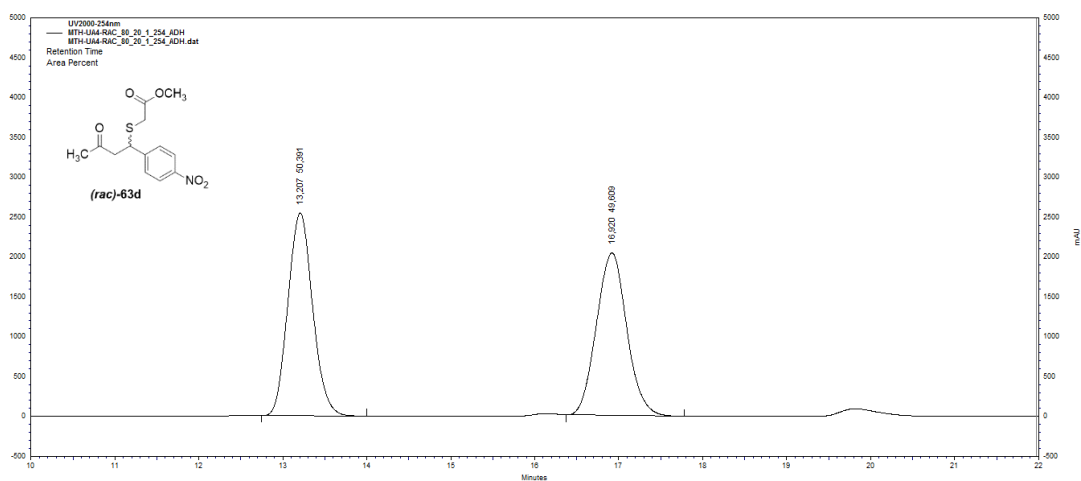


Figure B. 51 HPLC chromatogram of *rac*-**63d**

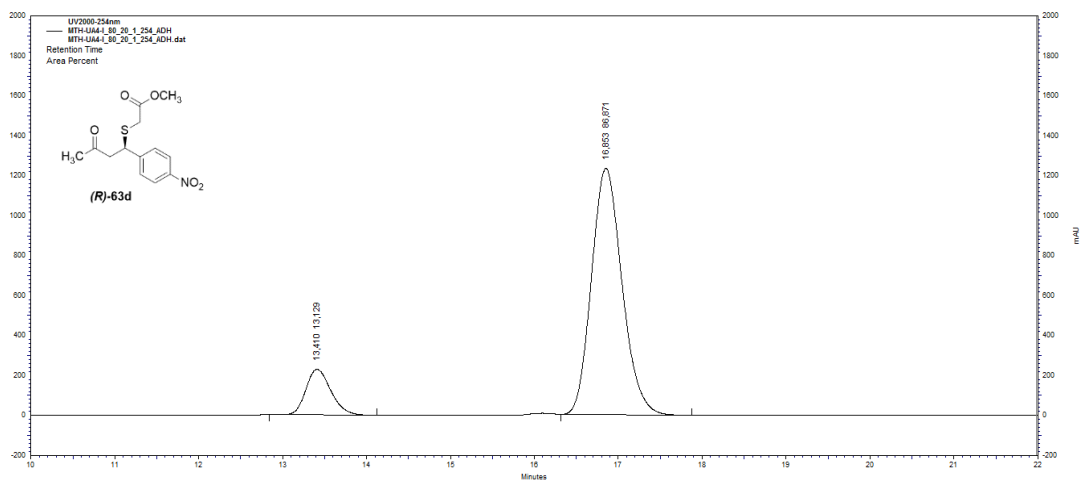


Figure B. 52 HPLC chromatogram of enantiomerically enriched **63d**

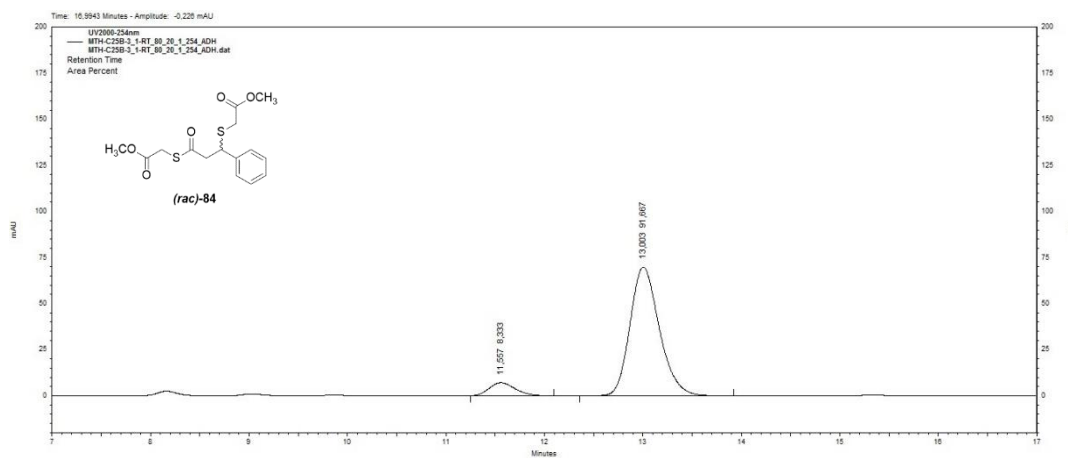


Figure B. 53 HPLC chromatogram of *rac*-**84**

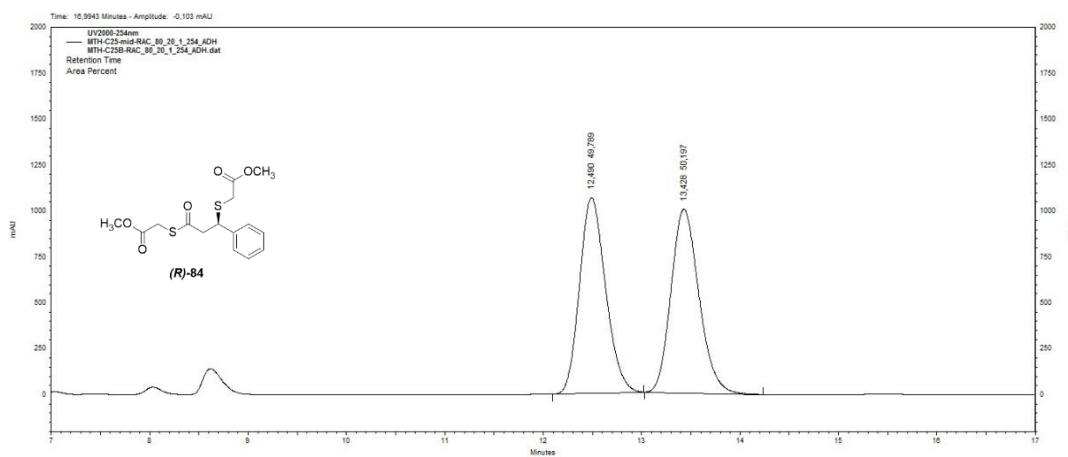


Figure B. 54 HPLC chromatogram of enantiomerically enriched **84**

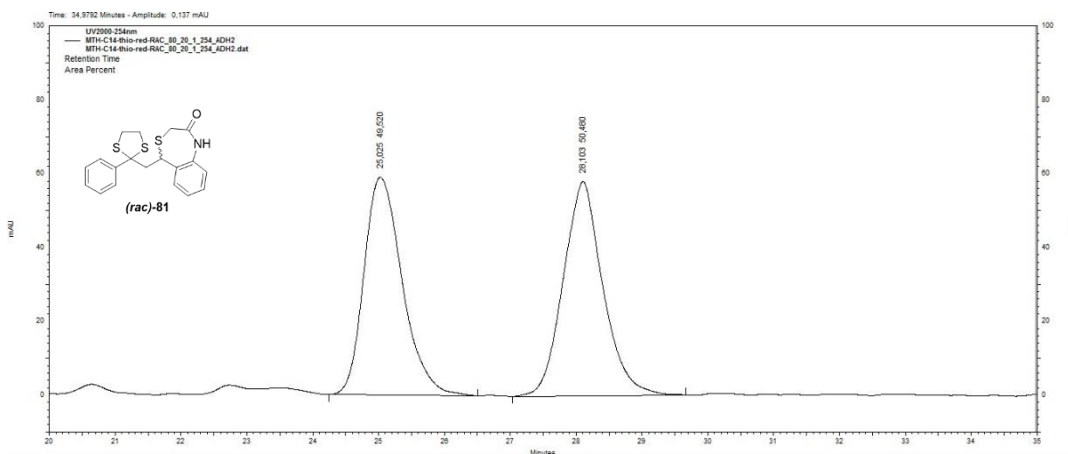


Figure B. 55 HPLC chromatogram of *rac*-**81**

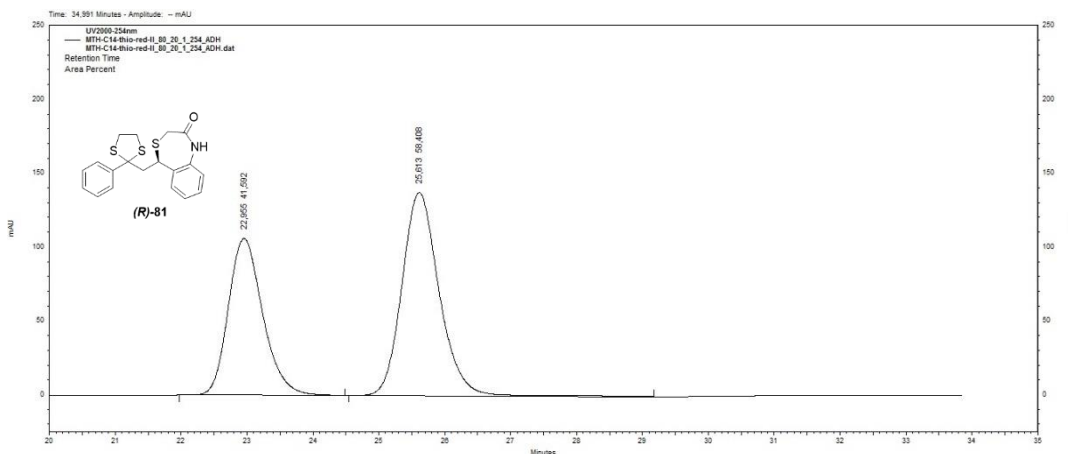


Figure B. 56 HPLC chromatogram of enantiomerically enriched **81**

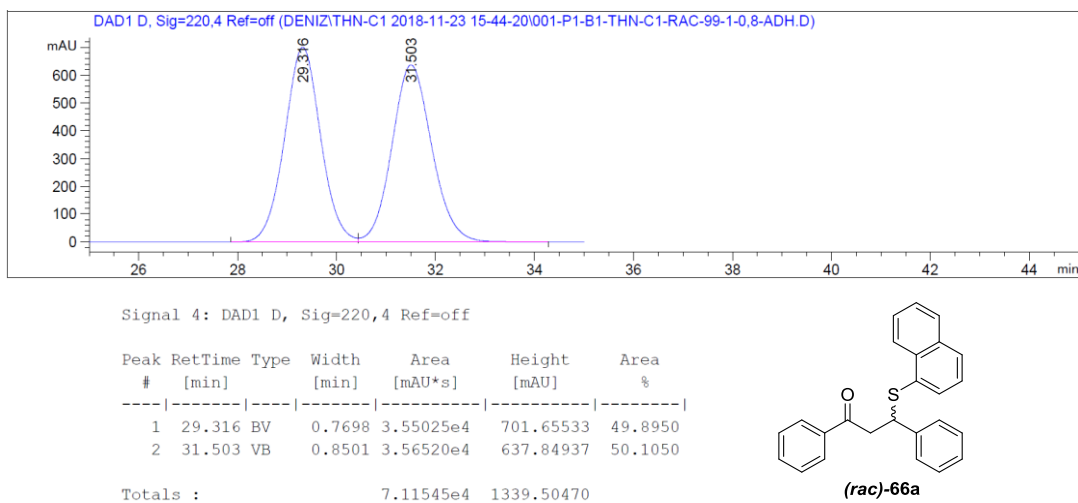


Figure B. 57 HPLC chromatogram of *rac*-66a

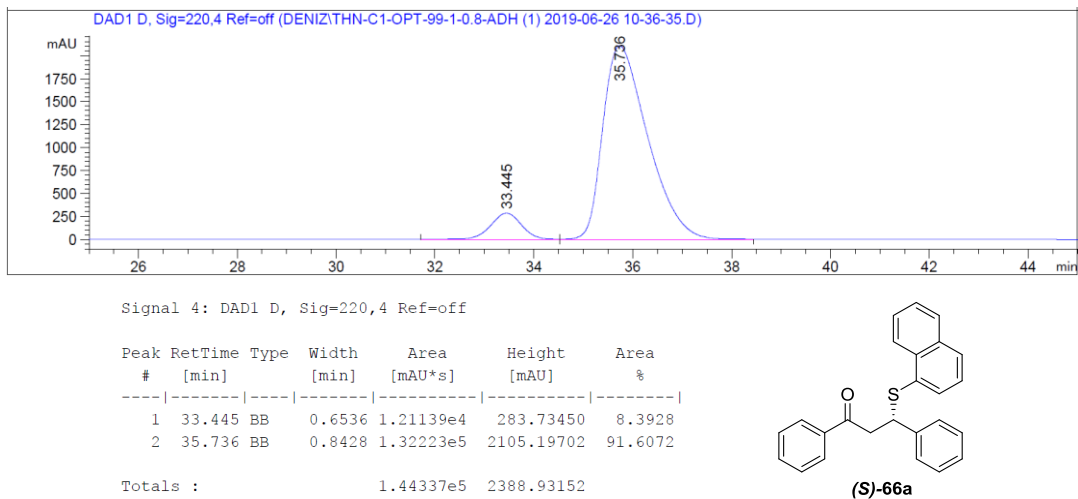
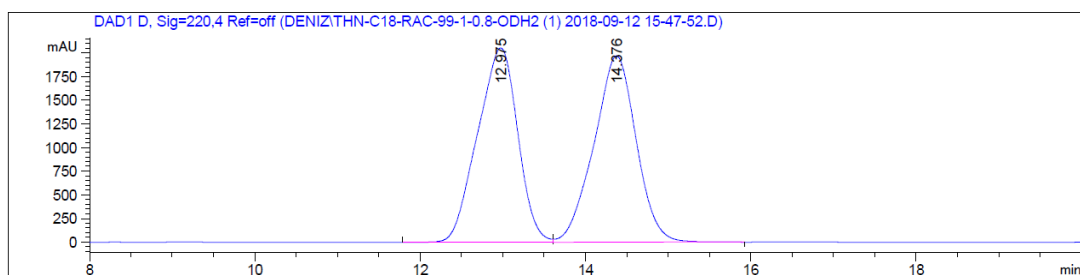


Figure B. 58 HPLC chromatogram of enantiomerically enriched 66a



Signal 4: DAD1 D, Sig=220,4 Ref=off

Peak #	RetTime [min]	Type	Width [min]	Area [mAU*s]	Height [mAU]	Area %
1	12.975	BV	0.4956	6.92892e4	2056.39526	49.7526
2	14.376	VB	0.5261	6.99784e4	1971.32837	50.2474

Totals : 1.39268e5 4027.72363

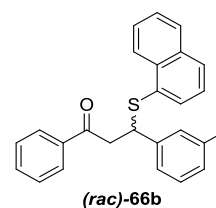
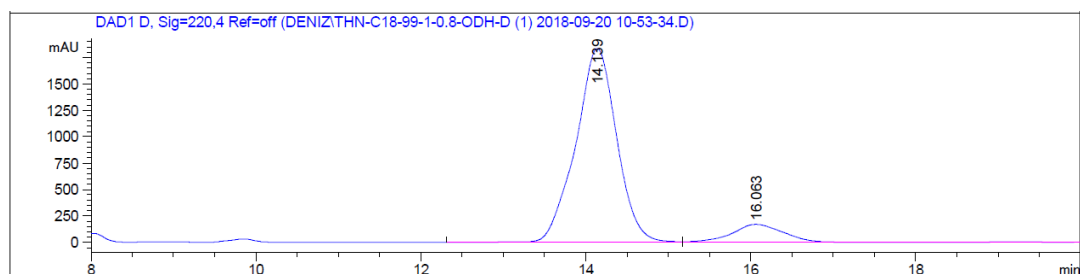


Figure B. 59 HPLC chromatogram of *rac*-66b



Signal 4: DAD1 D, Sig=220,4 Ref=off

Peak #	RetTime [min]	Type	Width [min]	Area [mAU*s]	Height [mAU]	Area %
1	14.139	BV	0.5148	6.34026e4	1836.55701	89.1188
2	16.063	VV R	0.6765	7741.29199	170.84424	10.8812

Totals : 7.11439e4 2007.40125

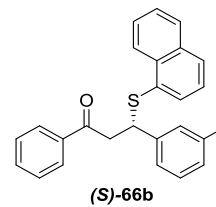


Figure B. 60 HPLC chromatogram of enantiomerically enriched 66b

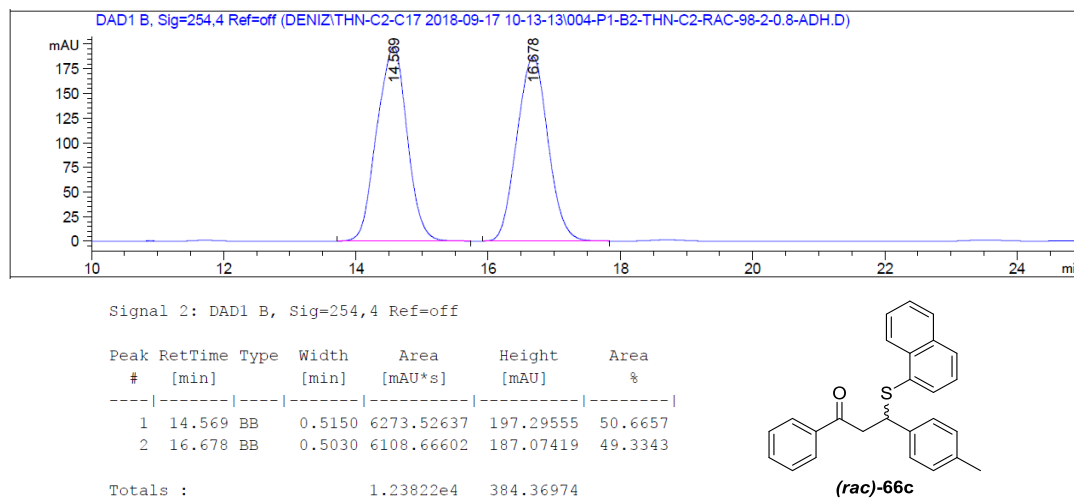


Figure B. 61 HPLC chromatogram of *rac*-**66c**

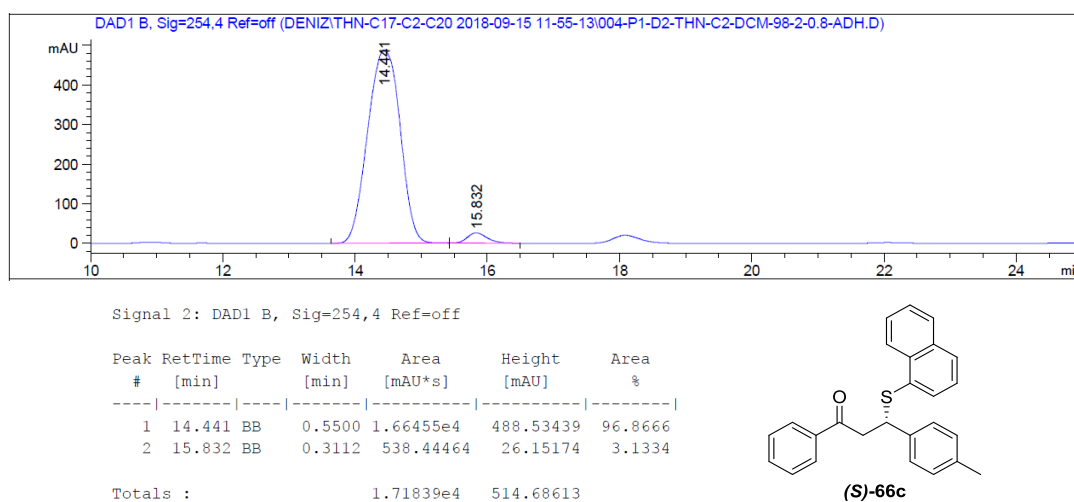


Figure B. 62 HPLC chromatogram of enantiomerically enriched **66c**

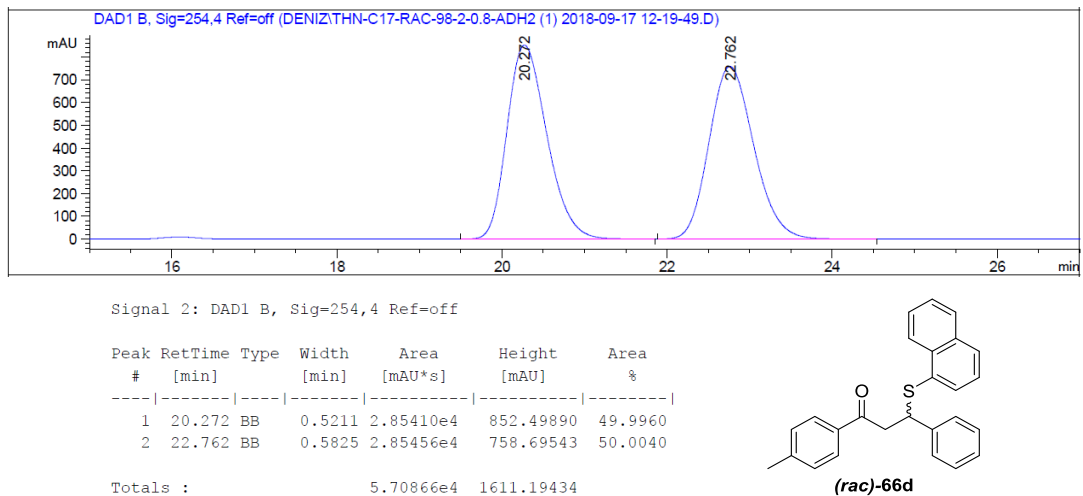


Figure B. 63 HPLC chromatogram of *rac*-**66d**

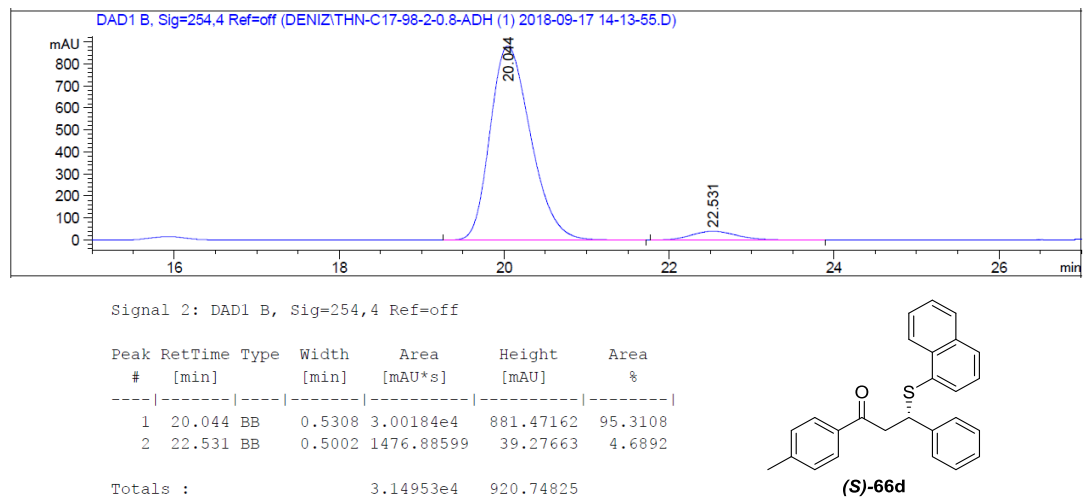
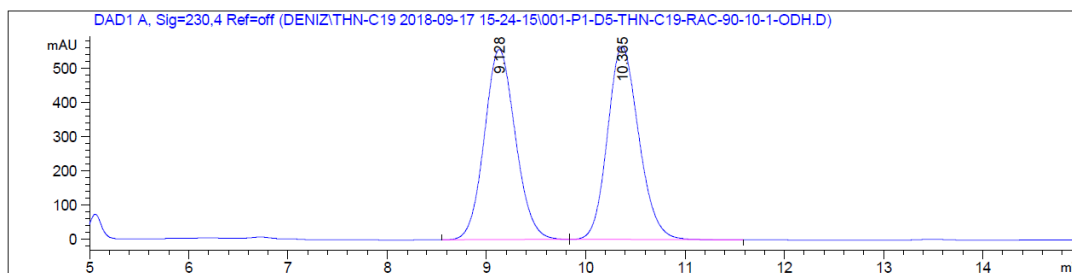


Figure B. 64 HPLC chromatogram of enantiomerically enriched **66d**



Signal 1: DAD1 A, Sig=230,4 Ref=off

Peak #	RetTime [min]	Type	Width [min]	Area [mAU*s]	Height [mAU]	Area %
1	9.128	BB	0.3359	1.21252e4	557.19781	49.4275
2	10.365	BB	0.3386	1.24061e4	566.28217	50.5725

Totals : 2.45312e4 1123.47998

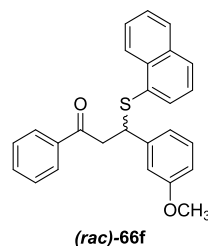
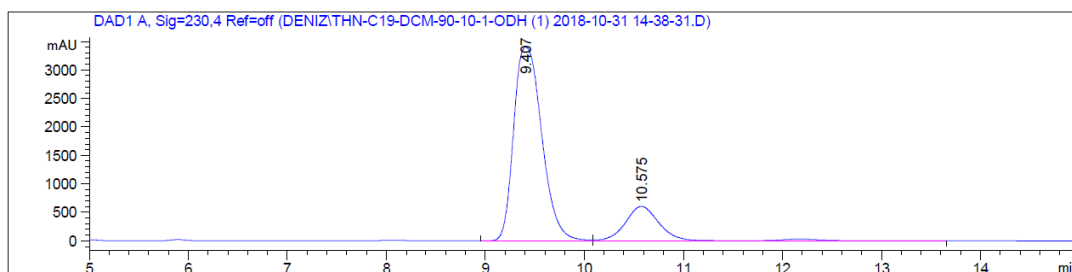


Figure B. 65 HPLC chromatogram of *rac*-66f



Signal 1: DAD1 A, Sig=230,4 Ref=off

Peak #	RetTime [min]	Type	Width [min]	Area [mAU*s]	Height [mAU]	Area %
1	9.407	BV	0.3099	6.70355e4	3402.12036	81.5014
2	10.575	VV R	0.3561	1.52152e4	604.47833	18.4986

Totals : 8.22507e4 4006.59869

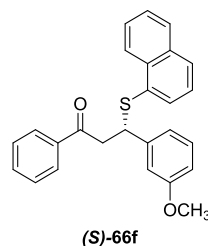
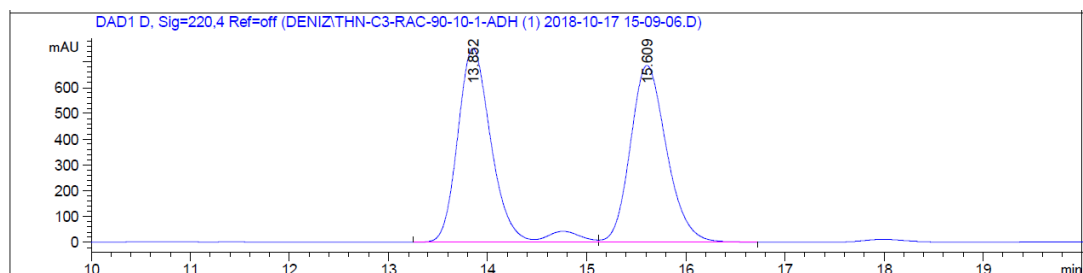


Figure B. 66 HPLC chromatogram of enantiomerically enriched 66f



Signal 4: DAD1 D, Sig=220,4 Ref=off

Peak #	RetTime [min]	Type	Width [min]	Area [mAU*s]	Height [mAU]	Area %
1	13.852	BV R	0.3547	1.82112e4	752.14575	51.2721
2	15.609	VB	0.3882	1.73076e4	685.24670	48.7279

Totals : 3.55188e4 1437.39246

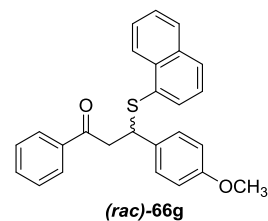
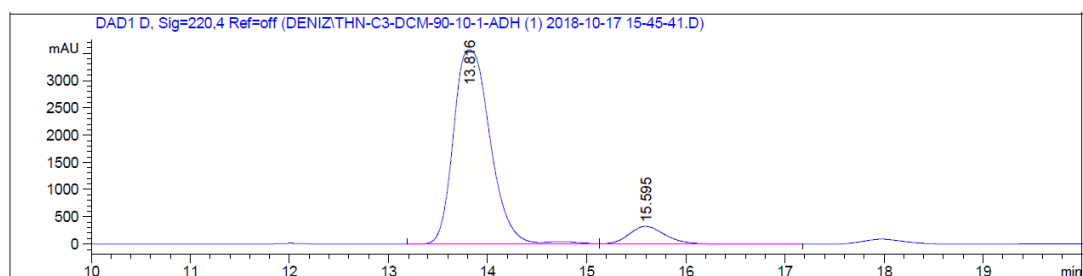


Figure B. 67 HPLC chromatogram of *rac*-66g



Signal 4: DAD1 D, Sig=220,4 Ref=off

Peak #	RetTime [min]	Type	Width [min]	Area [mAU*s]	Height [mAU]	Area %
1	13.816	BV R	0.2993	9.17834e4	3569.05933	91.7712
2	15.595	VB	0.3873	8229.84668	324.03961	8.2288

Totals : 1.00013e5 3893.09894

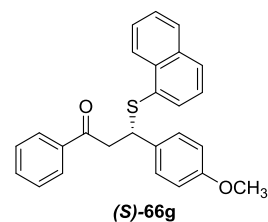
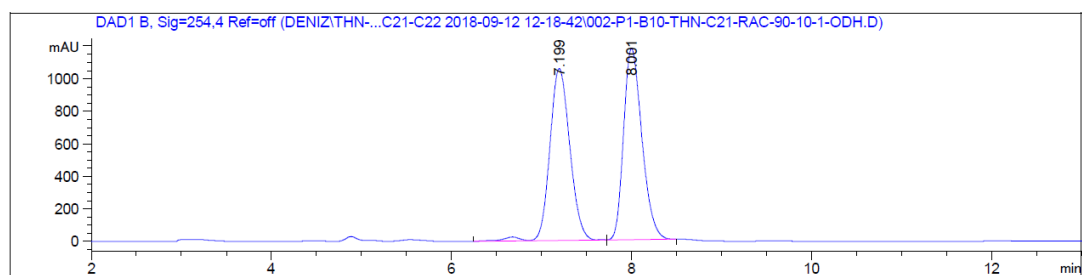


Figure B. 68 HPLC chromatogram of enantiomerically enriched 66g



Signal 2: DAD1 B, Sig=254,4 Ref=off

Peak #	RetTime [min]	Type	Width [min]	Area [mAU*s]	Height [mAU]	Area %
1	7.199	VV R	0.2365	1.63263e4	1055.59644	49.5946
2	8.001	BB	0.2194	1.65933e4	1173.67212	50.4054

Totals : 3.29196e4 2229.26855

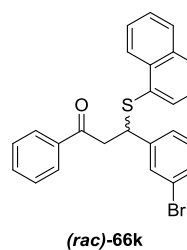
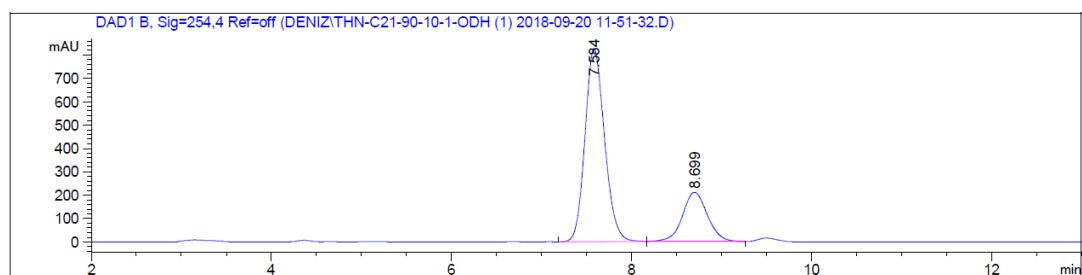


Figure B. 69 HPLC chromatogram of *rac*-66k



Signal 2: DAD1 B, Sig=254,4 Ref=off

Peak #	RetTime [min]	Type	Width [min]	Area [mAU*s]	Height [mAU]	Area %
1	7.584	BB	0.2336	1.24848e4	827.05249	75.4838
2	8.699	BV	0.2968	4054.90894	210.45692	24.5162

Totals : 1.65397e4 1037.50941

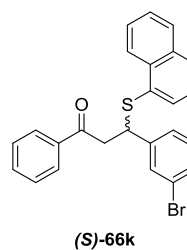
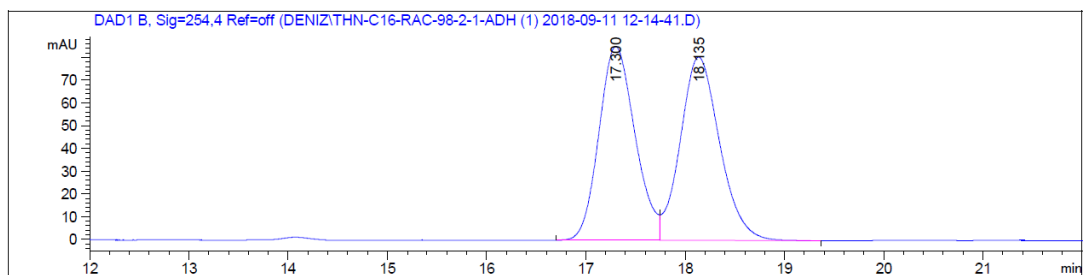


Figure B. 70 HPLC chromatogram of enantiomerically enriched 66k



Signal 2: DAD1 B, Sig=254,4 Ref=off

Peak #	RetTime [min]	Type	Width [min]	Area [mAU*s]	Height [mAU]	Area %
1	17.300	BV	0.3896	2160.08887	85.40229	49.1325
2	18.135	VB	0.4128	2236.36548	80.82732	50.8675
Totals :				4396.45435	166.22961	

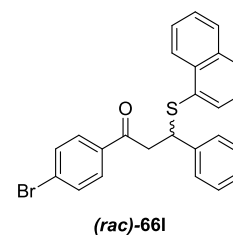
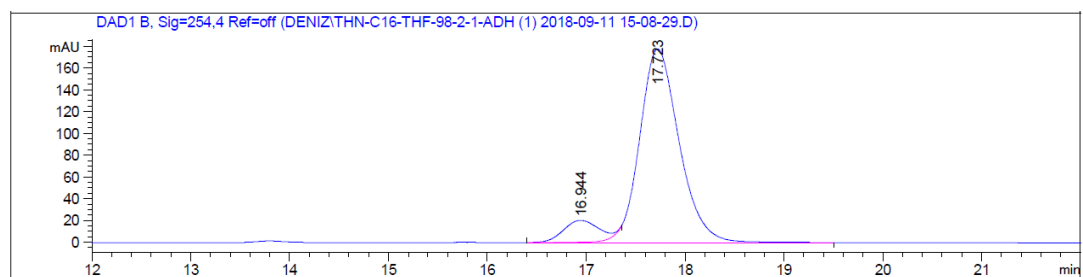


Figure B. 71 HPLC chromatogram of *rac*-**661**



Signal 2: DAD1 B, Sig=254,4 Ref=off

Peak #	RetTime [min]	Type	Width [min]	Area [mAU*s]	Height [mAU]	Area %
1	16.944	BV E	0.3540	498.38351	20.36371	9.1561
2	17.723	VB R	0.4235	4944.82568	178.06689	90.8439
Totals :				5443.20920	198.43061	

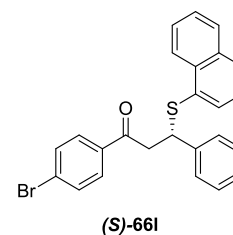
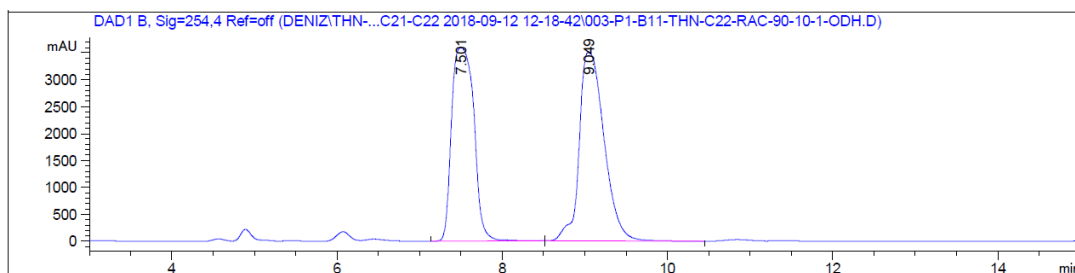


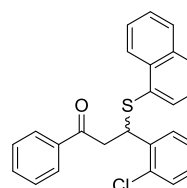
Figure B. 72 HPLC chromatogram of enantiomerically enriched **661**



Signal 2: DAD1 B, Sig=254,4 Ref=off

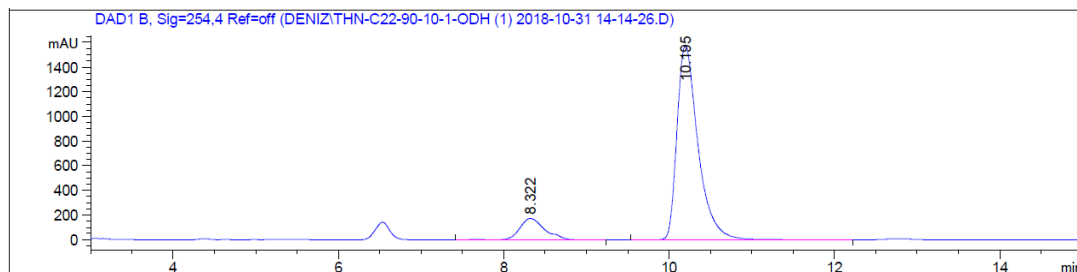
Peak #	RetTime [min]	Type	Width [min]	Area [mAU*s]	Height [mAU]	Area %
1	7.501	BB	0.3103	6.72355e4	3593.60767	47.7895
2	9.049	BB	0.3240	7.34555e4	3512.53784	52.2105

Totals : 1.40691e5 7106.14551



(rac)-66m

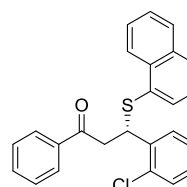
Figure B. 73 HPLC chromatogram of *rac*-66m



Signal 2: DAD1 B, Sig=254,4 Ref=off

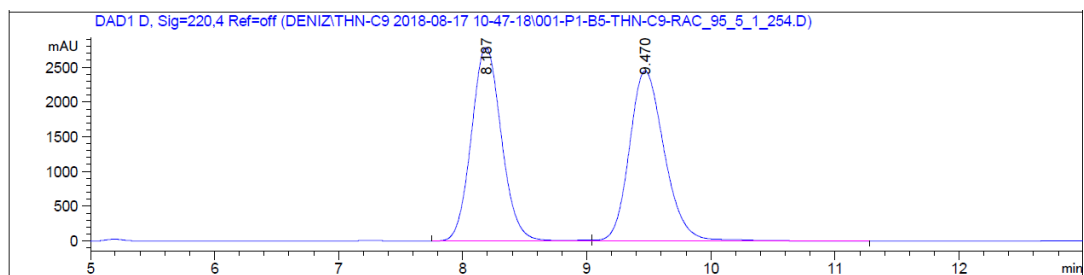
Peak #	RetTime [min]	Type	Width [min]	Area [mAU*s]	Height [mAU]	Area %
1	8.322	VB R	0.3137	3624.86670	172.64355	11.5050
2	10.195	BB	0.2682	2.78821e4	1577.27319	88.4950

Totals : 3.15069e4 1749.91675



(S)-66m

Figure B. 74 HPLC chromatogram of enantiomerically enriched 66m



Signal 4: DAD1 D, Sig=220,4 Ref=off

Peak #	RetTime [min]	Type	Width [min]	Area [mAU*s]	Height [mAU]	Area %
1	8.187	BV R	0.2594	4.69352e4	2785.85107	49.4771
2	9.470	VB	0.3026	4.79274e4	2446.08301	50.5229

Totals : 9.48626e4 5231.93408

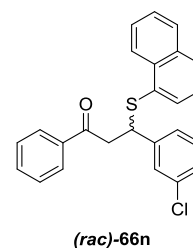
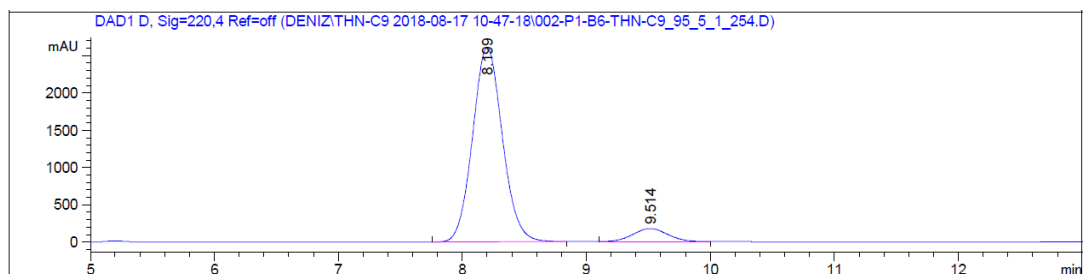


Figure B. 75 HPLC chromatogram of *rac*-66n



Signal 4: DAD1 D, Sig=220,4 Ref=off

Peak #	RetTime [min]	Type	Width [min]	Area [mAU*s]	Height [mAU]	Area %
1	8.199	BB	0.2573	4.35814e4	2609.86353	92.7353
2	9.514	BB	0.3016	3414.07690	175.42325	7.2647

Totals : 4.69955e4 2785.28677

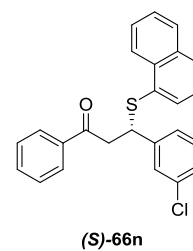
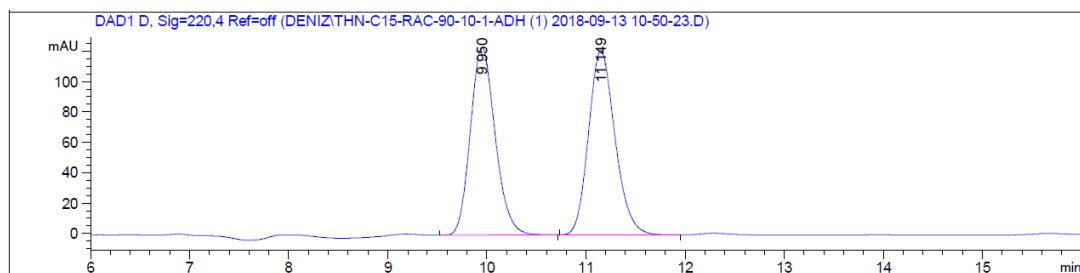


Figure B. 76 HPLC chromatogram of enantiomerically enriched 66n



Signal 4: DAD1 D, Sig=220,4 Ref=off

Peak #	RetTime [min]	Type	Width [min]	Area [mAU*s]	Height [mAU]	Area %
1	9.950	BB	0.2683	2156.46191	123.72632	48.8890
2	11.149	BB	0.2862	2254.47583	121.39420	51.1110

Totals : 4410.93774 245.12052

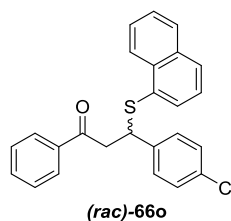
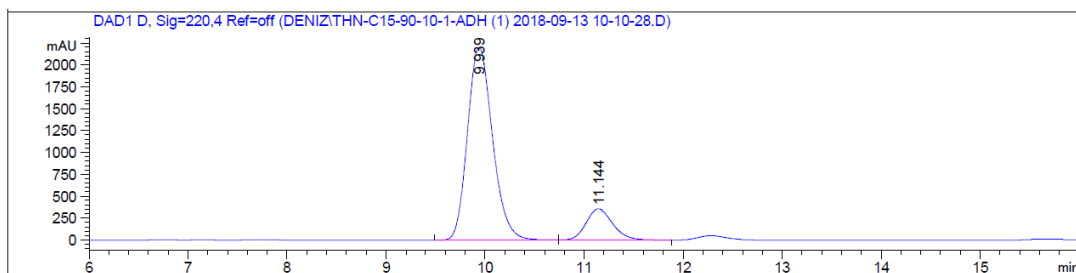


Figure B. 77 HPLC chromatogram of *rac*-660



Signal 4: DAD1 D, Sig=220,4 Ref=off

Peak #	RetTime [min]	Type	Width [min]	Area [mAU*s]	Height [mAU]	Area %
1	9.939	BV	0.2725	3.87236e4	2203.32349	85.4165
2	11.144	VB	0.2856	6611.40771	356.05481	14.5835

Totals : 4.53350e4 2559.37830

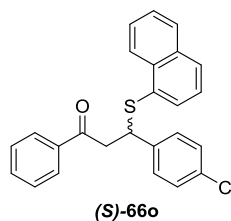
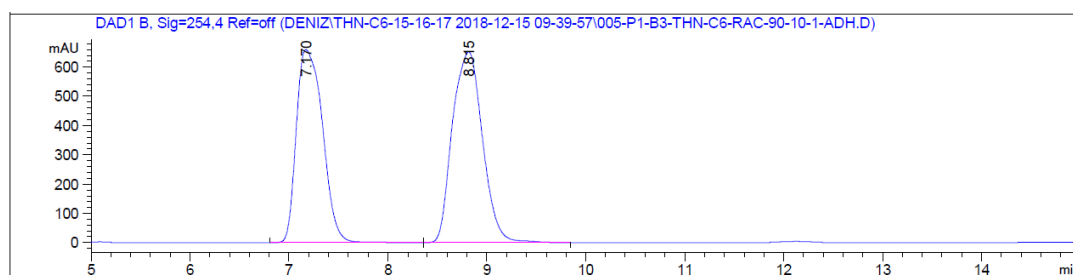


Figure B. 78 HPLC chromatogram of enantiomerically enriched 660



Signal 2: DAD1 B, Sig=254,4 Ref=off

Peak #	RetTime [min]	Type	Width [min]	Area [mAU*s]	Height [mAU]	Area %
1	7.170	BB	0.2999	1.21288e4	659.98712	46.8644
2	8.815	BB	0.3409	1.37519e4	652.39496	53.1356

Totals : 2.58807e4 1312.38208

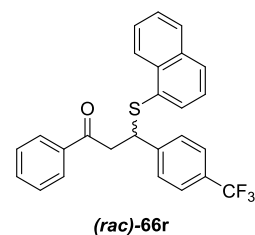
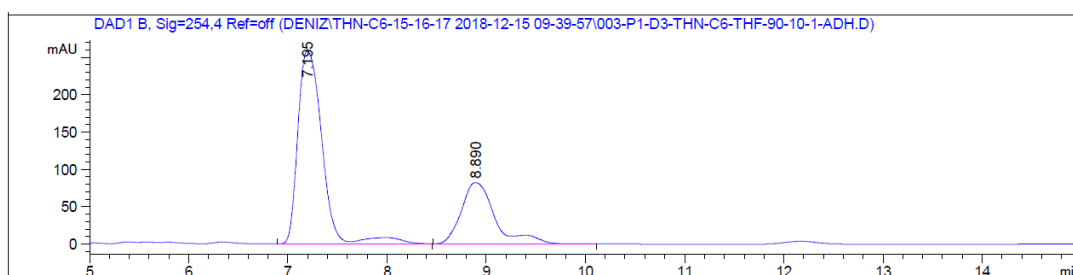


Figure B. 79 HPLC chromatogram of *rac*-66r



Signal 2: DAD1 B, Sig=254,4 Ref=off

Peak #	RetTime [min]	Type	Width [min]	Area [mAU*s]	Height [mAU]	Area %
1	7.195	BV R	0.2627	4425.58887	258.93863	69.4832
2	8.890	BV R	0.3337	1943.70544	82.17338	30.5168

Totals : 6369.29431 341.11201

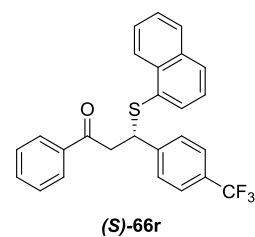
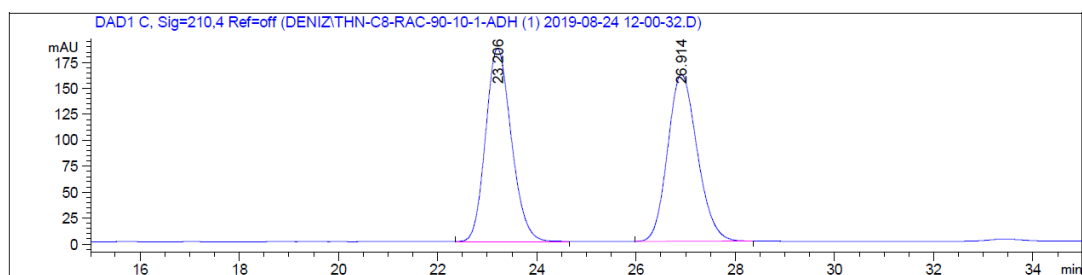


Figure B. 80 HPLC chromatogram of enantiomerically enriched 66r



Signal 3: DAD1 C, Sig=210,4 Ref=off

Peak #	RetTime [min]	Type	Width [min]	Area [mAU*s]	Height [mAU]	Area %
1	23.206	BB	0.5442	6688.13721	185.93582	50.1028
2	26.914	BB	0.6263	6660.69531	160.79277	49.8972

Totals : 1.33488e4 346.72859

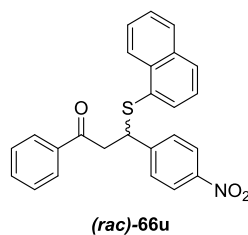
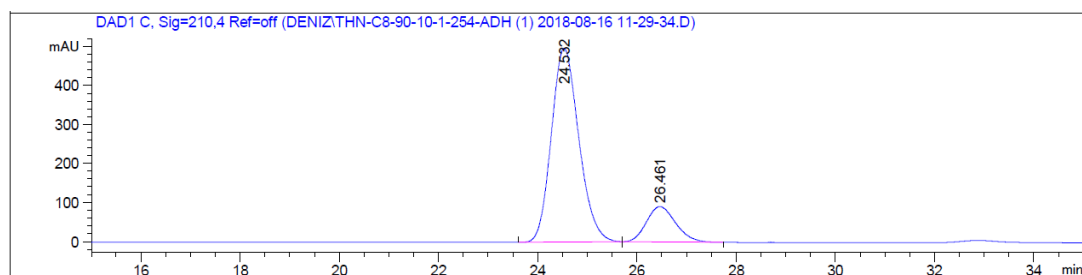


Figure B. 81 HPLC chromatogram of *rac*-66u



Signal 3: DAD1 C, Sig=210,4 Ref=off

Peak #	RetTime [min]	Type	Width [min]	Area [mAU*s]	Height [mAU]	Area %
1	24.532	BB	0.5899	1.91059e4	496.51318	83.7845
2	26.461	BB	0.5904	3697.71533	90.46827	16.2155

Totals : 2.28036e4 586.98145

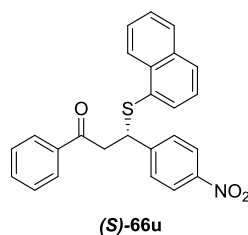


Figure B. 82 HPLC chromatogram of enantiomerically enriched 66u

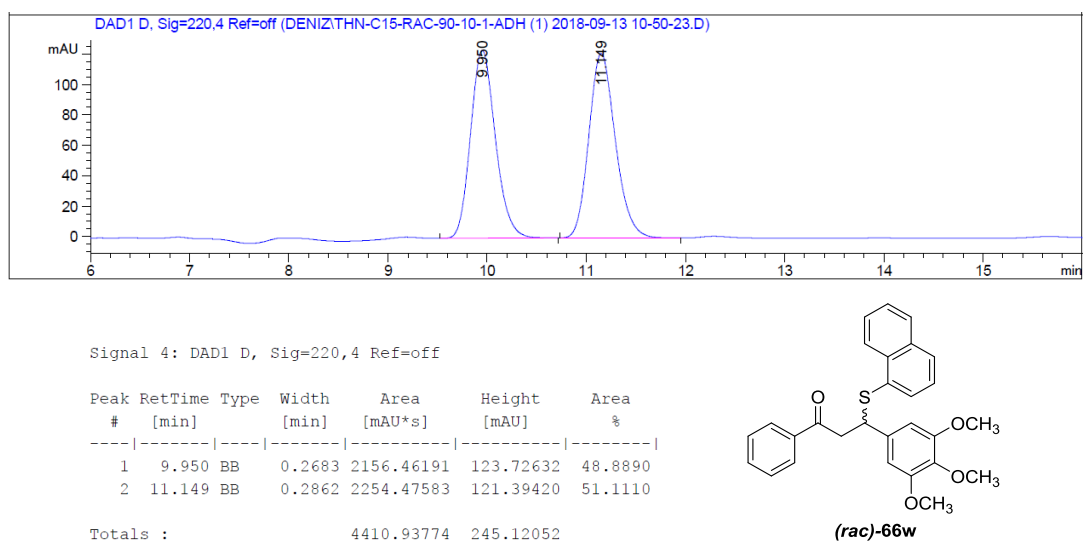


Figure B. 83 HPLC chromatogram of *rac*-66w

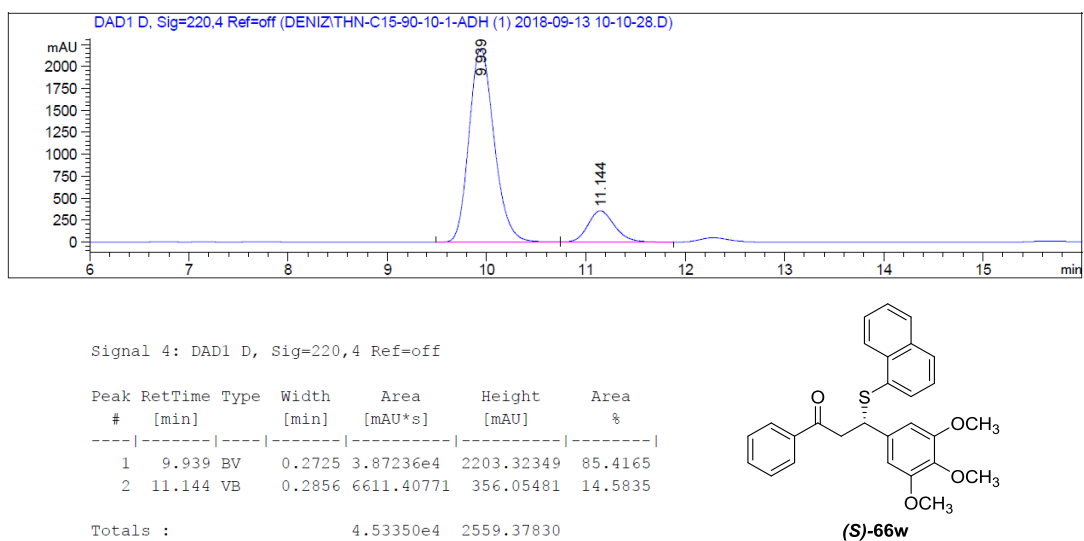
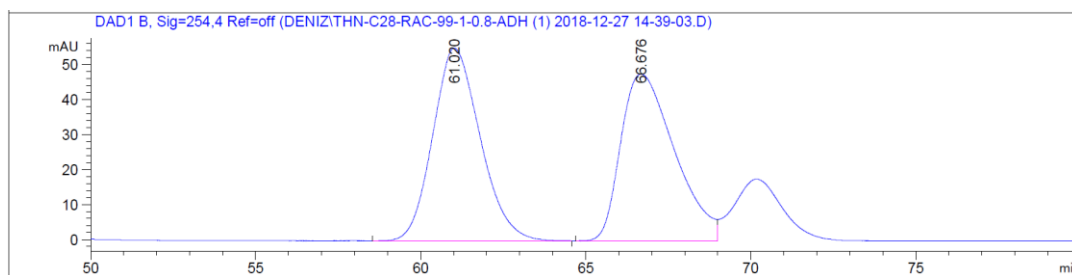


Figure B. 84 HPLC chromatogram of enantiomerically enriched 66w



Signal 2: DAD1 B, Sig=254,4 Ref=off

Peak #	RetTime [min]	Type	Width [min]	Area [mAU*s]	Height [mAU]	Area %
1	61.020	BB	1.5805	5495.46240	55.05659	50.4427
2	66.676	BV	1.7547	5399.01172	47.62256	49.5573

Totals : 1.08945e4 102.67915

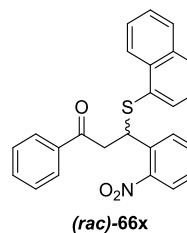
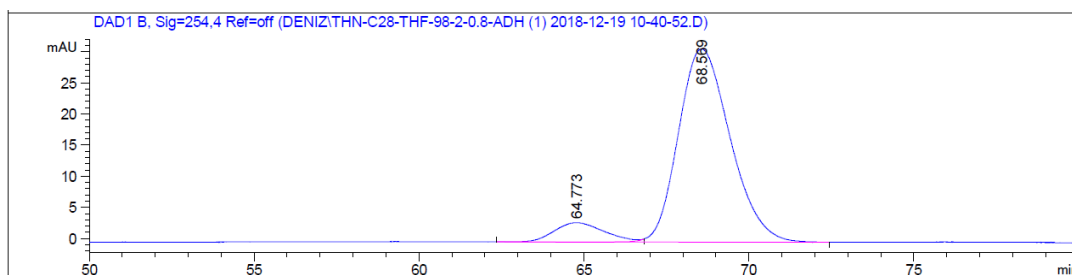


Figure B. 85 HPLC chromatogram of *rac*-**66x**



Signal 2: DAD1 B, Sig=254,4 Ref=off

Peak #	RetTime [min]	Type	Width [min]	Area [mAU*s]	Height [mAU]	Area %
1	64.773	BV E	1.6263	327.36319	3.11457	8.8062
2	68.569	VB R	1.7067	3390.04492	31.02762	91.1938

Totals : 3717.40811 34.14219

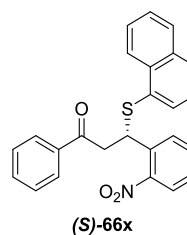


Figure B. 86 HPLC chromatogram of enantiomerically enriched **66x**

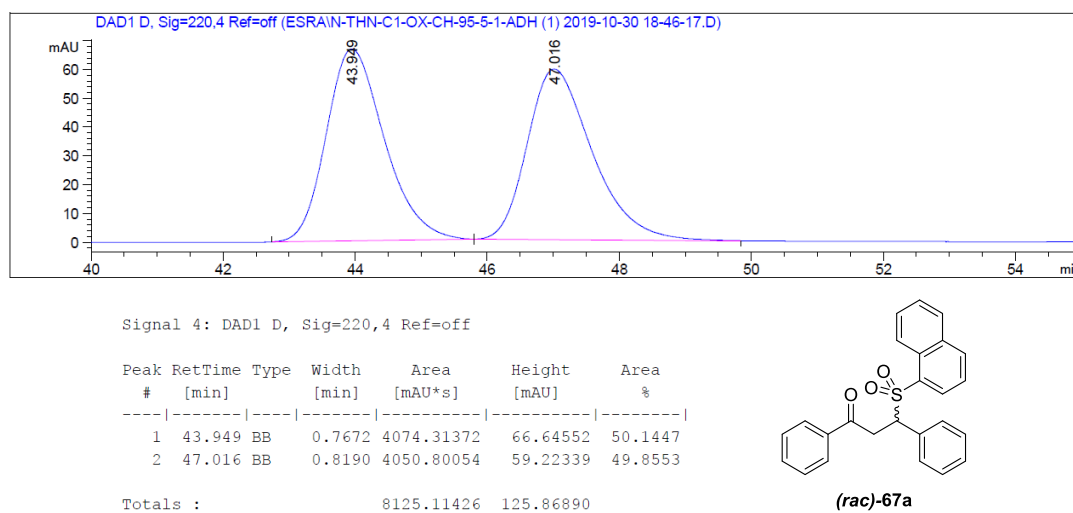


Figure B. 87 HPLC chromatogram of *rac*-**67a**

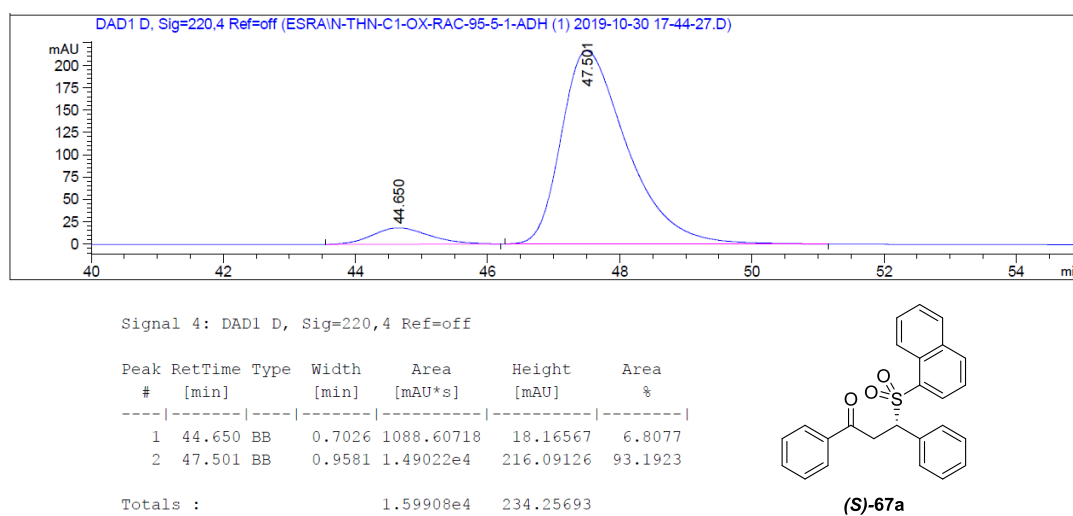
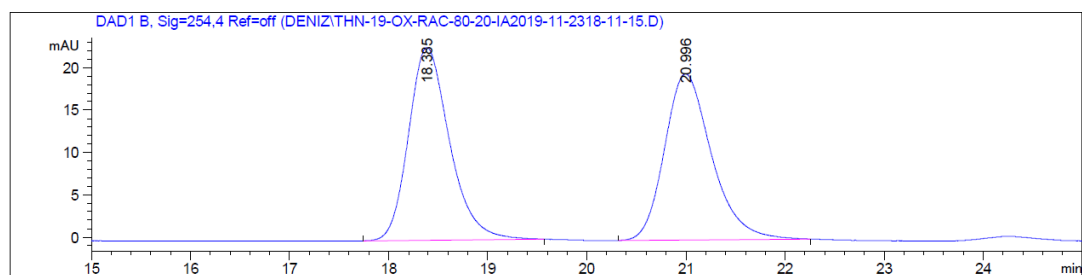


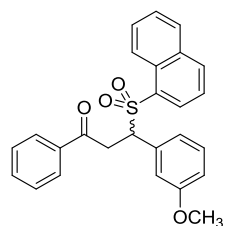
Figure B. 88 HPLC chromatogram of enantiomerically enriched **67a**



Signal 2: DAD1 B, Sig=254,4 Ref=off

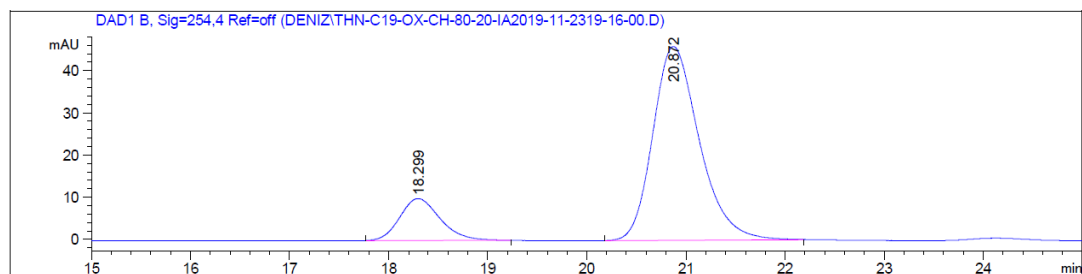
Peak #	RetTime [min]	Type	Width [min]	Area [mAU*s]	Height [mAU]	Area %
1	18.385	BB	0.3980	654.52106	22.75792	50.3000
2	20.996	BB	0.4316	646.71472	19.61943	49.7000

Totals : 1301.23578 42.37735



(rac)-67f

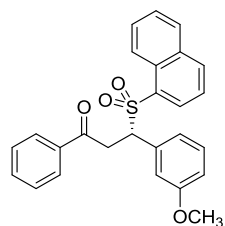
Figure B. 89 HPLC chromatogram of *rac*-**67f**



Signal 2: DAD1 B, Sig=254,4 Ref=off

Peak #	RetTime [min]	Type	Width [min]	Area [mAU*s]	Height [mAU]	Area %
1	18.299	BB	0.3332	278.74411	9.89344	15.7637
2	20.872	BB	0.4698	1489.52661	45.87250	84.2363

Totals : 1768.27072 55.76594



(S)-67f

Figure B. 90 HPLC chromatogram of enantiomerically enriched **67f**

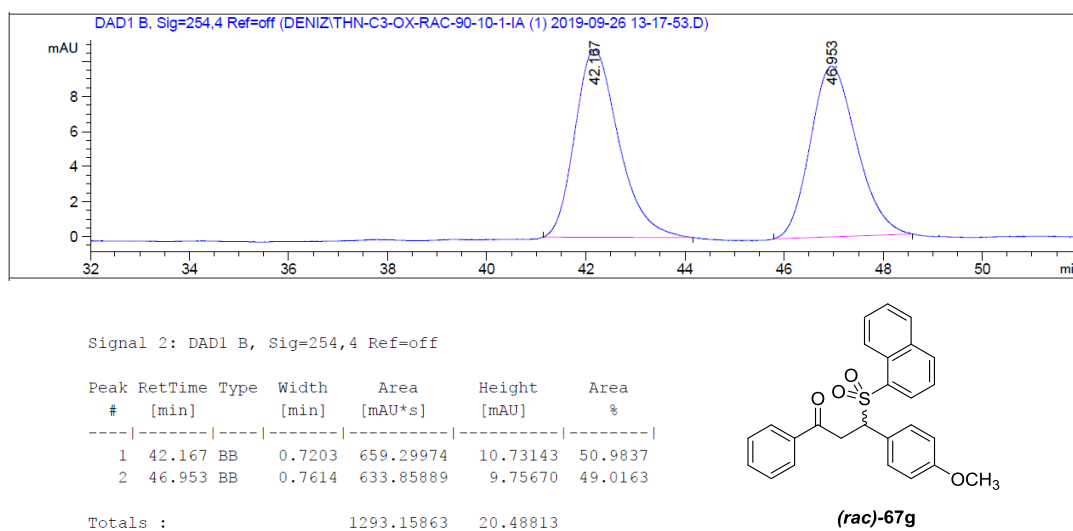


Figure B. 91 HPLC chromatogram of *rac*-67g

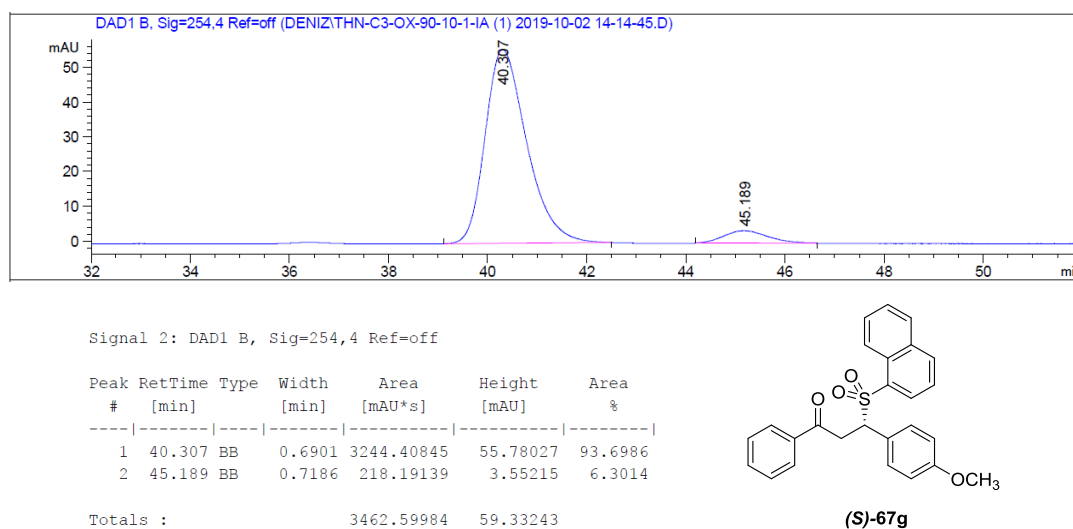
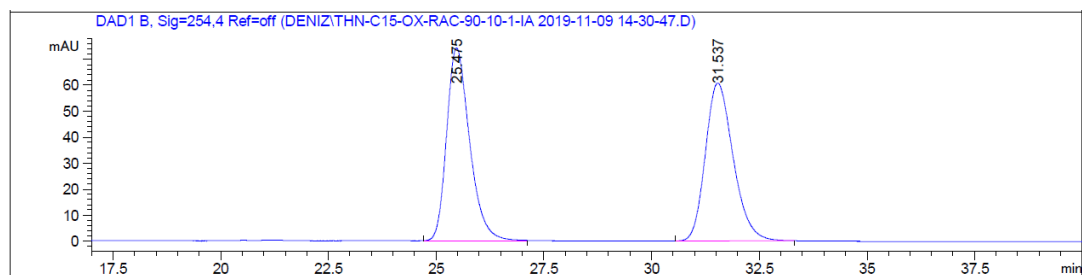


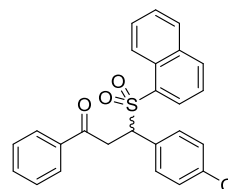
Figure B. 92 HPLC chromatogram of enantiomerically enriched 67g



Signal 2: DAD1 B, Sig=254,4 Ref=off

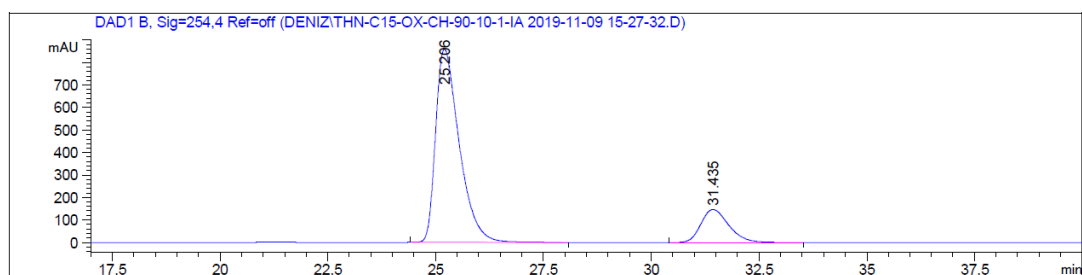
Peak #	RetTime [min]	Type	Width [min]	Area [mAU*s]	Height [mAU]	Area %
1	25.475	BB	0.5347	2746.05493	74.20673	50.1017
2	31.537	BB	0.6004	2734.90576	60.78342	49.8983

Totals : 5480.96069 134.99014



(rac)-67o

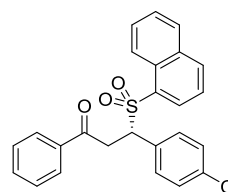
Figure B. 93 HPLC chromatogram of *rac*-67o



Signal 2: DAD1 B, Sig=254,4 Ref=off

Peak #	RetTime [min]	Type	Width [min]	Area [mAU*s]	Height [mAU]	Area %
1	25.206	BB	0.5778	3.27075e4	859.87500	83.1645
2	31.435	BB	0.6696	6621.16260	147.25027	16.8355

Totals : 3.93286e4 1007.12527



(S)-67o

Figure B. 94 HPLC chromatogram of enantiomerically enriched 67o

CURRICULUM VITAE

PERSONAL INFORMATION

Surname, Name: Tözendemir, Deniz
Nationality: Turkish (TC)
Date and Place of Birth: 16 July 1989, Ankara
Marital Status: Single
Phone: +90 538 865 95 56
email: 199740@metu.edu.tr

EDUCATION

Degree	Institution	Year of Graduation
MS	Hacettepe University Chemistry	2013
BS	Hacettepe University Chemistry	2010
High School	Etimesgut Anadolu High School, Ankara	2006

WORK EXPERIENCE

Year	Place	Enrollment
2019-Present	Roketsan Missiles Inc.	Engineer
2015-2019	METU Dept. of Chemistry	Research Assistant
2011-2013	Hacettepe Uni. Dept. of Chemistry	Research Assistant
2009 August	Turkish Aerospace Industries	Intern

FOREIGN LANGUAGES

Advanced English, Beginner German

PUBLICATIONS

Hasılciogulları, D.; Tanyeli, C. *Tetrahedron Letters*, **2018**, *59(14)*, 1414-1416.